

oml

**OAK RIDGE
NATIONAL
LABORATORY**

MARTIN MARIETTA

MARTIN MARIETTA ENERGY SYSTEMS LIBRARIES



3 4456 0268924 0

ORNL/TM-10362

Characterization of Solids in the Three Mile Island Unit 2 Reactor Defueling Water

D. O. Campbell

OAK RIDGE NATIONAL LABORATORY

CENTRAL RESEARCH LIBRARY

CIRCULATION SECTION

FORM RORR 175

LIBRARY LOAN COPY

DO NOT TRANSFER TO ANOTHER PERSON

If you wish someone else to see this report, send in name with request and the library will arrange a loan.

OPERATED BY
MARTIN MARIETTA ENERGY SYSTEMS, INC.
FOR THE UNITED STATES
DEPARTMENT OF ENERGY

Printed in the United States of America. Available from
National Technical Information Service
U.S. Department of Commerce
5285 Port Royal Road, Springfield, Virginia 22161
NTIS price codes—Printed Copy: A11 Microfiche A01

This report was prepared as an account of work sponsored by an agency of the United States Government. Neither the United States Government nor any agency thereof, nor any of their employees, makes any warranty, express or implied, or assumes any legal liability or responsibility for the accuracy, completeness, or usefulness of any information, apparatus, product, or process disclosed, or represents that its use would not infringe privately owned rights. Reference herein to any specific commercial product, process, or service by trade name, trademark, manufacturer, or otherwise, does not necessarily constitute or imply its endorsement, recommendation, or favoring by the United States Government or any agency thereof. The views and opinions of authors expressed herein do not necessarily state or reflect those of the United States Government or any agency thereof.

ORNL/TM-10362

Chemical Technology Division

CHARACTERIZATION OF SOLIDS IN THE
THREE MILE ISLAND UNIT 2 REACTOR DEFUELING WATER

D. O. Campbell

Date Published - December 1987

Prepared by
OAK RIDGE NATIONAL LABORATORY
Oak Ridge, Tennessee 37831
operated by
MARTIN MARIETTA ENERGY SYSTEMS, INC.
for the
U.S. DEPARTMENT OF ENERGY
under Contract No. DE-AC05-84OR21400

MARTIN MARIETTA ENERGY SYSTEMS LIBRARIES



3 4456 0268924 0

CONTENTS

LIST OF FIGURES. v

LIST OF TABLES vii

ABSTRACT 1

1. INTRODUCTION 2

2. EXAMINATION OF SAMPLES OF THE DWCS FILTERS 2

 2.1 MICROSCOPIC EXAMINATION 3

 2.2 CHARACTERIZATION OF FILM ON DWCS FILTERS. 9

3. FILTRATION TESTS WITH TMI-2 REACTOR DEFUELING WATER. 13

 3.1 NUCLEPORE FILTER TEST 1 14

 3.2 NUCLEPORE FILTER TEST 2A and 2B 15

 3.3 NUCLEPORE FILTER TEST 3 18

 3.4 NUCLEPORE FILTER TEST 4 19

4. EXAMINATION OF NUCLEPORE FILTERS BY SCANNING
ELECTRON MICROSCOPY 20

 4.1 INTERPRETATION OF SEM PHOTOGRAPHS 20

 4.2 PARTICLE SIZE DISTRIBUTION. 21

 4.3 INTERPRETATION OF ENERGY-DISPERSIVE X-RAY FLUORESCENCE
 (EDX) SPECTRA 26

 4.4 GENERAL OBSERVATIONS 28

 4.5 EXAMINATION OF NUCLEPORE FILTERS FROM TEST 1: WATER
 SAMPLE W1 (TURBIDITY = ~71 NTU) 32

 4.6 EXAMINATION OF NUCLEPORE FILTERS FROM TEST 2: WATER
 SAMPLE W1 (TURBIDITY = ~71 NTU) 35

 4.7 EXAMINATION OF NUCLEPORE FILTERS FROM TEST 3: WATER
 SAMPLE W2 (TURBIDITY = ~25 NTU) 39

 4.8 EXAMINATION OF NUCLEPORE FILTERS FROM TEST 4: WATER
 SAMPLE W3 (TURBIDITY = ~4 NTU) 44

5. ACKNOWLEDGMENTS 49

6. APPENDIXES 51

 Appendix A. Characterization Data for Stainless Steel
 DWCS Filter Media 53

 Appendix B. Analytical Studies of Films on DWCS Filters . . 61

 Appendix C. Particle Characterization Data for Sample W1
 (Turbidity = ~71 NTU): Filtration Test 1 95

 Appendix D. Particle Characterization Data for Sample W1
 (Turbidity = ~71 NTU): Filtration Test 2 111

 Appendix E. Particle Characterization Data for Sample W2
 (Turbidity = ~25 NTU): Filtration Test 3 147

 Appendix F. Particle Characterization Data for Sample W3
 (Turbidity = ~4 NTU): Filtration Test 4 203

LIST OF FIGURES

<u>Figure</u>		<u>Page</u>
1	Cross section of DWCS samples F2 (top) and F3 (bottom). Note film on surface of sample F2 and absence of film on sample F3	5
2	Cross section of sample F4 (top) and EDX spectrum of film region of same sample (bottom)	7
3	Cross section of surface of sample F4 (top) and silicon concentration map of same area (bottom)	8
4	Particles piled over pores of 2- μ m Nuclepore filter from Nuclepore filtration test 1: water sample W1 (turbidity = ~71 NTU). Note presence of very small particles	16
5	Particle size distribution of suspended solids	24
6	Aggregation of small particles on 0.1- μ m filter from Nuclepore filtration test 3: water sample W2 (turbidity = ~25 NTU)	31
7	Enlargement of the region shown in Fig. 6. Note the presence of rounded particles, very small particles, and aggregates	31

LIST OF TABLES

<u>Table</u>		<u>Page</u>
1	Results obtained in Nuclepore filter test 1	14
2	Results obtained in Nuclepore filter test 2A	17
3	Results obtained in Nuclepore filter test 3	18
4	Results obtained in Nuclepore filter test 4	19
5	Estimates of number and volume of particles in various size ranges	23

CHARACTERIZATION OF SOLIDS IN THE THREE MILE ISLAND UNIT 2 REACTOR
DEFUELING WATER

D. O. Campbell

ABSTRACT

Because of the impact of poor water clarity on defueling operations at the Three Mile Island Unit 2 Nuclear Power Station, a study was undertaken to characterize suspended particulates in the reactor defueling water. The examination included cascade filtration through Nuclepore filters of progressively smaller pore sizes, using three water samples obtained at different times and after varying degrees of clarification. The solids collected on the filters were examined with a scanning electron microscope and analyzed with energy-dispersive X-ray fluorescence.

A wide variety of solids was observed, and 26 elements were detected. These included all the materials expected from the reactor system (uranium, zirconium, silver, cadmium, indium, iron, chromium, and nickel), chemicals and zeolites used to decontaminate the water (aluminum, silicon, sodium), common impurities (potassium, chlorine, sulfur, magnesium, calcium, and others), as well as some unexpected metals (molybdenum, manganese, bromine, and lead). There was also evidence for the presence of organic material. A diverse assortment of particles with widely varying surface properties was found to be present.

Particles of all types were found in each size range. However, the larger ($>5\text{-}\mu\text{m}$) particles tended to contain predominantly lighter-atomic-weight elements, such as silicon, aluminum, and calcium, whereas the smaller ($<2\text{-}\mu\text{m}$) particles contained more core debris and less of the light elements. Individual core-debris particles tended to have a single major constituent (uranium, zirconium, stainless steel, or control rod); however, the different types of particles often aggregated into clusters. In addition, solids believed to be organic in origin appeared to dominate the smallest size range ($\sim 0.1\ \mu\text{m}$). As particles lodged over the filter pore openings, decreasing their effective size, progressively smaller particles were collected; consequently, the smallest particles eventually controlled the flow through the filter.

Stainless steel filter media from tests with reactor water were also examined, using a variety of surface analysis techniques. Although few particles were observed on these samples, media that had been effectively plugged were coated with a thin surface film which appeared to block pore openings. Similar media that had been "reclaimed" by soaking in hot boric acid solution showed no evidence for any film. Thus, the short filter life could result from flow blockage by either small particles or a film. Although efforts to characterize the film were not definitive, they indicated that the nature of the film changed from a primarily organic material in an early sample (prior to extensive water clarification operations) to a primarily siliceous film (after water clarity has been markedly improved by filtration and diatomaceous earth had been used extensively).

1. INTRODUCTION

The maintenance of acceptable water clarity for effective defueling activities at the Three Mile Island Unit 2 (TMI-2) nuclear power station has presented serious problems. Although excellent clarity had been achieved on a few occasions, this had not generally been the case following the commencement of active defueling at the end of 1985 - especially after the "core drill" operation which was carried out during the summer of 1986. Water clarity has been degraded by a variety of suspended solids of diverse origin. In addition to the generation and dispersal of inorganic particulate material as a result of the mechanical defueling, a biological growth developed which also interfered with visibility. The microorganisms have been controlled by the addition of hydrogen peroxide; however, their growth periodically recurs.

During the latter half of 1986, the impact of the water clarity problem became more apparent and several tasks were undertaken (1) to find a means to alleviate the problem in the short term and (2) to gain a better understanding of it for the longer term. One of these tasks was the characterization of suspended matter in the reactor defueling water and of the material that was causing unsatisfactorily short operating life of the Defueling Water Cleanup System (DWCS) filters.

2. EXAMINATION OF SAMPLES OF THE DWCS FILTERS

Samples of Paul-Trinity stainless steel filter media, identical to that used in the TMI-2 DWCS filters, were used in a laboratory test rig at TMI-2 to filter samples of defueling water. Four filter samples were

sent to ORNL for examination, and three of them had been used to filter defueling water. The samples were identified as follows:

Sample F1 - An unused (new) filter.

Sample F2 - A filter operated in the test rig with 71-NTU water until the flow had decreased to a very low rate (the filter was effectively plugged).

Sample F3 - A filter operated in a manner similar to sample F2 and then "reclaimed" by soaking in hot boric acid solution to restore flow.

Sample F4 - A filter operated in the test rig with 4-NTU water (at a later date than samples F2 and F3) until the flow had decreased to a very low rate.

No precipitate was observed on any of the filters with the naked eye under conditions of rather poor visibility. On filters exposed to water, one side was several times more radioactive than the other, as measured with an open-window survey instrument, and that was presumed to be the upstream side.

2.1 MICROSCOPIC EXAMINATION

The first observations were made on sample F1 to determine the nature of the filter. Scanning electron microscope (SEM) photographs showed a tortuous flow path of interlinked crevices of varying thickness, typically about 0.5 μm . The filter composition determined by energy-dispersive X-ray fluorescence (EDX) was representative of Type 316 stainless steel: Fe, Cr, and Ni, with measurable levels of Si and a small amount of S.

Small specimens of samples F2 and F3 were mounted for metallographic examination. In each case, one sample was mounted vertically so the

polished section was perpendicular to the surface; one was mounted at a small angle to the horizontal; and the third was mounted horizontally with the upstream side on top after polishing. These specimens were examined with both an optical microscope and the SEM. The angled specimens did not show any features different from the others and were not further examined. The filter surface was sufficiently curved that the polished surface of the horizontal mount cut very gradually into the metal of the filter surface. No unusual definitive features were observed.

The cross section of sample F2 showed clear evidence of a thin film on the surface, particularly in surface pores on the upstream side, but there was no such indication for sample F3. More complete information is included in Appendix A. Examination by EDX of the region containing the film showed primarily the components of stainless steel ($\text{Fe} > \text{Cr} > \text{Ni}$), with smaller amounts of Si and Al in varying proportions (Fig. A.8). Unfortunately, the sample had been ground with alumina and polished with silica, so the last two elements could have been introduced during sample preparation. Iron depleted in Cr and Ni, a likely corrosion product, was not observed.

The same samples were reground using diamond abrasive and polished with chromium oxide to avoid these interferences. Reexamination again indicated the presence of a film in sample F2 but not in sample F3 (Fig. 1). The EDX analyses showed silicon (in addition to the stainless steel elements) and a large Compton-scattering component characteristic of organic material. (The white areas in Fig. 1 are stainless steel, while the uniform dark areas are the epoxy mounting.) The dark appearance of the film indicates a material of low atomic number (Z), probably organic. The film was also visible by optical microscopy.

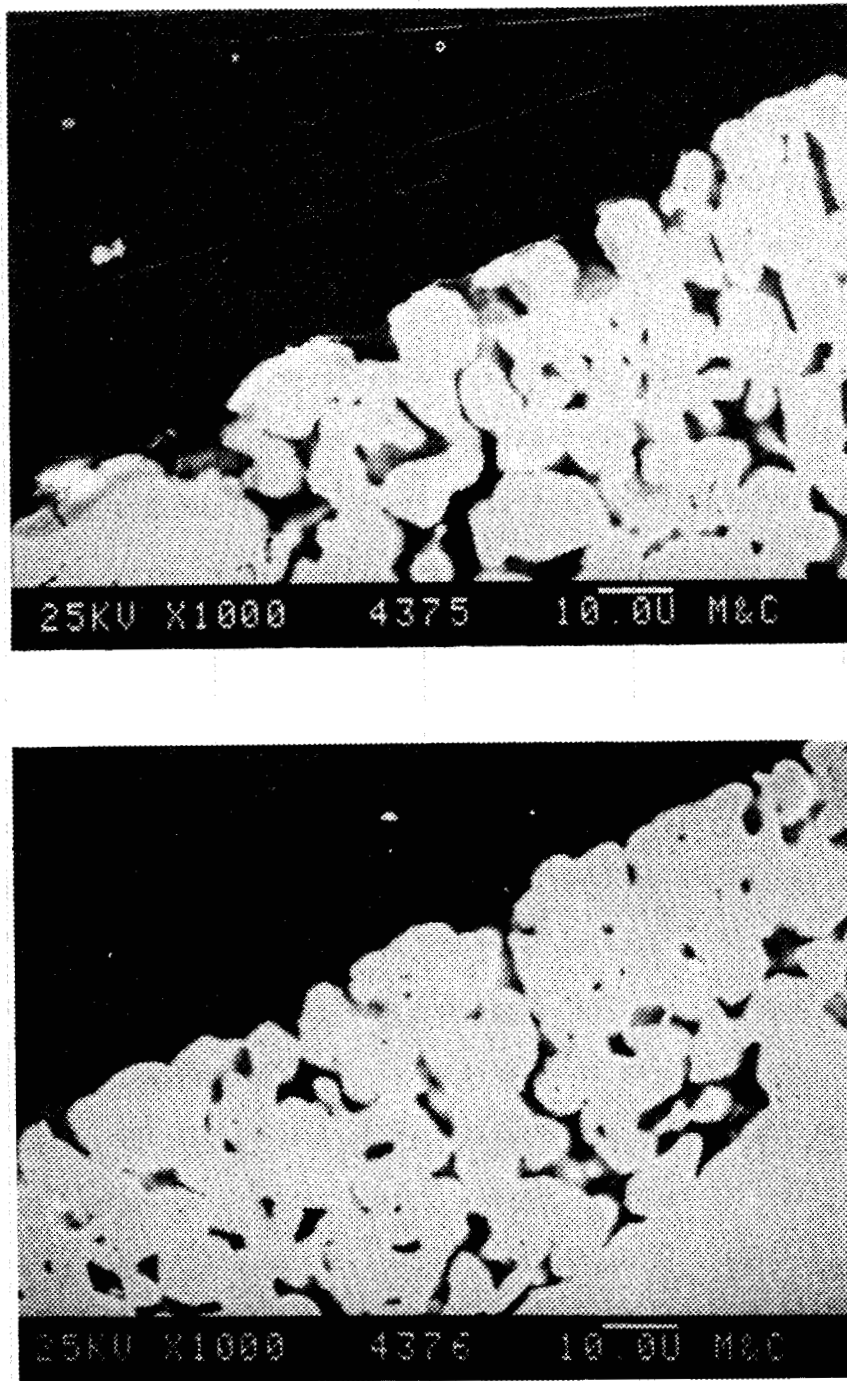


Fig. 1. Cross section of DWCS samples F2 (top) and F3 (bottom). Note film on surface of sample F2 and absence of film on sample F3.

These observations suggest that, in addition to the anticipated filtration problem from small particulates, a thin surface film may be a significant contributor to plugging of the filters. Moreover, the film probably contains silicon but may be largely organic in nature, and it is removed by the filter reclamation process, which consists of soaking in hot boric acid solution.

The leached filter (sample F3) also showed greater porosity, or a greater void fraction, than sample F2. Since the boric acid leach would not be expected to dissolve a significant amount of the stainless steel filter medium, this characteristic was presumed to be an artifact of the fabrication.

Sample F4 was acquired at a later date and examined in the same manner. The upstream surface was coated with a film that was much thicker than that for sample F2 (up to 5 to 7 μm); there was no evidence for a film on the downstream surface (Fig. 2). The film had been pulled away from the filter surface in many areas during sample preparation (potting in epoxy), leaving a crevice either between the metal and the film or between the film and the epoxy. This suggests that the film might be easily removed physically, as during sample handling. The film was analyzed by EDX, which clearly showed that it contained silicon; in addition, an elemental map showed silicon in the film on both sides of the crevice (Fig. 3). The film could also contain organic material that cannot be defined by EDX.

Sample F4 had been tested with low-turbidity water of relatively low solids concentration, but it had plugged more quickly than the filters tested with high-turbidity water. This behavior indicates that whatever

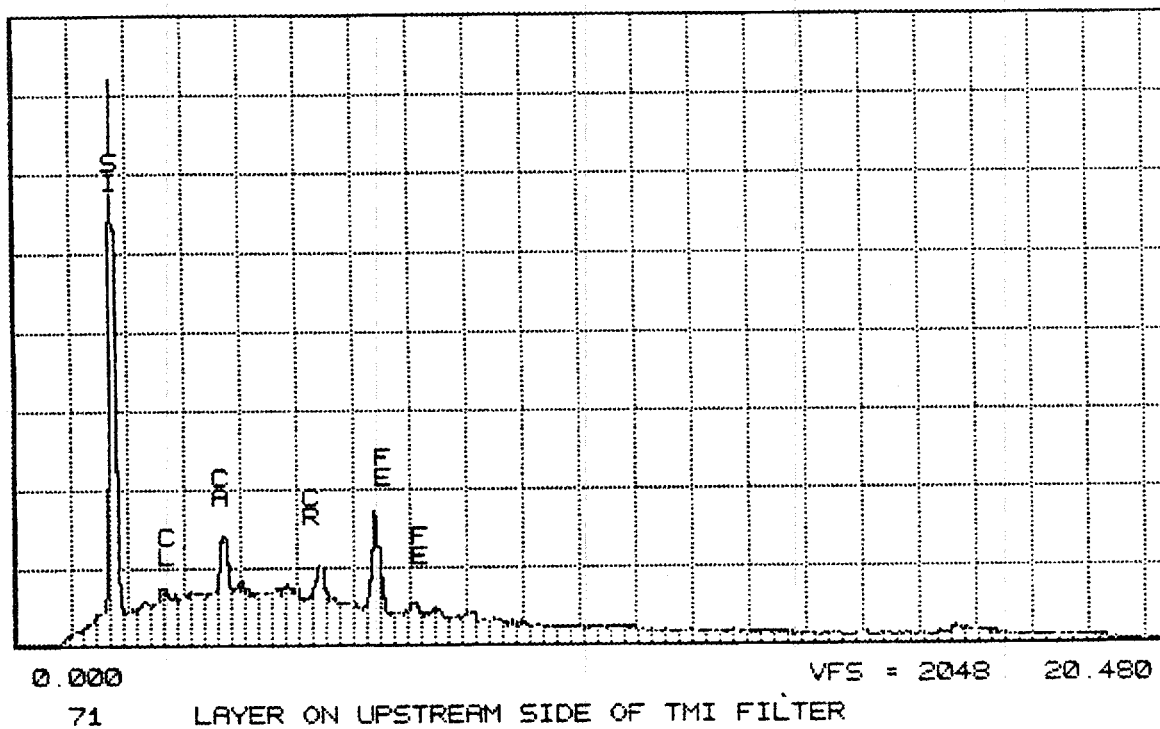
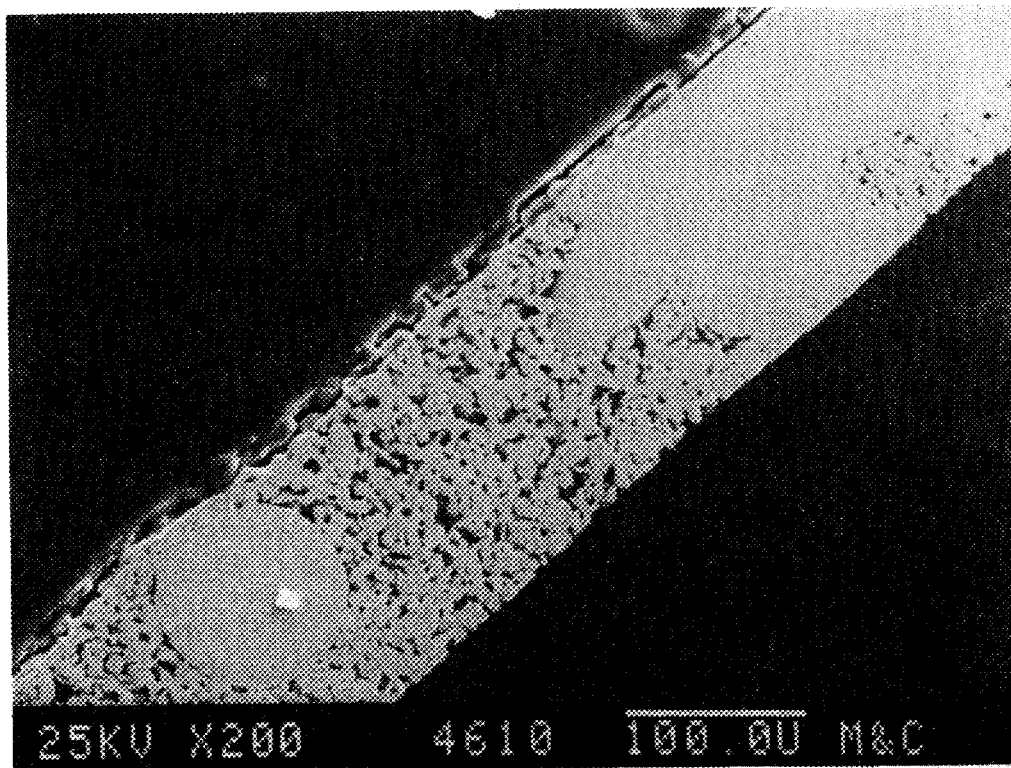


Fig. 2. Cross section of sample F4 (top) and EDX spectrum of film region of same sample (bottom).

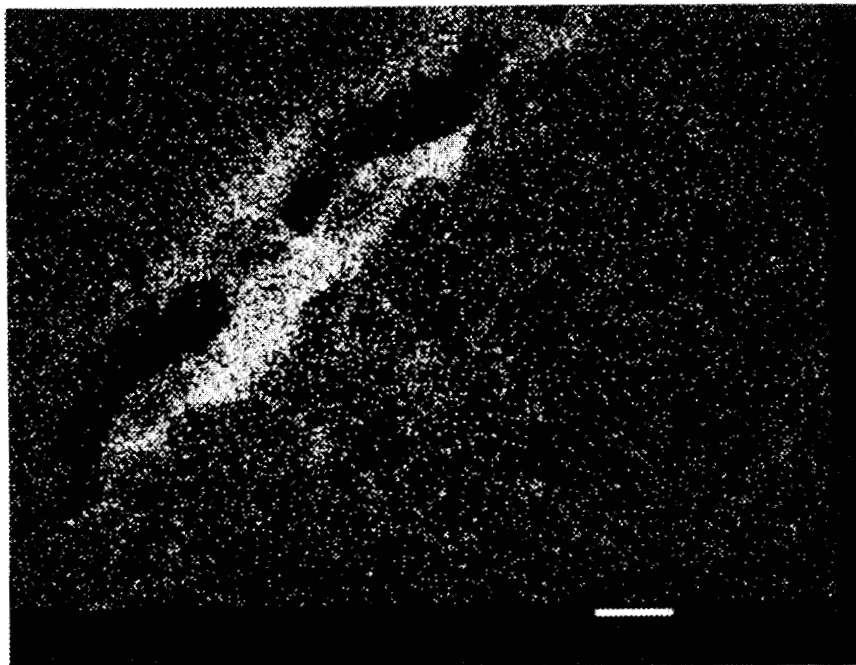
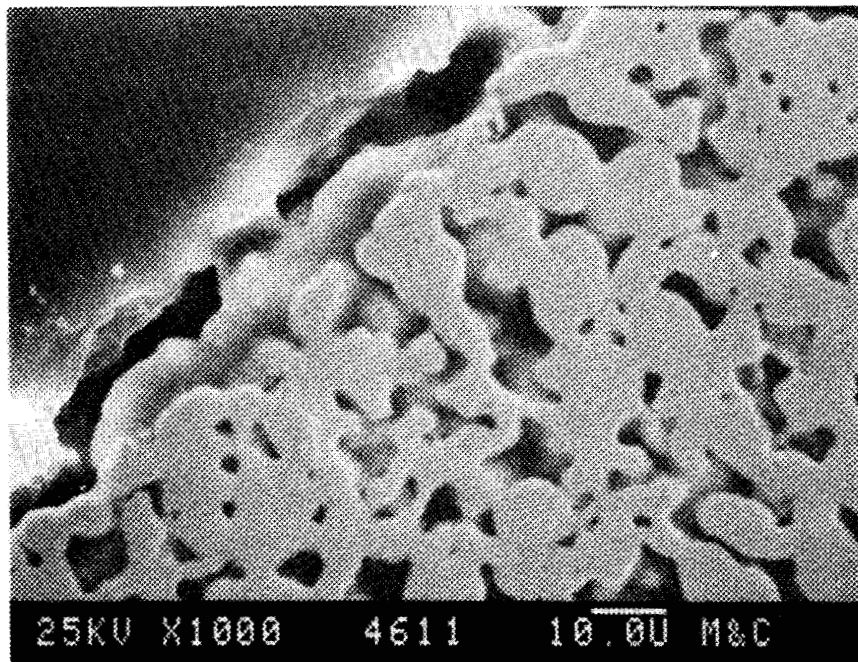


Fig. 3. Cross section of surface of sample F4 (top) and silicon concentration map of same area (bottom).

caused the film had not been removed from the water as effectively as the particulate material that contributed to turbidity. Alternatively, it is possible that particulates in the high-turbidity water formed, in effect, a precoat which extended the filter surface and delayed formation of the film.

Very few foreign particles were observed on the perpendicular cross sections of any filter, but the surface area of the filter under examination was extremely small - a line that was, at most, a few hundred micrometers long and a particle diameter wide. One particle of core debris (5 to 10 μm , Zr > U > Fe > Cr) was found on the downstream side of sample F2 (Figs. A.5 and A.7); it may have been knocked off the original surface during shipping and handling. The film showed no evidence of particulates or crystalline structure except for a very few regions with tiny particles containing some lanthanum and cerium. These elements could possibly be contaminants from sample grinding and polishing, although that is thought to be unlikely; no other potential source is known.

2.2 CHARACTERIZATION OF FILM ON DWCS FILTERS

The possible effectiveness of a film in causing plugging of filters and the very small quantity of particulate inorganic material observed on these samples led us to perform additional studies to attempt to determine whether a film really did exist and, if so, to characterize it. These studies, which were applied to both the front and the back sides of samples F2 and F4, included surface analysis by secondary ion mass spectrometry (SIMS), ion scattering spectrometry (ISS), infrared and

Raman spectrometry, and laser-desorption Fourier Transform mass spectrometry (FTMS). The results are given in Appendix B.

Analytical studies relating to the films on samples F2 and F4 are qualitative and indicative, but not conclusive. All the data generally support the presence of films which are of predominantly different composition in the two cases. The film on sample F2 appeared to be primarily organic with some silicon or organic silicate, whereas that on sample F4 was predominantly silicon with possibly some organic component. Some inconsistencies that were observed were probably related to the different thicknesses of the surface layer that the methods analyze.

The ISS method examines a very thin surface layer (only a few atoms thick). Carbon and oxygen were detected on both sides of each filter; however, there was less carbon (relative to oxygen) on sample F4, suggesting that its film contained more oxide. The amount of silicon was small, if it was present at all, on sample F2; however, it was found on both sides of sample F4 (more on the front than on the back). Iron and chromium were found on both sides of sample F4, indicating that at least some metal filter medium was very close to the surface; it was noted above that the film may have flaked off part of the surface of this filter. These elements were not observed on sample F2 until after repeated scans (which eroded the surface to the extent of perhaps 0.1 μm); then they appeared only on the back side. Thus, the coating on the upstream side of sample F2 was relatively thick. There was also evidence for a small amount of FeO on the front surface of sample F4.

The SIMS method, which examines a much thicker layer (up to the order of 0.1 μm thick), gives results generally consistent with the foregoing.

Significant peaks characteristic of organic compounds were present on both sides of sample F2, with the larger peaks found on the front. Such peaks were notably absent on sample F4. The silicon peak was large on sample F4 and enriched on the front surface, while it was small on sample F2. The sodium peak was larger on the back of each filter than on the front. Aluminum was present on all surfaces. Peaks for the filter-medium metals, chromium and iron, were much larger on sample F4 than on F2, suggesting that the film was thinner or may have flaked off part of the surface of sample F4. Note that the filter presents a very rough surface; therefore, the film varies in thickness from very thick over the pores to quite thin over the high points, as shown in Figs. 1 and 2.

The FTMS method, which analyzes an even thicker surface layer than does the SIMS method, also showed the two samples to be different. Both have a large signal at mass 43, which is probably methyl silicon (from organic silicate) but could possibly be BO_2 . Several other peaks are indicative of silicon, and there is no evidence for boron in any of the other determinations (above). The data also indicated that the film was very nonuniform, with substantial variations occurring from point to point on the sample.

Two additional materials were tested with the FTMS method for comparison: (1) the borated hydraulic fluid, which was known to have been spilled into the water; and (2) sugar, which is representative of polysaccharides that are reasonable products of biological activity (cell membranes). In the case of sample F2, the peaks for sugar correlated well with the observed spectra, but those for hydraulic fluid did not; this supports the suggestion that the film is at least partly derived

from biological material. For sample F4, there was poorer agreement with the peaks for either material and a siliceous film was indicated.

Diffuse-reflectance infrared spectra from the front of sample F4 showed some weak, but meaningful, absorption in regions characteristic of hydrocarbons and silicon-oxygen functionalities, and possibly also bonding between silicon and organic carbon. These findings also support the existence of a siliceous film on the front of sample F4. The back side showed only the hydrocarbon bands. It is possible that all stainless steel surfaces are covered with a thin coating of hydraulic fluid, but this coating does not constitute the film. Sample F2 was not examined by this method.

These results support the presence of films on the DWCS filter samples and suggest that the nature of the material forming the film changed between the times samples F2 and F4 were taken. The film on sample F2 had a large organic component that was probably derived from biological growth. Although the production of this material has been largely eliminated, a reservoir of it may still exist somewhere in the system. One might expect the problem arising from this component to diminish with time since the material is gradually removed from the system and is not replenished.

The film on sample F4 contained a large amount of silicon and much less organic material than did that on sample F2. The silicon probably originated from the diatomaceous earth (DE) precoat used in the swimming pool filter during the time between the test which generated sample F2 and that which generated sample F4. The use of DE is expected to continue, so this source of a film will probably persist; therefore, it will

be necessary to deal with such siliceous material throughout defueling. Two approaches that are generally used (either alone or in combination) are: (1) to provide an extended surface by precoating and continuously renewing the surface by "body feed" and (2) to coagulate the very small particles into larger agglomerates by modifying their surface properties with a polymer additive. These methods are currently being used for water treatment in the plant.

3. FILTRATION TESTS WITH TMI-2 REACTOR DEFUELING WATER

Filtration tests were carried out using a series of Nuclepore filters, in succession, to separate the insoluble material into different size ranges that could be further characterized. With one exception, each of these tests was performed with 30 mL of water. A 25-mm-diam filter was used in test 1; the larger (47-mm-diam) filter was used in all others. The exposed diameters were 19 and 37 mm, giving areas of 2.84 and 10.8 cm², respectively. The "loadings" with 30 mL of feed were 10.6 and 2.8 mL per cm² of surface area, corresponding to filtration of water at initial depths of only 10.6 and 2.8 cm.

The turbidity of the water was measured after each filtration. Relative radiation levels of each filter (measurements made ~0.5 in. away) and of the water after each filtration (measurements made at the side of a polyethylene graduate) were determined with a survey instrument. Finally, a sample of each filter was examined with an SEM with EDX capability; the results are summarized in Sect. 4.

The three different water samples that were supplied by GPU Nuclear can be described as follows:

- W1 - This sample was taken on September 8, 1986, after a bleed/feed procedure, following core bore, and prior to swimming pool filter operation; the turbidity was reported to be 71 NTU. Filter sample F2 was used to filter similar water.
- W2 - This sample was taken on September 22, 1986, after swimming pool filter operation; the turbidity was reported to be 25 NTU.
- W3 - This sample was taken on October 16, 1986, after DWCS operation; the turbidity was reported to be 4 NTU. (Filter sample F4 was used to filter similar water.)

3.1 NUCLEPORE FILTER TEST 1

Test 1 was carried out with water sample W1 (turbidity = ~71 NTU). The Nuclepore filters were 25 mm OD with an exposed diameter of 19 mm. The 30 mL of water (10.6 mL/cm²) was vacuum filtered through a sequence of filters of successively smaller pore sizes. After passage of the water through each filter, the radiation levels of the filter and the filtered water were measured and the turbidity of the water was determined. These data are listed in Table 1.

Table 1. Results obtained in Nuclepore filter test 1

Pore size of filter (μm)	Turbidity of filtered water (NTU)	Radiation level (mR/h)	
		Filter	Filtered water
10.0	90	30	60
2.0 ^a	29	800	30
1.0 ^b	15	120	24
0.6 ^b	5.1	110	24
0.4	2.2	24	21
0.1	0.24	25	19

^aFilter collected a large amount of solids smaller than 2 μm, in addition to the 2- to 10-μm fraction, leaving less of the finer material for subsequent filters.

^bFilter contained some material smaller than nominal pore size.

Because of the buildup of solids over the pores of the 2- μm filter, the effective pore size was decreased and the filter collected a large quantity of solids with particle sizes much smaller than 2 μm . Accordingly, less solid material was left in the water that was fed to the filters with smaller pores. The 1- μm filter similarly collected particles smaller than 1 μm , but not to so great an extent. Thus, the 2- μm filter collected more solids than were actually in the 2- to 10- μm size range, and the filters smaller than 1 μm collected less solids than were present in the defueling water in their appropriate size ranges.

The behavior of the 2- μm filter may explain the problem from plugging in the large DWCS filters. A pile of particles collected over each filter pore (Fig. 4), and the surface of the pile is composed largely of very small particles. Regardless of the pore size of the filter media, partial blockage of the pores decreases the size of the flow paths so that successively smaller particles are collected. This process continues until the finest particles present to any substantial extent will determine the effective pore size of the filter.

3.2 NUCLEPORE FILTER TEST 2A AND 2B

Water sample W1 was also used for both parts of this test. In part 2A, the test procedure was the same as that used in Nuclepore filter test 1 except (1) intermittent swirling of the solution was used to disperse particles away from the pores; (2) a larger (47-mm-diam) filter was used to provide more efficient size fractionation and thinner deposits, which were more appropriate for SEM particle characterization; and (3) two additional filters, 5- and 0.8- μm , were added to the sequence. Some buildup of small particles still occurred on the 2- μm filter, but not on the others. Radiation and turbidity data from test 2A are given in Table 2.

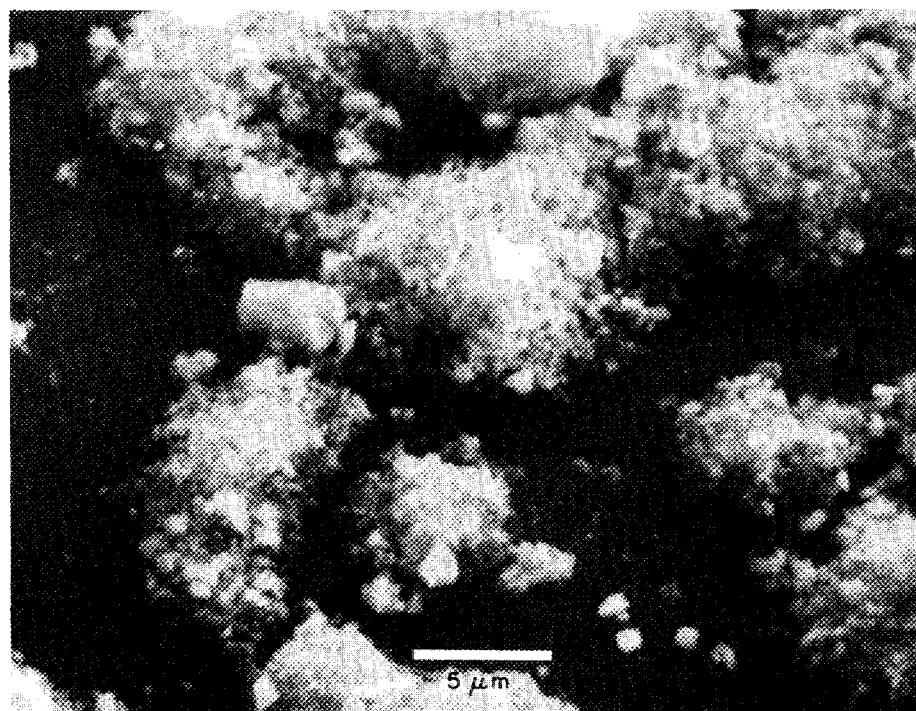
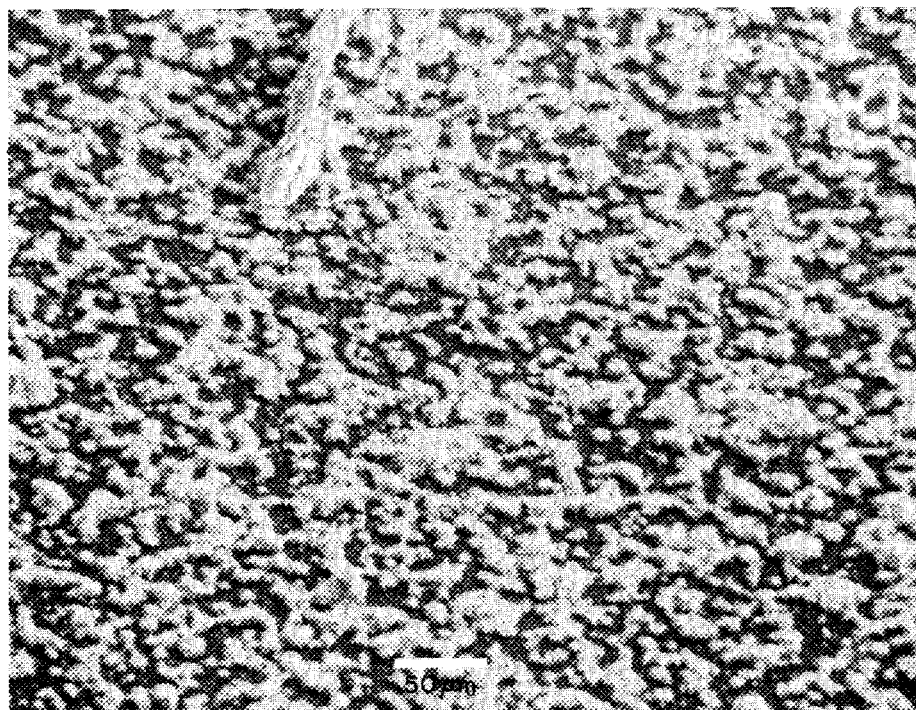


Fig. 4. Particles piled over pores of 2- μm Nuclepore filter from Nuclepore filtration test 1: water sample W1 (turbidity = ~ 71 NTU). Note presence of very small particles.

Table 2. Data obtained in Nuclepore filter test 2A

Pore size of filter (μm)	Turbidity of filtered water (NTU)	Radiation level (mR/h)	
		Filter	Filtered water
Initial	93		60
10.	88	38	58
5.	90	43	53
2.0 ^a	49	360 ^b	30
1.0	24	130	28
0.8	19.6	25	23
0.6	12.1	49	21
0.4	5.4	56	19
0.1	0.34	50	18

^aFilter collected some solids smaller than 2 μm .

^bRadioactivity level of 2- μm filter after filtration of 5 mL of solution measured 32 mR/h, corresponding to 192 mR/h for this test.

In part 2B, 10-, 5-, and 2- μm filters (all 47-mm-diam) were used to filter only 5 mL of sample W1 water. This avoided the pileup of diverse particles over the pore openings and yielded a 2- to 5- μm sample which had well-separated particles and was more suitable for SEM examination. Such samples were designated as "diluted 2 μm ."

The radioactivity level of the water in the original bottle of sample W1 measured 900 mR/h at the bottom and 15 mR/h at the top before shaking; after shaking, it measured 200 mR/h at the middle. (All determinations were made at a distance of 1/2 in. from the bottle.)

3.3 NUCLEPORE FILTER TEST 3

Water sample W2 (turbidity, ~25 NTU) was filtered successively through a similar series of Nuclepore filters to separate particles into narrow size fractions, as was done in test 2 (see Sect. 3.2). There was little, if any, pore blockage with this water. The test was performed with 30 mL of water on 47-mm-diam filters. The radiation levels of the filters and the filtered water and the water turbidity determinations after each filtration are reported in Table 3.

Table 3. Results obtained in Nuclepore filter test 3

Pore size of filter (μm)	Turbidity of filtered water (NTU)	Radiation level (mR/h)	
		Filter	Filtered water
Initial	22		36
10.	21	4	37
5.	21	4	34
2.0	21	9	32
1.0	16.2	42	31
0.8	13.0	20	28
0.6	8.8	46	25
0.4	4.2	54	22
0.1	0.30	63	20

The radioactivity level of the original bottle of sample W2 measured 460 mR/h at the bottom and 75 mR/h at the top, before shaking, and 120 mR/h at the middle, both before and after mixing. (All determinations were made at a distance of 1/2 in. from the bottle.)

3.4 NUCLEPORE FILTER TEST 4

The same filtration sequence was carried out with water sample W3, which had a turbidity of ~4 NTU. Again, 30 mL of water was used with 47-mm filters. The filters were very lightly loaded with particles. The radiation levels of the filters and the water turbidity measurements after the various filtration steps are reported in Table 4.

Table 4. Data obtained in Nuclepore filter test 4

Pore size of filter (μm)	Turbidity of filtered water (NTU)	Radiation level (mR/h)	
		Filter	Filtered water
Initial	2.5		29
10.0	2.3	<1	28
5.0	2.3	<1	25
2.0	2.2	2	24
1.0	1.6	2	25
0.8	1.3	4	25
0.6	0.9	3	25
0.4	0.51	6	22
0.1	0.20	6	21

The radioactivity level of the bottle of sample W3 measured 130 mR/h at the bottom, 100 mR/h at the middle, and 92 mR/h at the top before mixing; it was 110 mR/h at the middle after mixing.

4. EXAMINATION OF NUCLEPORE FILTERS BY SCANNING ELECTRON MICROSCOPY

Small sections of each Nuclepore filter from the tests described in the preceding section were examined with an SEM, and various areas of the filters and of individual particles were analyzed by EDX. The results of these observations are summarized here; complete data are included in the Appendixes. Two different SEM instruments were used. One, which gave significantly better resolution for small particles, was used to examine the smaller pore-size filters; the other was used to examine the larger pore-size filters. Data from the two instruments are presented in different formats (see the Appendixes).

4.1 INTERPRETATION OF SEM PHOTOGRAPHS

The summary presented later in this section briefly describes some of the particles. SEM photographs of each filter are included in the Appendixes. These photographs were made at several magnifications, up to 20,000X in a few cases. Since the magnification is changed during photographic reproduction, a calibration scale is provided on each figure for estimating particle sizes. The filter pores are also an indication of scale.

Particle appearances vary greatly. Recognizable material includes diatoms from filter precoat and core-debris fragments with sharp edges and corners, presumably from the core-drilling operations. Many particles show no particular structure, and many appear to be agglomerates of much smaller fundamental particles. In the case of very small particles, the fundamental particles were of the proper size to have passed through the previous filter; however, the aggregates are larger, so they were presumably formed between filtrations. The smaller size fractions, in particular, contain globular or spherical particles.

An important, but qualitative, feature is the apparent brightness of the particles. Most photographs are secondary electron images (SEI), which provide, in general, a topographic view of the surface. Elements of higher atomic number (Z) scatter electrons more efficiently than those of lower Z; thus, high-Z particles appear brighter or white, while low-Z material is gray. A reference point is the smooth organic filter material itself. Since the brightness and contrast controls of the instrument can be varied over a wide range, such observations are only qualitative at best. However, in many cases, they provide an indication of which particles contain, for example, light (Si, Al, Ca), intermediate (Zr, Cd, Ag), or heavy (U) elements.

This difference can be greatly accentuated by using the backscatter electron image (BEI), which was done in several cases. Backscattering by an angle of nearly 180° is more efficient with heavy elements but practically nonexistent for light elements. As a result, organic particles, consisting predominantly of low-Z elements (C, H, O) are effectively invisible. A comparison of the SEI and BEI images of the same area gives a good indication of the fractions of the particles that are of reasonably high Z and of low Z. Low-Z particles that do not contain elements heavier than sodium are most likely to be organic in nature.

4.2 PARTICLE SIZE DISTRIBUTION

An effort was made to estimate the density of particles in each size range by counting the number of particles in the SEM photographs. Also, a rough estimate of the volume of solids in each size range was made by calculating the volume of the solid particles, assuming that each particle diameter was equal to, or slightly less than, the mean of the filter

pore size range in which the particle was collected. For example, particles that were collected on the 1- μm filters were assumed to have a diameter of 1.4 μm . For those particles collected on the 10- μm filter (the largest pore-size filter used), the particle diameter was assumed to be 15 μm . The results of these estimates are summarized in Table 5, and the estimated particle size distribution is shown in Fig. 5. The accuracy of these data was poor in some cases because either (1) too few particles were present to permit a statistically significant count, (2) the particles were not distributed uniformly, (3) so many particles were present that they covered each other, or (4) many small particles were agglomerated into larger clumps. The precision of data obtained from different SEM photographs of particles within the same size range varied from a factor of 2 (in most cases) to much larger factors (in a few cases). Even though some of the results may be inaccurate, the data as a whole were analyzed and some interesting observations were noted, as described below.

For water sample W1 (turbidity = ~ 71 NTU), which represents the state of the defueling water after the core bore operations and a period of settling (but before any filtration), the particle size distribution of the contained solids was reasonably close to a log-normal distribution, as evidenced by the approximately linear plots shown in Fig. 5.

For water sample W2 (turbidity = ~ 25 NTU), which represents the state of the defueling water after some filtration through the swimming pool filter containing a diatomaceous earth (DE) precoat, the number of core-debris particles within the 1- to 10- μm size range was reduced substantially. At the same time, relatively large DE particles were introduced (and observed in the SEM photographs). The net result was

Table 5. Estimates of number and volume of particles in various size ranges

Filter pore size (μm)	Number of particles/cm ²			Relative particle size distribution (% larger than specific size)					
	Water sample W1 ^a	Water sample W2 ^b	Water sample W3 ^c	Water sample W1 ^a		Water sample W2 ^a		Water sample W3 ^c	
				No. of particles	Volume of solids	No. of particles	Volume of solids	No. of particles	Volume of solids
10	5E3	3E3	4E3	0.00	5.7	0.00	11	0.00	50
5	5E4	5E3	5E3	0.00	13	0.00	13	0.00	58
2	2E6	8E4	7E4	0.15	35	0.01	16	0.04	67
1	3E7	1E7	7E5	2.4	69	0.9	51	0.4	75
0.8	1E7	5E6	2E6	3.1	72	1.3	56	1.1	80
0.6	1E8	4E7	5E6	11	86	4.8	74	3.4	88
0.4	2E8	1E8	8E6	26	97	13.4	90	7.1	93
0.1	1E9	1E9	2E8	100	100	100	100	100	100
Total	1.3E9	1.2E9	2.2E8						

^aTurbidity of water sample W1 = ~71 NTU.

^bTurbidity of water sample W2 = ~25 NTU.

^cTurbidity of water sample W3 = ~4 NTU.

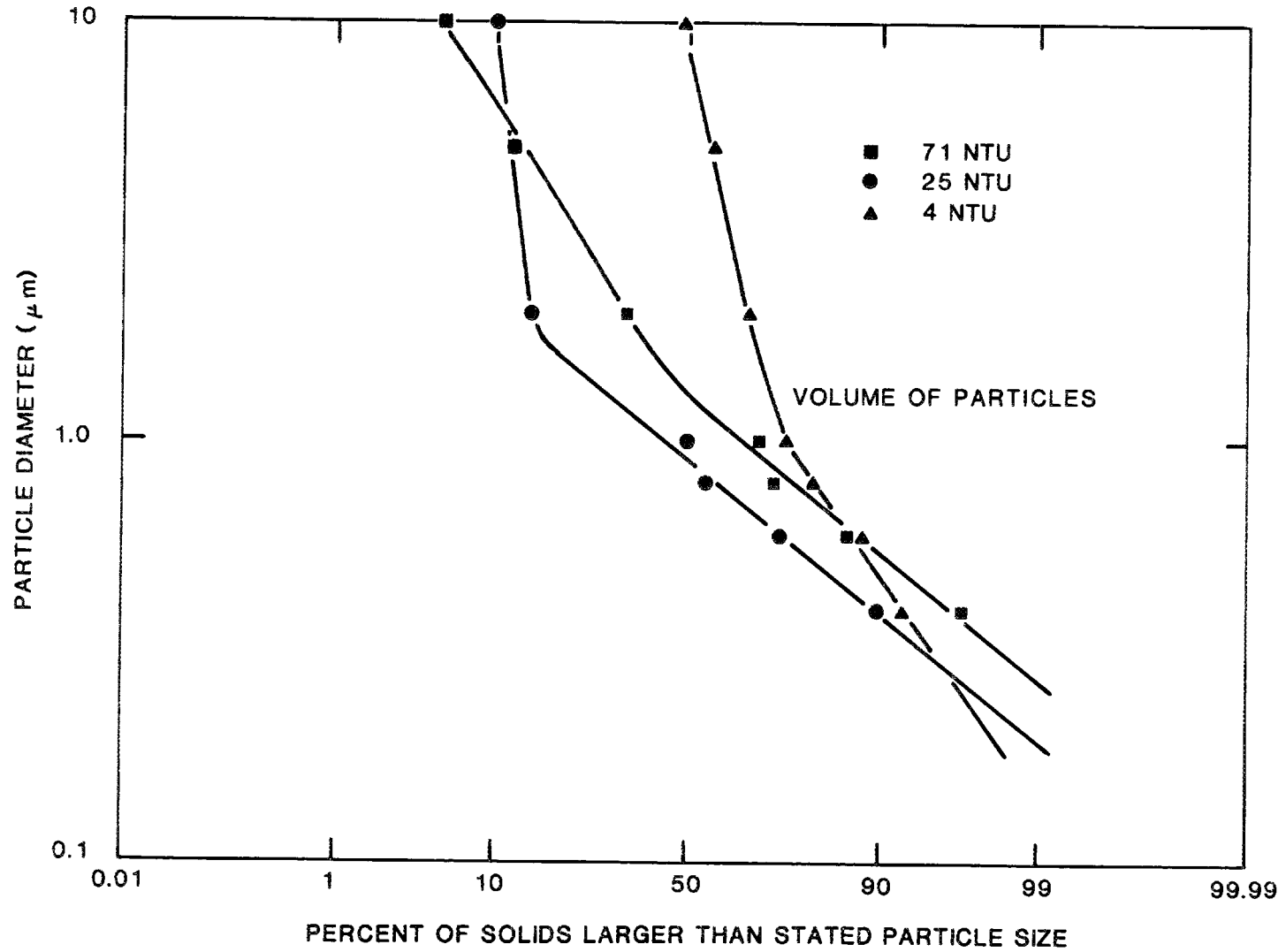


Fig. 5. Particle size distribution of suspended solids.

was that the number of particles in the $>10\text{-}\mu\text{m}$ size range was about the same, but the particles were of different composition.

In the case of water sample W3 (turbidity = ~ 4 NTU), which represents the state of the defueling water after additional filtration through the DE-precoat swimming pool filter and also some filtration through the $0.5\text{-}\mu\text{m}$ -rated DWCS filters, the number of particles in the $>2\text{-}\mu\text{m}$ range was not reduced as compared with sample W2. This was because of (1) the effectiveness of the swimming pool filter in removing the larger core-debris particles in both cases and (2) the addition of the larger DE particles. In contrast, the number of particles in the $<2\text{-}\mu\text{m}$ size range was substantially decreased by the $0.5\text{-}\mu\text{m}$ -rated DWCS filters.

The introduction of DE fragments biased the particle size distribution extensively. The increased component from these large particles appears in the curves of Fig. 5 as a steeper slope, especially at the upper end of the lines and as a displacement of the curves to the right.

These data demonstrate that sample W3 (turbidity = ~ 4 NTU) contained a relatively higher percentage of large-particle material; this was derived from DE fragments and was, therefore, silica-rich as compared with the particles that would be expected if the DE material was not present. This silica source dominated the total water impurity content. Waste clarification methods currently being used depend on the injection of DE "body feed," and it is possible that some of these solids will escape the filtration system. It is likely that DE particles will be controlled more effectively with DWCS filters than with the swimming pool filter, which was used during the time that the water samples studied here were obtained. Accordingly, the DE particulates should occur to a smaller extent than is indicated by the results of this study.

The smaller-size (<1- μ m) particles appear to be derived predominantly from the reactor system (core debris and possibly some organic material). Since ongoing defueling operations will continue to resuspend existing core-debris particulates and generate new debris, that source of solids should be expected to persist throughout defueling. These small particles scatter light much more effectively than larger ones, although large particles may constitute the bulk of the solids. Consequently, small particles from the core debris will probably continue to represent a potential visibility problem.

4.3 INTERPRETATION OF ENERGY-DISPERSIVE X-RAY FLUORESCENCE (EDX) SPECTRA

The summary presented at the end of this section identifies and estimates the inorganic elements observed in the EDX scans. They are listed generally in the order of decreasing intensity (or peak height) of the characteristic X-ray lines observed for each element. Very light elements ($Z < \sim 11$) were not detected; this range includes boron (known to be present) and carbon (from organic material, which may be present). All other elements can be detected, although with varying efficiencies.

It should be emphasized that these listings are not quantitative measures of relative abundance; in fact, they may not even be in the proper qualitative order. Different groups of elements were detected by means of different orders of X-rays: K X-rays were used to detect "light elements" (Z from ~ 12 to ~ 45); L X-rays were used to detect heavier elements ($Z > \sim 35$); and M X-rays were used to detect the heaviest elements, notably uranium for which both L-type and M-type X-rays appeared. There were important interferences which, in a few cases, made element identification uncertain.

The emission intensities of the different orders of X-rays vary, and the efficiencies for exciting them decrease monotonically with increasing Z. Interactions that involve the absorption of primary X-rays and the emission of secondary ones occur within the material being examined. Although corrections can be applied so that quantitative X-ray fluorescence determinations can be made with ideal samples (smooth surface and thick), this is not practical with small samples of small particles, such as those encountered in the present study. Because of the considerations noted here, even an estimate of the qualitative order of abundance is uncertain. Accordingly, the listings reported should be interpreted only as approximations.

In most cases, X-ray spectra were obtained for individual particles or small aggregates of particles, ranging from a few micrometers to submicron size, by focusing the electron beam on the particle of interest. There is often some contribution to such spectra from material immediately adjacent to and underneath the particle of interest. Area scans of the solids on the filter, representing the entire surface of the corresponding photograph, are given in some cases. Area scans represent many particles (usually hundreds or thousands) and are, therefore, a sort of average composition plus a contribution from the filter media that may dominate.

There is a natural tendency to select for analysis those particles which are of unusual appearance and to examine only a relatively few particles typical of the bulk of the material, so it is not easy to convert the analyses for individual particles to an average for all solids present. This can be done, to some extent, by estimating the

relative quantities of particles of similar characteristics or appearances in the photographs. The least that can be said is that those compositions which are observed do, in fact, exist in this system.

The X-ray spectra from light elements, such as those found in organic material and the filter media, generally appear as Compton backgrounds with small X-ray peaks denoting any trace elements present. A significant Compton background is always present in scans of very small particles or of areas. This background appears to be suppressed if large X-ray peaks are present because the Y-axis scale (counts) is expanded to match the largest peak. In the Appendixes, the Y-axis scale is indicated on the spectra either by a number followed by "FS" (e.g., 125FS) or by "VFS=" (e.g., VFS=1024). If the Compton background dominated the spectrum, no large X-ray peaks were present; in such cases, the Y-axis scale is relatively small. This suggests that there was no significant quantity of any element heavier than sodium.

4.4 GENERAL OBSERVATIONS

At least 26 elements were found in the various solids; in addition, light elements such as carbon and boron must be present. The elements detected include Na, Mg, Al, Si, S, Cl, K, Ca, Ti, Cr, Mn, Fe, Ni, Cu, Zn, Br, Zr, Mo, Ag, Cd, In, Ba, Ce, Pb, Bi, and U. Of these, Al, Cl, Cu, and Zn were present, to some extent, as artifacts due to sample preparation and mounting; in many samples, however, Al, Cl, and, in some cases, Cu were present far in excess of such amounts.

Many of these elements were expected, such as Fe, Cr, Ni, Zr, Ag, Cd, In, and U (from the reactor system) and Cl, S, Al, Si, and Ca (as

common or known impurities). However, some were unexpected; these include Mo in quite a few samples, Br in several, Pb and possibly Bi in a very few, K in large amounts in a few, Mn in a few, and rarely Ce and Ba (the Ba X-ray could be an artifact from the decay of ^{137}Cs in fuel-bearing material).

A wide range of particle sizes and compositions was observed in all water samples, but there were systematic variations in the nature of the solids according to particle size. In general, the larger ($>5\text{-}\mu\text{m}$) particles were composed of light elements (Si, Al, Ca, and sometimes Fe that was usually free of Cr and Ni); there was also a small amount of other materials, including core debris (Zr, U, and Ag), which was probably associated with some of these larger particles as agglomerates. The large particles were relatively few in number and probably do not contribute significantly to the water problem.

A change in character of the particles was observed starting with the 2- to 5- μm fraction for water sample W1 (turbidity = ~ 71 NTU) and the 1- to 2- μm fractions from samples W2 (turbidity = ~ 25 NTU) and W3 (turbidity = ~ 4 NTU). As the particle size decreased through these ranges, a larger amount of solids appeared and the solids contained less of the light elements but more core debris. Individual debris particles, in most cases, were composed predominantly, or almost entirely, of only one element: U, Zr, or some mixture of control rod metals (Ag, Cd, and In were each dominant in different particles). Iron was also present, sometimes relatively pure and sometimes mixed with Cr, Ni, or both. In addition, aggregates of several types of particles occurred.

As the particle size decreased below 1 μm , the light-element fraction (Al, Si, Ca) decreased greatly and the fraction of core-derived material generally increased. There was also a tendency for some particles in the few-tenths micrometer size range to be rounded or globular, suggesting that they resulted from molten material (control rod) or aerosol condensation (refractory oxides, uranium), although some fragmented material was observed as well.

As the particle size decreased further, there was increasing evidence for particles containing only low-Z elements (e.g., organic material); and that appeared to dominate in the smallest fraction, 0.1 to 0.4 μm . A substantial amount of material was found in this size range (Fig. 5). Under higher magnification, many particles were rounded and particles even smaller than 0.1 μm were observed (Figs. 6 and 7); however, there was still some core-derived material in this fraction (i.e., the bright core in the particle near the center). In the smaller-size material, especially, there was evidence for the aggregation of small, often spherical, particles into small clusters.

Particles with the same general characteristics were observed in each of the three water samples. The primary difference involved the amount of solids present; substantially less of the metal-containing solids (but still a very significant amount) was found in the lower-turbidity waters, especially sample W3. There was also less small-sized low-Z material (presumably organic) in the lower-turbidity waters, but it probably did not decrease as much as did the amount of larger-sized (metal-containing) solids. However, it is difficult to estimate the amount of such material accurately.

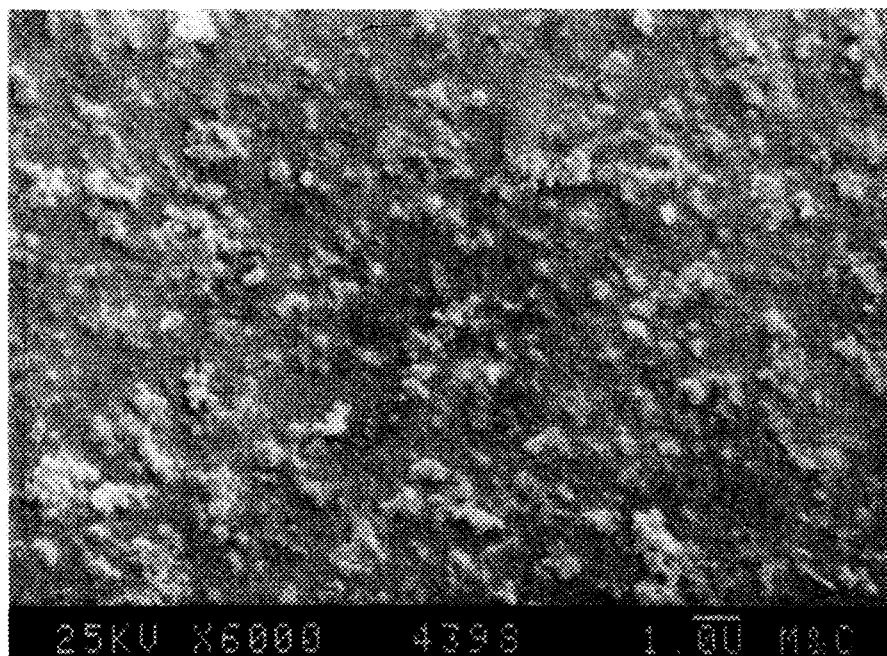


Fig. 6. Aggregation of small particles on 0.1- μ m filter from Nuclepore filtration test 3: water sample W2 (turbidity = \sim 25 NTU).

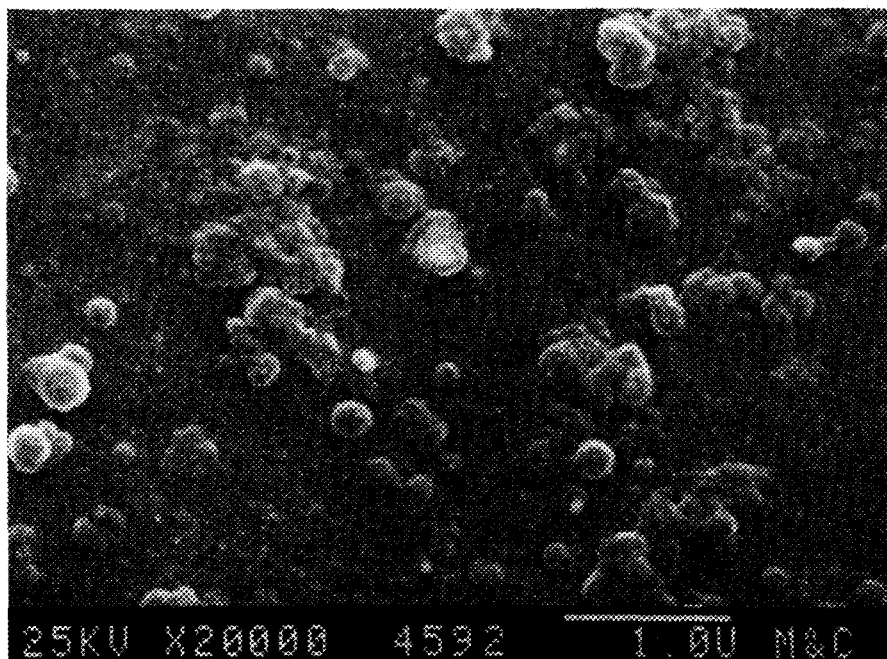


Fig. 7. Enlargement of the region shown in Fig. 6. Note the presence of rounded particles, very small particles, and aggregates.

The filters were examined using an SEM with EDX capability. The analytical data reports (photographs and EDX spectra) are detailed in Appendixes C through E; the results for each analysis are summarized in the subsections that follow. For cross reference, each photograph is referred to by its identification number, which is given at the left margin of the listing that follows, as well as on the photographs in the Appendixes. Each photograph also includes a scale indicated by a line labeled with its corresponding length in micrometers (designated as "U" or " μm "). Within a given EDX analysis, elements are generally listed in the order of decreasing relative X-ray peak heights; these values are not necessarily the same as their relative abundances.

4.5 EXAMINATION OF NUCLEPORE FILTERS FROM TEST 1: WATER SAMPLE W1 (TURBIDITY = ~ 71 NTU)

10- μm Filter (Figures C.1-C.2)

<u>Photograph</u>	<u>Comments</u>
18412	Few large particles; widely separated
18413	10- to 13- μm ill-defined particle— Ca > Si >> Cl, Al > Fe
18414	1. 5- μm -diam x 30- μm -long rod; essentially all silica 2. Cluster of small particles on end of rod— Fe >> Al, Ni > Si > Cl, Cd (no Cr) 3. 5 x 10 μm poorly defined particle— large Compton background and no metals; probably organic

2- μm Filter (Figures C.3-C.4)

<u>Photograph</u>	<u>Comments</u>
18415	Very heavy deposit; particles (some $\ll 2 \mu\text{m}$) piled over pores
18415	Area scan; X-ray spectrum of area is complex. Some peaks may be misidentified— Cd (Ag, In), Fe > Zr > Al, Si > Cl; Ni appears smaller than in SS, and Cr is absent; U was not detected but could be present in small concentration
18416	Scan of small area; most particles $\ll 1 \mu\text{m}$; largest, $2 \times 4 \mu\text{m}$ — Cd, (Ag, In), Fe > Zr > Al, Si, Cl > Ni
18417	Area scan similar, but possibly U present

1- μm Filter (Figures C.5-C.6)

<u>Photograph</u>	<u>Comments</u>
18418	Large area, moderately heavy deposit; some particles piled over pores, but many pores visible. Area scan— complex spectrum: Mo, Zr, Fe, Cd, Al, Si, Pb, (Bi), Zr
18419	Small area— K, Cd? \gg Al, Mo, Ag, Fe, Zr, Cl, Cr, Ni, Pb; Si peak small, if present at all
18420	Agglomerate of small particles— Fe, Pb, Bi, Mo, Al

0.6- μm Filter (Figure C.7)

<u>Photograph</u>	<u>Comments</u>
18421	Large area, moderately heavy deposit; rounded particles tend to pile over pores; some particles appear spherical or globular. Area scan— Mo, Fe, Pb, Bi, Zr, Al
18422	Fuel or control rod residue in white particles; spheres are fuel residue or Ag-Cd in separate particles

0.4- μ m Filter (Figure C.8)

<u>Photograph</u>	<u>Comments</u>
18424	Moderate deposit; lighter, but similar, to 0.6- μ m filter; both white and gray particles; tendency toward more spheres. Area scan—Al, Cl, Fe, Si, Compton background (from filter media)
18425	Individual particles variable— some U, Ag—Cd, Si—Al

0.1- μ m Filter (Figure C.9)

<u>Photograph</u>	<u>Comments</u>
18426	Small, but significant, deposit of small particles, plus a very few larger, apparently aggregated particles. Area scan— mainly Compton background; very small indication of Cl, Fe; mostly low-Z material, probably organic
18427	3000X— many small (<0.1- to 0.3- μ m) poorly defined particles. Area scan— mainly Compton; trace Cl, Fe

0.4- μ m Filter; reexamination with different SEM (Figures C.10—C.19)

<u>Photograph</u>	<u>Comments</u>
4367	Both white and gray particles; many rounded or spherical
4368	Area scan— Br, Cl, Ag, Si, Fe; all small peaks over large Compton <ol style="list-style-type: none"> 1. Two small white cores in bright particle— nearly pure Zr; trace Al, Si, Fe, Cl, Ag 2. Rounded white core in gray particle— pure U 3. Similar to (2)— nearly pure U; trace Al, Si, Fe 4. Gray sphere— Compton background dominant; trace Al, Si, Cl, Fe, Cu, Br? 5. Light gray in gray— Ag > Zr; trace Al, Si, Fe; maybe Mo, Cl, U
4365	Note white core in some gray particles
4366	20,000X shows agglomerate of 0.2- to 0.4- μ m spheres

4.6 EXAMINATION OF NUCLEPORE FILTERS FROM TEST 2: WATER SAMPLE W1
(TURBIDITY = ~71 NTU)

10- μ m Filter (Figures D.1-D.4)

<u>Photograph</u>	<u>Comments</u>
18428	Widely spaced large particles
18429	1. Diatom particle— nearly pure Si
18430	2. Diatom particle— nearly pure Si
18431	3. 4 x 7 μ m particle with regular shape— Al, Si \gg Fe, Ba, Ce, Cl
18432	4. 10- μ m irregular particle, agglomerate?— Fe \gg Ni > Cd, Cl, Al, Si 5. Small "flake," irregular— Fe \gg Ni, Al, Cl, Cd, Si
18433	6. 10- μ m rounded particle, rough surface— In, Cd?, Ag > Mo > Fe, Al, Cl, Si 7. Diatom— pure Si

5- μ m Filter (Figures D.5-D.8)

<u>Photograph</u>	<u>Comments</u>
18434	Widely spaced particles
18435	1. 9 x 12 μ m fuzzy agglomerate— Fe \gg Cd, Si, Mo, Ni, Al, Cl 2. 5- μ m particle with square corners— Si (diatom fragment?)
18436	3. 4 x 7 μ m particle— Fe > Ni > Si, Al, Cd, Cl, Mo
18437	4. 4 x 8 μ m pointed particle— Al, Si \gg Ba, Fe, Ni, Sn? 5. 5- μ m plus small crystals— Al, Si > Fe > Ba, Mo, Cd, Sn? 6. 6 x 8 μ m particle— Fe \gg Al > Si, Ni, Cd
18438	7. 7- μ m, rounded particle— Fe \gg Al, Cd (In?), Ni, Si, maybe Zr 8. Sharply edged particle— Zr > Ag \gg trace Fe 9. 7- μ m fuzzy particle— trace Fe, Ba, Si, Al, Zr, Cl

2- μm Filter (Figures D.9-D.10)

<u>Photograph</u>	<u>Comments</u>
18446	Heavy deposit; particles piled over pore openings A. Cylinder, 7 μm diam x 50 μm long— Si > Ca > Al B. Identical particle (Si/Ca/Al, ~4/2/1)
18447	1. Bright 3 x 4 μm particle— Fe > Al, Si, Ni > Cd, Ag, In, Zr, Cl, Cr 2. Small particles over pore— Cd, In, Ag, Fe > Zr, Al, Si 3. Similar to (2) plus 2- μm sphere— Fe > Ag, Cd, In, Cl, Al, Si, Zr 4. Large agglomerate— Si, Zr > Fe, In, Cd, Ag > Al > Ni, Cl

"Diluted 2- μm " Filter (Figures D.11-D.15)

<u>Photograph</u>	<u>Comments</u>
18439	Well separated particles
18440	1. 12- μm -long, thin, rough surface— trace Al, Fe, probably organic
18441	2. Large agglomerate— Cl > Al, Si > Fe 3. Bright, smooth, curved surface— Cd >>> Zr, Fe, Al, Cl 4. 2 x 3 μm agglomerate; bright region— Fe, In (Ag, Cd), Al > Mo, Si 5. 3- μm grain; rough surface— U > Zr > trace Al, Fe
18442	6. 8 x 10 μm angular particle— Al >>> Mo > trace Fe 7. 6- μm thin flake— Zr >>> Ag, Cd, Fe, Cr, Ni, Al 8. 1- μm round particle— Fe = Cr > Al
18443	9A. 3 x 4 μm bright, sharp-edged, angular particle— Zr > U >> Fe, Al 9B. 2- μm , rounded, fuzzy particle— Fe >> Al, Si, Ni, U, trace Cl 9C. 1 x 2 μm , grain— U > Zr >> Fe, Al, Cl 9D. 2 x 3 μm gray, rounded, fuzzy particle— Al, Si >> Ba, Fe 9E. 4 μm , sharp grain— U > Zr

1- μm Filter (Figures D.16-D.18)

<u>Photograph</u>	<u>Comments</u>
18444	Good distribution of 1- to 2- μm white and gray particles
18445	<ol style="list-style-type: none"> 1. Bright particle in agglomerate— U >>> Al, Fe, Ni 2. Gray agglomerate— Fe, Al, Si > Cl; large Compton 3. White angular particle— Ag > In > Mo > Fe, Al, Cl 4. White angular particle— U > Zr > trace Al, Cr, Fe, Cl 5. Gray area of agglomerate— Fe > Al, Cl > Cd, Mo, Zr (Compton) 6. Bright area, same agglomerate— U > Zr > Fe, Al, Si, Cl 7. Mixed agglomerate— Fe, Zr, Ag-Cd-In, Al > Si, Cl > trace Ni 8. Bright, rounded particle— In (Ag, Cd) > Zr, Fe > Al > Si, Cl, trace Ni 9. Dull gray particle— Fe > trace Al; mostly Compton

0.8- μm Filter (Figures D.19-D.26)

<u>Photograph</u>	<u>Comments</u>
4387	<p>Widely scattered particles and agglomerates</p> <p>Bright 0.8-μm particle with smaller gray particles— Fe > Al; trace Ni, Cl, Si, S, probably Zr, Cl, In, maybe Cd</p>
4388	White sphere with gray shell around it— Ag > Zr, S
4389	Small white spheroid in small bright particle— pure U
4390	Cluster of bright particles, each <1 μm — Zr >> U

0.6- μm Filter (Figures D.27-D.33)

<u>Photograph</u>	<u>Comments</u>
4391	Scattered white and gray particles and agglomerates 1. White sphere, 0.7 μm — pure Ag 2. Bright 0.5- μm sphere, gray shell— Zr >> Cr, trace Fe, U, Al, Si 3. Gray round particle— Fe, Br >>> Ag, Ni, Cu, Cl, Si, Zr 4. Light spot in transparent shell— large Compton background; Fe, Br, Ag, (Cd) > trace Si, Zr, Sn
4392	Area scan— U > Zr, trace Fe, Al, Si

0.4- μm Filter (Figures D.34-D.39)

<u>Photograph</u>	<u>Comments</u>
4393	Scattered bright and gray particles and agglomerates Area scan— U >> Fe > Zr, Al, Si
4395	White angular particle— Zr >> Ag, (Cd), Fe, Si, Al
4394	"Normal" secondary electron image (SEI); shows topography with some dependence of brightness on Z
4396	Backscatter electron image (BEI) of same area; high-Z elements are bright, while low-Z elements are dark

0.1- μm Filter (Figures D.40-D.45)

<u>Photograph</u>	<u>Comments</u>
4397	BEI
4398	SEI; heavy scatter of agglomerates and small particles down to submicron size; many particles rounded 1. Small, white particle— U, trace Fe, Al, Si, Zr, S, Cl 2. Three different particles, rounded, small; light on SEI but nearly invisible in BEI— Fe >> Al, Si, Cl, Cu, Compton background; Fe, Ag, S, Al, Si, Compton background; Fe >> Zr, Cu, Ca, Cl, S, Si, Al, Compton background 3. Gray; faint in BEI— Fe >> Zr, Cu > trace Al, Si, S, Cl, Ca, Zn

4.7 EXAMINATION OF NUCLEPORE FILTERS FROM TEST 3: WATER SAMPLE W2
(TURBIDITY = ~25 NTU)

10- μ m Filter (Figures E.1-E.5)

<u>Photograph</u>	<u>Comments</u>
18448	Very few particles
18449	1. 8 x 30 μ m long particle— Compton background; low-Z elements; some Cl
18450	2. 7 x 14 μ m agglomerate— Fe, Ag, Cd, In > Zr > Mo, Cl, Al > Si, maybe U 3. Bright, 5 x 10 μ m particle— Si > Cl > Fe
18451	Very few particles; some <10 μ m
18452	1. 11 x 22 μ m agglomerate— Zr >> U, Cd, Ag, In, trace Cl, Fe
18453	2. Gray, layered structure— Compton background; trace Cl
18454	3. 3- μ m, white, rounded particle— Compton background > trace Si, Cl 4. 2.4 x 4 μ m pointed particle— Compton background > trace Cl, Si 5. 2- to 3- μ m gray agglomerate; small particles— Cl; Compton background
18455	6. 3 x 8 μ m particle with small spheres on surface— Compton background; Cl > Si
18456	7. 6 x 8 μ m rounded particles, similar to (6)— Compton background; Si, Cl

5- μ m Filter (Figures E.6-E.9)

<u>Photograph</u>	<u>Comments</u>
18457	Very few widely scattered particles
18458	1. 15 x 20 μ m, nebulous— Compton background; trace Cl
18459	2. 8 x 24 μ m particle, similar to (1)— Compton background; trace Cl

- 18460 3. Aggregate; ~5 x 8 μm particle— Fe >> Cl > Al, Si, Zr, S, Ca
 4. 5- μm fuel grain shape— U, trace Zr, Cl
- 18461 5. 4 x 6 μm agglomerate— Fe > Al, Cl, U > Si, Zr, Ni > Ca
- 18462 6. Thin, bent shell or flake— Si
 7. 1.5- μm small aggregate— Compton background; Cl, maybe Al, Si
- 18463 8. 8- μm , rounded, maybe layered particle— Compton background; Cl
- 18464 9. 3 x 8 μm elongated particle— Compton background; Cl > Si

2- μm Filter (Figures E.10-E.13)

<u>Photograph</u>	<u>Comments</u>
18465	Scattered particles 1. Large particle— pure Si 2. Small, round particle— Zr >> Ag > U > trace Fe, Cl 3. Fe, Cr > Mn > U, Cd, In, Zr > Cl, Al, Ca 4. Fe (no Cr) > Cd, In, Ag > Al, Cl, Mo > trace Si, Ni 5. Pure U 6. Fe >> trace Si, Al, Cd, Cl 7. Fe >> trace Ni, Cl, Al, Si
18466	8. 1 x 2 μm , bright, jagged particle— Zr > Si, Ag, Cd, In, Cl, U? 9. Diatom fragment— Si
18467	10. 2 x 4 μm smooth particle— Zr > trace U, Ag, Fe
18468	11. 2 x 4 μm irregular (melted?) particle— Ag, Cd, In >> Mo > Zr, Fe

1- μm Filter (Figures E.14-E.25)

<u>Photograph</u>	<u>Comments</u>
4400	Normal SEI showing topography
4399	BEI of same area showing high-Z elements as white A. Large white, rounded particle— Cd >> U >> trace Zr B. Small white particle, $\sim 1 \mu\text{m}$ — U >> trace Zr C. Less-white, 2- μm aggregate of fines— In > trace Fe > maybe Si, Al D. Near-white, pointed, 1 x 2 μm particle— U >> trace Zr E. White, rounded, near 2- μm particle— U >> maybe trace Zr
4401	BEI (F, G, and H are invisible)
4402	SEI of same area (F, G, and H are gray) F. About 1- μm particle, pointed at one end— Zr >> trace Ag, In, Al?, Si?, Fe? G. <1- μm , elongated particle— Fe >> Al, Ni, maybe Si H. About 1- μm , gray flake— Compton background; slight trace Si, S

0.8- μm Filter (Figures E.26-E.39)

<u>Photograph</u>	<u>Comments</u>
4412	SEI (2000X)
4411	BEI of same area (2000X) A. Bright particle, <1 μm — Zr, U >> maybe trace Fe, Si, Al B. Round, bright particle, $\sim 1 \mu\text{m}$ — U >> trace Fe, Cr, Al, Zr C. Round, bright particle, <1 μm — U >> trace Fe, Cr, Al, Zr D. Bright particle, <1 μm — U > Zr >> trace Al, Si, Fe E. Smaller, round bright particle— U > Zr > trace Al, Si, Fe?

F. Small light-gray particle— Fe >> trace Ni, Al, Si, S, Cl, Ca?

Area scan— Compton background, maybe trace Fe, Al, Zr, U

4414 BEI (6000X)

4413 SEI of same area (6000X)

G. Rough, large particle, dim in BEI— Compton background, maybe Al, Si, Cl

H. <1- μ m gray particle dim in BEI— Compton background, some Al, Si, Zr, Ti, Fe, Cu

I. 0.8- μ m aggregate, moderately bright in BEI— Fe > trace Al, Si, Ni > maybe S, Cl

0.6- μ m Filter (Figures E.40-E.56)

<u>Photograph</u>	<u>Comments</u>
4416	SEI (2000X)
4415	BEI of same area (2000X) Area scan— Compton background, trace Al, Cl, Fe, Br, Si
4417	SEI (6000X)
4418	BEI of same area (6000X)
	A. Bright, angular particle, 0.5 x 1 μ m— U > trace Zr, Fe, Al, Si
	B. Bright, rounded, 0.5- μ m particle— U > Zr > trace Fe, Si, Cr
	C. Gray (SEI/BEI), pointed, 0.5- μ m particle— In, Ag > trace Al, S > Si, Fe
	D. White, 0.5 x 0.8- μ m particle with corners— U
	E. White BEI, gray SEI, end of crystal clump— U, Zr
	F. White BEI, gray SEI, <0.5- μ m particles— U > trace Al, Fe > Si?, Zr?
	G. Gray cluster of ~0.7- μ m particles— Zr > Ag > trace Fe, Al, Si, Br

- H. White, pointed, angular particle, 0.4 x 1 μm — U > Zr > trace Al, Si
- I. Gray, rounded, <0.5- μm particle— Fe > Al > trace Si, Br
- J. Similar to (I)— Fe > Al > trace Si, Br, Zr
- 4417 L. Large, gray structureless area— Compton background; trace Al, Br, Fe
- M. Dark gray cluster, faint on BEI— Si > trace Fe, Al, Zr, Br

0.4- μm Filter (Figures E.57-E.71)

<u>Photograph</u>	<u>Comments</u>
4590	BEI image shows a thin scatter of white particles (2000X)
4588	SEI image of same area, with a good assortment of particles
4589	BEI image shows a few white particles (6000X)
4587	SEI image of same area, with many particles and agglomerates Area scan— mostly Compton background; trace Cl, S, K > Cu, Fe, Si, Al, Zn, Na
	1. White, rounded 0.5- μm particle— U >>> trace Fe, Al, Si?
	2. 1- μm , gray agglomerate— Fe >> K, Al, S, Cl, Si > Ni, Cu, Zr
	3. Gray agglomerate— Fe >> K, Al, S, Cl, Si > In, Cu, Ni, Na
	4. Small white particle— U >>> possibly trace Al, Si, Zr, S, Cu
	5. Large gray agglomerate— mostly Compton background; trace S, K, Cl, Cu, Al
	6. 1- μm gray platelet— Compton background; Fe >> trace K, Al, S, Si, Cl, Cu
	7. 0.5- μm white particle— U >> Zr >> possibly Al, Si, Fe
	8. 1- μm agglomerate— mostly Compton background; trace Fe, K, S, Cl
	9. Small white particle— U >> Zr >> trace Fe, Al
	10. Gray agglomerate— Compton background; trace Cl, S, K, Si, Fe

0.1- μm Filter (Figures E.72-E.84)

<u>Photograph</u>	<u>Comments</u>
4591	SEI image; good assortment of small particles and agglomerates
4593	BEI image of same area, with very few bright particles (6000X)
4591	Area scan— Compton background; Cl, S > Si, U or K, Cu > Ag, Fe, Al <ol style="list-style-type: none"> 1. Tiny white particle in gray agglomerate— Compton background; trace S, Si, Cl, Fe, Cu 2. Rounded white particle— U, Zr >> trace Fe, Cu, Si, Al 3. Bright area in gray particle— U >>> trace Al, Si, Cl, Cu, Fe
4592	Blowup of No. 3 (20,000X); 0.15- μm white core in 0.4- μm gray blob; note other spheres and agglomerates <ol style="list-style-type: none"> 4. Bright spots in gray agglomerate— Compton, Fe, Ag, Si, S > Al, Cu 5. Gray agglomerate— Cl > Fe > Cu, K, S, Si, Al 6. Gray agglomerate— Compton background; Cl > Fe, Co, Ag, Si, Al > trace K 7. Small white area in gray blob— U > Cl >> Zr > trace Cu, Fe, Si 8. Gray agglomerate— Compton background; small Ag, Cl, Fe, Si, S, Cu, Zn, Al 9. Gray sphere— Compton background; trace S, Si, Cu, Cl

4.8 EXAMINATION OF NUCLEPore FILTERS FROM TEST 4: WATER SAMPLE W3
(TURBIDITY = ~4 NTU)10- μm Filter (Figures F.1-F.4)

<u>Photograph</u>	<u>Comments</u>
18469	Few large particles <ol style="list-style-type: none"> 1. Large flake, 40 x 20 μm— no structure; Fe (no Cr, Ni)
18470	<ol style="list-style-type: none"> 2. Similar to (1)— same composition + trace Si, Mo, Cl

- 18471 3. Gray particle, ~20 μm , with small white globules on surface— Si, Ca > Cl > Al, Mg, Mo, K, Fe, Ti
- 18572 4. 10- μm agglomerate— Mo, Si, Cl > K, Ca, Al, Mg > Fe; Compton
5. Small (6 to 8 μm), rounded particle— Ca >> Mg > trace Si, Cl, Fe
6. Odd-shaped particle, 20 to 30 μm — Compton background, trace Cl, Mo, Fe, Ni, Ca
7. 5 x 10 μm pointed particle— Ca > Si >> Cl, Al, Mg, S, K, Fe
8. ~10- μm particle plus small fragments— Fe >> Ni, Mo, Cl, K
- 18473 9. Lump on filter; tiny surface particles— Ti (maybe La), Mo, Cl > Al > Si, Fe, Ni, K, Ca

5- μm Filter (Figures F.5-F.8)

<u>Photograph</u>	<u>Comments</u>
18474	Very few particles
	1. 8- μm cotton ball— Si > Al > Ca, Fe > trace Cl, K, Mo
18475	2. 3- μm agglomerate— Cl > Si, maybe Mg
	3. 3- μm fluff— Compton background; trace Si, Cl, Fe
	4. Agglomerate of small gray particles— Ni > Cl > Mo > trace Al, K
18476	5. Agglomerate of small particles— Ni, Cl >> trace Si, S, Al
	6. Large agglomerate of small particles— Cl, Ni > S, Ca > Si, Al
18477	7. 12 x 15 μm ; no structure— Compton background; trace Cl
	8. 6- μm agglomerate of small particles— U (maybe Cd), Zr > Al, Cl, Fe
18478	9. 3 x 10 μm particle; no structure— Compton background; trace Cl

2- μ m Filter (Figures F.9-F.12)

<u>Photograph</u>	<u>Comments</u>
18479	Scattered small particles
18480	1. 15 x 20 μ m agglomerate— Si > Cl 2. 2 x 5 μ m crystal— Zr, Fe > Cr, Cd, Cl > Ni
18481	3. 2- μ m agglomerate— Fe > Cr > Ni > trace Si, Cl 4. <1- μ m rounded particle— Fe >> Cr > trace Si, Al (no Cr, Ni) 5. 3 x 4 μ m particle with little structure— Fe > Si, Cl 6. Bright agglomerate— Fe, Al > Ni, Cl > trace Si
18482	7. Agglomerate of small round particles— Fe > Si, Cl > S, Ni, Al 8. Small gray agglomerate, rounded— Fe > K, Cl, Al > trace Si, Ni 9. 3- μ m agglomerate— Fe > K, Cl > Si, S, Al 10. Large agglomerate— Fe > K, Cl > Si, S 11. <1- μ m particles— K > Cl > Fe 12. 2- μ m, rounded particle— Si >> K, Cl

1- μ m Filter (Figures F.13-F.16)

<u>Photograph</u>	<u>Comments</u>
18483	Scattered small particles
18484	1. 2 x 4 μ m agglomerate— Fe, Cl, Compton background 2. 1 x 3 μ m agglomerate— Compton background; Cd, trace Cl 3. Similar to (2)— Compton background; trace Fe, Cl 4. Smaller agglomerate— Fe > Cl, Al, Compton background 5. Agglomerate— Fe, trace Cl, Compton background 6. Agglomerate— trace Fe, Cl

- 18485 7. Agglomerate— Si, Al, Cl, Compton background
 8. 2- μ m rounded agglomerate— U > Ag > Fe > trace Cl, Al
 9. Agglomerate— Cl, Fe, Compton background
 10. 0.5 x 1 μ m, rounded— Zr > Ag, Cl, Fe

0.8- μ m Filter (Figures F.17-F.26)

<u>Photograph</u>	<u>Comments</u>
4606	Few particles, both white and gray
4616	Three particles close together 1. Angular, bright particle, 0.6 x 0.8 μ m— Zr >> U > trace Fe 2. Irregular, bright particle, 0.4 x 0.8 μ m— Fe >> Cu, Al, Si, Ni Larger, light-gray agglomerate between (1) and (2)— same as (2)
4617	0.1- μ m white sphere inside gray shell— Ag, U, S > Cl, Cu
4618	0.4 x 0.8 μ m globular white particle— Zr >> U
4619	0.7- μ m gray sphere plus smaller white spheres— Fe >> Cu, Ni > trace Al, Si, Cl

0.6- μ m Filter (Figures F.27-F.30)

<u>Photograph</u>	<u>Comments</u>
4558	Very few white particles and gray particles (2000X)
4559	Few particles of any kind (6000X) Particle near center— Zr > Al > Fe > U, Ni, Si
4560	0.6- μ m particle with white core (lower right on 4559)— similar to 4559
4615	0.4- μ m white sphere— U > Al, Zr, Fe

0.4- μm Filter (Figures F.31-F.44)

<u>Photograph</u>	<u>Comments</u>
4531	Few particles, white or gray; many spherical or rounded 0.6- μm white sphere— Ag > Al, Mo, Cu, Ni > Fe, Cl
4557	Very few white particles; more gray (2000X)
4555	Scattered white and gray particles (6000X) 1. Rounded, white particle, 0.6 μm — Ag >> S > Al > Cu 2. Rounded, white particle, 0.8 μm — U >> Al, P > Si, Cu, Bi 3. Gray particle, 0.8 μm — Al, Si >> Cu, Ba, Fe 4. Dark-gray sphere, 0.4 μm — mainly Compton background; trace Al, Cu
4556	Three small particles (20,000X) 1. Rounded white particle, 0.5 μm — Zr >> U > trace Al, Si, Cu 2. Gray particle, 0.5 x 1 μm — mainly Compton background; S > Al > Cu 3. Gray crystal, 0.6 μm — Fe >> Al >> Cu, Si (no Cr, Ni)

0.1- μm Filter (Figures F.45-F.49)

<u>Photograph</u>	<u>Comments</u>
4529	Several small (0.1- to 0.2- μm) spheres and other gray, low-Z particles; 10% heavier than Si Rounded 0.5- μm particle (or flake)— Compton background; faint trace Al, Cu (organic)
4530	Very few small white particles (0.1 to 0.2 μm); more gray particles 1. White globular particle, 0.2 to 0.3 μm — U > Cu > Zn, Si 2. White sphere, 0.1 to 0.2 μm — U >> Cu > Al Most material appears to be organic; small amount of fuel or control rod material; little, if any, light elements

5. ACKNOWLEDGMENTS

The author wishes to acknowledge the extensive analytical work performed to characterize these samples. Major contributions were made by many members of the ORNL Analytical Chemistry Division, particularly D. S. Zingg, M. B. Wise, C. S. MacDougall, and the group of D. A. Costanzo. In addition, much of the SEM work was done by R. S. Crouse's group in the Metals and Ceramics Division. All of the work was coordinated by J. H. Stewart, Jr., of the Analytical Chemistry Division.

6. APPENDIXES

Appendix A. CHARACTERIZATION DATA FOR STAINLESS STEEL DWCS FILTER MEDIA

<u>Figure</u>	<u>Page</u>
A.1 Optical-microscope photograph of sample F2. Note the thin film on the upstream (lower-left) surface.	55
A.2 Optical-microscope photograph of sample F3. Note absence of film.	55
A.3 Optical-microscope photograph of sample F2. Note film on the surface.	56
A.4 Optical-microscope photograph of sample F3. Note absence of film.	56
A.5 Scanning-electron-microscope photograph of sample F2. Upstream surface, lower right.	57
A.6 Scanning-electron-microscope photograph of sample F2. Upstream surface	57
A.7 EDX of particle on downstream surface of Fig. A.5.	58
A.8 EDX of film on upstream surface of Fig. A.6.	58
A.9 Scanning-electron-microscope photograph of sample F4. Filter and epoxy mounting separated at film on upstream surface.	59
A.10 Scanning-electron-microscope photograph of sample F4. Same region as shown in Fig. A.9	59

Y-207034

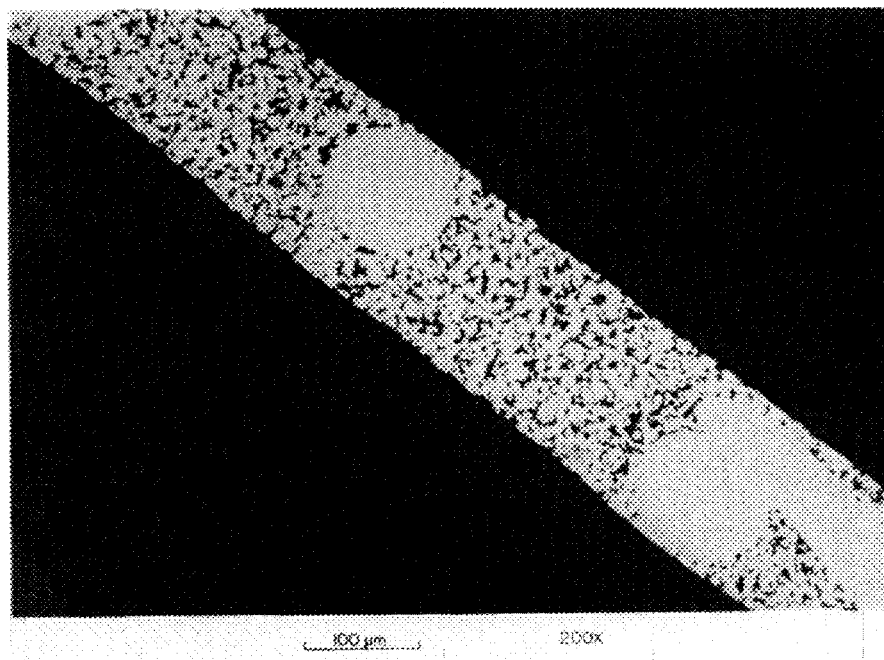


Fig. A.1. Optical-microscope photograph of sample F2. Note the thin film on the upstream (lower-left) surface.

Y-207038

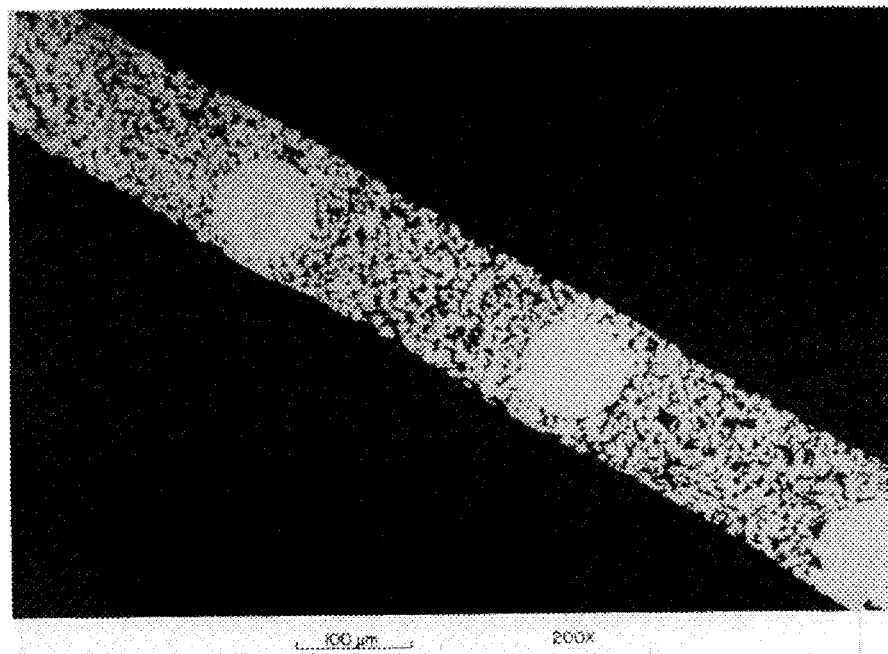


Fig. A.2. Optical-microscope photograph of sample F3. Note absence of film.

Y-207035

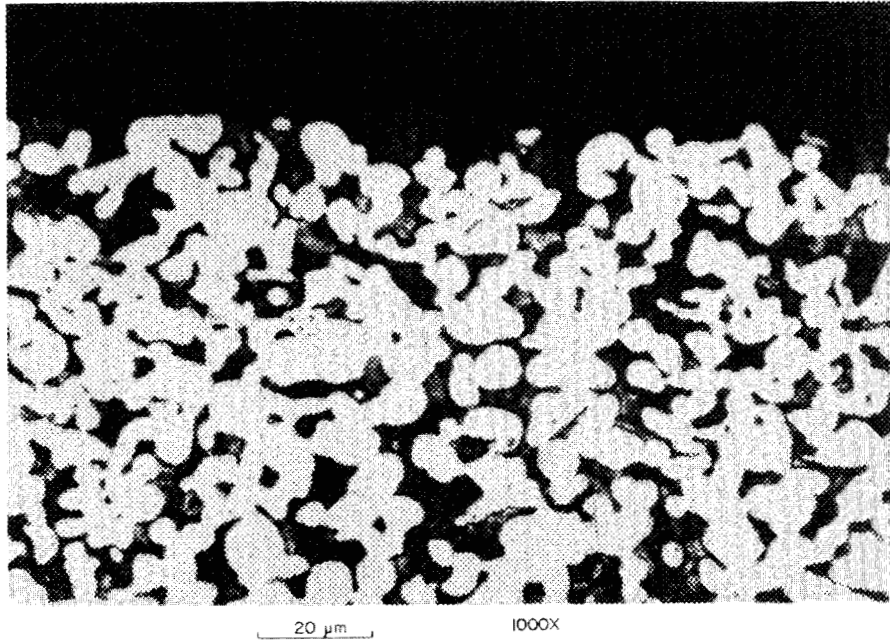


Fig. A.3. Optical-microscope photograph of sample F2. Note film on the surface.

Y-207039

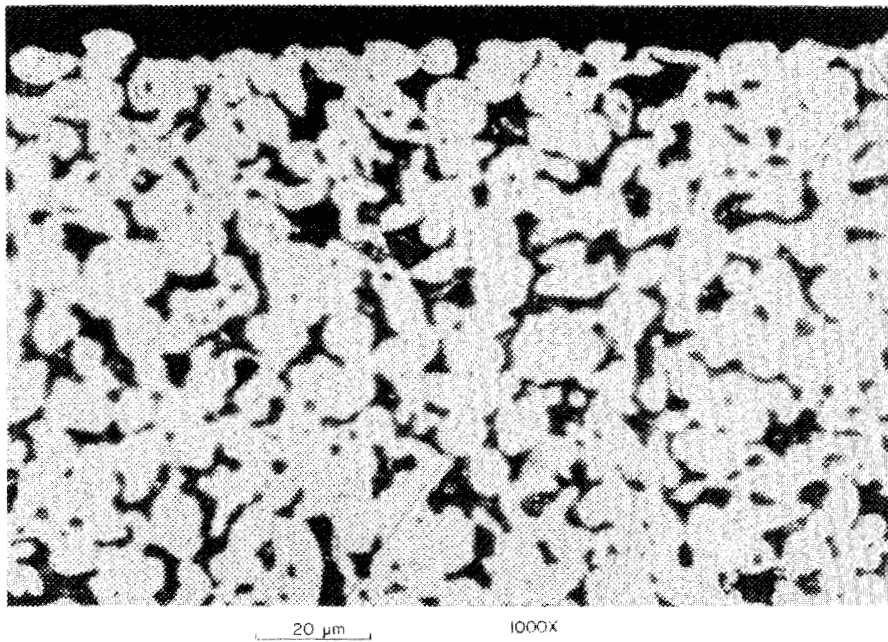


Fig. A.4. Optical-microscope photograph of sample F3. Note absence of film.

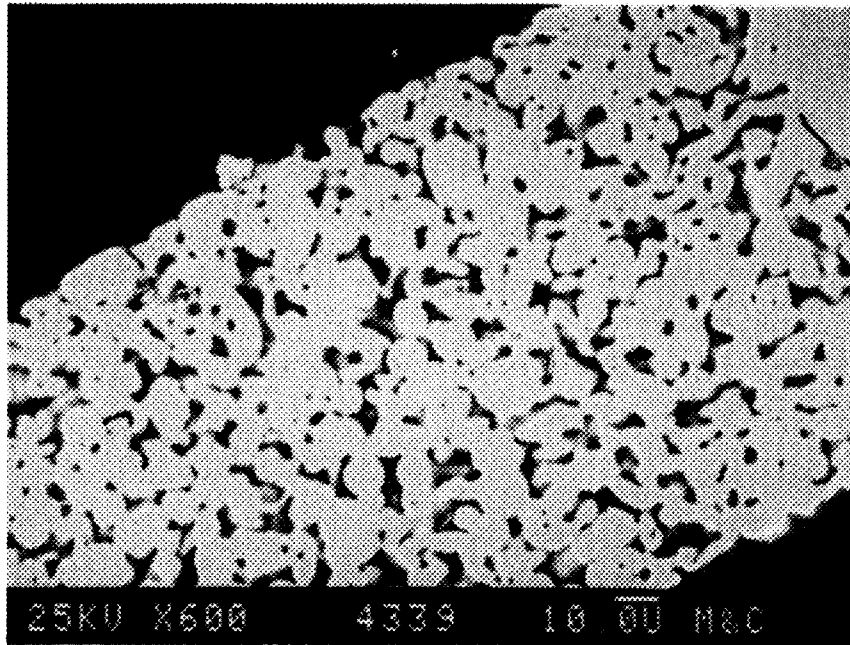


Fig. A.5. Scanning-electron-microscope photograph of sample F2. Upstream surface, lower right.

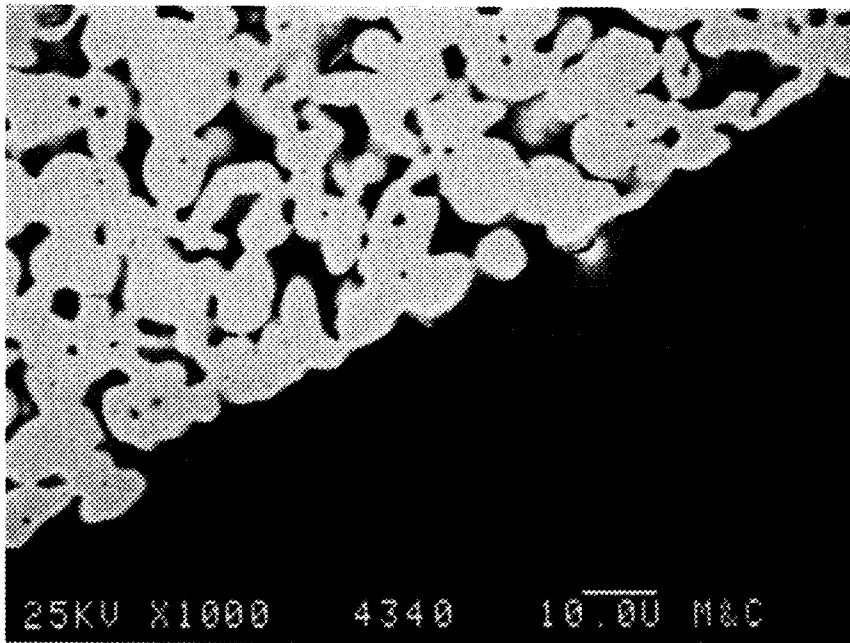


Fig. A.6. Scanning-electron-microscope photograph of sample F2. Upstream surface.

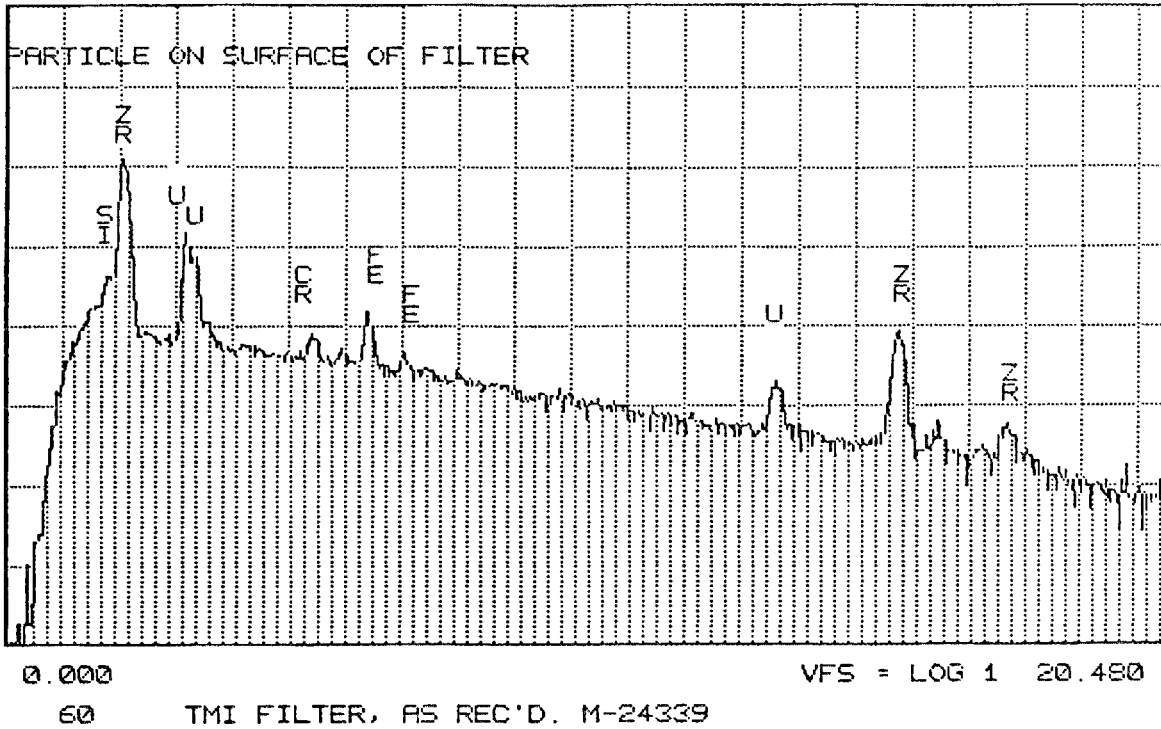


Fig. A.7. EDX of particle on downstream surface of Fig. A.5.

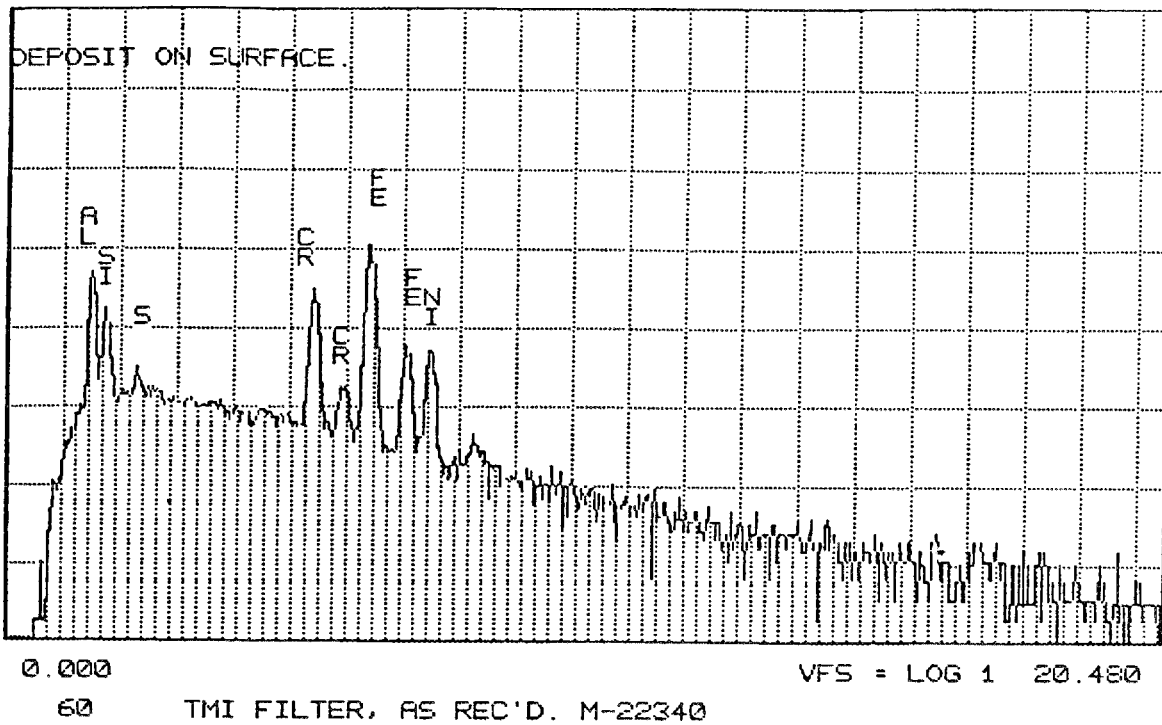


Fig. A.8. EDX of film on upstream surface of Fig. A.6.

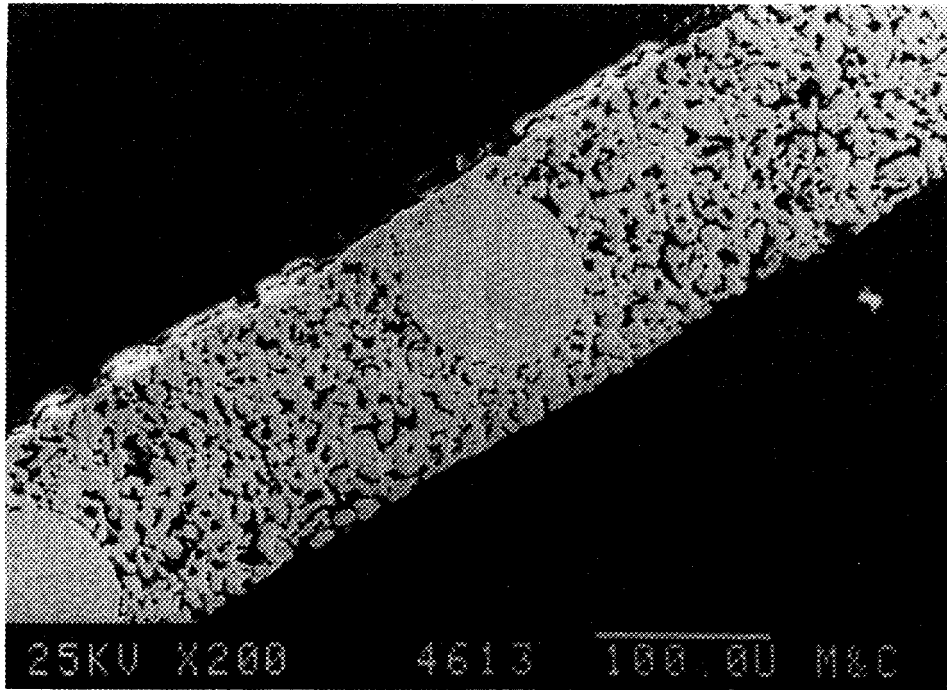


Fig. A.9. Scanning-electron-microscope photograph of sample F4. Filter and epoxy mounting separated at film on upstream surface.

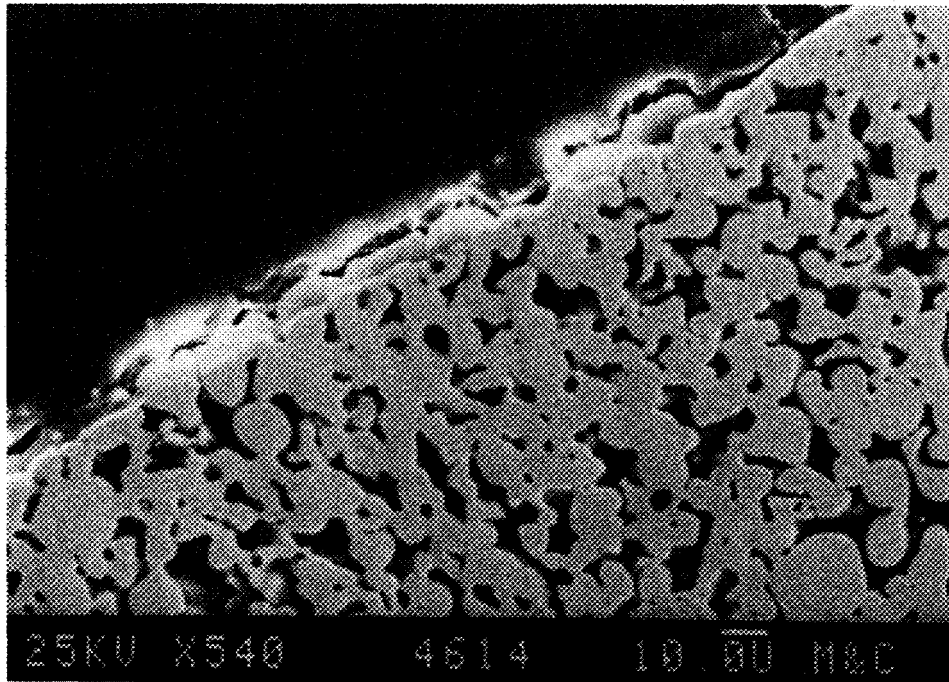


Fig. A.10. Scanning-electron-microscope photograph of sample F4. Same region as shown in Fig. A.9.

Appendix B. ANALYTICAL STUDIES OF FILMS ON DWCS FILTERS

<u>Reference</u>	<u>Memorandum to D. O. Campbell</u>	<u>Page</u>
B.1	R. L. Hettich and M. B. Wise, "Qualitative Analysis of Organic Film on Three Mile Island Filter Sample," Dec. 12, 1986.	63
B.2	D. S. Zingg, "Surface Analysis of Stainless Steel Filter Segments," Jan. 20, 1987.	75
B.3	J. E. Caton, Request No. 91035, Jan. 9, 1987	83

To: David O. Campbell

Date: December 12, 1986

Subject: Qualitative analysis of organic film on
Three Mile Island filter sample.

Summary of Experiments

Two samples of filter materials were examined by laser desorption Fourier transform mass spectrometry (FTMS) and diffuse reflectance infrared absorption spectrometry. In addition, several standard compounds were examined under similar mass spectral conditions for comparison. These standards included sucrose, ketones, and borated hydraulic fluid, each coated onto a clean stainless steel surface. In addition, double-sided tape was examined as a possible source of contamination.

Summary of Findings

Both sides of the filter samples were analyzed. In each case, only one side yielded spectra indicative of a coating on the surface.

Positive ion laser desorption mass spectrometry indicated peaks characteristic of stainless steel (iron, chromium, cobalt and potassium). No other ions were reproducibly generated that could be identified as originating from an organic surface coating.

Negative ion spectra were the more informative with the most intense peaks tentatively identified as organo-silicon compounds. Other ions observed have been tentatively identified as polysaccharide products and possibly borated oil.

Diffuse reflectance infrared spectra revealed very weak but characteristic bands at approximately 2950 cm^{-1} and 1050 cm^{-1} which may correspond to hydrocarbon and silicon-oxygen functionalities, respectively.

Experimental Details

Positive ion mass spectra consisted primarily of the metal ions (K^+ , Cr^+ , and Fe^+) which were generated from the stainless steel screen.

Negative ion mass spectra were calibrated using fluoride ion and the two isotopes of chloride ion. The major peak observed in the negative ion mass spectra was at nominal mass m/z 43. Exact mass determination of this ion consistently indicated two possible formulas; SiCH_3^- or BO_2^- , with SiCH_3^- as the closest match. An ion observed at m/z 42 has approximately the correct isotopic intensity to be 10BO_2^- , but the exact mass measurement of this ion suggests that the either 10BO_2^- or SiCH_2^- could be the correct formula. Both m/z 42 and 43 are also observed in the mass spectra of the borated oil sample and correspond to BO_2^- according to exact mass measurements. Peaks observed at m/z 79, 84 and 100 amu appear to be organosilicon ions, however, the lack of calibrant ions in this mass range may result in some

degree of inaccuracy in these assignments. Peaks that were observed in the mass range of 100-400 amu showed a close correlation to the peaks that were observed in the negative mass spectra of sucrose. These laser ionization experiments also suggest that the coating on the filter samples is not homogeneous as indicated by variations in spectra that were obtained at different locations on the surface.

It is important to realize that the apparent relative abundance of observed ions does not necessarily correspond to the relative amounts of these compounds present in the film. For example, compounds with high electron affinities such as silicon oxides may be enhanced in the negative ion spectra relative to organic ions.

Diffuse reflectance infrared absorption measurements of the coated side of the filter showed very weak but detectable peaks which may be due to the presence of organosilicon compounds. The peaks observed in this spectrum are reasonably similar to those observed in the infrared spectrum of silicone lubricant (see attached figures). The infrared spectrum of the uncoated side of the filter was essentially featureless. These spectra were obtained using a clean piece of stainless steel as a reference sample and 1,000 spectra were signal averaged in order to enhance the signal-to-noise.

Robert L. Hettich

Robert L. Hettich

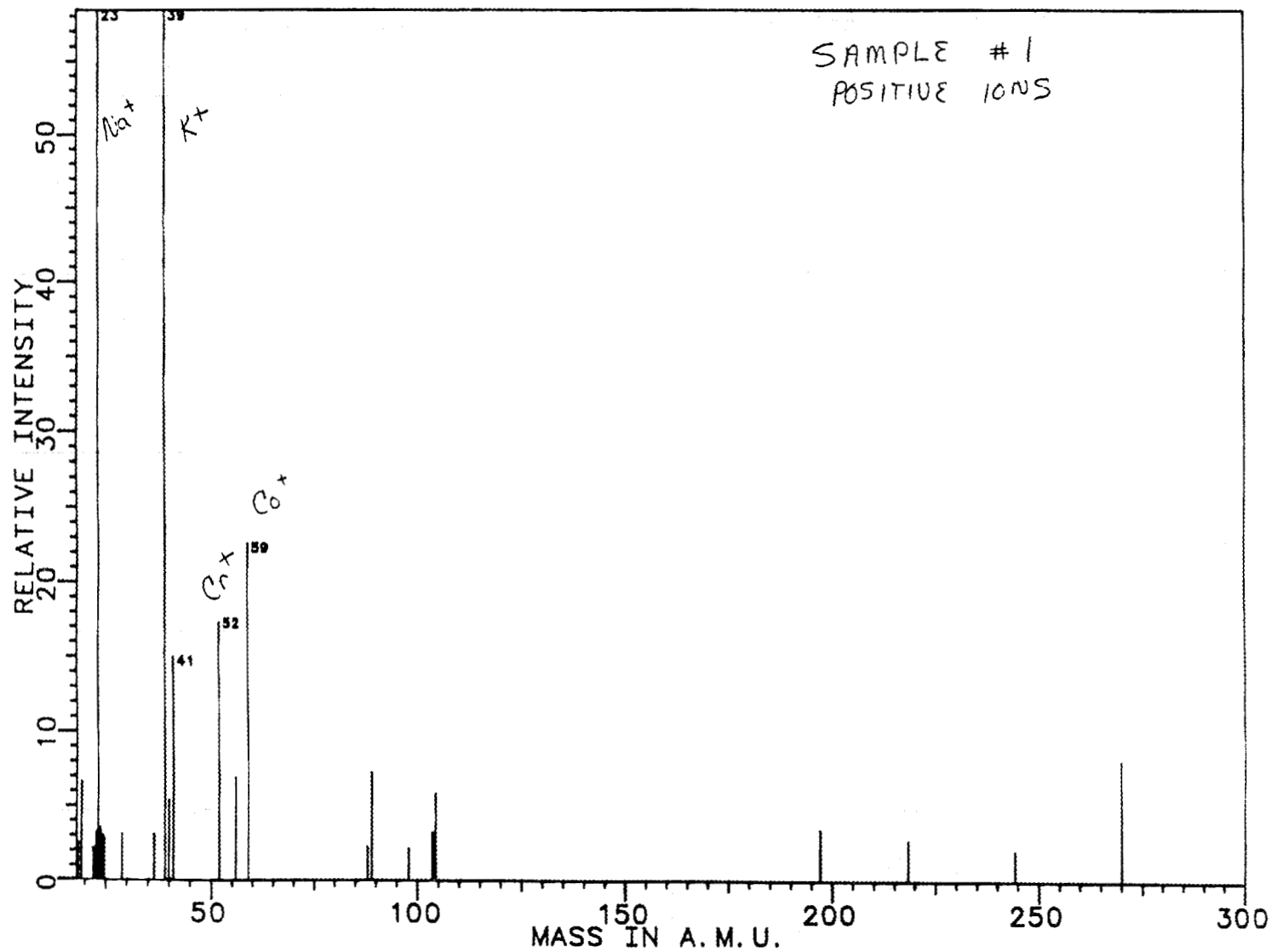
Marcus B. Wise

Marcus B. Wise

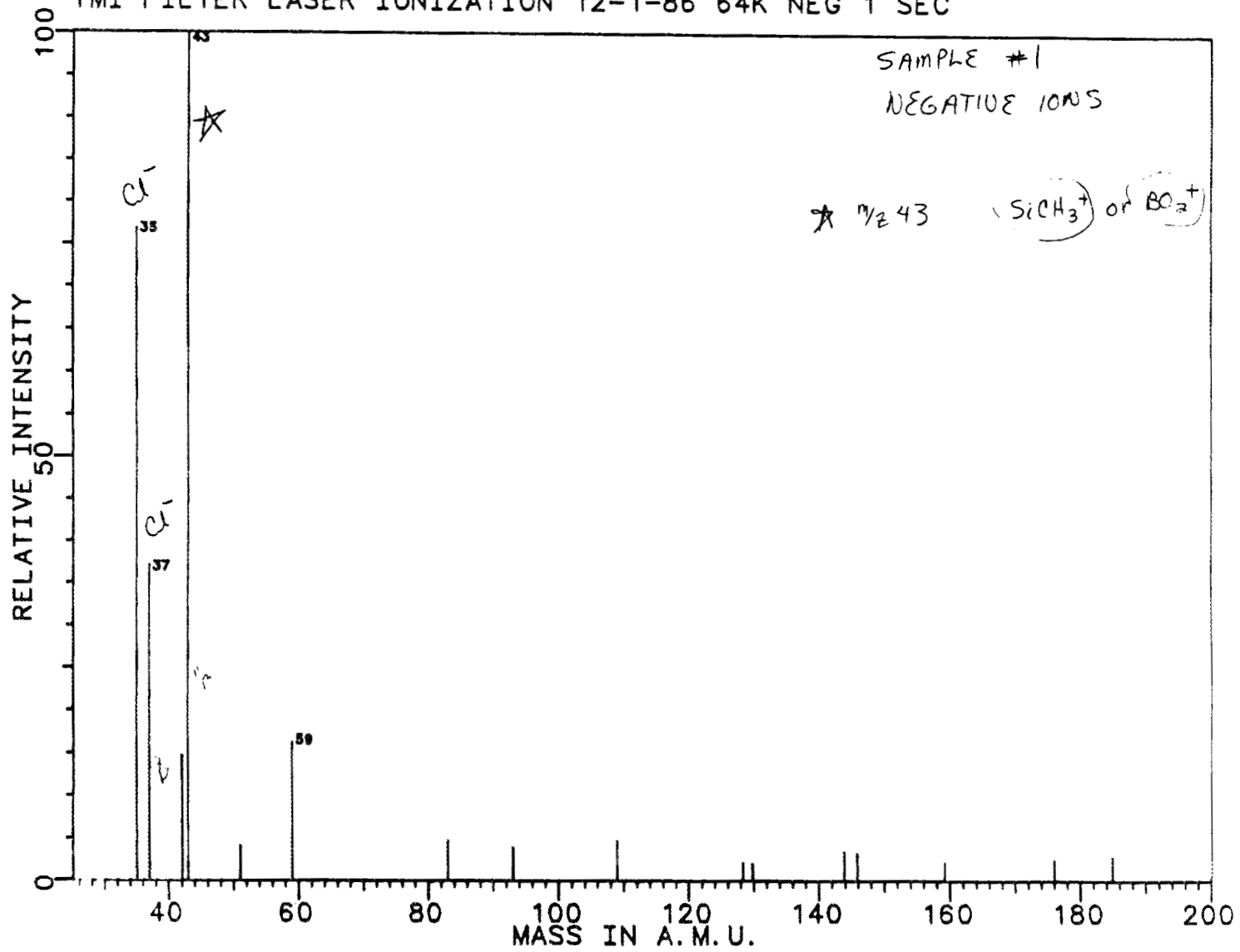
Certified by Michelle V. Buchanan

M. V. Buchanan
Organic Analysis Group
Analytical Chemistry Division

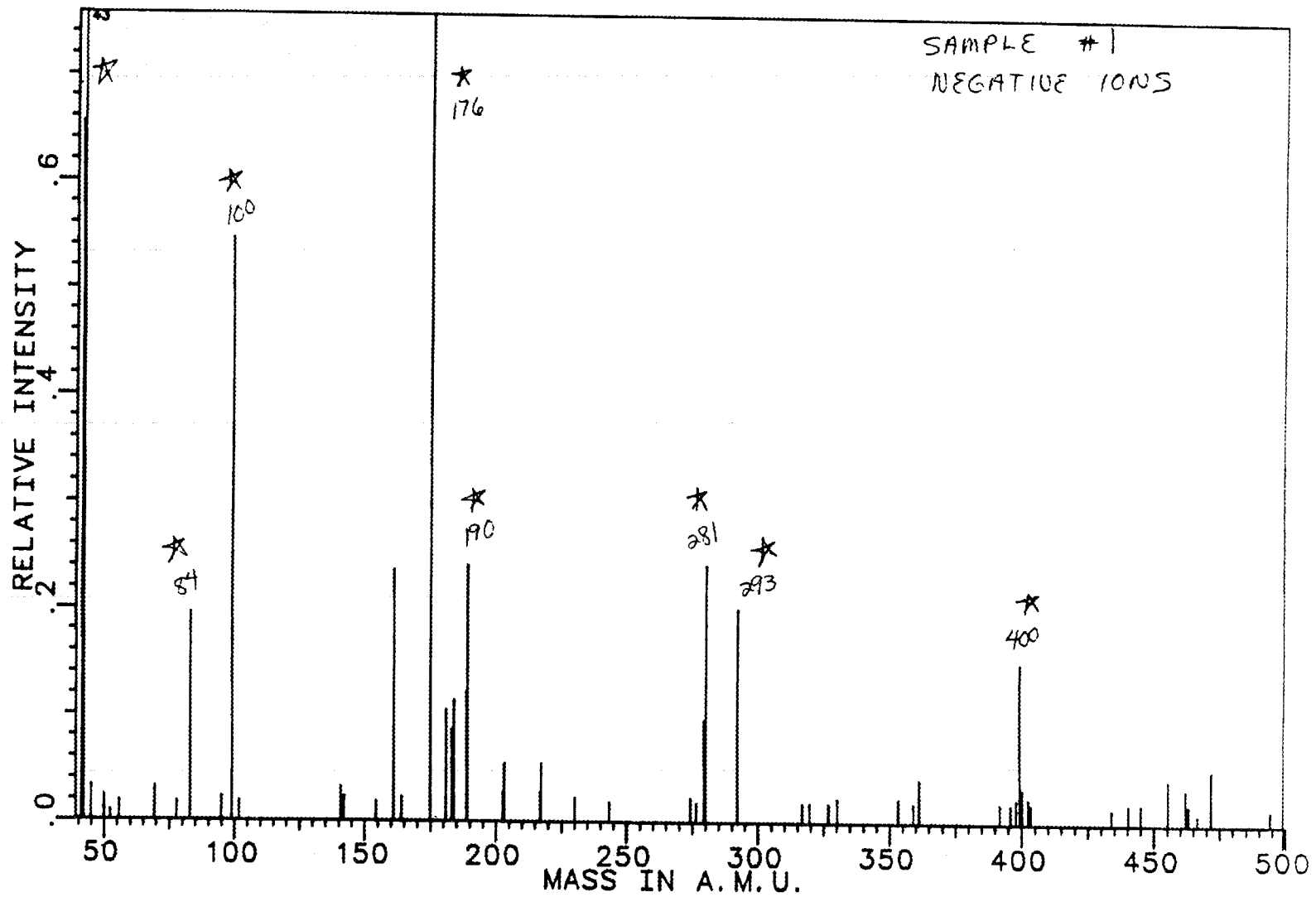
TMI FILTER LASER IONIZATION 12-1-86 64K POS 0.5 SEC



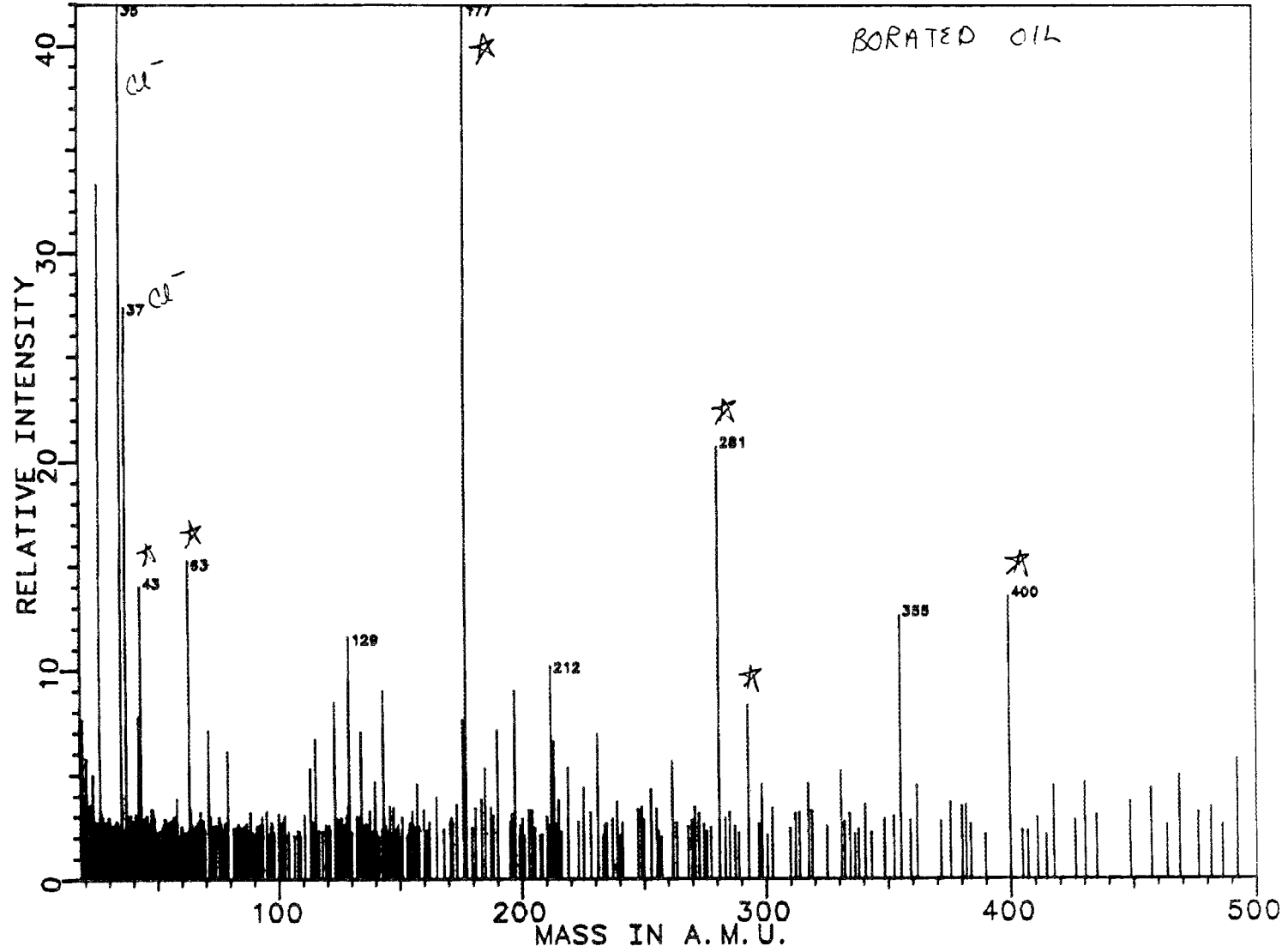
TMI FILTER LASER IONIZATION 12-1-86 64K NEG 1 SEC



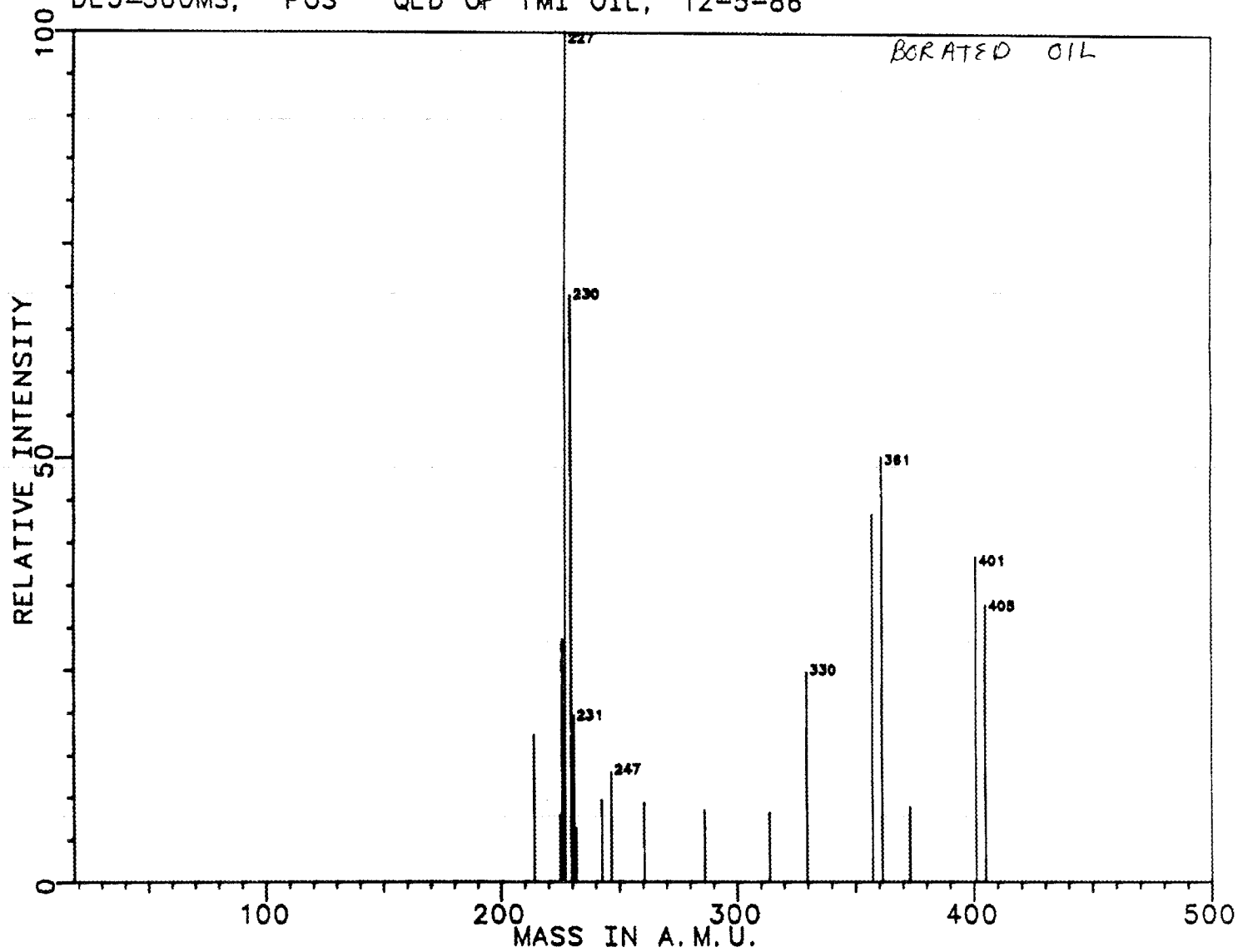
TMI FILTER QS LASER IONIZATION 12-1-86 NEG 1 SEC



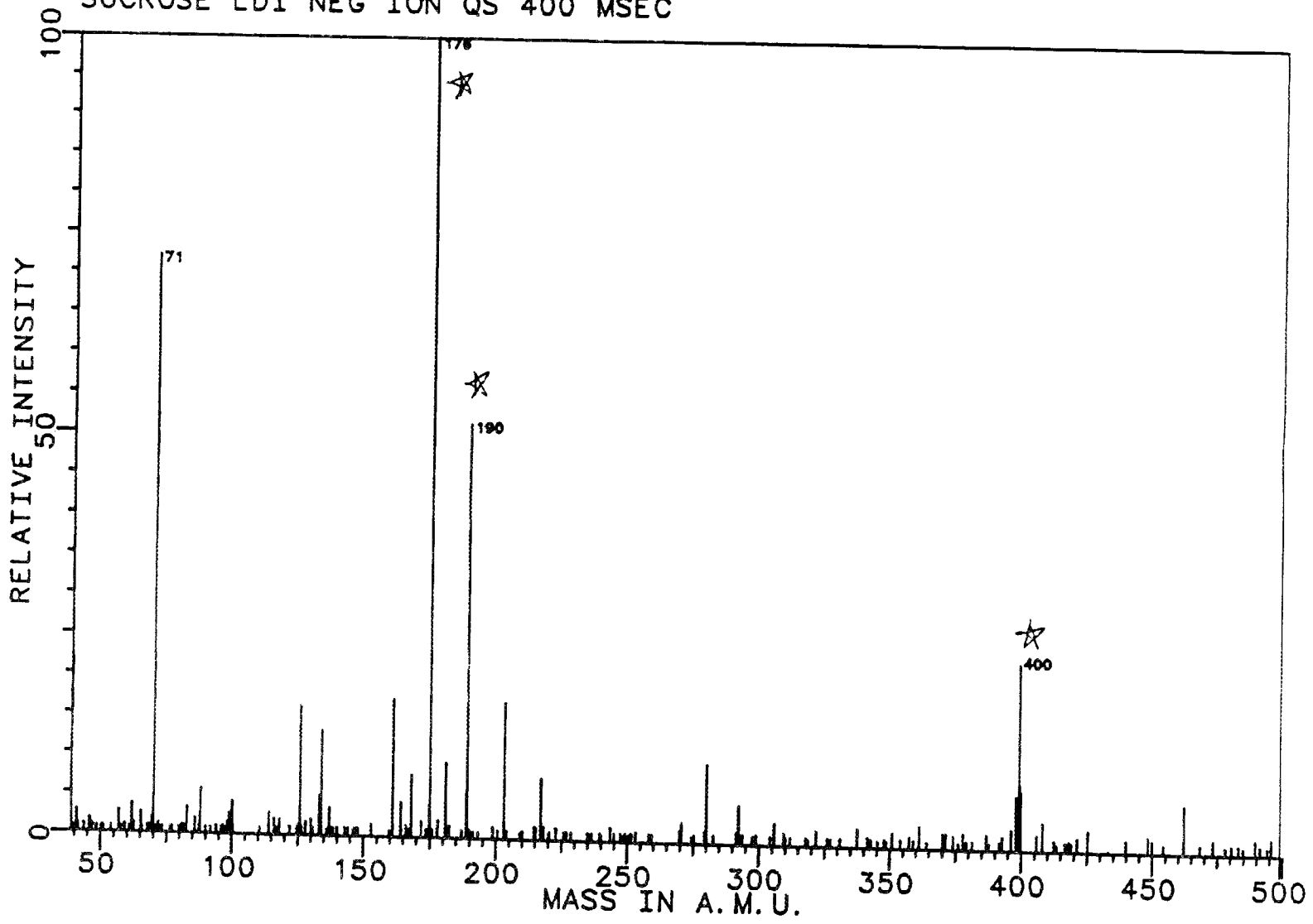
DL3=300MS, NEG QLD OF TMI OIL, 12-5-86

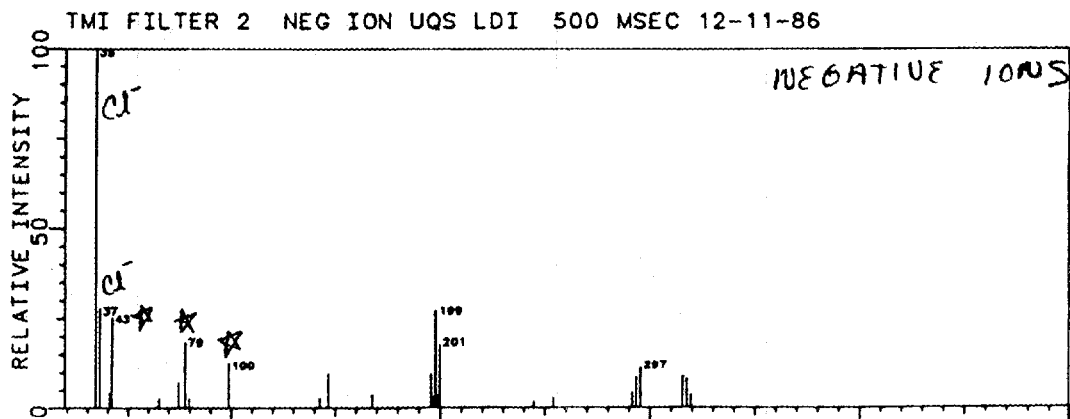
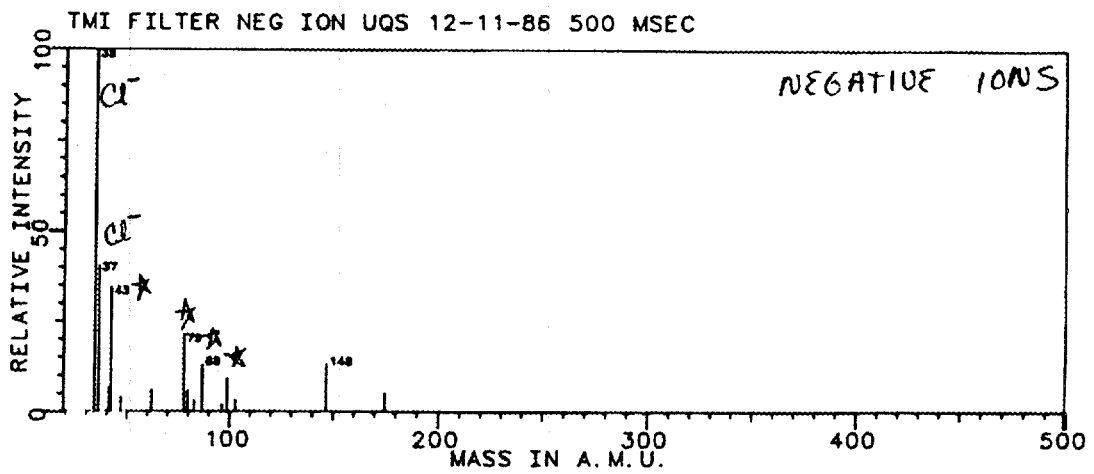
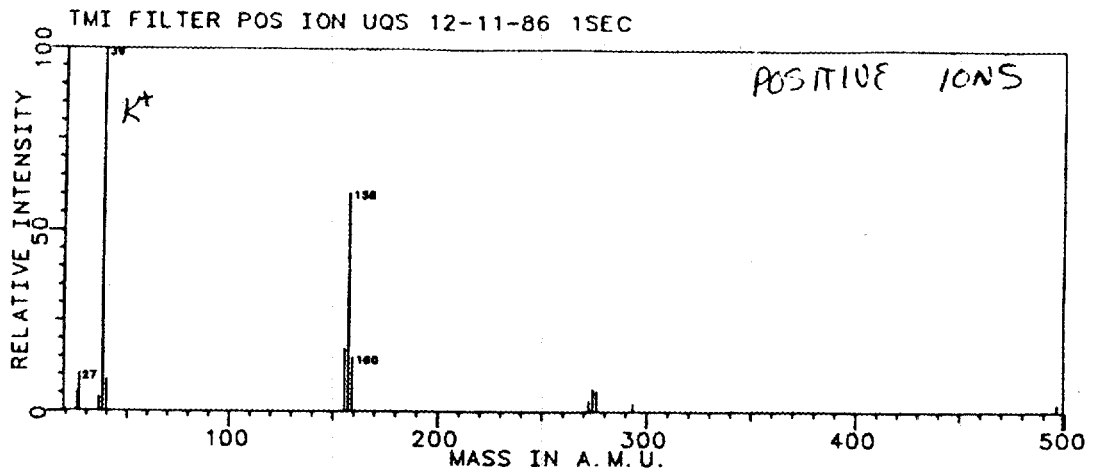


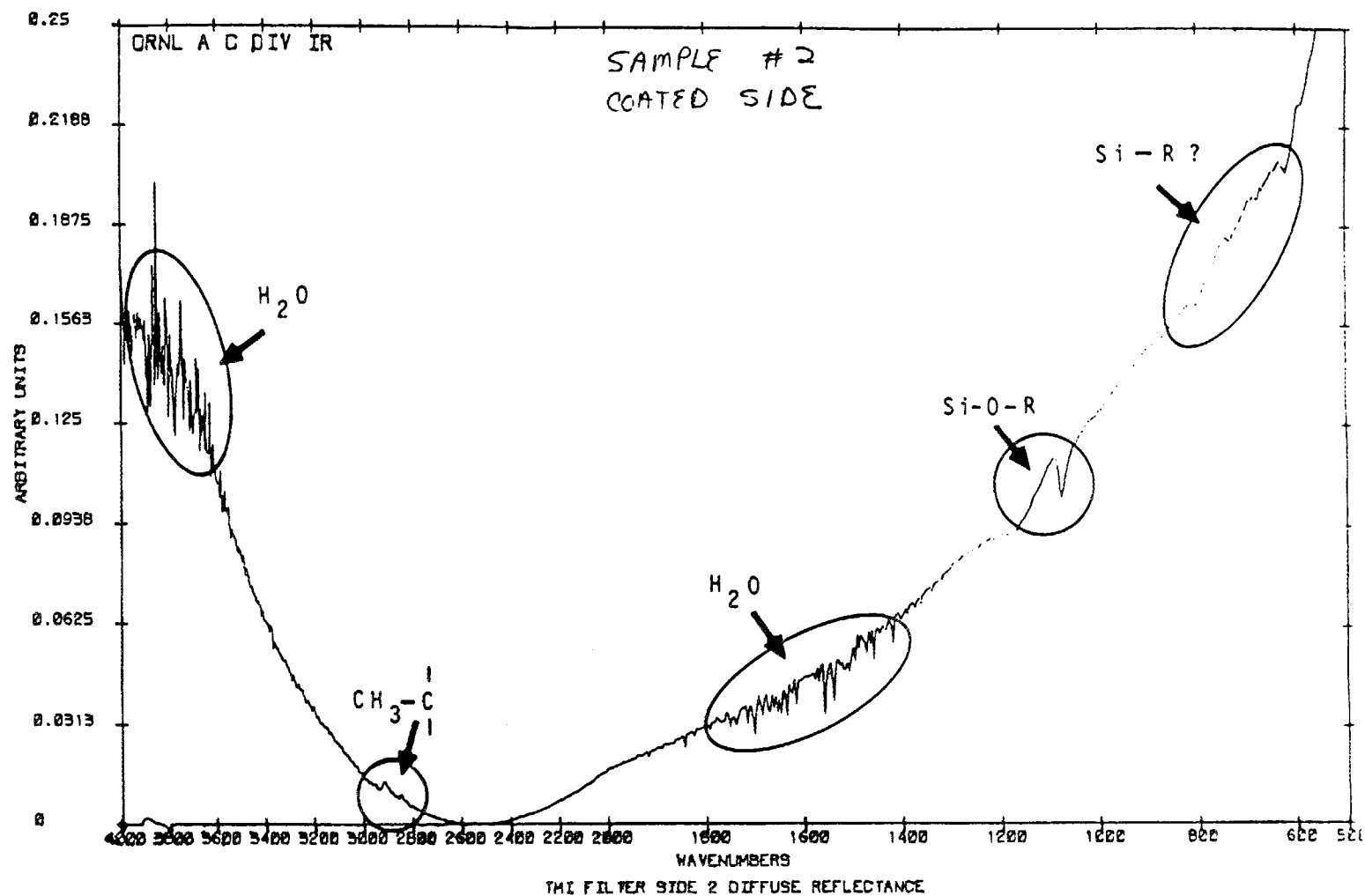
DL3=300MS, POS QLD OF TMI OIL, 12-5-86



SUCROSE LDI NEG ION QS 400 MSEC



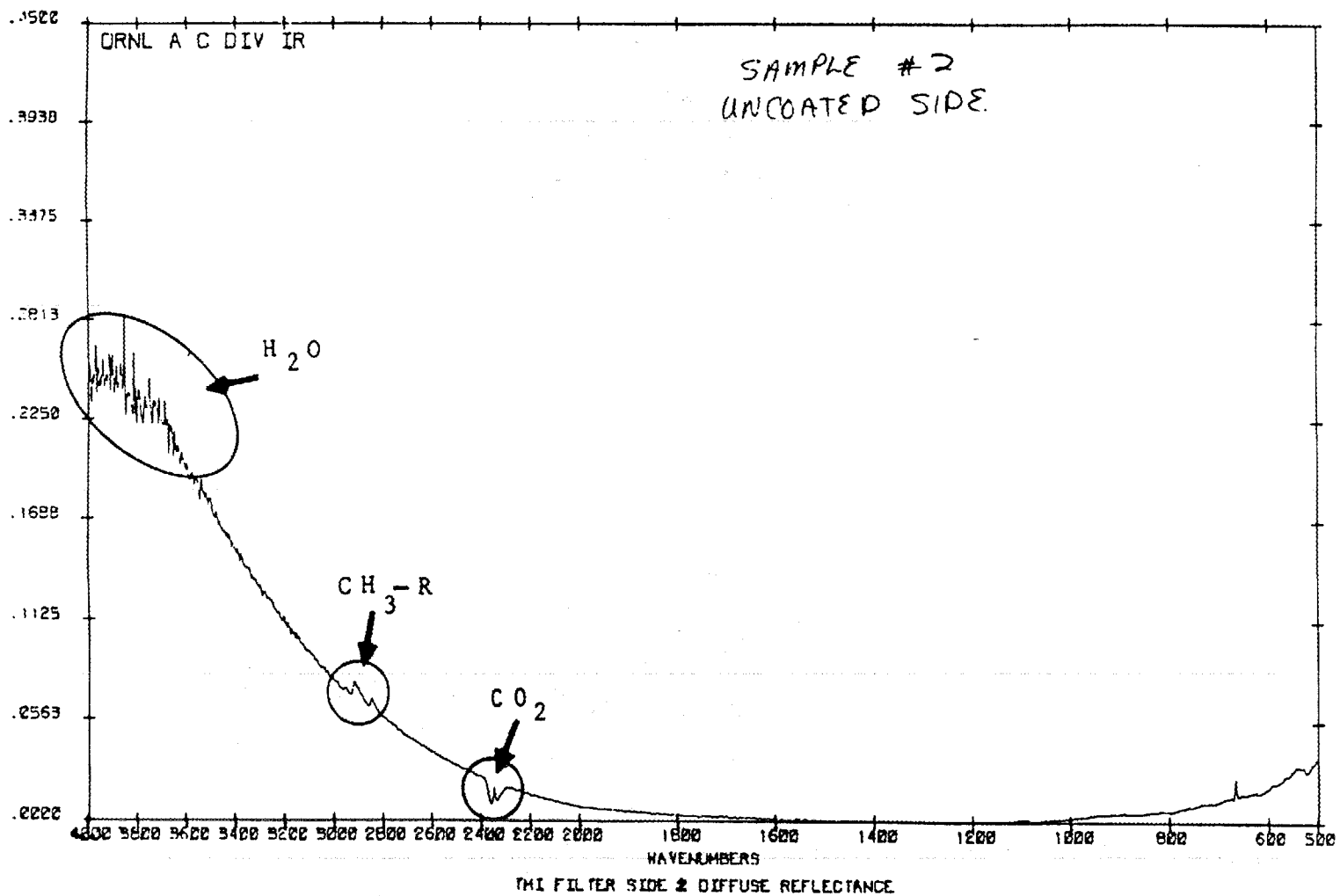




SFL=KMPLOT
NSCANS=1000
PLM=9

RES=4 DP

12/11/96 12:43:28



9FL=KHPLQT
NSCANS=1000
PLM=9

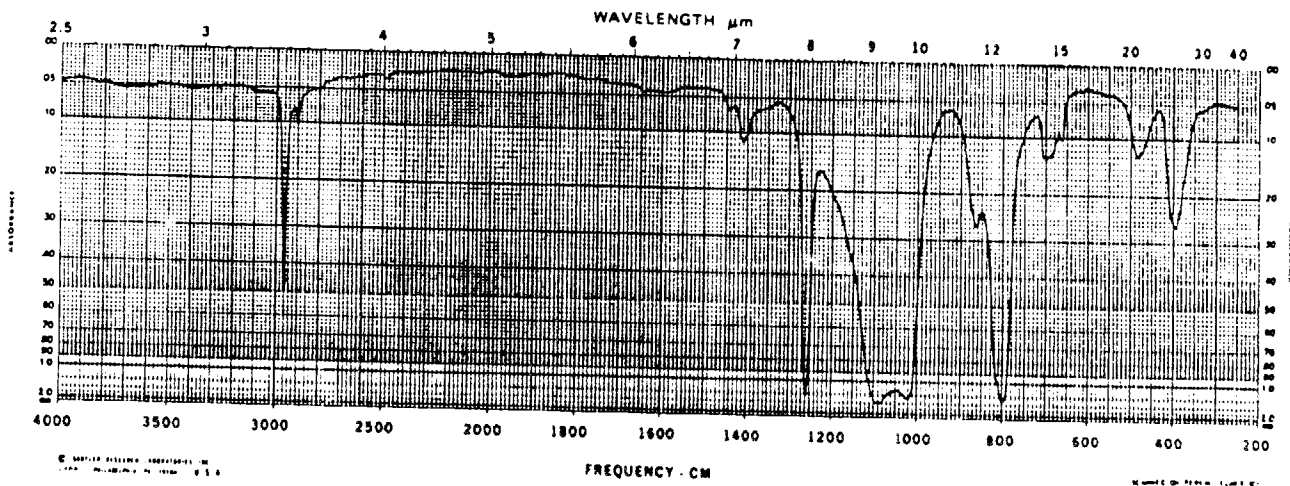
RES=4 DP

12/11/86 10:37

SILICONE LUBRICANT

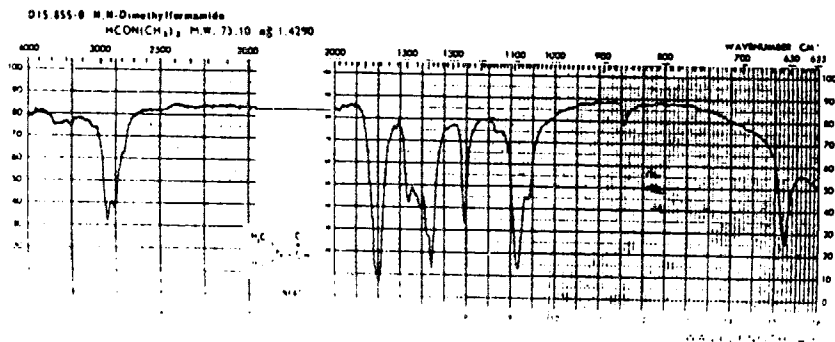
Source: Dow Corning Corp.
Capillary Cell

No. 27



74

No. 28



Internal Correspondence

MARTIN MARIETTA ENERGY SYSTEMS, INC.

January 20, 1987

David O. Campbell, 4500-N, MS B12, ORNL

Surface Analysis of Stainless Steel Filter Segments

Two stainless steel filter samples were submitted to the ORGDP Analytical Chemistry Department for surface analytical work utilizing Secondary Ion Mass Spectrometry (SIMS) and Ion Scattering Spectrometry (ISS). The purpose of the work was to determine the reason for the premature plugging of the filters. Data already obtained (SEM pictures) indicated the possible presence of some type of film covering the surface of the filter. Confirmation and further characterization of this film was the desired result. The two samples (HDO and HSJ) were a followup to a sample which was submitted and analyzed at an earlier date. This report attempts to summarize the results of the analyses performed.

The two techniques used for the analysis of the samples were Secondary Ion Mass Spectrometry (SIMS) and Ion Scattering Spectrometry (ISS). Both of these techniques are surface analysis techniques. The depth into the sample from which information is obtained utilizing these techniques varies depending on the sample matrix but is generally quoted to be about 100 Å for SIMS and about 3 Å for ISS. Both techniques utilize an inert gas primary ion beam with energies in the 1-5 keV range. The SIMS technique utilizes a quadrupole mass spectrometer to analyze the mass of charged atomic and molecular particles sputtered from the sample surface. The ISS technique measures the kinetic energy of the backscattered inert gas primary ions using a cylindrical mirror analyzer. The energy loss suffered by the primary ions can be related to the elemental composition of the surface through the application of the laws of conservation of momentum and conservation of energy. A knowledge of instrumental parameters allows characteristic energy ratios (measured kinetic energy/initial primary ion beam kinetic energy) for each element to be calculated for individual inert gas ions. A measurement of the primary ion beam energy distribution after a collision with the surface of interest yields a qualitative elemental analysis of the surface.

The analysis of the first sample was inconclusive. The data obtained on this sample compared the underside of the sample (clean) to the topside which was the heavily contaminated side. The SIMS and the ISS spectra obtained are contained as attachments 1 and 2. The positive ion SIMS data indicates that both sides of the sample were contaminated with organics as indicated by the clusters of peaks (65-73, 77-85, and 89-97) separated by 12 amu. This is confirmed by the presence of a small carbon peak at $E/E_0=0.29$ in the ISS. This contamination layer is thick enough to all but prevent the detection of iron and chromium ($E/E_0=0.75$), the major components of the filter material. Although the level of contamination differed from topside and underside, it appears that both sides had a significant amount of organic contamination. The second set of filter samples received had a significantly different appearance. A comparison of the positive ion SIMS spectra of the first sample (attachment 1) and the second set of samples (attachment 3) reveal that the organic contamination present on the first sample is absent on the second set of samples. The major peaks seen in the spectra of the second set of samples correspond to chromium ($m/e=52$) and iron ($m/e=56$). Table 1 gives a comparison of the ratios of the various elements detected on the surface of the sample. To obtain the numbers shown in Table 1

D. O. Campbell
 Page 2
 January 20, 1987

Table 1. Comparison of elemental ratios (SIMS)

M	M/Cr	
	HSU	HSD
Na	0.25	0.65
Al	0.26	0.20
Si	0.98	0.17
Fe	0.40	0.22

the area of the various metal peaks was ratioed to that of chromium in an attempt to account for matrix effects. If the chromium surface concentration varies significantly from HSD to HSU the meaning of these numbers becomes questionable. It is assumed that the actual surface concentration of chromium is remaining constant and any variation in the chromium signal is the result of matrix effects and/or contamination. The numbers in Table 1 seem to indicate an enrichment or accumulation of silicon or a silicon containing compound on the HSU side. There also appears to be a slight enrichment of iron. Attachment 4 is a scale expansion of the spectra contained in attachment 3, one noticeable difference is the presence of a peak at $m/e=72$ on the HSU sample which is all but absent on the HSD sample. The peak at $m/e=72$ is probably due to a FeO^+ molecular cluster ion. Table 2 is a comparison of cluster ion intensities for the two samples. The data contained in Table 2 further indicate that an oxidic

Table 2. Comparison of cluster ion intensities

M	M/Cr	
	HSU	HSD
CrO	7.2e-03	9.1e-03
FeO	2.0e-02	4.7e-03

iron compound may be being deposited on the surface of the HSU sample. It is also justification for referencing peak areas to the absolute area of the chromium peak. There is very little change in the CrO/Cr ratio between the HSU and the HSD sample.

A similar type of analysis can be carried out utilizing the peak areas generated from the ISS spectra contained as attachment 5. The spectra obtained have peaks which show the presence of carbon ($E/E_0=0.295$), oxygen ($E/E_0=0.410$), sodium ($E/E_0=0.540$), silicon ($E/E_0=0.607$), and iron/chromium ($E/E_0=0.780$). Table 3 show the results of the analysis. The major concentration difference seen is

D. O. Campbell
 Page 3
 January 20, 1987

Table 3. Comparison of elemental ratios (ISS)

M	M/Cr	
	HSU	HSD
C	0.09	0.15
O	0.37	0.34
Na	0.10	0.11
Si	0.23	0.11

once again the enrichment of silicon on the HSU surface. The magnitude of enrichment determined utilizing the two techniques is significantly different (SIMS=5.8,ISS=2.1) but can be explained by realizing that the sampling depth of the SIMS technique is significantly greater than that of the ISS technique.

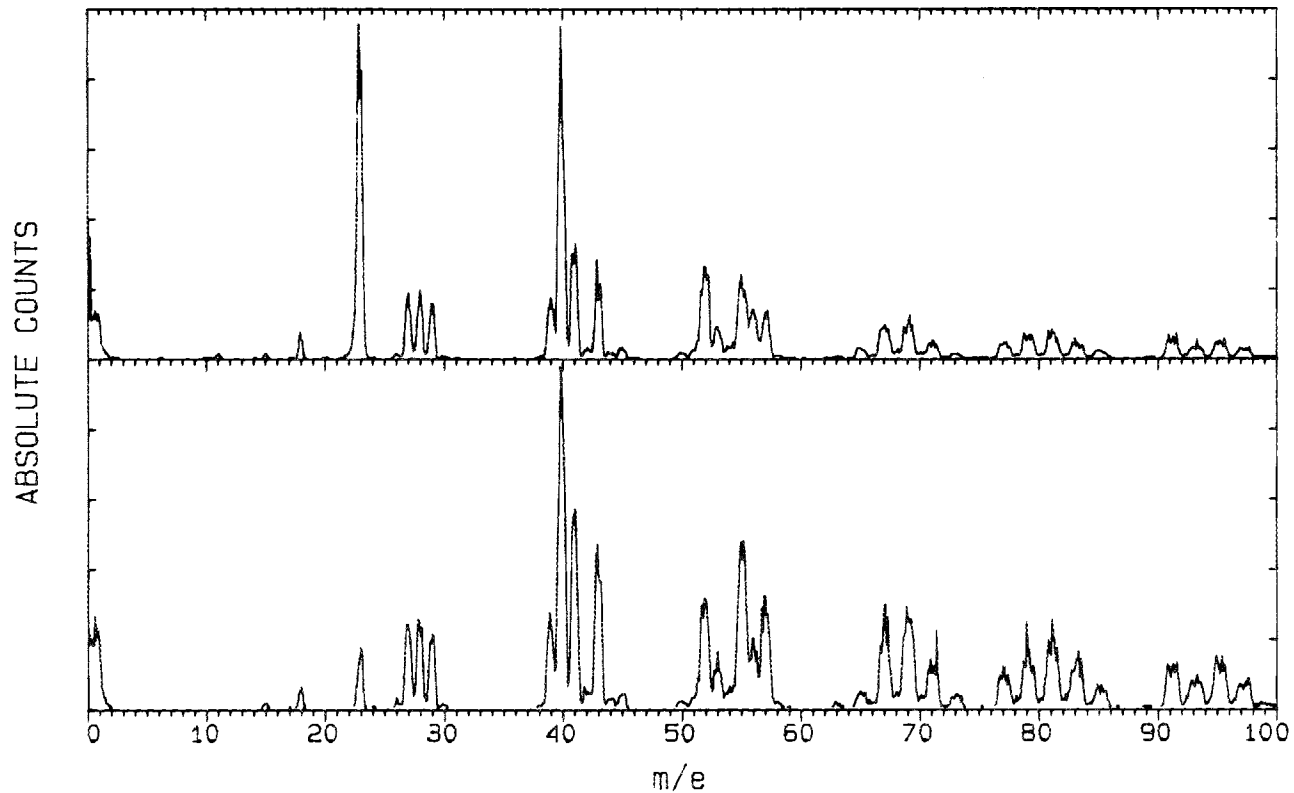
In conclusion, a comparison of the HSU and HSD samples reveal that there appears to be a enrichment (deposition) of silicon or some type of silicon compound on the surface of the HSU sample. In addition there is good evidence for the deposition of an oxidic iron compound on the HSU surface. The ISS/SIMS data alone is not sufficient to determine if either of the differences discussed is responsible for the premature failure of the filters.

D. S. Zingg

D. S. Zingg, K-1004-B, MS 449 (6-4517) - NoRC

cc: J. H. Stewart Jr., 4500-S, MS 140, ORNL
 R. W. Morrow
 L. W. McMahon

POSITIVE ION SIMS



UPPER: UNDERSIDE 2 SCANS

LOWER: TOPSIDE 2 SCANS

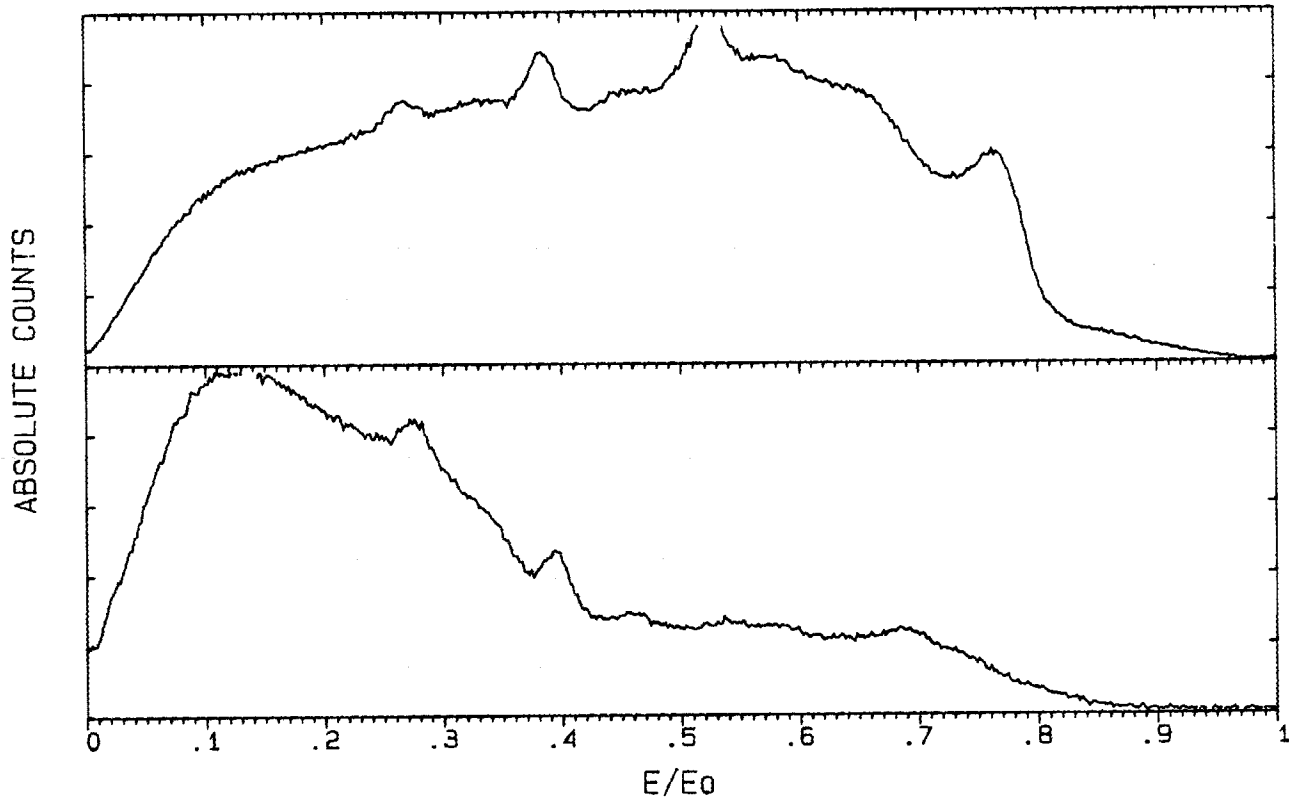
DATE: 11/11/86

PROCESS SUPPORT DIV.

ANALYTICAL CHEM DEPT.

SURFACE ANALYSIS LAB

4HE ISS



UPPER: UNDERSIDE NEW AREA 50 SCANS

LOWER: TOPSIDE NEW AREA 50 SCANS

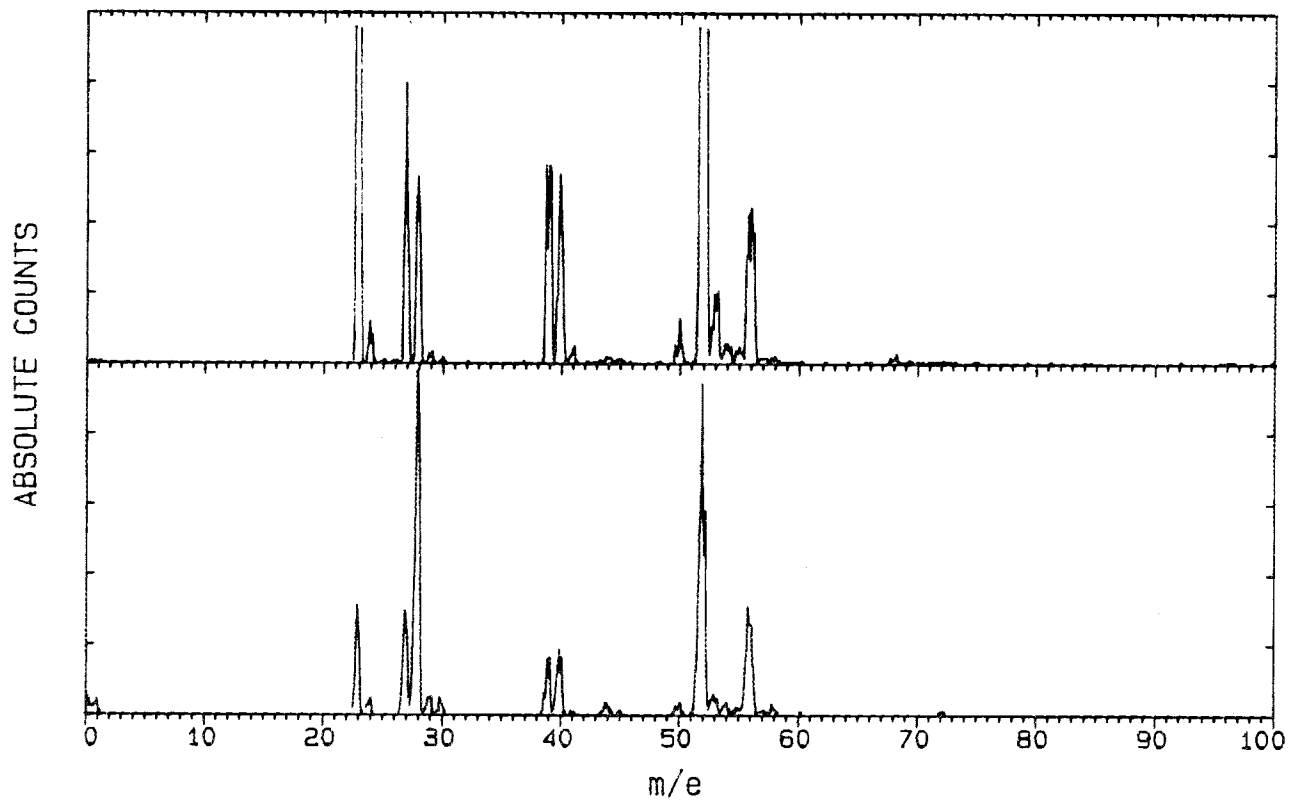
DATE: 11/11/86

PROCESS SUPPORT DIV.

ANALYTICAL CHEM DEPT.

SURFACE ANALYSIS LAB

POSITIVE ION SIMS

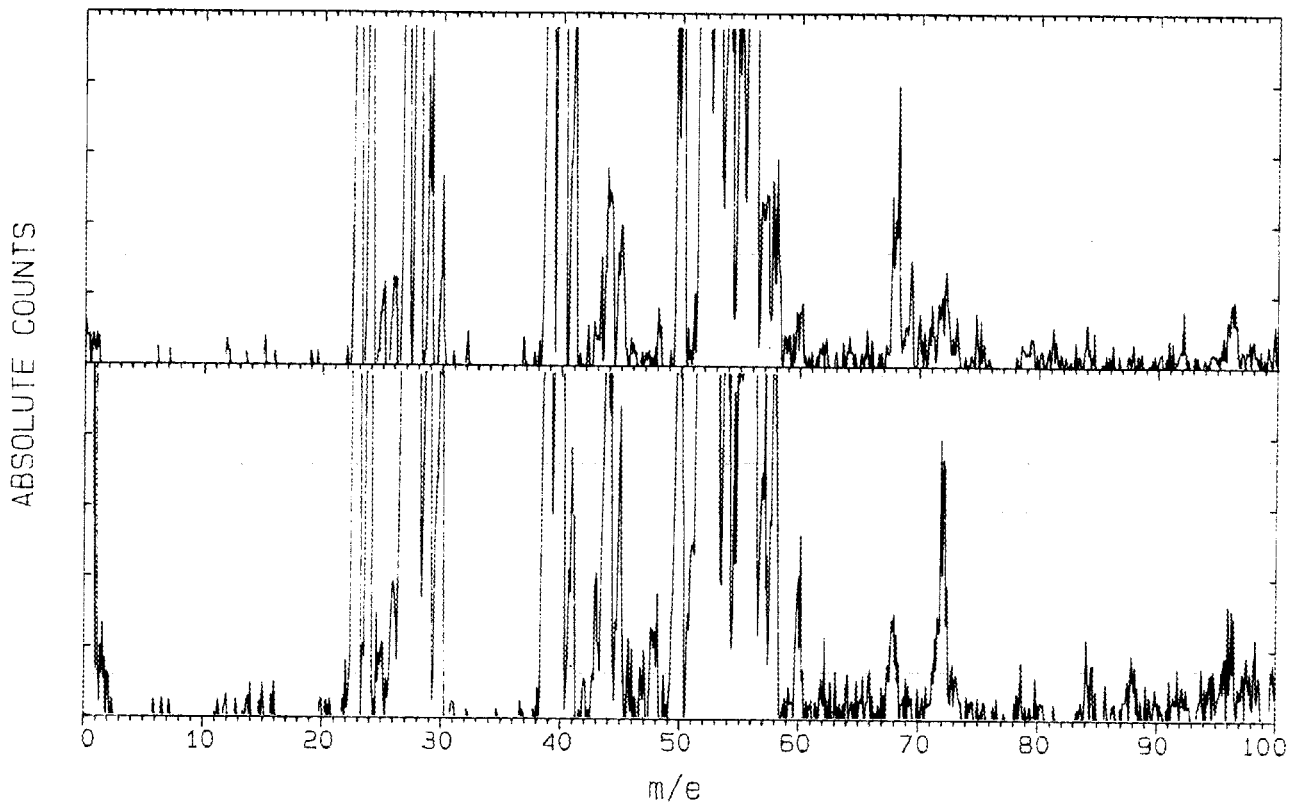


UPPER: HOT SIDE DOWN

LOWER: HOT SIDE UP

PROCESS SUPPORT DIV.
ANALYTICAL CHEM DEPT.
SURFACE ANALYSIS LAB

POSITIVE ION SIMS



UPPER: HSD (60x expansion)

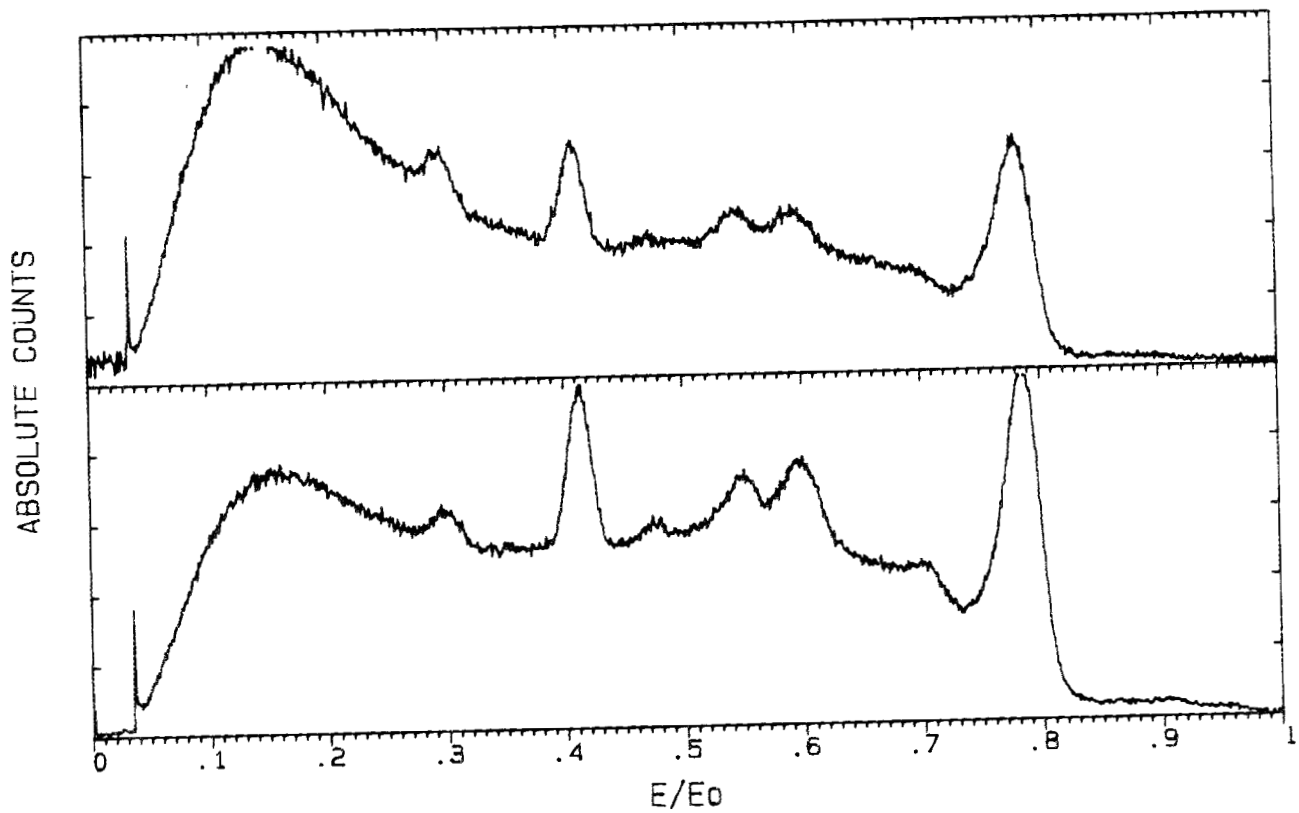
LOWER: HSU (60x expansion)

PROCESS SUPPORT DIV.

ANALYTICAL CHEM DEPT.

SURFACE ANALYSIS LAB

4HE ISS



UPPER: HOT SIDE DOWN

LOWER: HOT SIDE UP

PROCESS SUPPORT DIV.

ANALYTICAL CHEM DEPT.

SURFACE ANALYSIS LAB

MARTIN MARIETTA

Internal Correspondence

MARTIN MARIETTA ENERGY SYSTEMS, INC

January 9, 1987

D. O. Campbell

Request No. 91035

Using gas chromatograph/mass spectrometry, the sample identified as 4NTU chromatographed as one large peak at a retention time of 33.3 minutes on a J&W DB-5 capillary column (non-polar) with a primary mass of 129. (There were also several minor peaks shown on the total ion chromatogram on pp. 5-15). This mass is characteristic of an oxygenated compound such as an ester. The chromatogram of the second sample, 71NTU showed peaks at 29.6, 32.3, 35.6, 38.1, 40.7, and 44.5 minutes as well as many minor peaks. The primary mass for each of these peaks was 59, which is also characteristic of an oxygenated compound, such as alcohol.

Typical mass spectra for these species are shown in attached figures (Figure 1, primary mass of 129; Figure 2, primary mass of 59). Reversed Phase Liquid chromatography showed a major peak at 2 minutes for each of these extracts. (Eluting solution was 65% methanol in water.) This indicates a fairly polar species.

JEC:SKH:ldg

Attachments

John E. Caton /SKH

John E. Caton
Group Leader
Organic Analysis Group
Organic Chemistry Section
Analytical Chemistry Division

December 30, 1986

John E. Caton, 4500S, MS 120

Details of Sample Preparation of Aqueous Three Mile Island Samples

Two of the three existing aqueous Three Mile Island samples, viz. 70 and 4 NTU, were prepared as we discussed this morning.

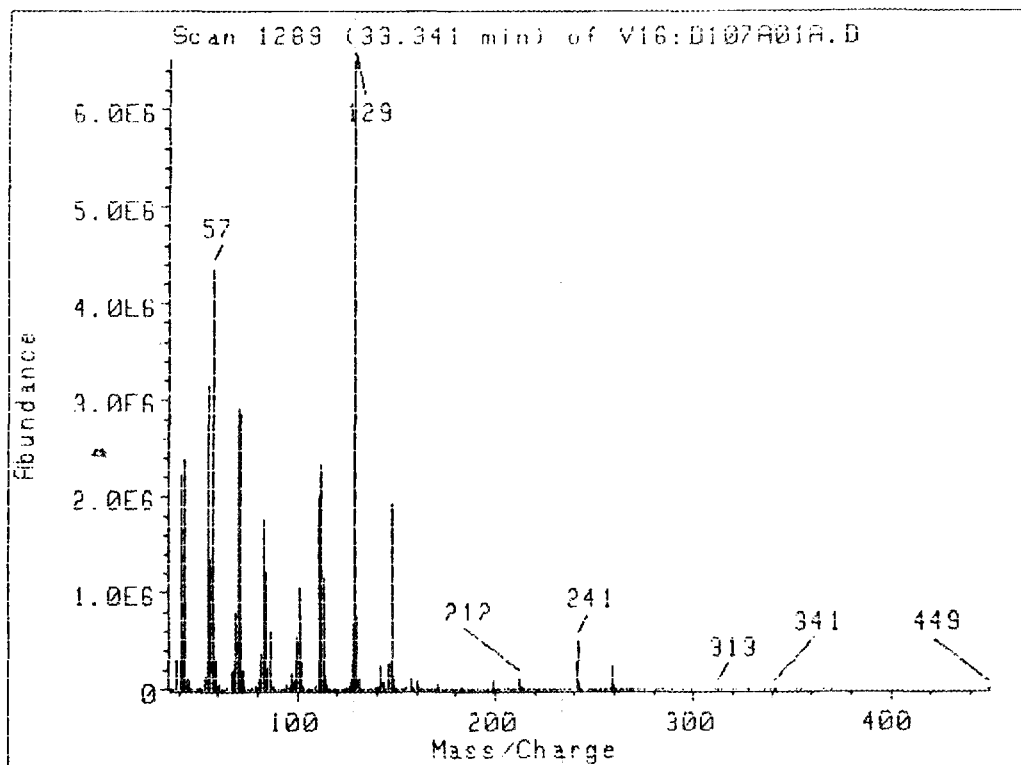
Briefly, 1.75 mL isopropanol were added to 10 mL of either aqueous sample, which was processed as received (viz., no pH adjustment, filtration, etc.). This solution was then passed through an OCTADECYL SPE column which had been conditioned with methanol and 15% vol/vol isopropanol/water, in that order. The sorbed organics (if any) were eluted with four 500 uL aliquots of acetonitrile, which were concentrated to a final volume of 300 uL using dry, flowing nitrogen.

In both cases, a thin brown ring (heavier for 70 NTU, almost nonexistent for 4 NTU, as expected) appeared just under the frit of the SPE column, indicating that particles were removed effectively from the sample. These particles were modestly radioactive (ca. 100 mrad/hr beta/gamma radioactivity), yet they apparently did not enter the final acetonitrile solution. The latter exhibited no beta/gamma radiation exceeding background.

BAT.

Bruce A. Tomkins, 2026, MS 043, 6-6692

4-NTU WATER SAMPLE



Scan 1289 (33.341 min) of V16:D107A01A.D
 SAMPLE #4487 + IS SPE TOMKINS

m/z	abund.	m/z	abund.	m/z	abund.	m/z	abund.
39.05	5	69.05	12	99.05	1	130.95	2
41.10	34	70.05	45	99.95	8	141.90	4
42.10	9	71.00	44	100.95	16	143.00	1
43.10	37	72.00	3	102.00	4	146.00	4
44.10	2	73.00	3	103.00	1	147.00	29
45.00	1	79.00	1	108.90	1	147.05	2
53.10	2	81.00	2	111.00	3	156.95	2
53.05	24	82.10	6	112.00	3	157.95	1
56.05	21	83.00	27	113.00	18	171.00	1
57.05	67	84.00	19	114.00	2	199.00	1
58.05	4	85.00	3	115.00	1	211.95	2
59.05	5	86.95	9	126.05	1	241.05	8
59.95	1	87.95	1	126.95	2	242.05	1
61.05	1	93.05	1	128.05	10	259.00	4
67.05	3	97.05	2	128.95	100	260.00	1
68.05	3	98.05	1	129.95	11		

FIGURE 1

4-NTU WATER SAMPLE (CONTINUED)

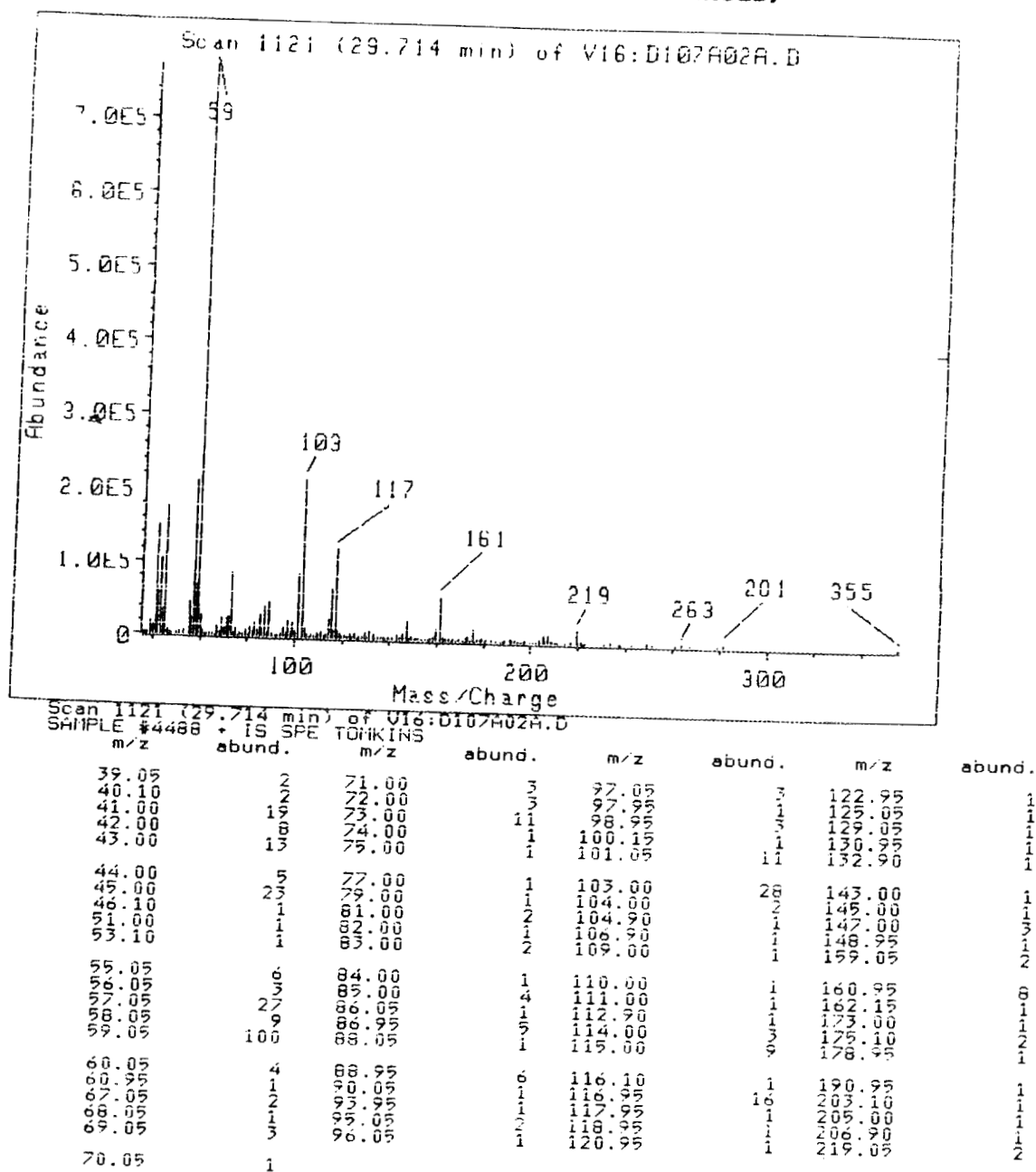


FIGURE 2

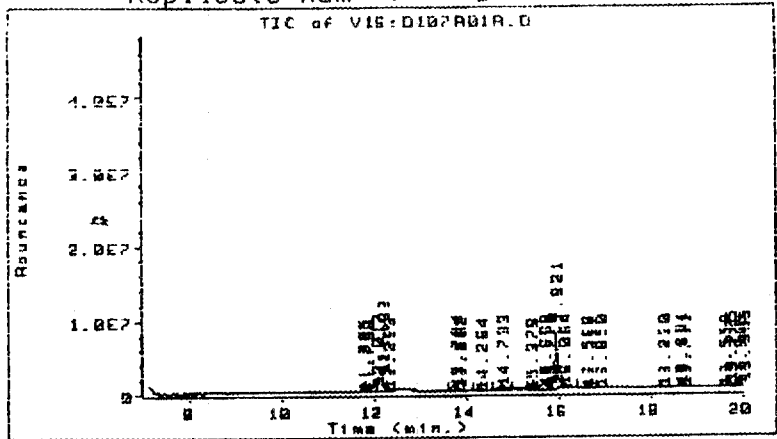
TOTAL-ION CHROMATOGRAM OF 4-NTU WATER SAMPLE

Data file: V16:D107A01A.D
 File type: GC / MS DATA FILE

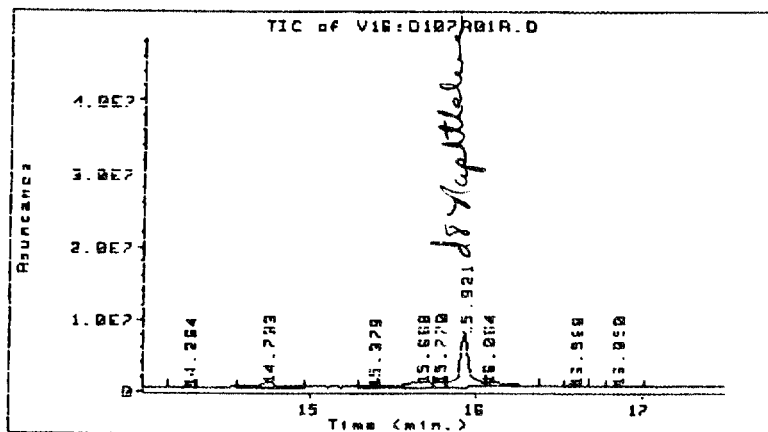
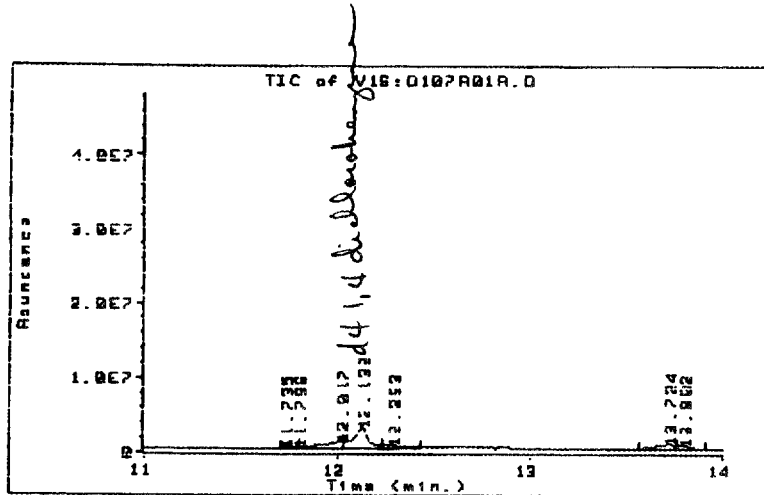
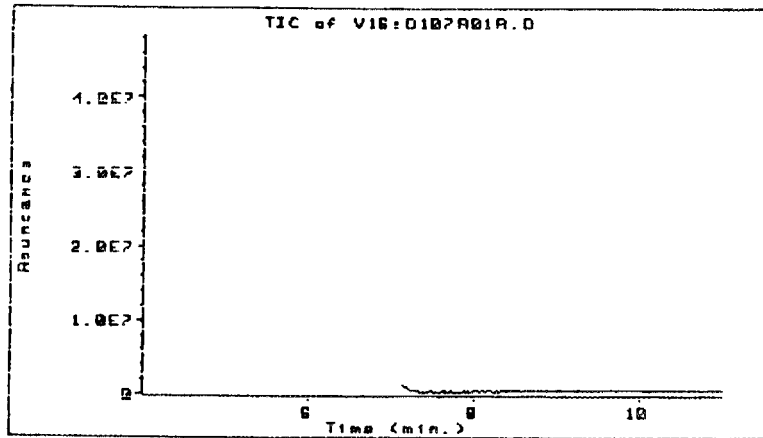
Name Info: SAMPLE #4487 + IS SPE TOMKINS
 Misc Info: J&W 30M DB5 30(5)-30008 D
 Operator : HARMON/TREESE

Date : 7 Jan 87 3:08 pm
 Instrument: MS_5970
 Inlet : GC

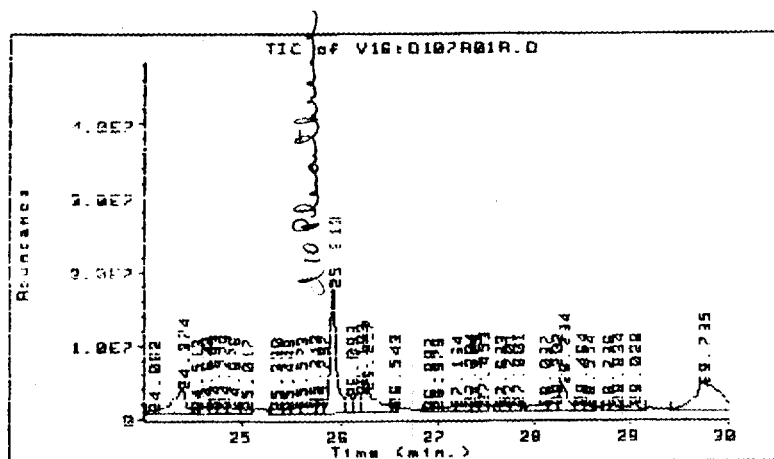
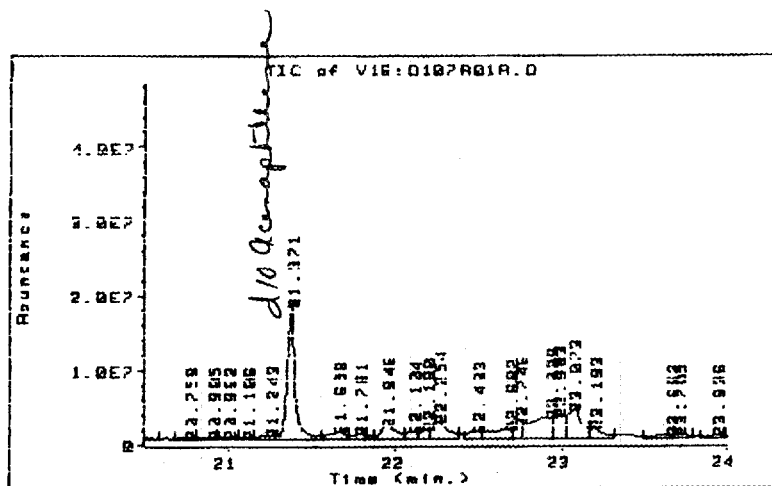
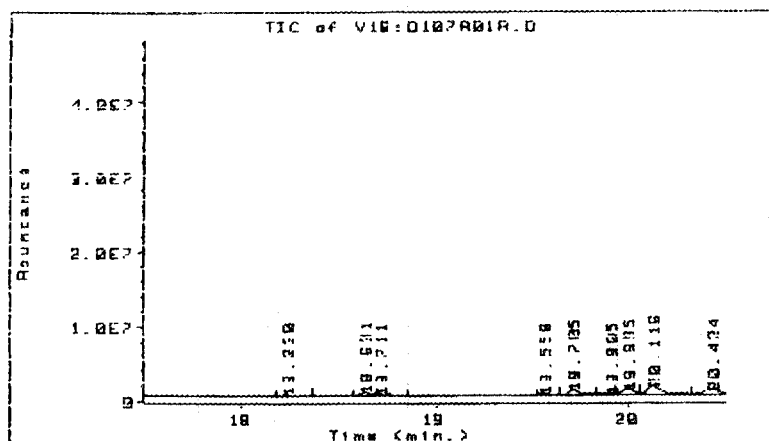
Sequence index : 1
 This bottle num : 1
 Replicate num : 1



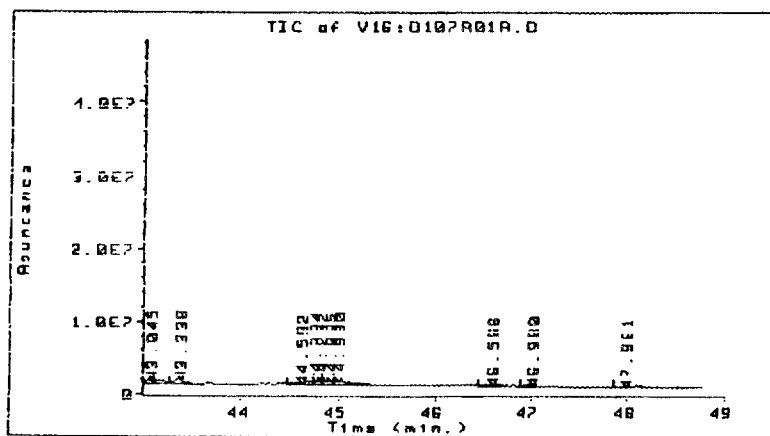
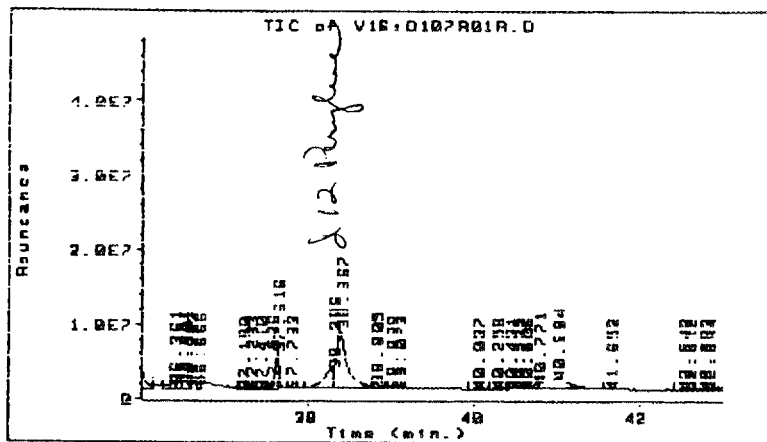
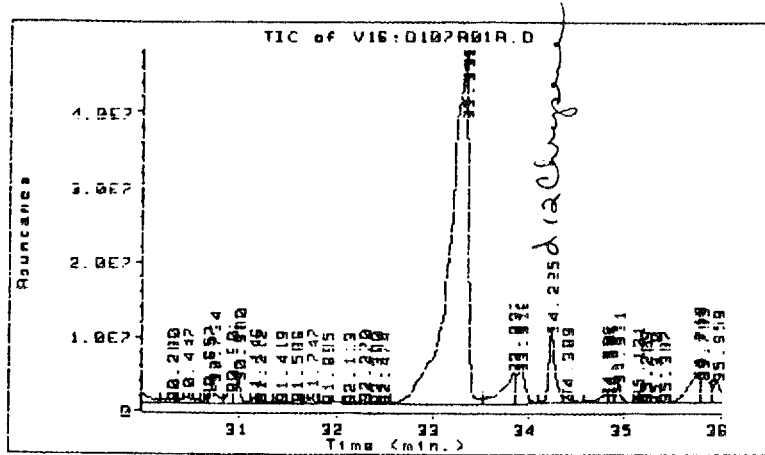
TOTAL-ION CHROMATOGRAM OF 4-NTU WATER SAMPLE
(CONTINUED)



TOTAL-ION CHROMATOGRAM OF 4-NTU WATER SAMPLE
(CONTINUED)

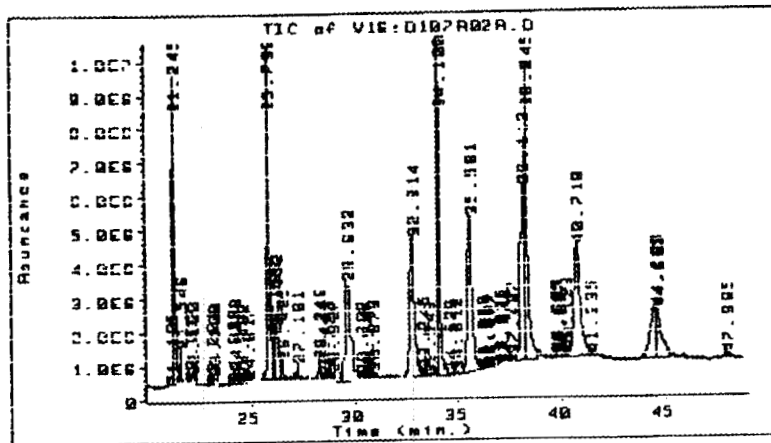
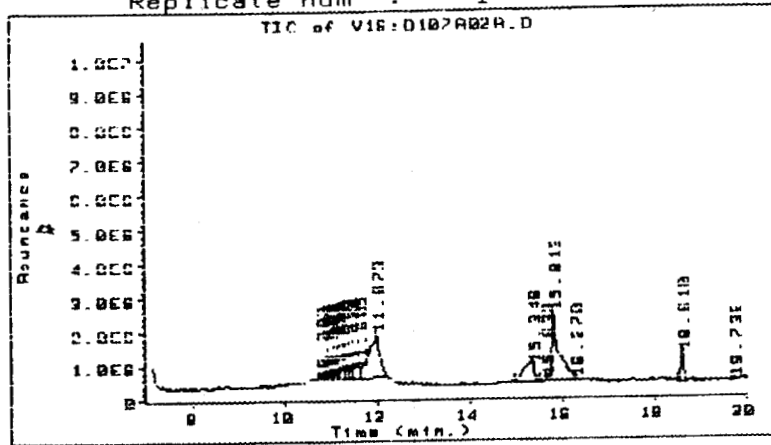


TOTAL-ION CHROMATOGRAM OF 4-NTU WATER SAMPLE
(CONTINUED)

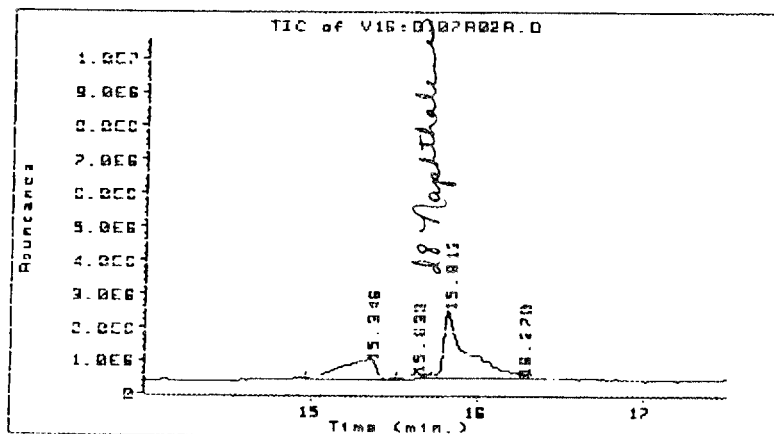
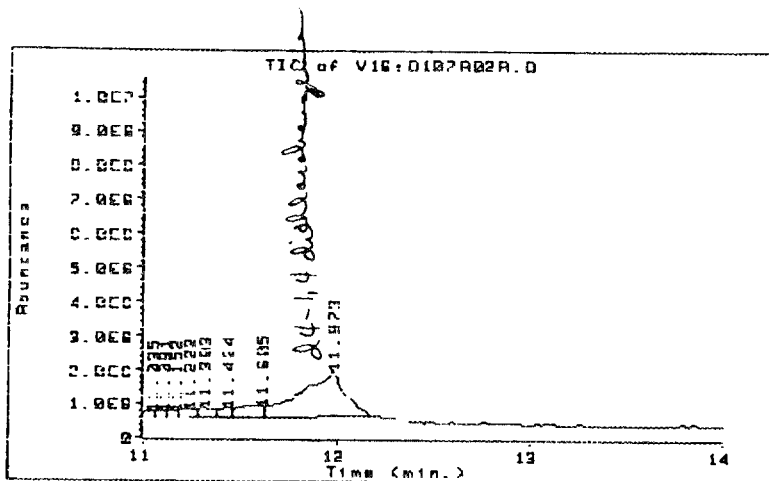
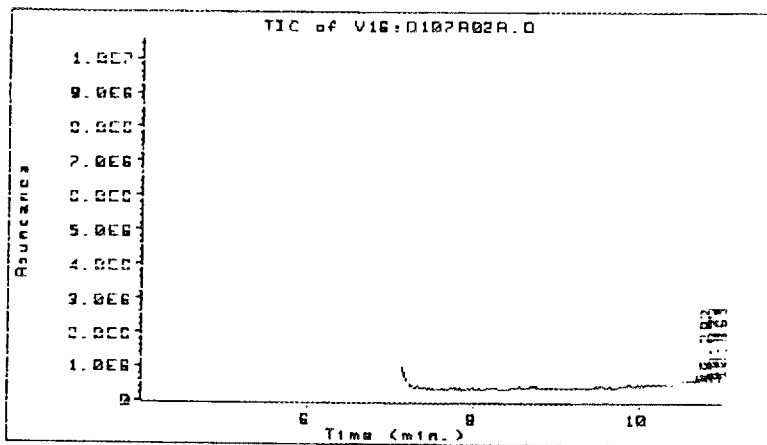


TOTAL-ION CHROMATOGRAM OF 70-NTU WATER SAMPLE

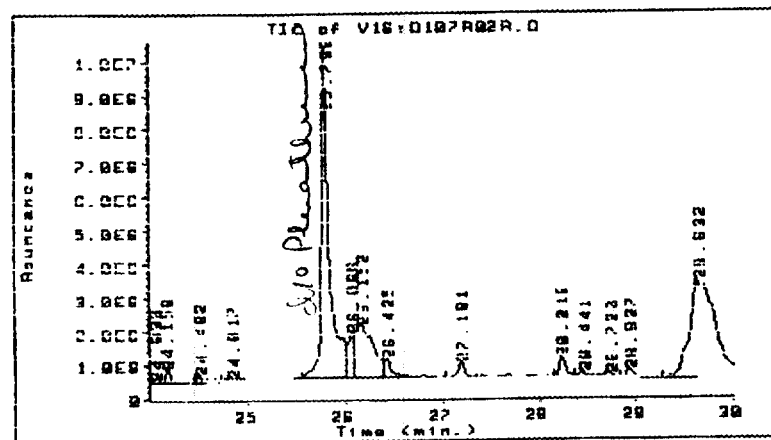
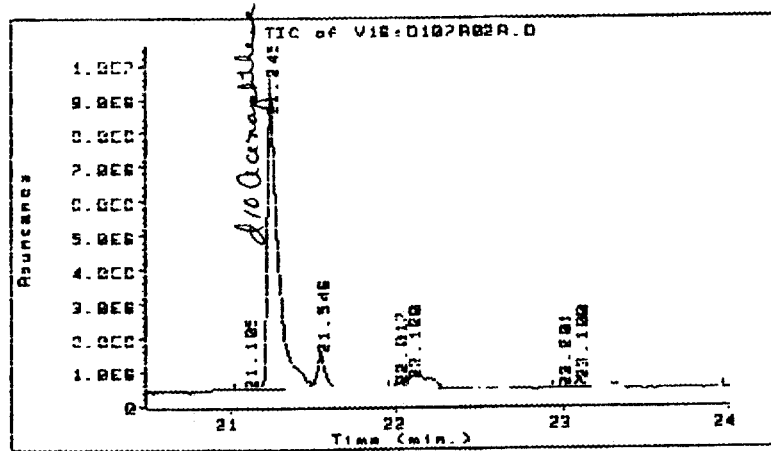
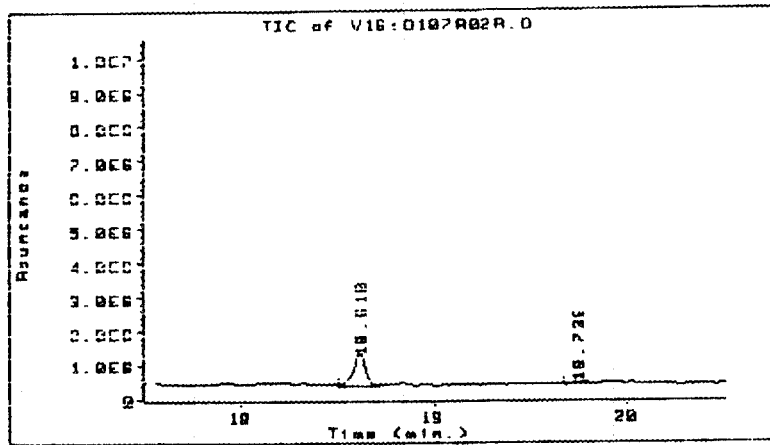
Data file: V16:D107A02A.D
 File type: GC / MS DATA FILE
 Name Info: SAMPLE #4488 + IS SPE TOMKINS
 Misc Info: J&W 30M DB5 30(5)-300@B D
 Operator : HARMON/TREESE
 Date : 7 Jan 87 4:18 pm
 Instrument: MS_5970
 Inlet : GC
 Sequence index : 1
 His bottle num : 1
 Replicate num : 1



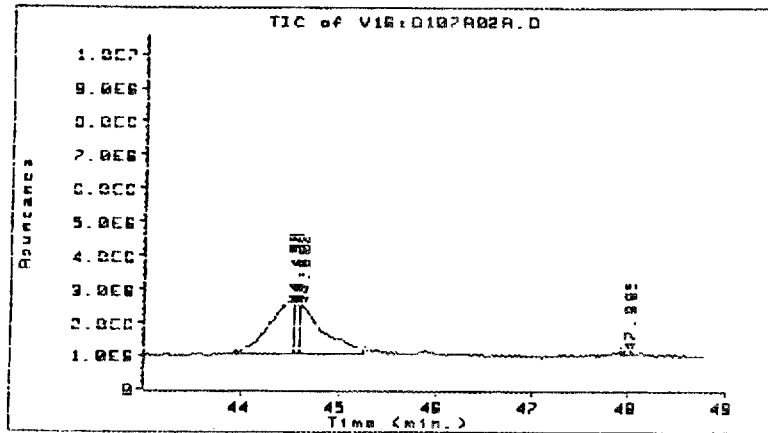
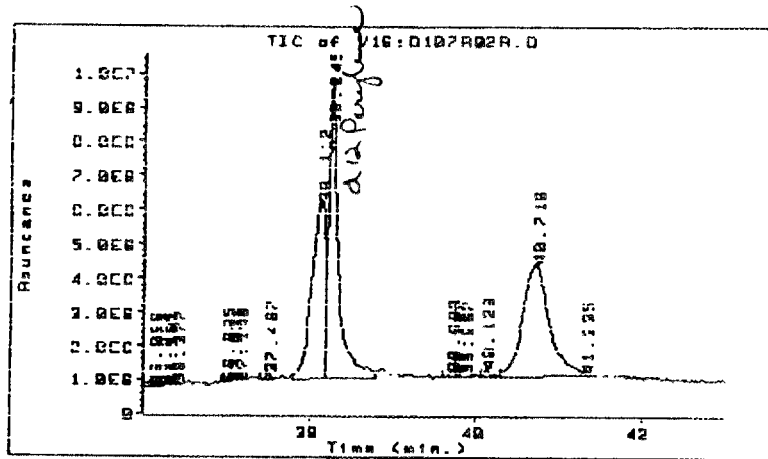
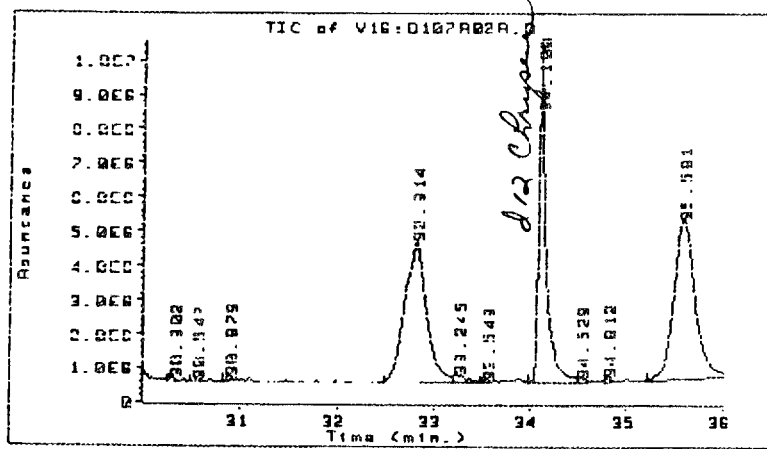
**TOTAL-ION CHROMATOGRAM OF 70-NTU WATER SAMPLE
(CONTINUED)**



TOTAL-ION CHROMATOGRAM OF 70-NTU WATER SAMPLE
(CONTINUED)



**TOTAL-ION CHROMATOGRAM OF 70-NTU WATER SAMPLE
(CONTINUED)**



**Appendix C. PARTICLE CHARACTERIZATION DATA FOR SAMPLE W1
(TURBIDITY = ~71 NTU): FILTRATION TEST 1**

<u>Figure</u>	<u>Page</u>
C.1 Nuclepore filter test 1 with 71-NTU water sample W1, 10- μ m filter.	97
C.2 Nuclepore filter test 1 with 71-NTU water sample W1, 10- μ m filter.	98
C.3 Nuclepore filter test 1 with 71-NTU water sample W1, 2- μ m filter	99
C.4 Nuclepore filter test 1 with 71-NTU water sample W1, 2- μ m filter	100
C.5 Nuclepore filter test 1 with 71-NTU water sample W1, 1- μ m filter	101
C.6 Nuclepore filter test 1 with 71-NTU water sample W1, 1- μ m filter	102
C.7 Nuclepore filter test 1 with 71-NTU water sample W1, 0.6- μ m filter	103
C.8 Nuclepore filter test 1 with 71-NTU water sample W1, 0.4- μ m filter	104
C.9 Nuclepore filter test 1 with 71-NTU water sample W1, 0.1- μ m filter	105
C.10 Nuclepore filter test 1 with 71-NTU water sample W1, 0.4- μ m filter	106
C.11 Nuclepore filter test 1 with 71-NTU water sample W1, 0.4- μ m filter	106
C.12 EDX of area of 4368 (see Fig. C.11)	107
C.13 EDX of particle No. 1, 4368 (see Fig. C.11)	107
C.14 EDX of particle No. 2, 4368 (see Fig. C.11)	108
C.15 EDX of particle No. 3, 4368 (see Fig. C.11)	108
C.16 EDX of particle No. 4, 4368 (see Fig. C.11)	109

<u>Figure</u>		<u>Page</u>
C.17	EDX of particle No. 5, 4368 (see Fig. C.11).	109
C.18	Nuclepore filter test 1 with 71-NTU water sample W1, 0.4- μ m filter.	110
C.19	Nuclepore filter test 1 with 71-NTU water sample W1, 0.4- μ m filter.	110

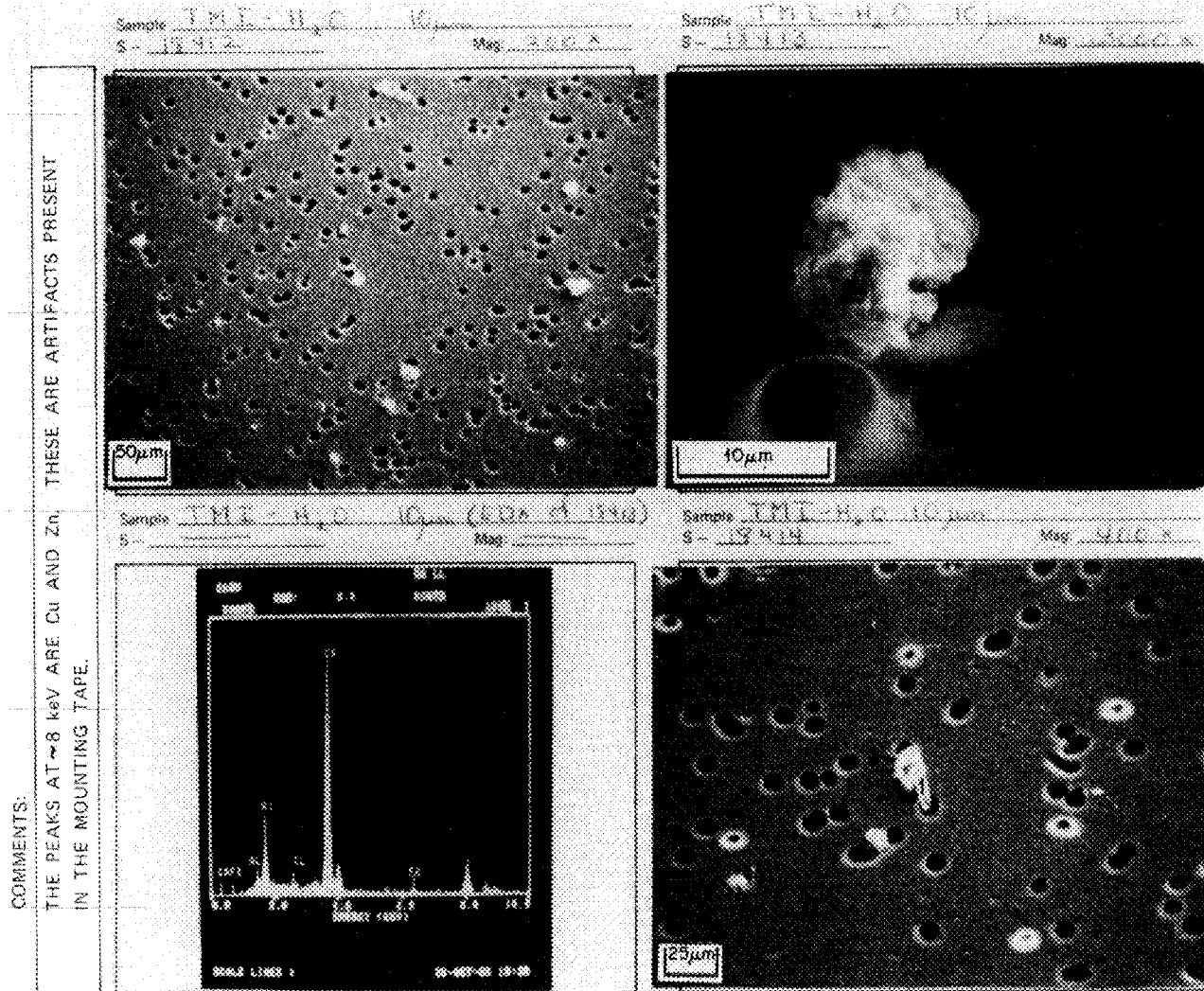
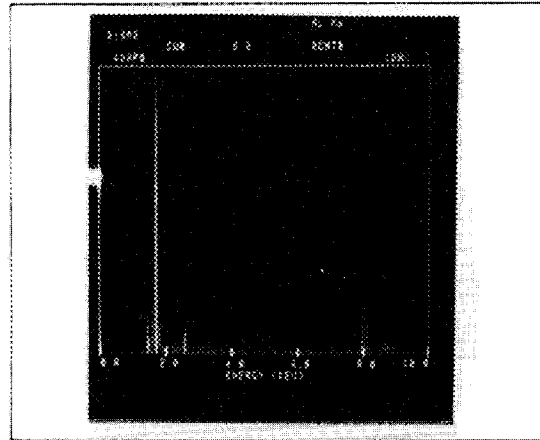
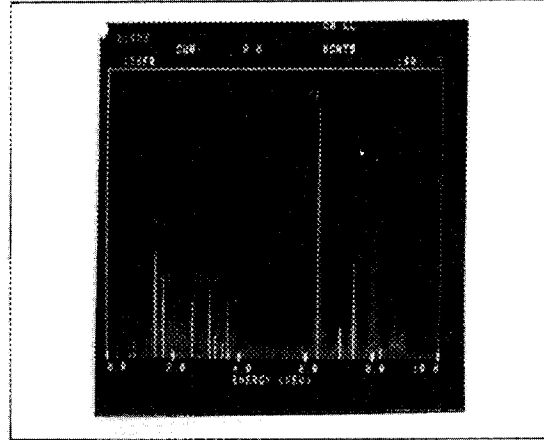


Fig. C.1. Nucleopore filter test 1 with 71-NTU water sample W1, 10-µm filter.

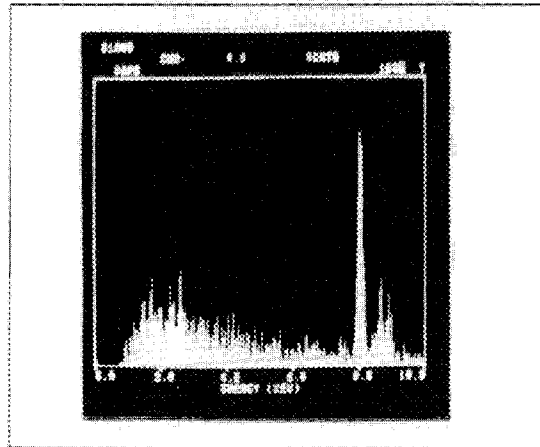
Sample TMI-H₂O 10µm (COX #1) (1874)
S - _____ Mag: _____



Sample TMI-H₂O 10µm (COX #1) (1874)
S - _____ Mag: _____



Sample TMI-H₂O 10µm (COX #1) (1874)
S - _____ Mag: _____



Sample _____
S - _____ Mag: _____

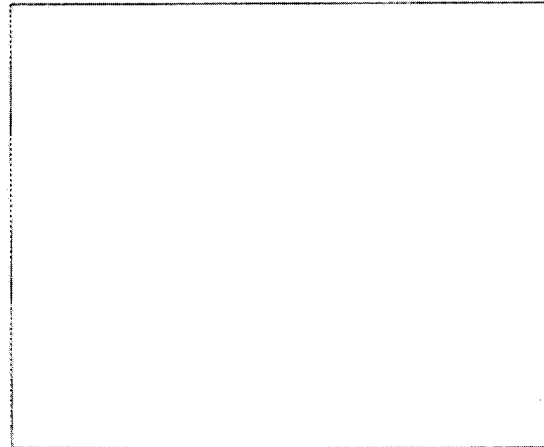


Fig. C.2. Nuclepore filter test 1 with 71-NTU water sample W1, 10-µm filter.

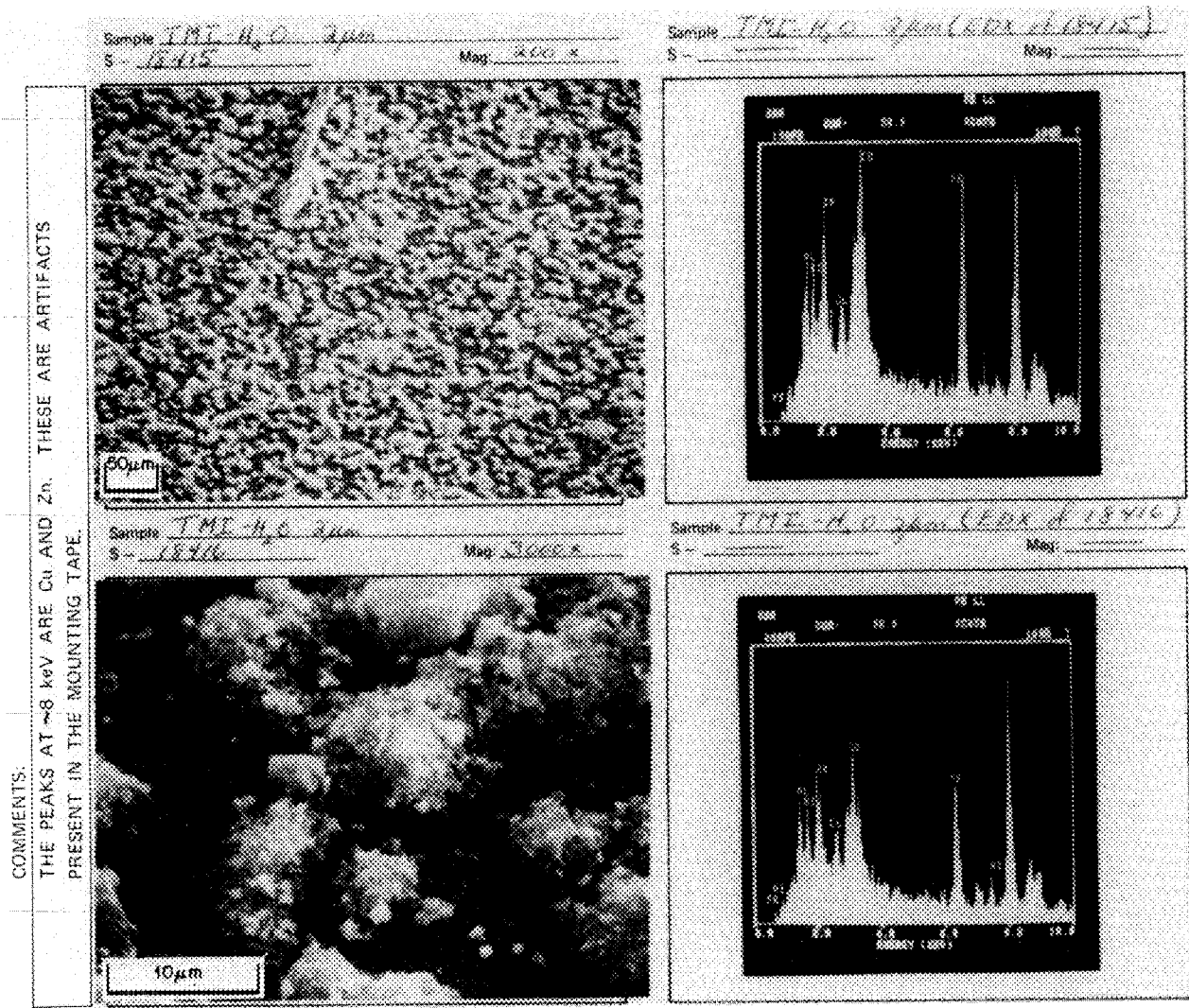
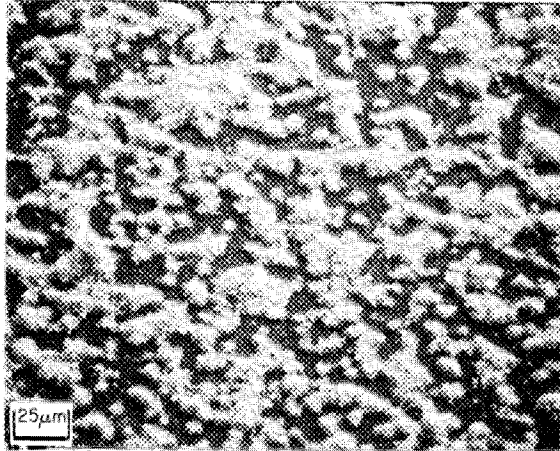
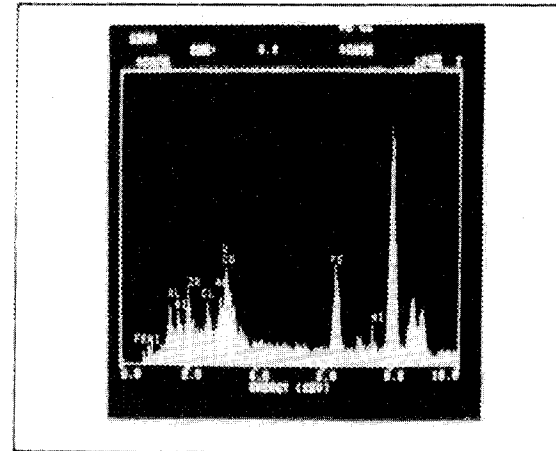


Fig. C.3. Nucleopore filter test 1 with 71-NTU water sample W1, 2-µm filter.

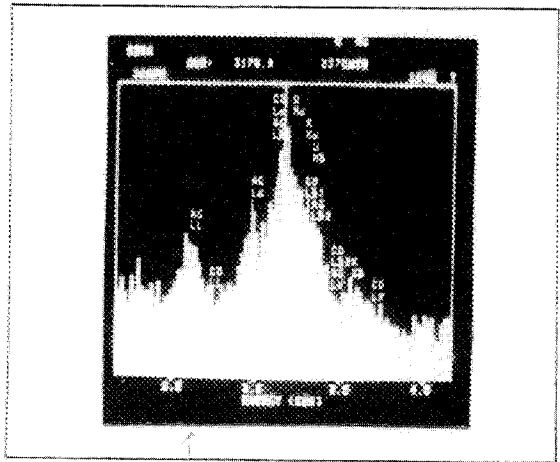
Sample TME-11.6 9um
S - 1347 Mag: 750x



Sample TME-11.6 9um (EDX of 1347)
S - _____ Mag: _____



Sample TME-11.6 9um (EDX of 1347)
S - _____ Mag: _____



Sample _____
S - _____ Mag: _____

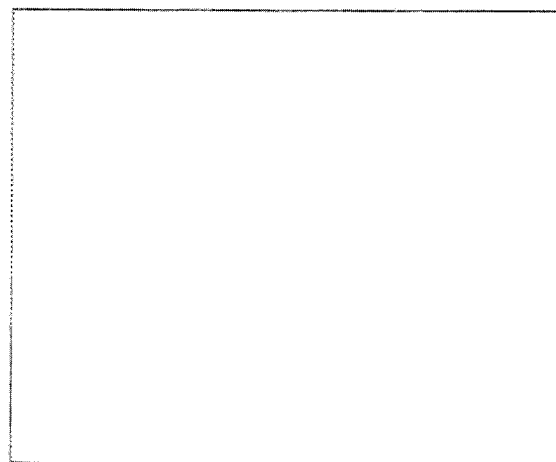


Fig. C.4. Nuclepore filter test 1 with 71-NTU water sample W1, 2- μ m filter.

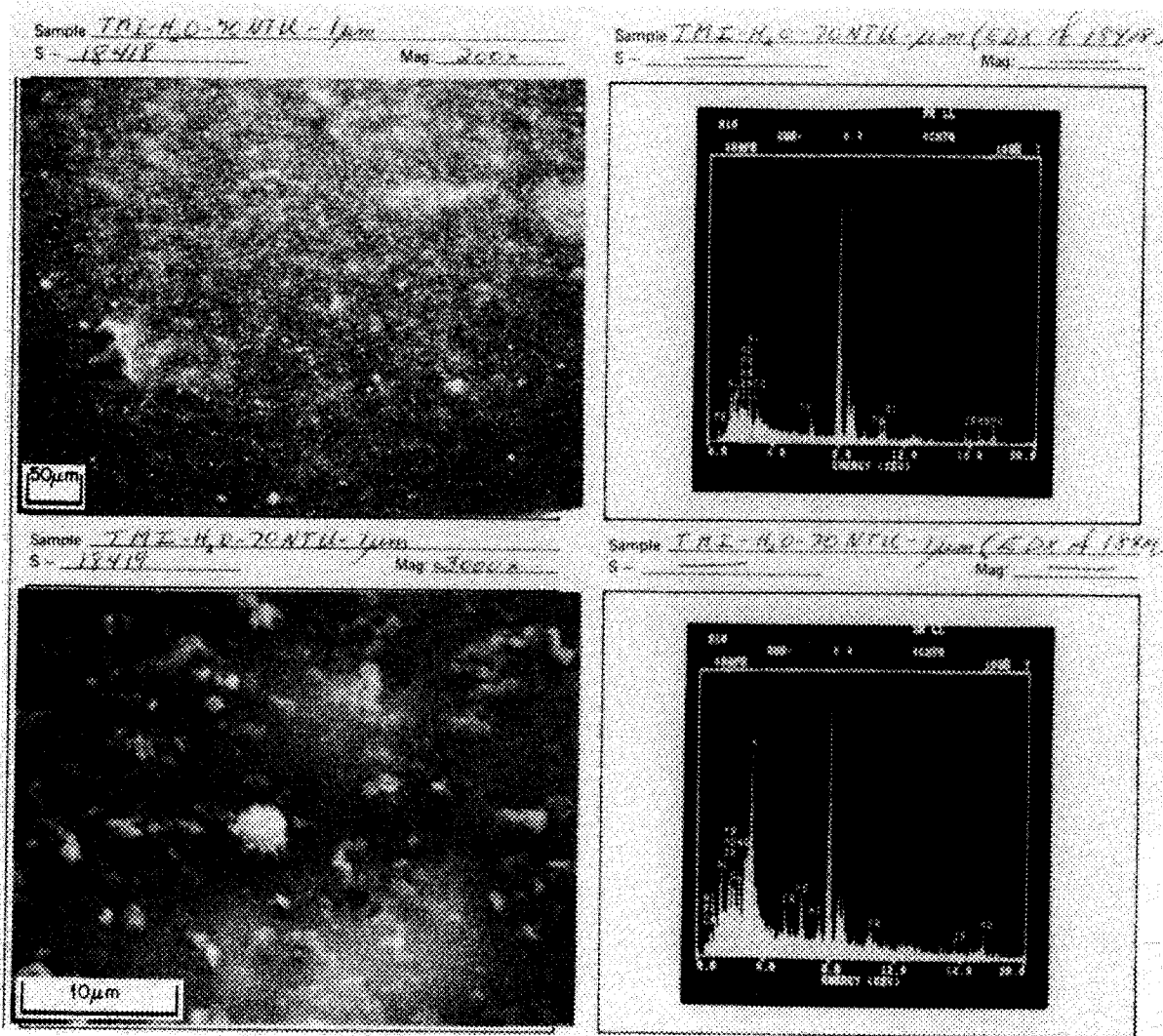
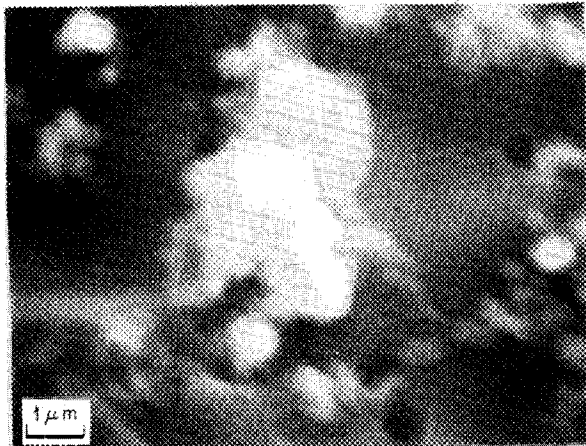
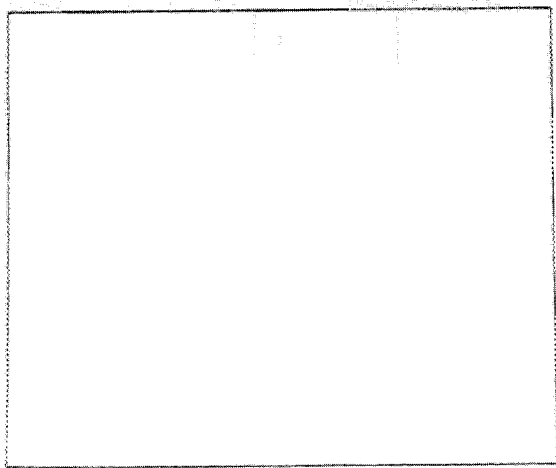


Fig. C.5. Nuclepore filter test 1 with 71-NTU water sample W1, 1-µm filter.

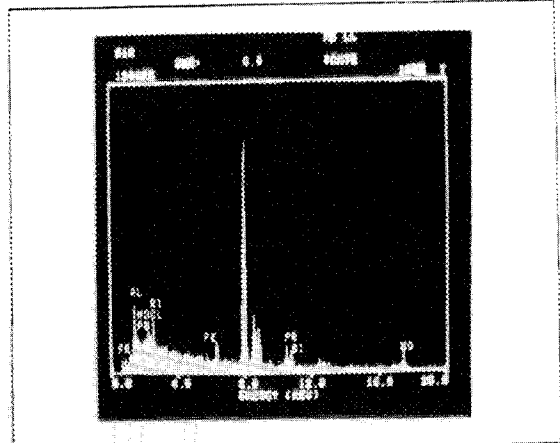
Sample TMI-H₂O-70 NTU 1µm
S - 18428 Mag: 10,000x



Sample _____
S - _____ Mag: _____



Sample TMI-H₂O-70 NTU 1µm (EDX)
S - _____ Mag: _____



Sample _____
S - _____ Mag: _____

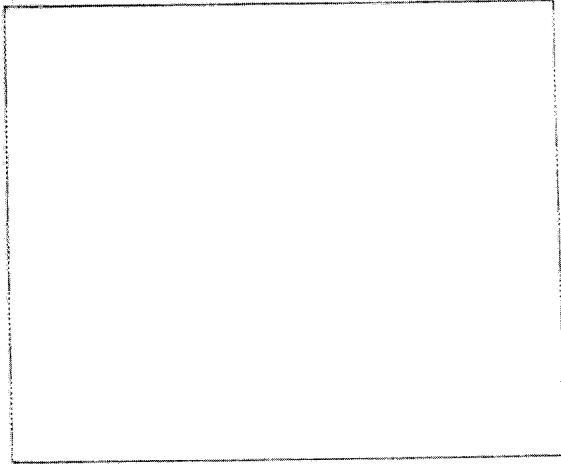


Fig. C.6. Nucleopore filter test 1 with 71-NTU water sample W1, 1-µm filter.

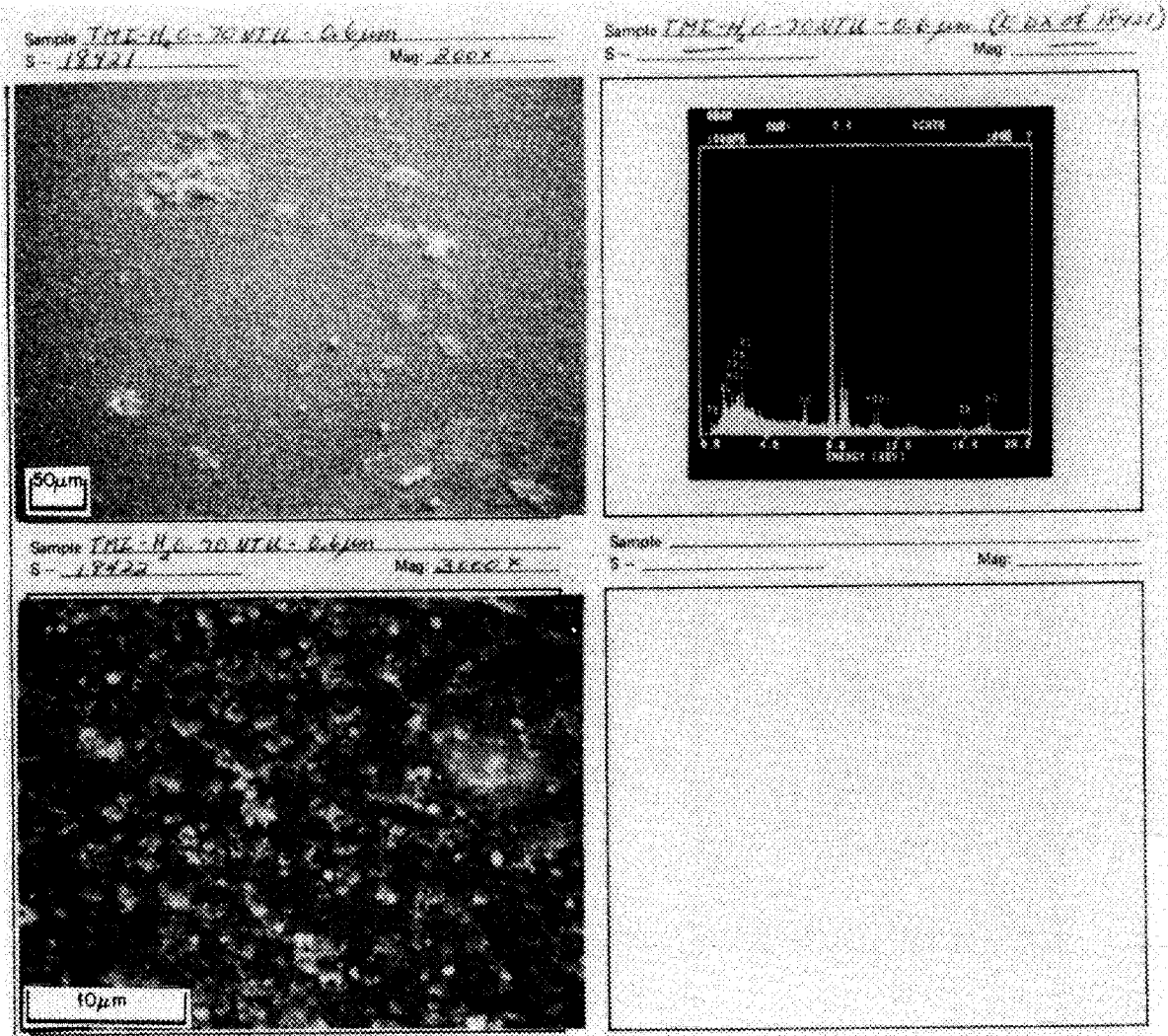
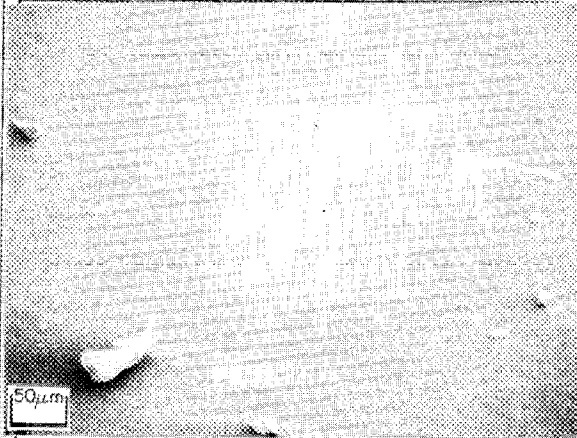
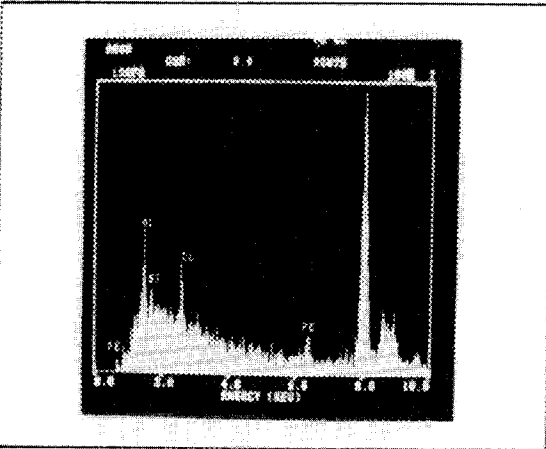


Fig. C.7. Nuclepore filter test 1 with 71-NTU water sample W1, 0.6-µm filter.

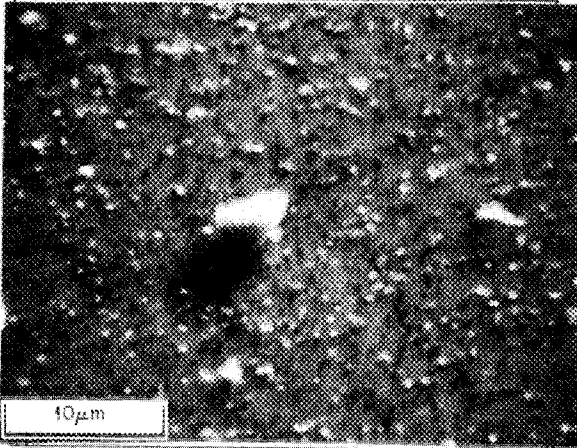
Sample TMI-H₂O-70 NTU-0.4µm
S - 18424 Mag: 200x



Sample TMI-H₂O-70 NTU-0.4µm (EDX of 18424)
S - _____ Mag: _____



Sample TMI-H₂O-70 NTU-0.4µm
S - 18425 Mag: 2000x



Sample _____
S - _____ Mag: _____

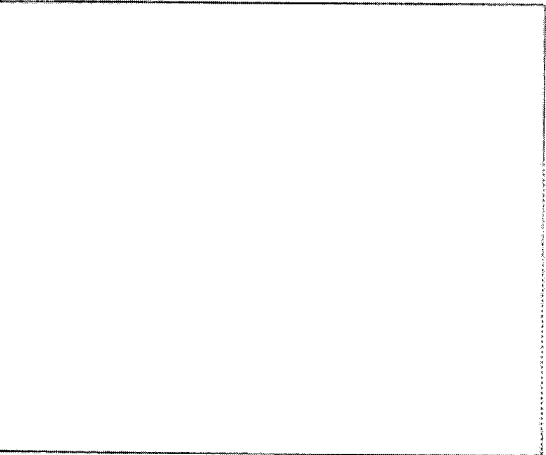


Fig. C.8. Nuclepore filter test 1 with 71-NTU water sample W1, 0.4-µm filter.

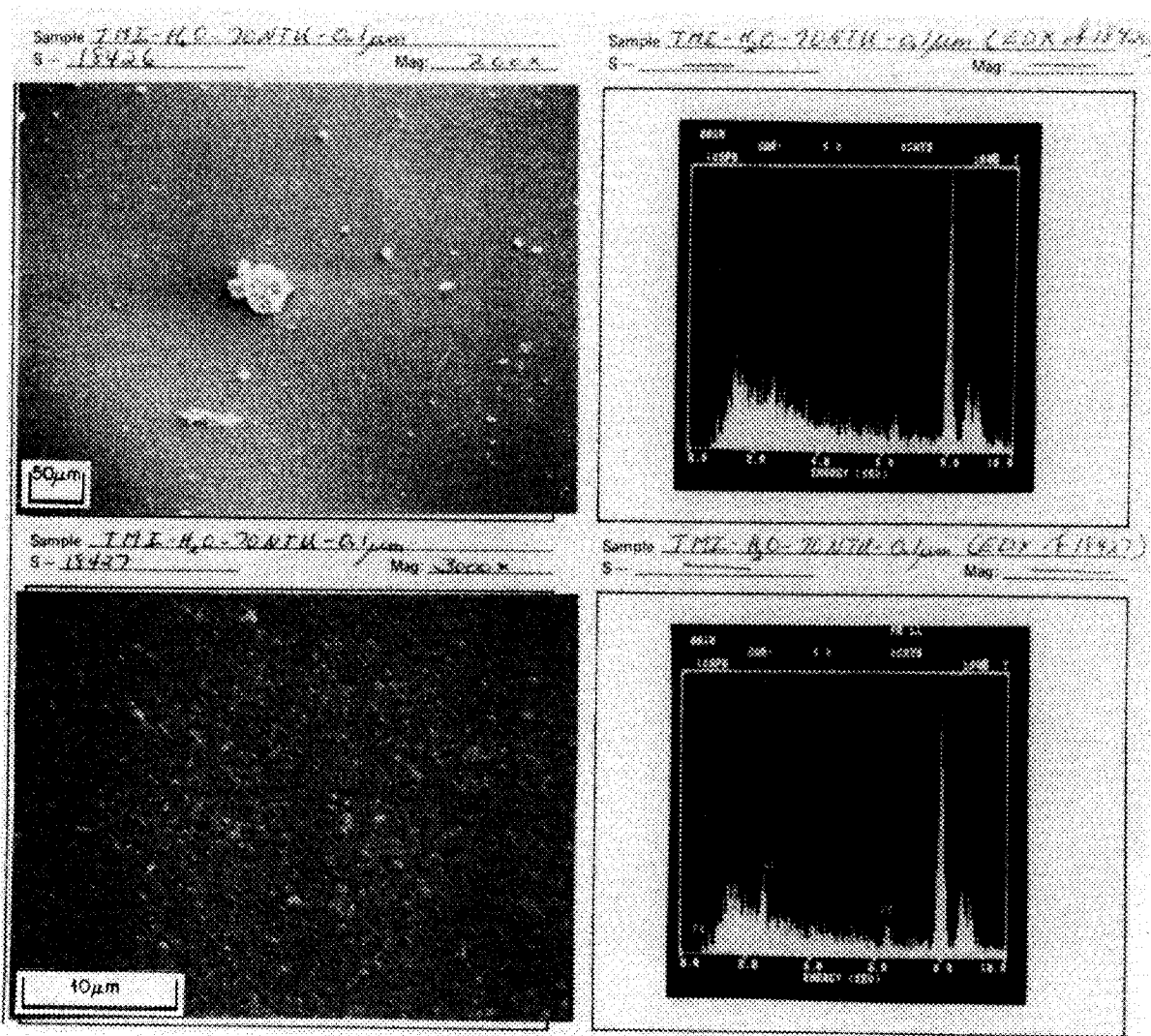


Fig. C.9. Nucleopore filter test 1 with 71-NTU water sample W1, 0.1-µm filter.

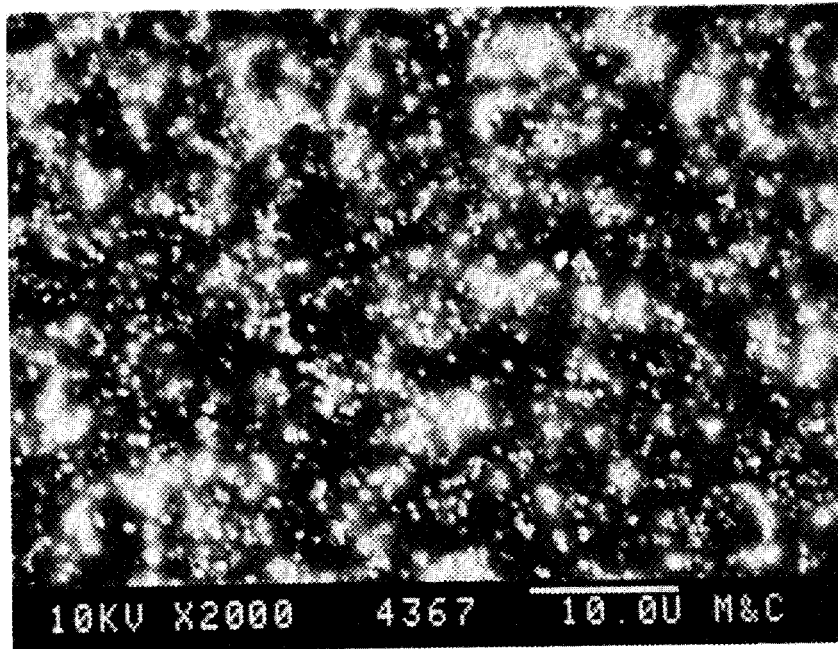


Fig. C.10. Nuclepore filter test 1 with 71-NTU water sample W1, 0.4- μm filter.

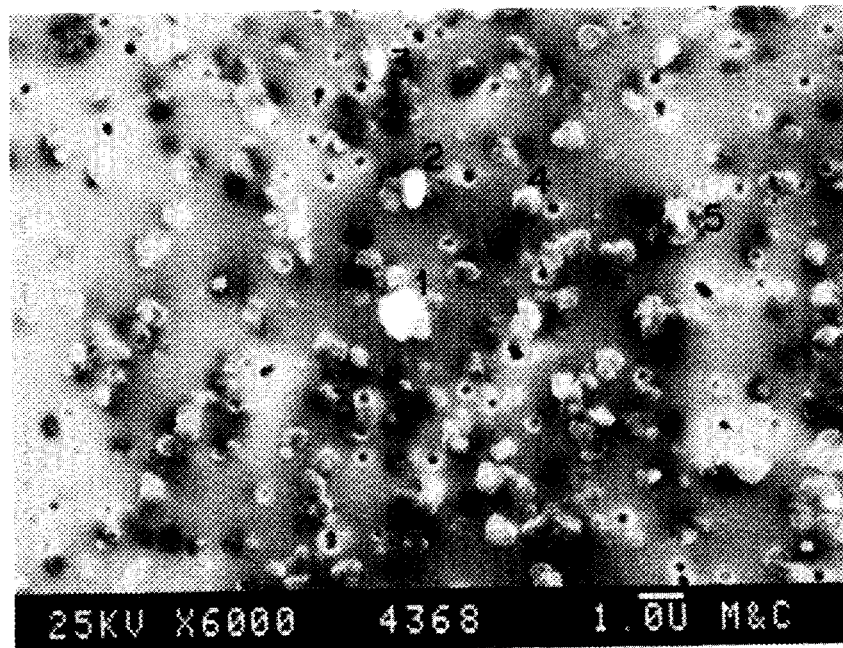


Fig. C.11. Nuclepore filter test 1 with 71-NTU water sample W1, 0.4- μm filter.

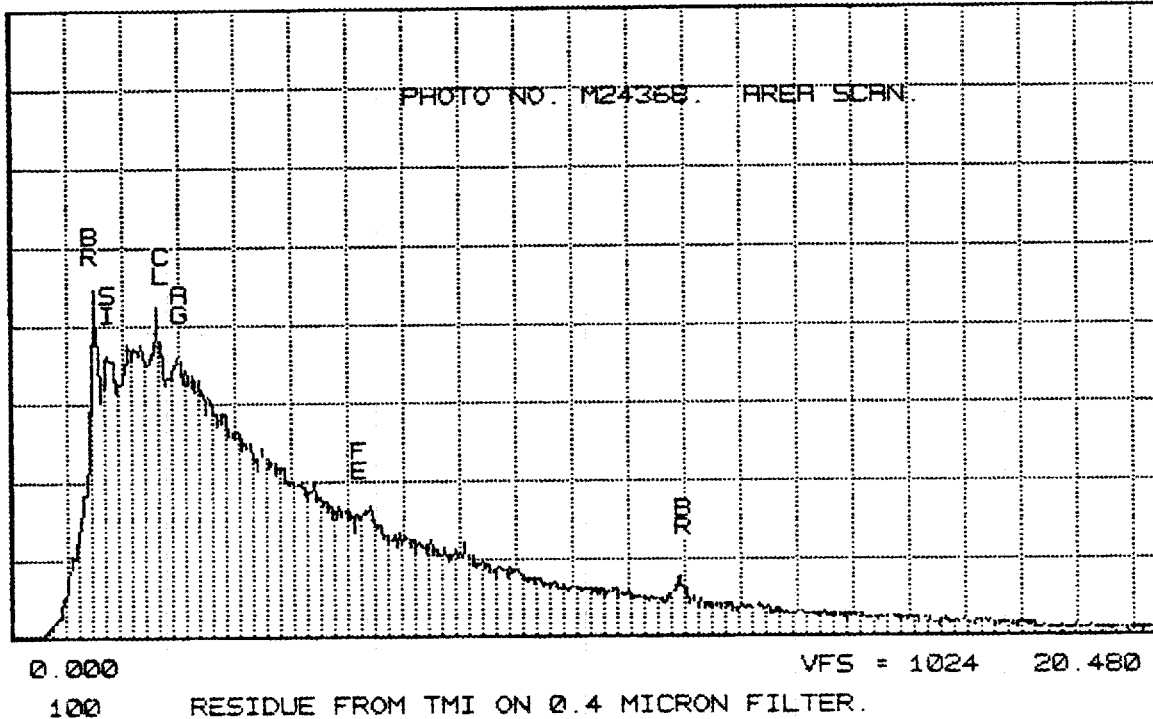


Fig. C.12. EDX of area of 4368 (see Fig. C.11).

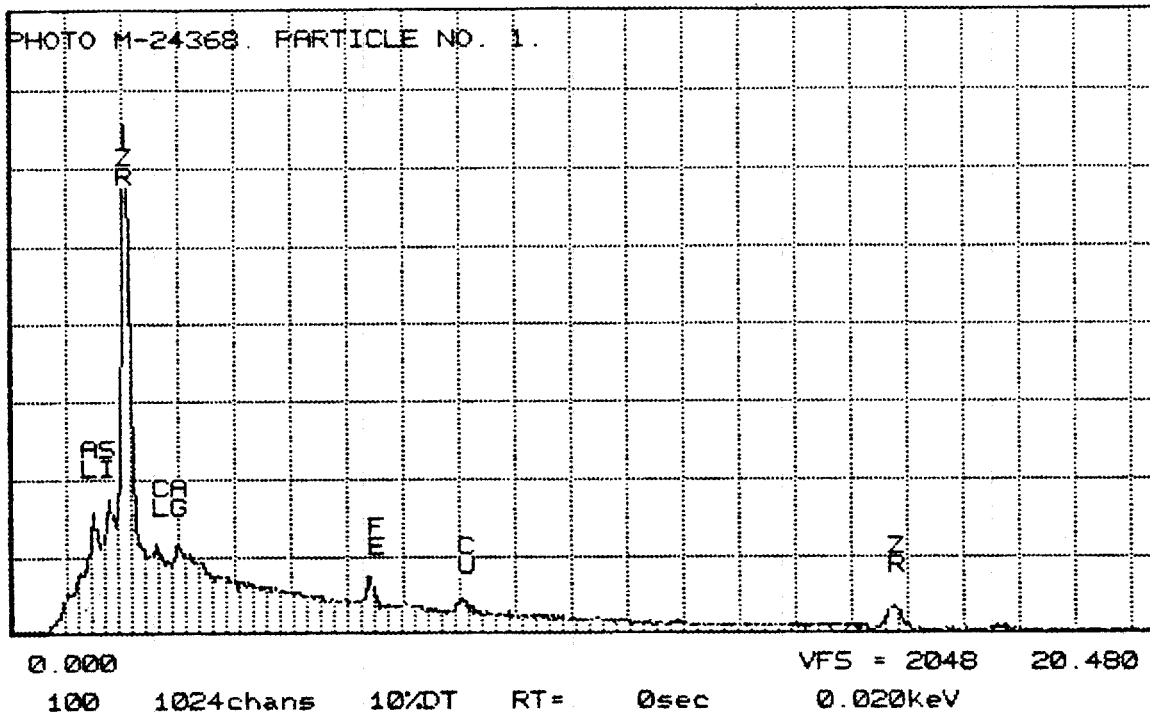


Fig. C.13. EDX of particle No. 1, 4368 (see Fig. C.11).

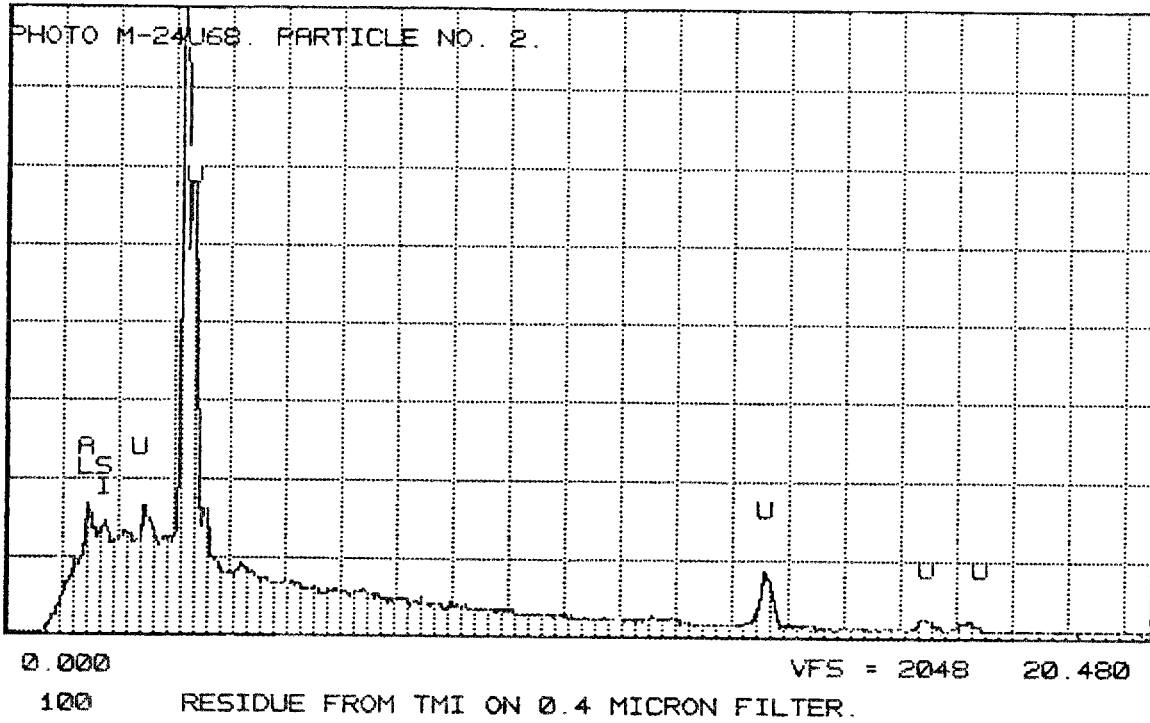


Fig. C.14. EDX of particle No. 2, 4368 (see Fig. C.11).

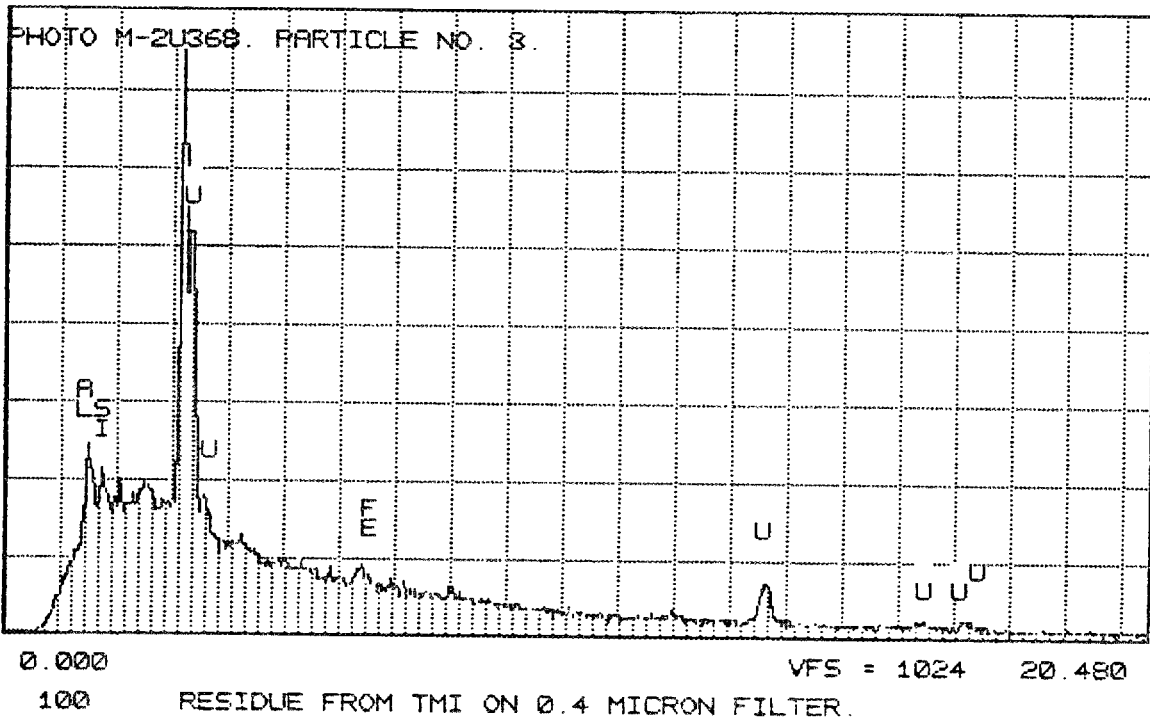


Fig. C.15. EDX of particle No. 3, 4368 (see Fig. C.11).

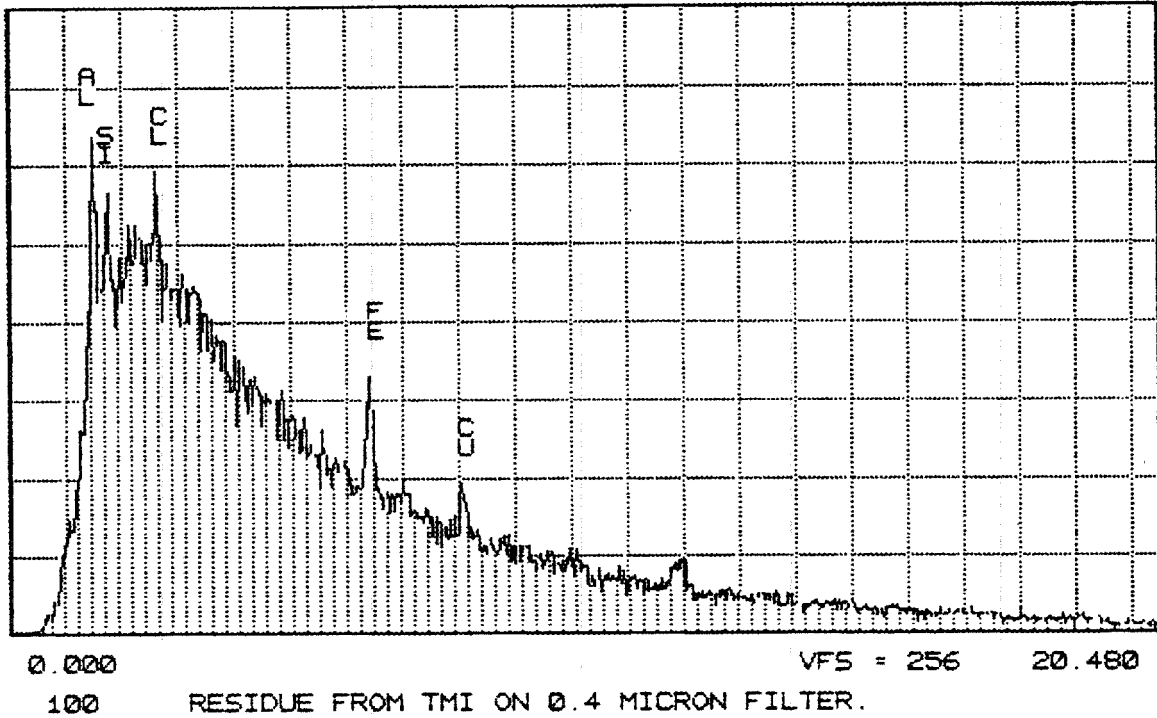


Fig. C.16. EDX of particle No. 4, 4368 (see Fig. C.11).

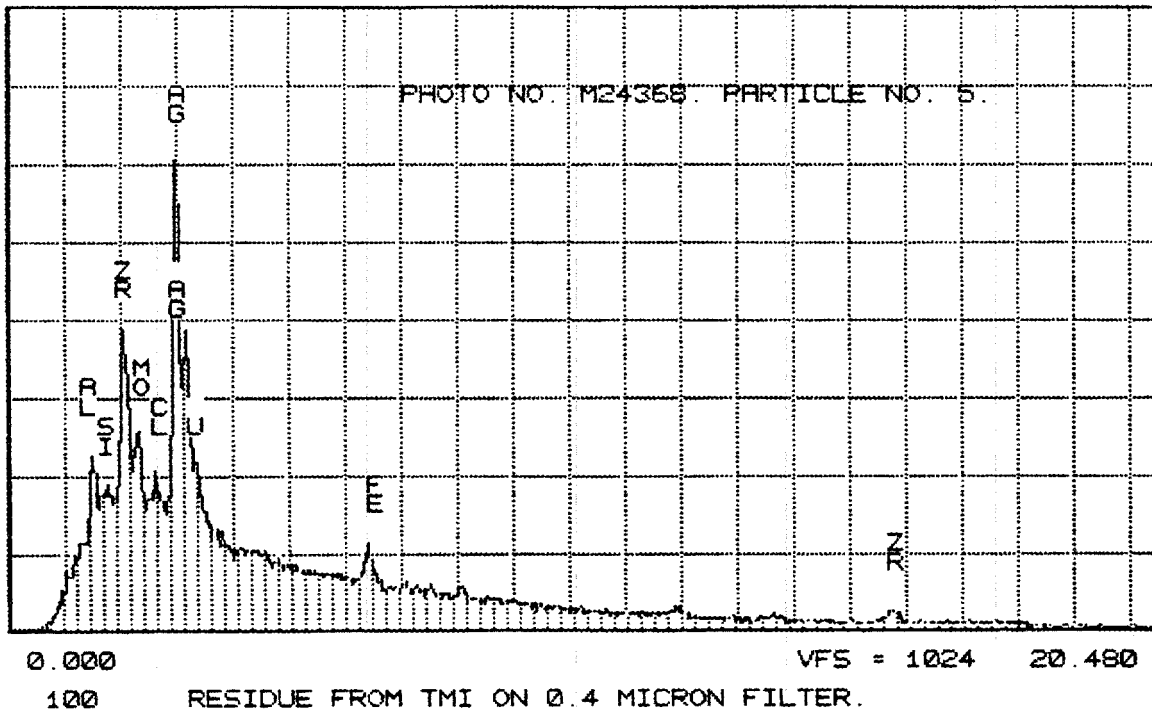


Fig. C.17. EDX of particle No. 5, 4368 (see Fig. C.11).

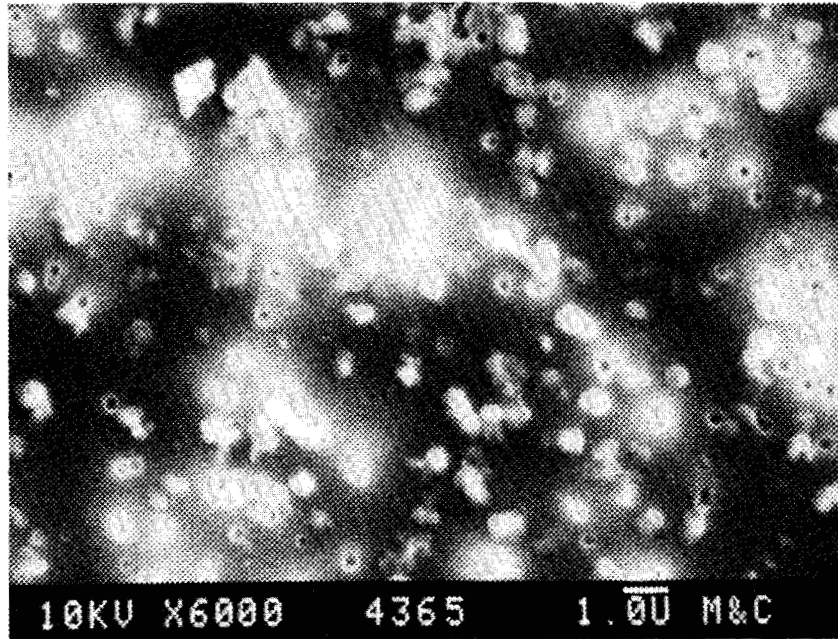


Fig. C.18. Nucleopore filter test 1 with 71-NTU water sample W1, 0.4- μm filter.

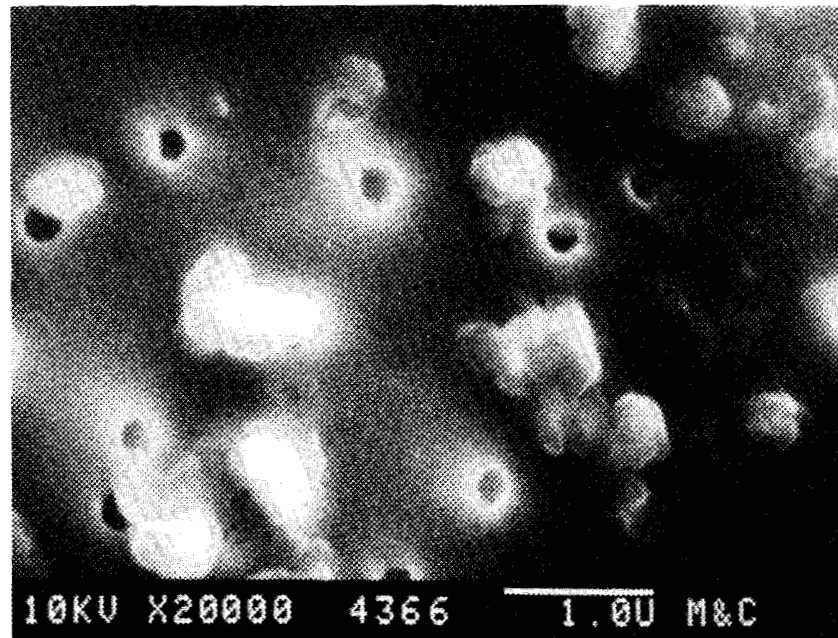


Fig. C.19. Nucleopore filter test 1 with 71-NTU water sample W1, 0.4- μm filter.

**Appendix D. PARTICLE CHARACTERIZATION DATA FOR SAMPLE W1
(TURBIDITY = ~71 NTU): FILTRATION TEST 2**

<u>Figure</u>		<u>Page</u>
D.1	Nuclepore filter test 2 with 71-NTU water sample W1, 10- μ m filter.	115
D.2	Nuclepore filter test 2 with 71-NTU water sample W1, 10- μ m filter.	116
D.3	Nuclepore filter test 2 with 71-NTU water sample W1, 10- μ m filter.	117
D.4	Nuclepore filter test 2 with 71-NTU water sample W1, 5- μ m filter	118
D.5	Nuclepore filter test 2 with 71-NTU water sample W1, 5- μ m filter	119
D.6	Nuclepore filter test 2 with 71-NTU water sample W1, 5- μ m filter	120
D.7	Nuclepore filter test 2 with 71-NTU water sample W1, 5- μ m filter	121
D.8	Nuclepore filter test 2 with 71-NTU water sample W1, 2- μ m filter	122
D.9	Nuclepore filter test 2 with 71-NTU water sample W1, 2- μ m filter	123
D.10	Nuclepore filter test 2 with 71-NTU water sample W1, diluted 2- μ m filter	124
D.11	Nuclepore filter test 2 with 71-NTU water sample W1, diluted 2- μ m filter	125
D.12	Nuclepore filter test 2 with 71-NTU water sample W1, diluted 2- μ m filter	126
D.13	Nuclepore filter test 2 with 71-NTU water sample W1, diluted 2- μ m filter	127
D.14	Nuclepore filter test 2 with 71-NTU water sample W1, diluted 2- μ m filter	128
D.15	Nuclepore filter test 2 with 71-NTU water sample W1, 1- μ m filter	129

<u>Figure</u>	<u>Page</u>
D.16	Nuclepore filter test 2 with 71-NTU water sample W1, 1- μ m filter 130
D.17	Nuclepore filter test 2 with 71-NTU water sample W1, 1- μ m filter 131
D.18	Nuclepore filter test 2 with 71-NTU water sample W1, 0.8- μ m filter 132
D.19	EDX of particle cluster, 4387 (see Fig. D.18) 132
D.20	Nuclepore filter test 2 with 71-NTU water sample W1, 0.8- μ m filter 133
D.21	EDX of "fish-egg" particle near center, 4388 (see Fig. D.20). 133
D.22	Nuclepore filter test 2 with 71-NTU water sample W1, 0.8- μ m filter 134
D.23	EDX of bright particle near center, 4389 (see Fig. D.22). 134
D.24	Nuclepore filter test 2 with 71-NTU water sample W1, 0.8- μ m filter 135
D.25	EDX of bright cluster near center, 4390 (see Fig. D.24). 135
D.26	Nuclepore filter test 2 with 71-NTU water sample W1, 0.6- μ m filter 136
D.27	EDX of area of 4392 (see Fig. D.26) 136
D.28	Nuclepore filter test 2 with 71-NTU water sample W1, 0.6- μ m filter 137
D.29	EDX of particle No. 1, 4391 (see Fig. D.28) 137
D.30	EDX of particle No. 2, 4391 (see Fig. D.28) 138
D.31	EDX of particle No. 3, 4391 (see Fig. D.28) 138
D.32	EDX of particle No. 4, 4391 (see Fig. D.28) 139
D.33	Nuclepore filter test 2 with 71-NTU water sample W1, 0.4- μ m filter 140
D.34	EDX of area of 4394 (see Fig. D.33) 140

<u>Figure</u>		<u>Page</u>
D.35	Nuclepore filter test 2 with 71-NTU water sample W1, 0.4- μ m filter.	141
D.36	EDX of white particle near center, 4395 (see Fig. D.35)	141
D.37	Nuclepore filter test 2 with 71-NTU water sample W1, 0.4- μ m filter.	142
D.38	Nuclepore filter test 2 with 71-NTU water sample W1, 0.4- μ m filter, BEI	142
D.39	Nuclepore filter test 2 with 71-NTU water sample W1, 0.1- μ m filter.	143
D.40	Nuclepore filter test 2 with 71-NTU water sample W1, 0.1- μ m filter, BEI	143
D.41	EDX of particle No. 1, 4398 (see Fig. D.39).	144
D.42	EDX of particle No. 2a, 4398 (see Fig. D.39)	144
D.43	EDX of particle No. 2b, 4398 (see Fig. D.39)	145
D.44	EDX of particle No. 3, 4398 (see Fig. D.39).	145

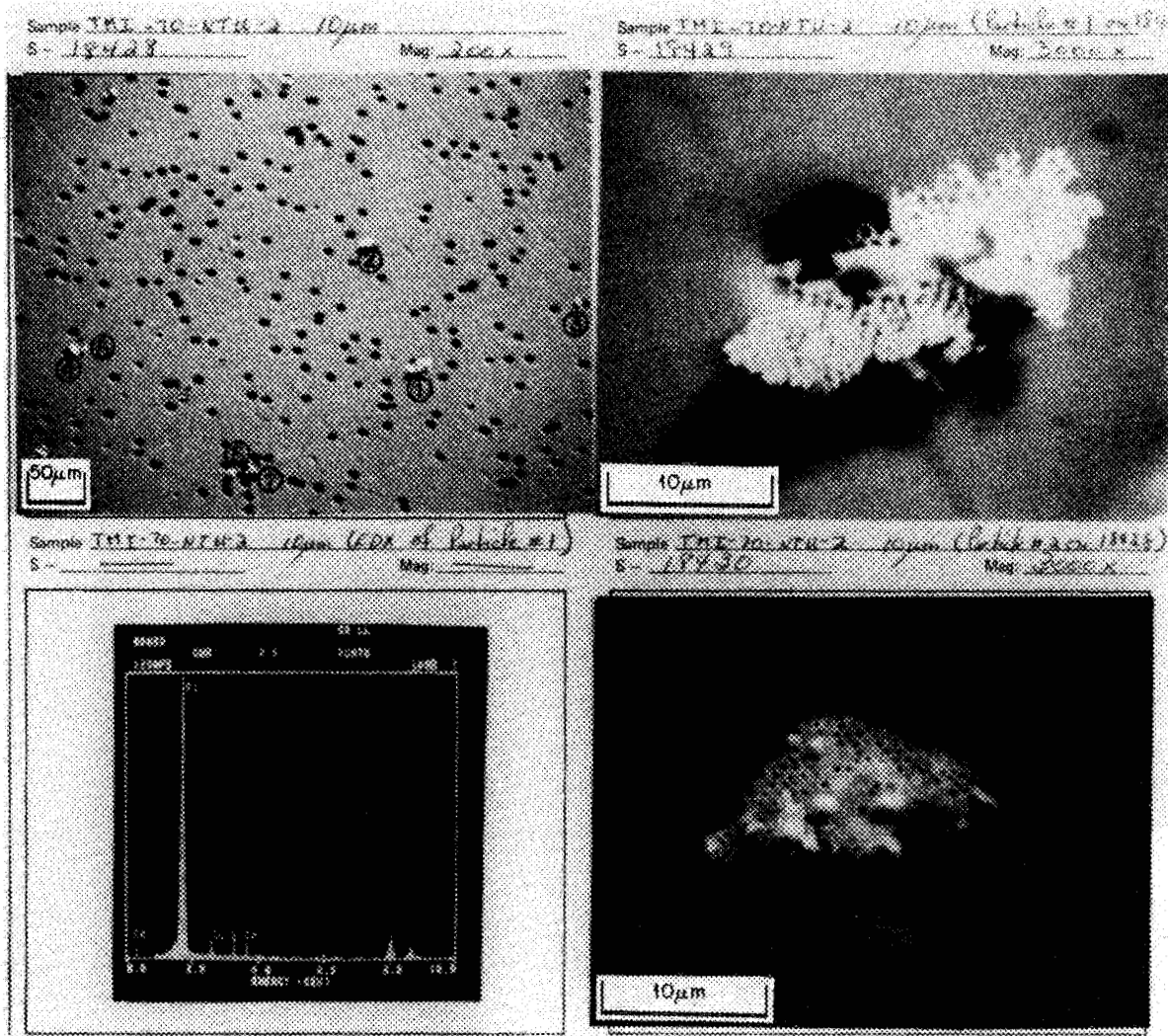
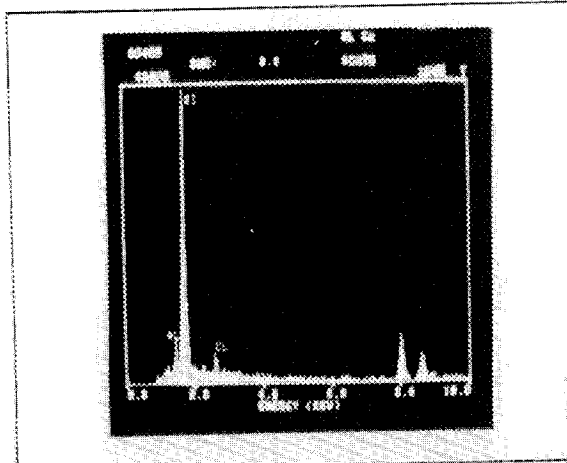
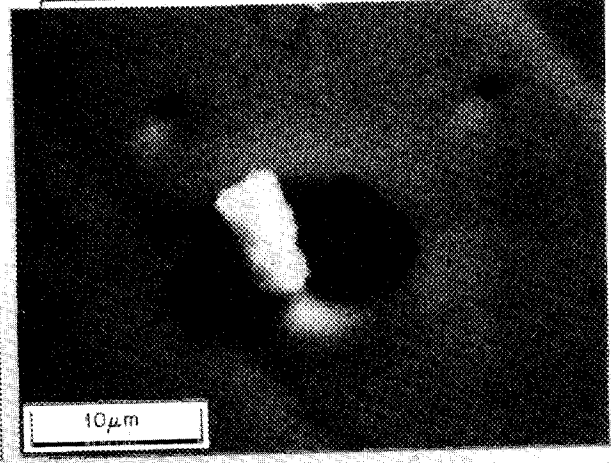


Fig. D.1. Nuclepore filter test 2 with 71-NTU water sample W1, 10-µm filter.

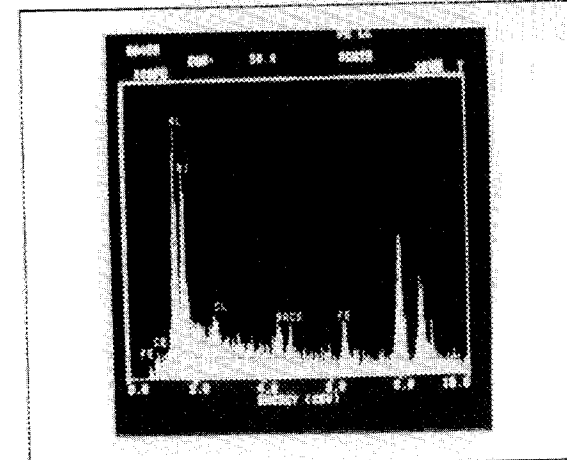
Sample 71-NTU-2 10µm (EPA of Parkville #2)
S - 18431 Mag: 3000x



Sample 71-NTU-2 10µm (EPA of Parkville #2)
S - 18431 Mag: 3000x



Sample 71-NTU-2 10µm (EPA of Parkville #2)
S - 18432 Mag: 3000x



Sample 71-NTU-2 10µm (EPA of Parkville #2)
S - 18432 Mag: 3000x

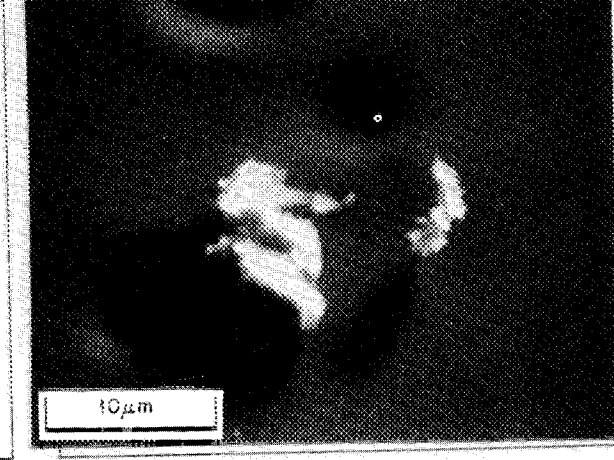


Fig. D.2. Nuclepore filter test 2 with 71-NTU water sample W1, 10-µm filter.

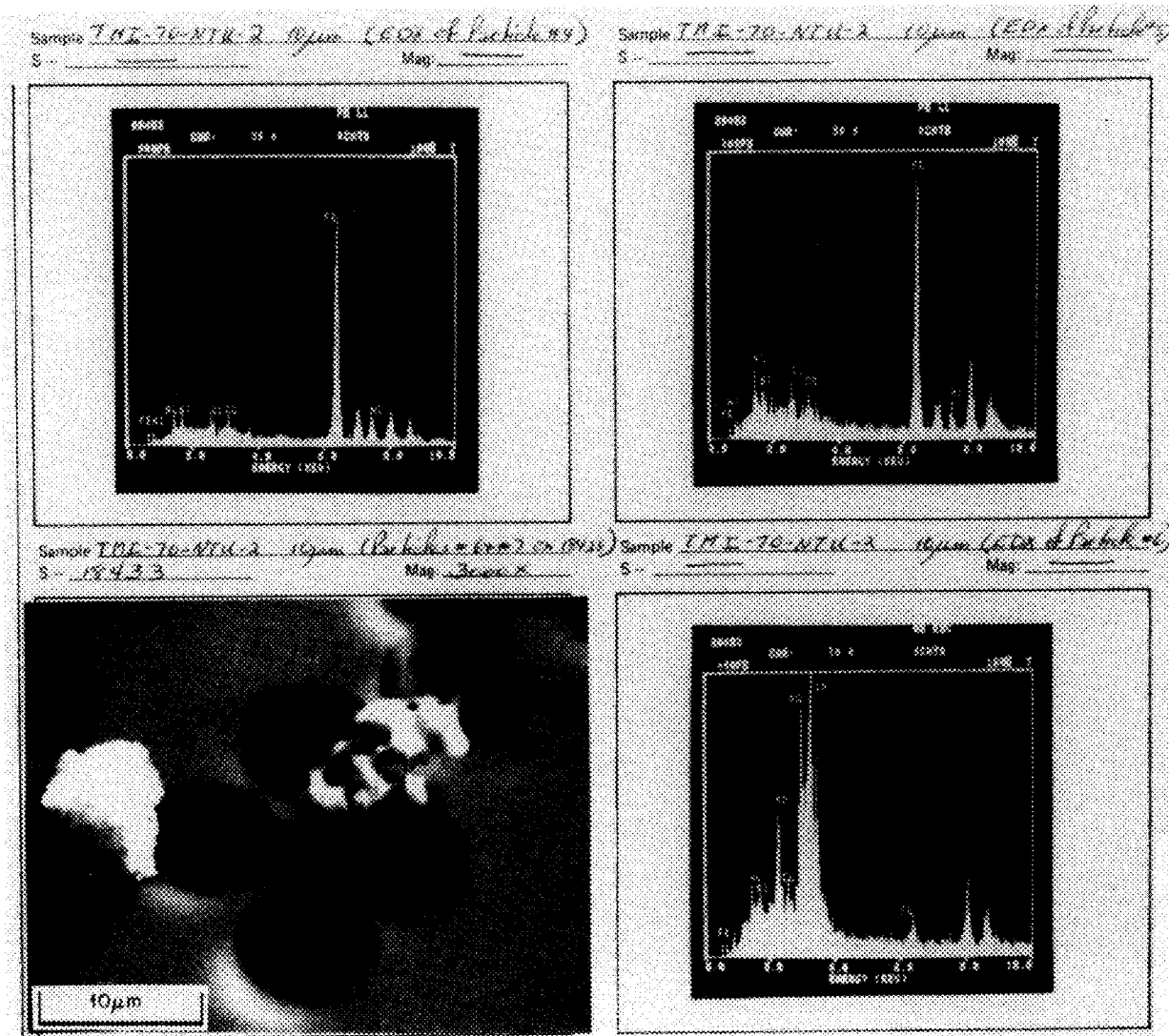
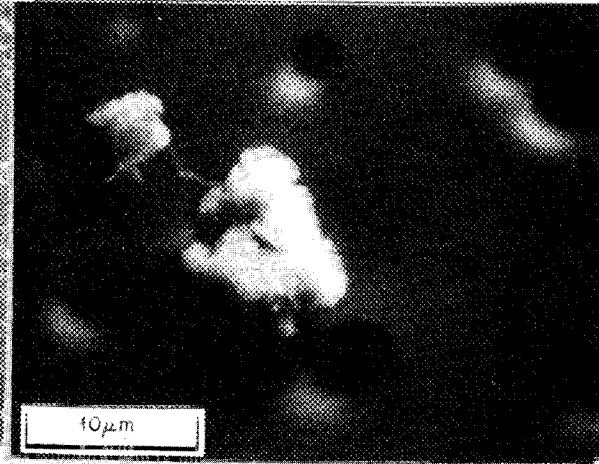
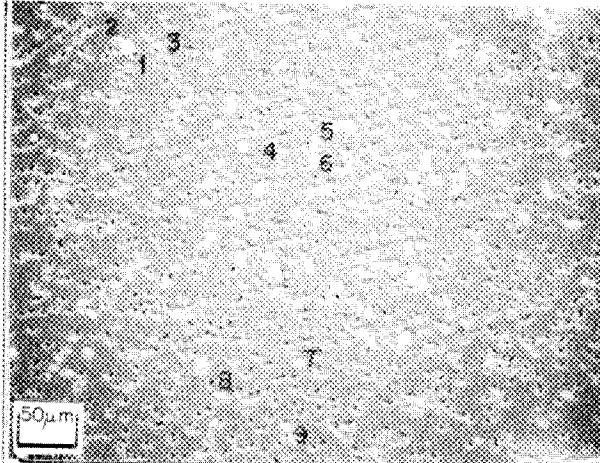


Fig. D.3. Nucleopore filter test 2 with 71-NTU water sample W1, 10-µm filter.

Sample 71E-70-NTU-2 5µm
S - 18434 Mag: 200X

Sample 71E-70-NTU-2 5µm (EDX of particle #1)
S - 18435 Mag: 3000X



Sample 71E-70-NTU-2 5µm (EDX of particle #1)
S - _____ Mag: _____

Sample 71E-70-NTU-2 5µm (EDX of particle #2)
S - _____ Mag: _____

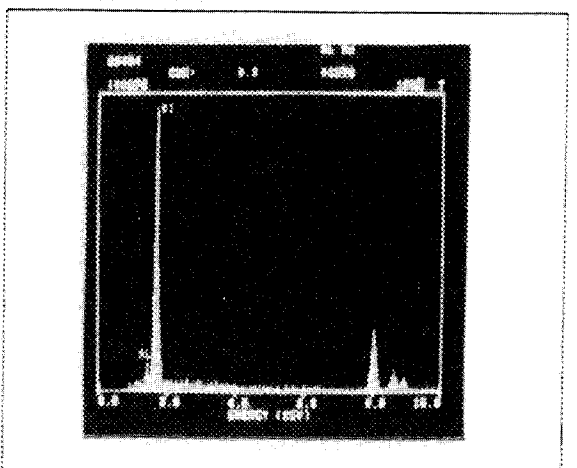
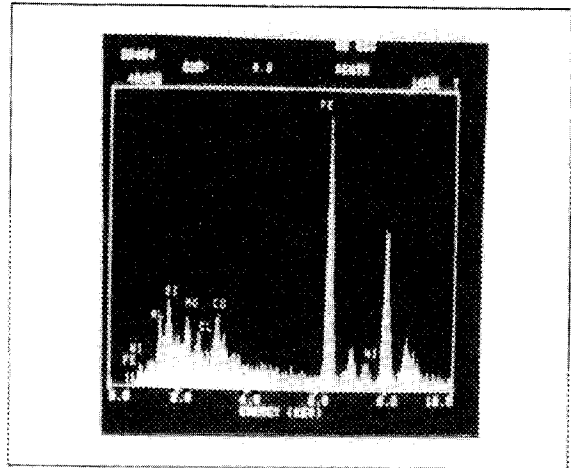


Fig. D.4. Nuclepore filter test 2 with 71-NTU water sample W1, 5-µm filter.

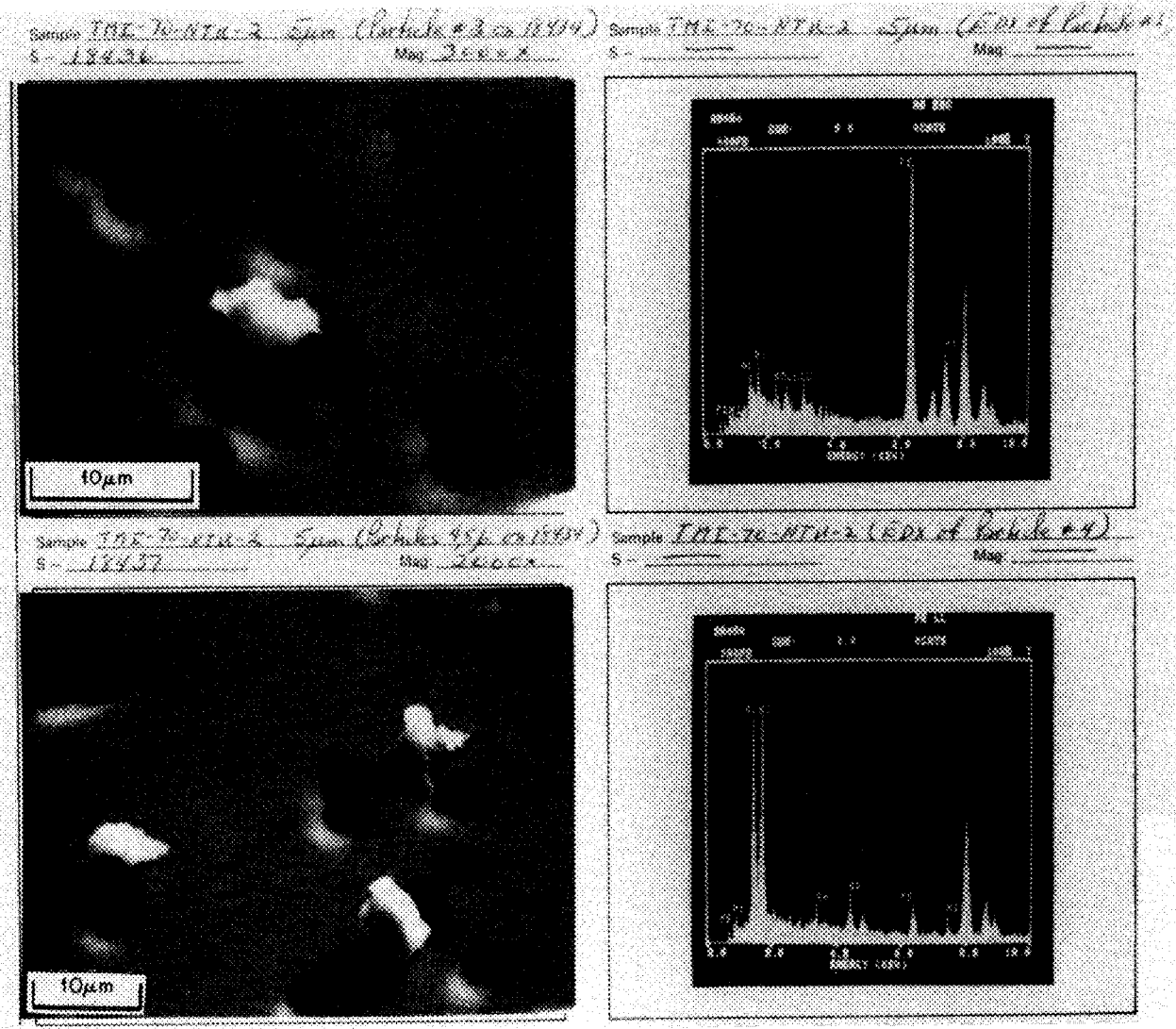


Fig. D.5. Nuclepore filter test 2 with 71-NTU water sample W1, 5-µm filter.

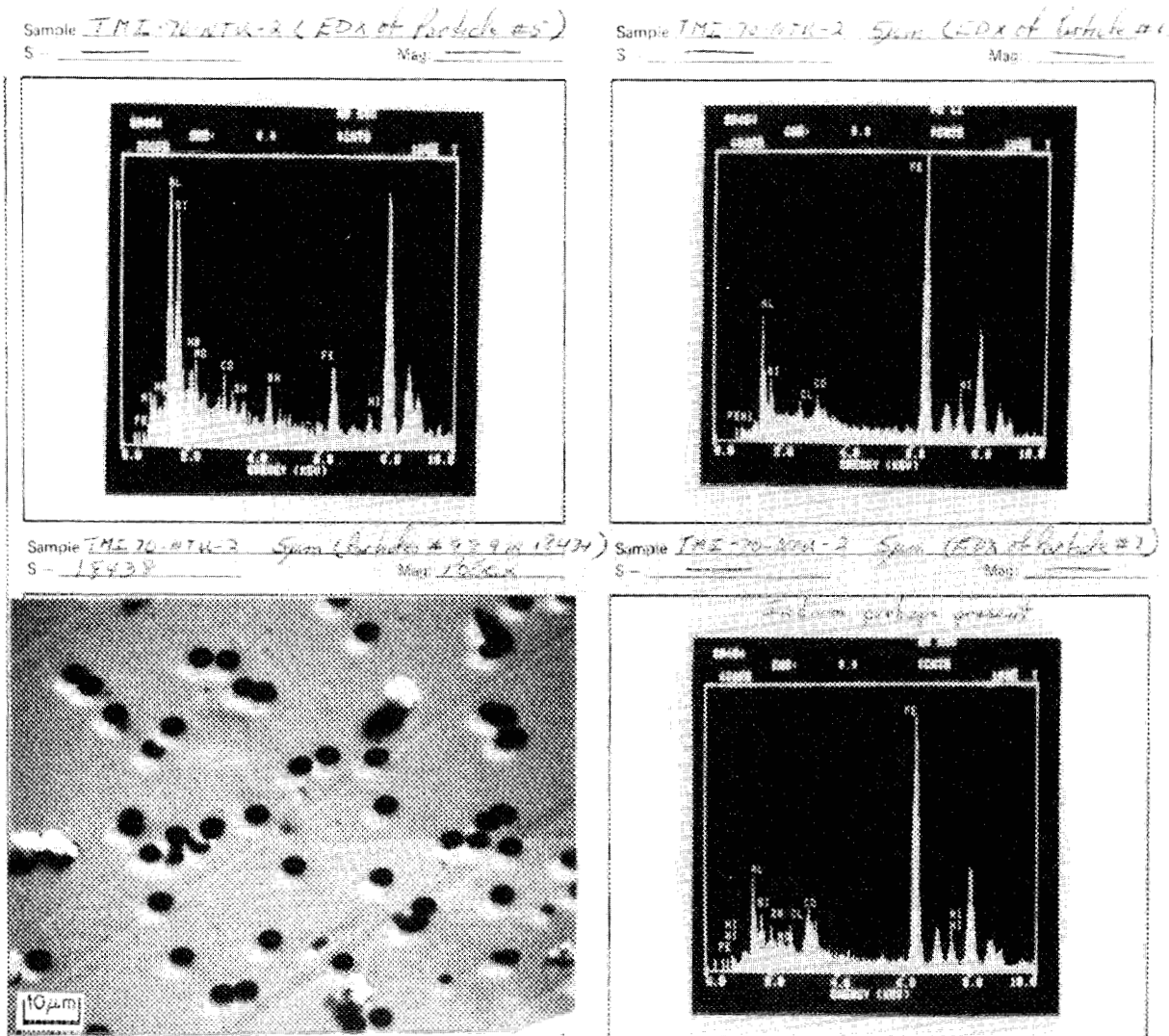


Fig. D.6. Nucleopore filter test 2 with 71-NTU water sample W1, 5- μ m filter.

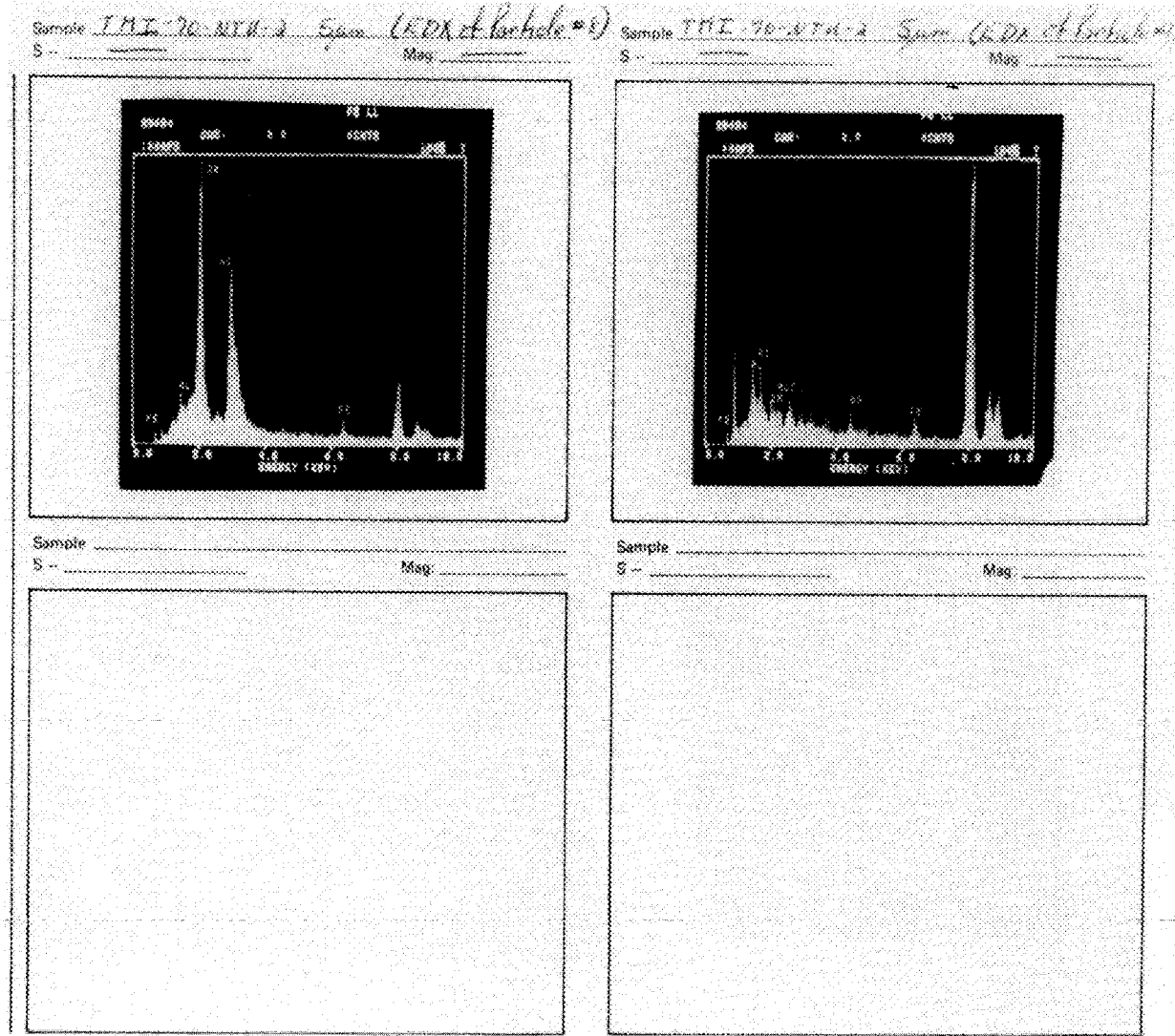
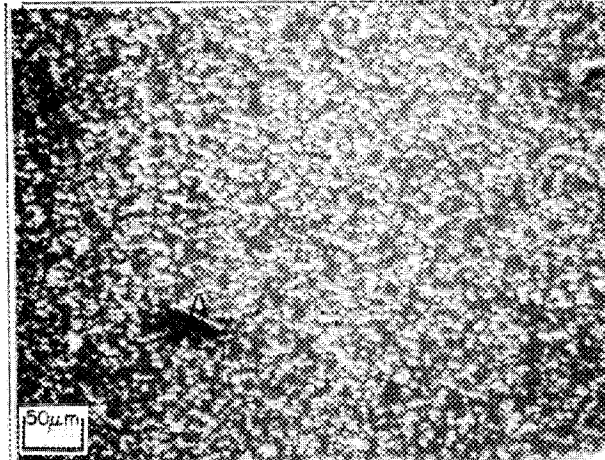
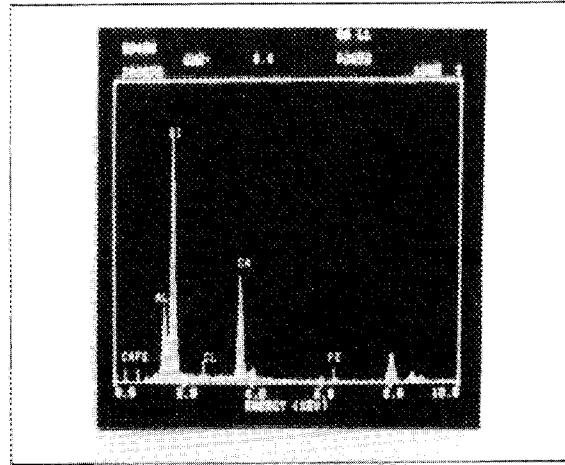


Fig. D.7. Nucleopore filter test 2 with 71-NTU water sample W1, 5-µm filter.

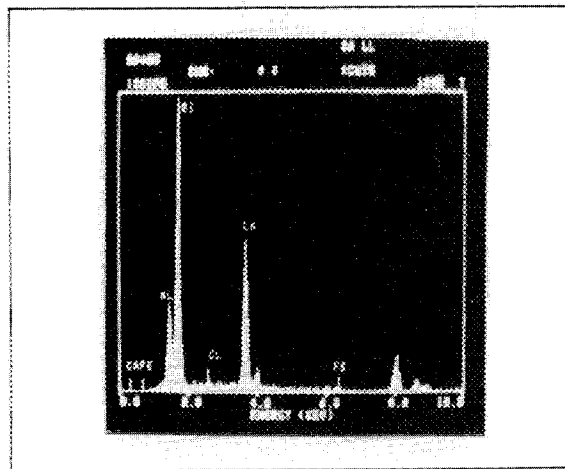
Sample IME-70-NTU-2 2µm
S- 18442 Mag 200x



Sample IME-70-NTU-2 3µm LED A/B on 18442
S- _____ Mag _____



Sample IME-70-NTU-2 2µm LED A/B on 18442
S- _____ Mag _____



Sample IME-70-NTU-2 2µm
S- 18442 Mag 200x

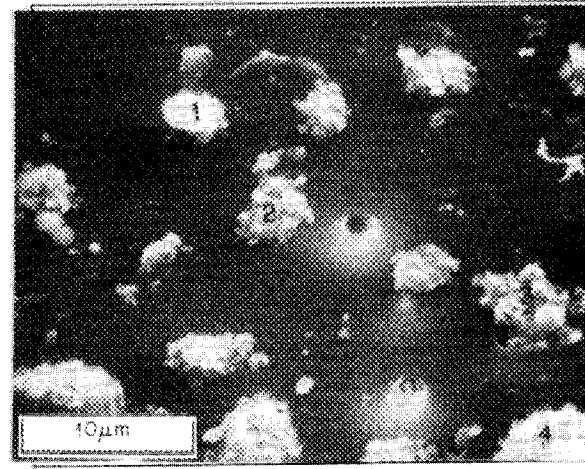


Fig. D.8. Nucleopore filter test 2 with 71-NTU water sample W1, 2-µm filter.

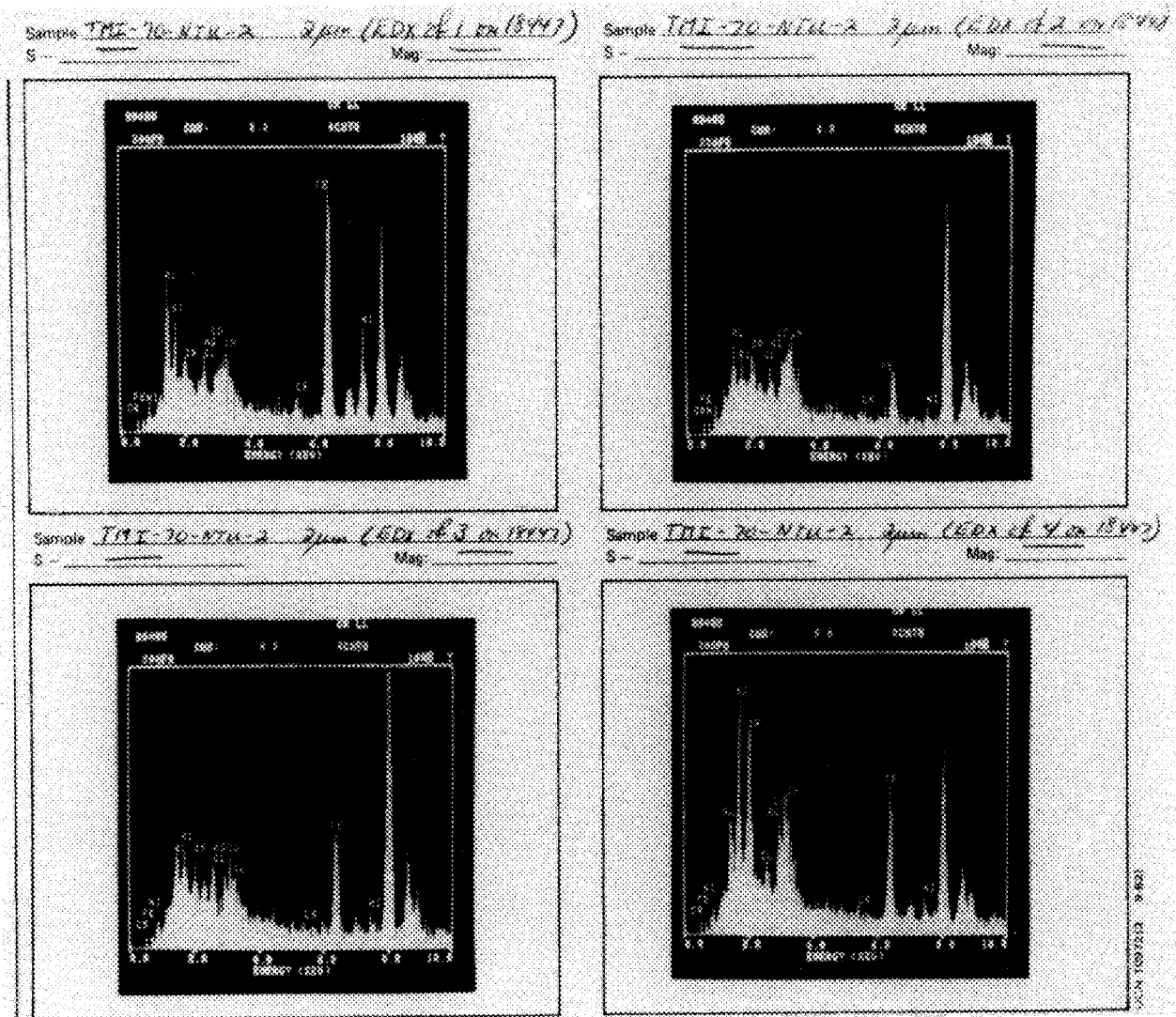


Fig. D.9. Nuclepore filter test 2 with 71-NTU water sample W1, 2-µm filter.

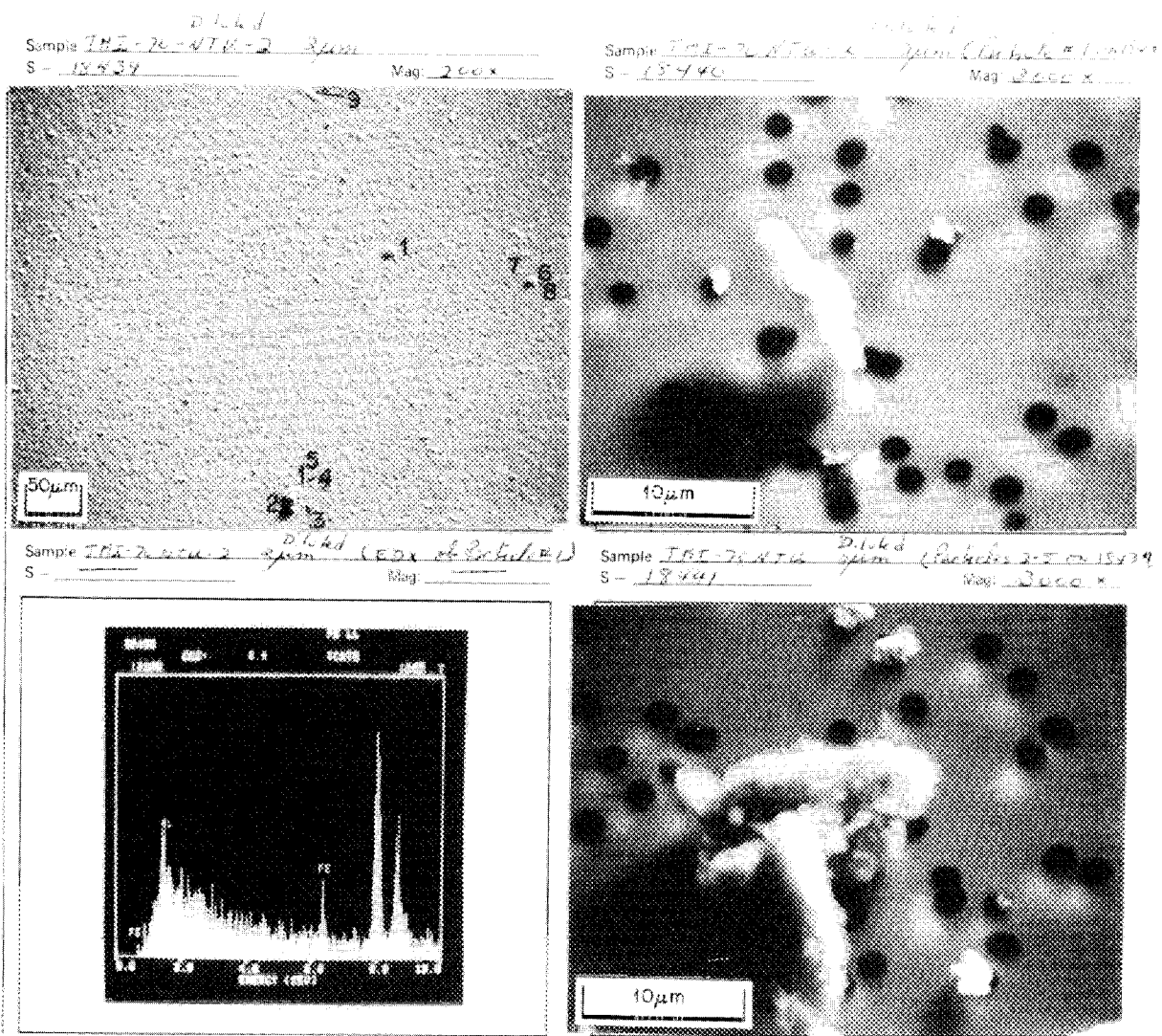


Fig. D.10. Nucleopore filter test 2 with 71-NTU water sample W1, diluted 2-µm filter.

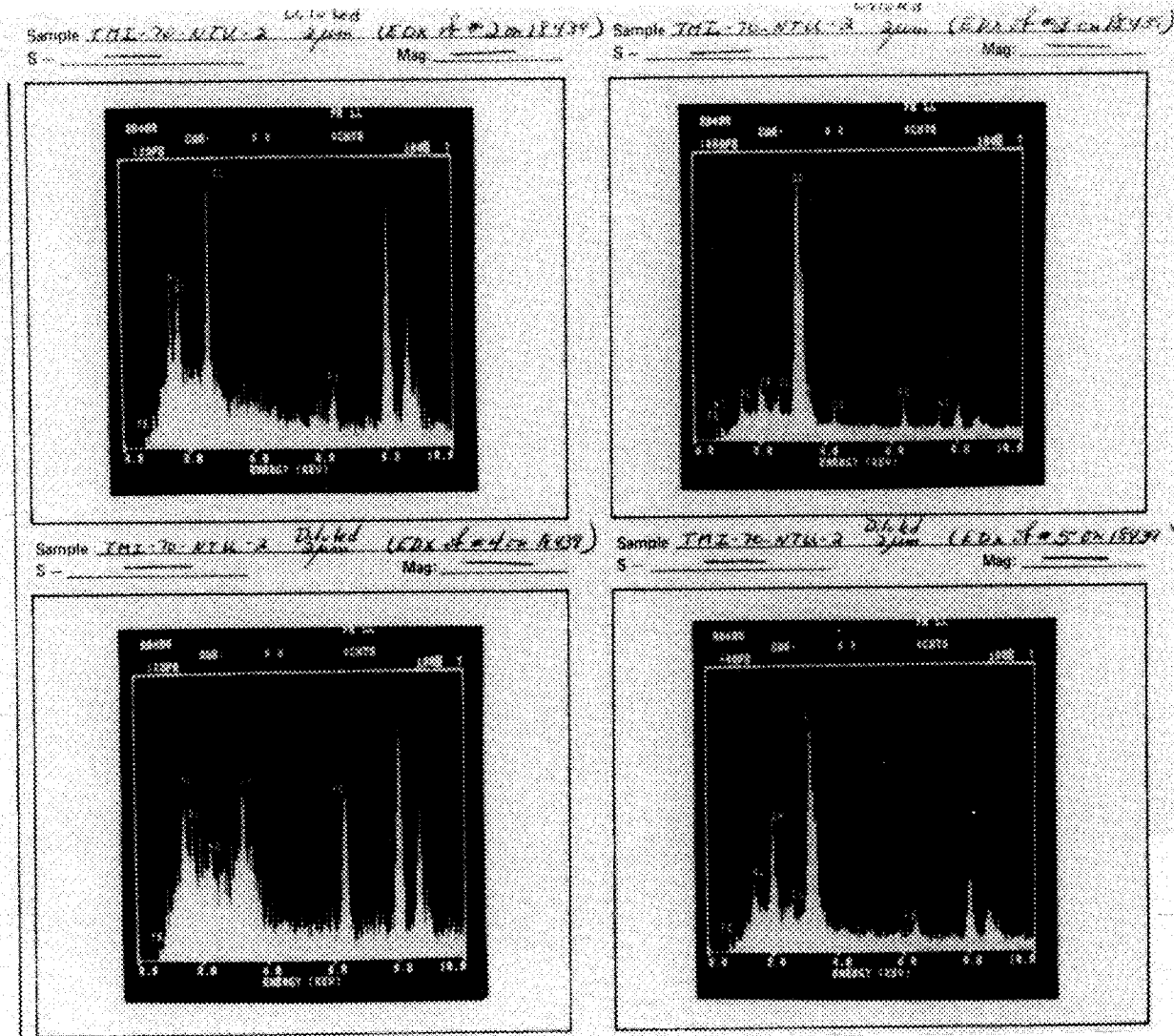


Fig. D.11. Nuclepore filter test 2 with 71-NTU water sample W1, diluted 2-µm filter.

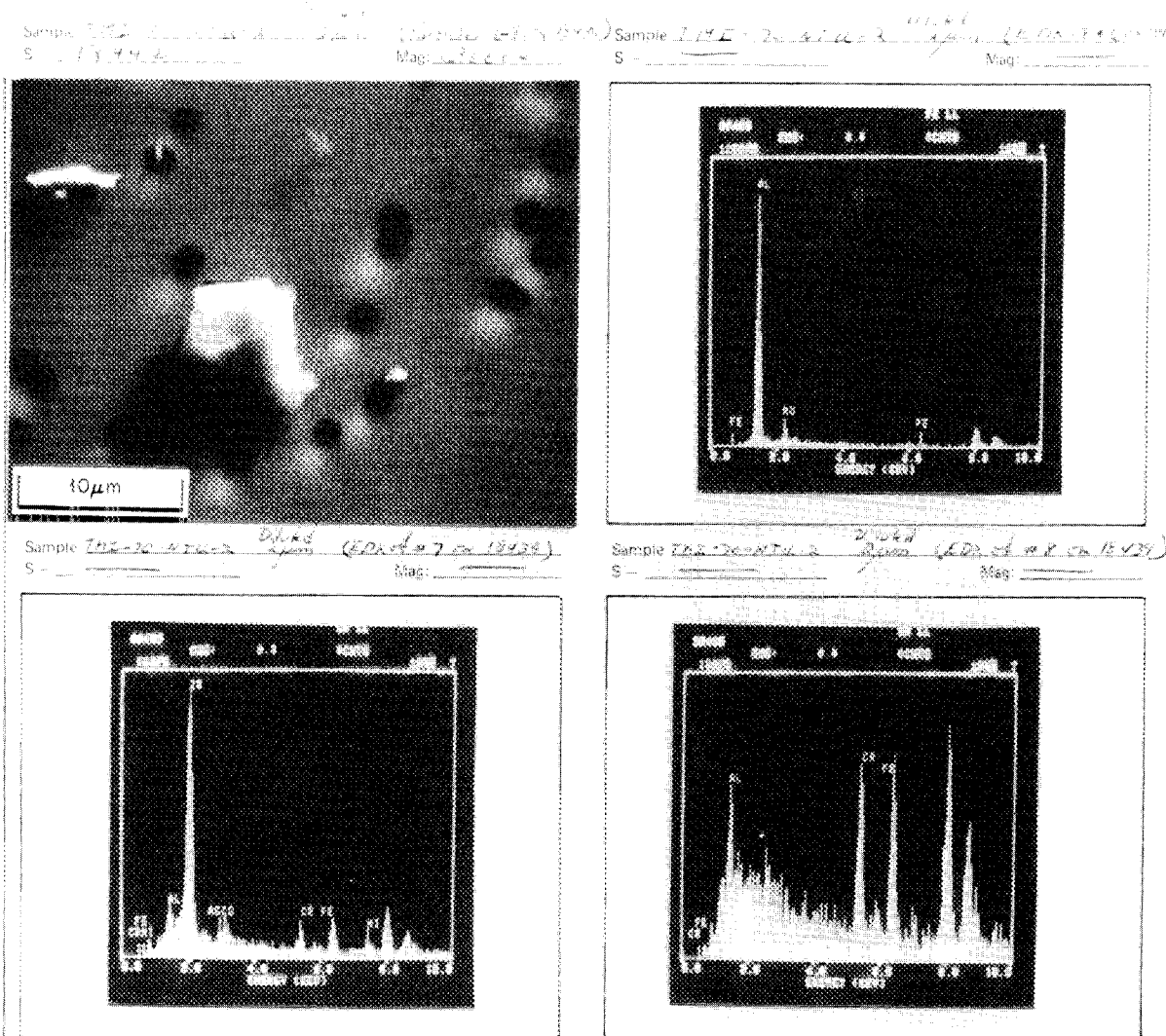


Fig. D.12. Nucleopore filter test 2 with 71-NTU water sample W1, diluted 2-µm filter.

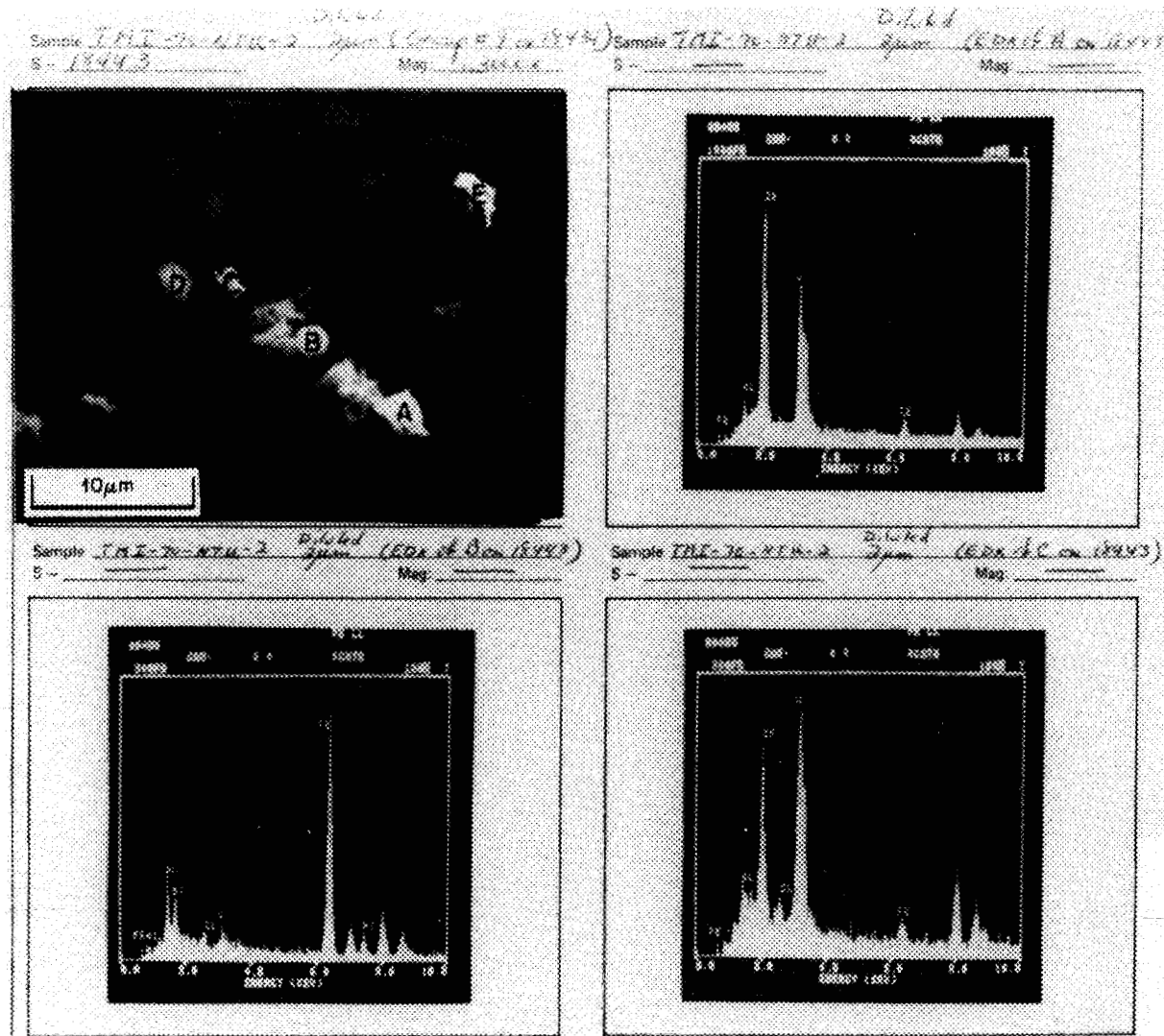
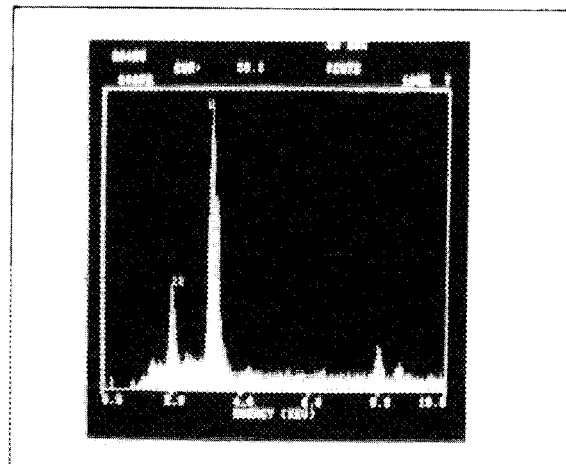
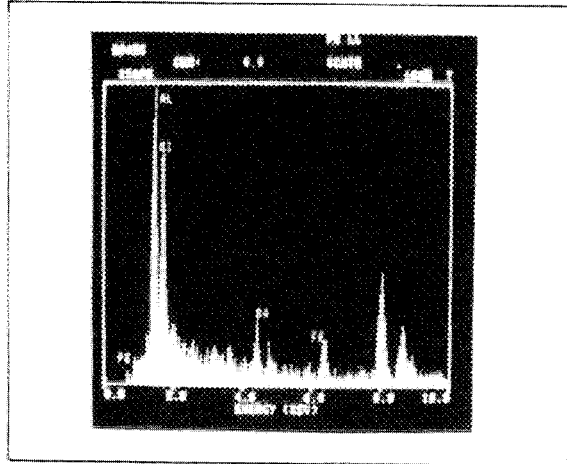


Fig. D.13. Nucleopore filter test 2 with 71-NTU water sample W1, diluted 2-µm filter.

Sample IME-70-W11-2 ^{Vols 6 & 7} 3µm (EDAC/DMAB)
S _____ Mag: _____

Sample IME-70-W11-2 ^{Vols 6 & 7} 3µm (EDAC/DMAB)
S _____ Mag: _____



Sample _____
S _____ Mag: _____

Sample _____
S _____ Mag: _____

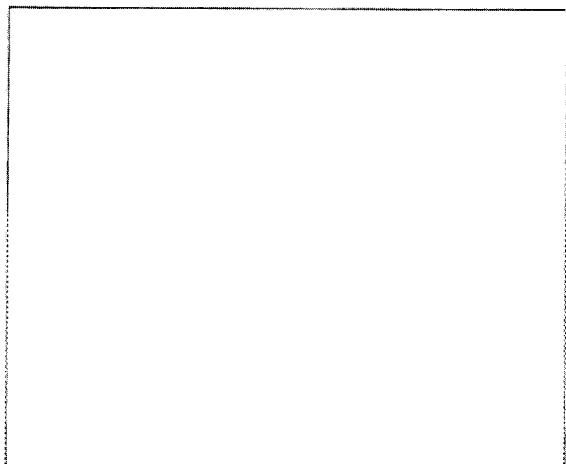
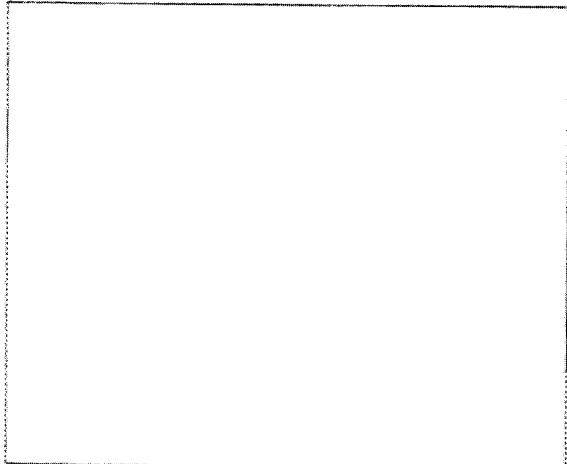


Fig. D.14. Nucleopore filter test 2 with 71-NTU water sample W1, diluted 2-µm filter.

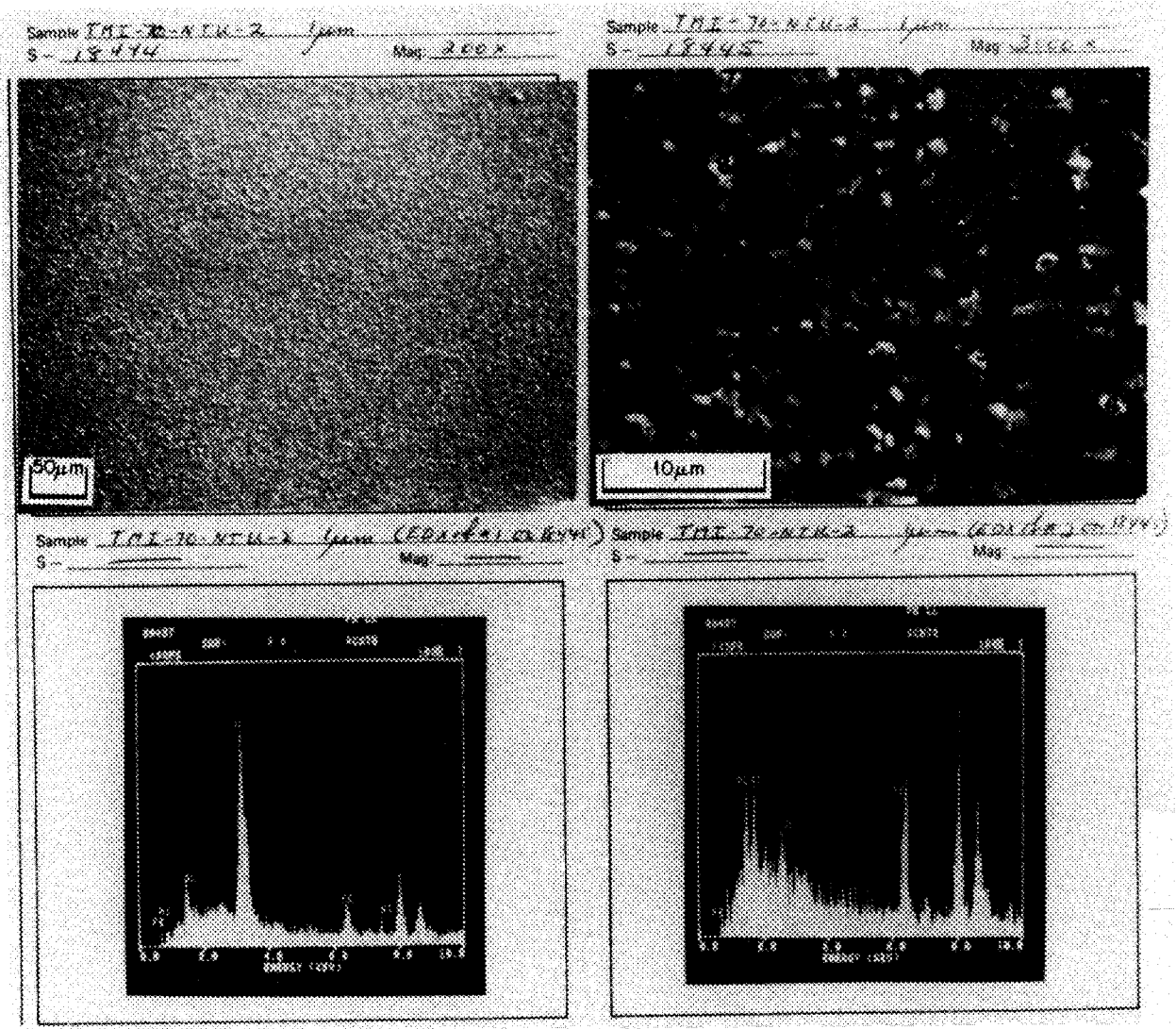
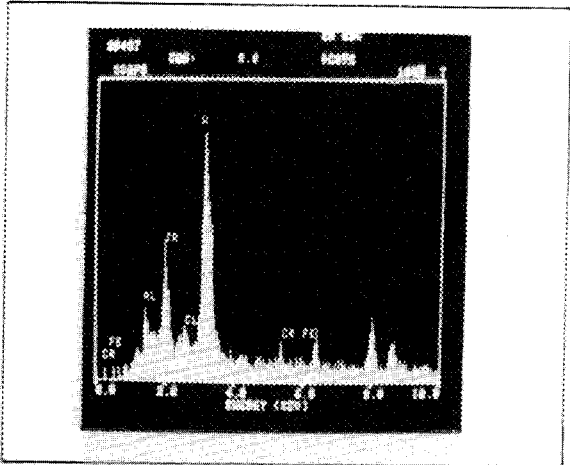
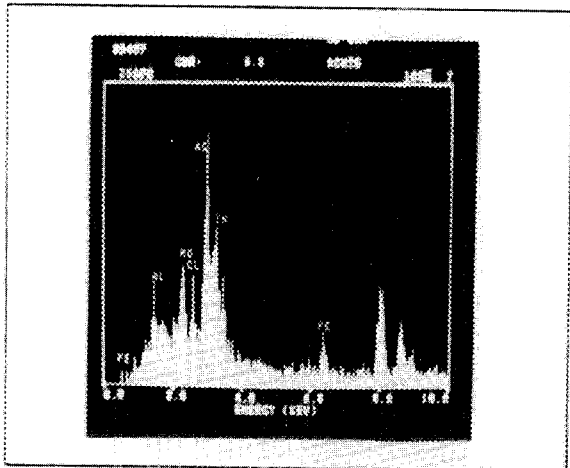


Fig. D.15. Nucleopore filter test 2 with 71-NTU water sample W1, 1-µm filter.

Sample IME-70-NTU-2 1µm (EDA # 3 ON 15445) Sample IME-70-NTU-2 1µm (EDA # 4 ON 15445)
S - _____ Mag: _____ S - _____ Mag: _____



Sample IME-70-NTU-2 1µm (EDA # 5 ON 15445)
S - _____ Mag: _____

Sample IME-70-NTU-2 1µm (EDA # 6 ON 15445)
S - _____ Mag: _____

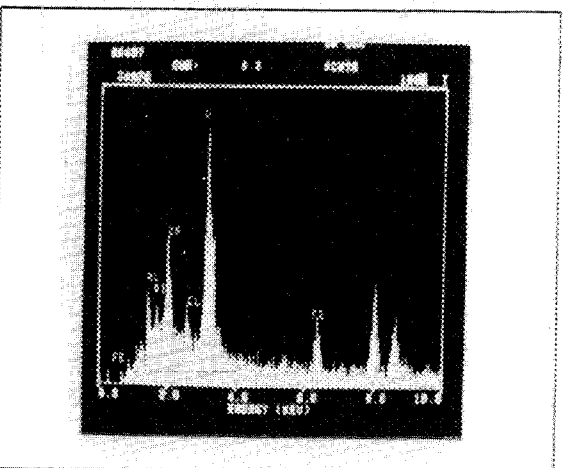
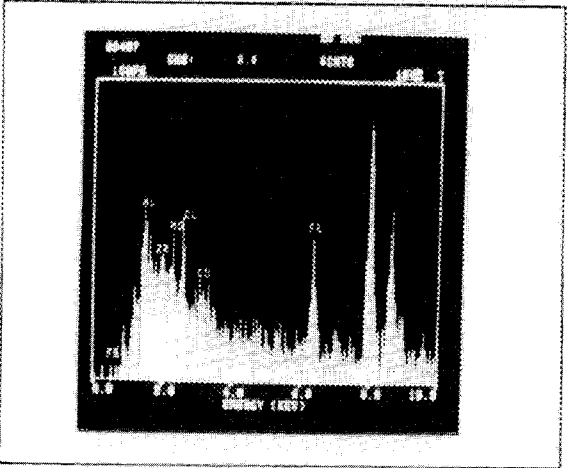


Fig. D.16. Nuclepore filter test 2 with 71-NTU water sample W1, 1-µm filter.

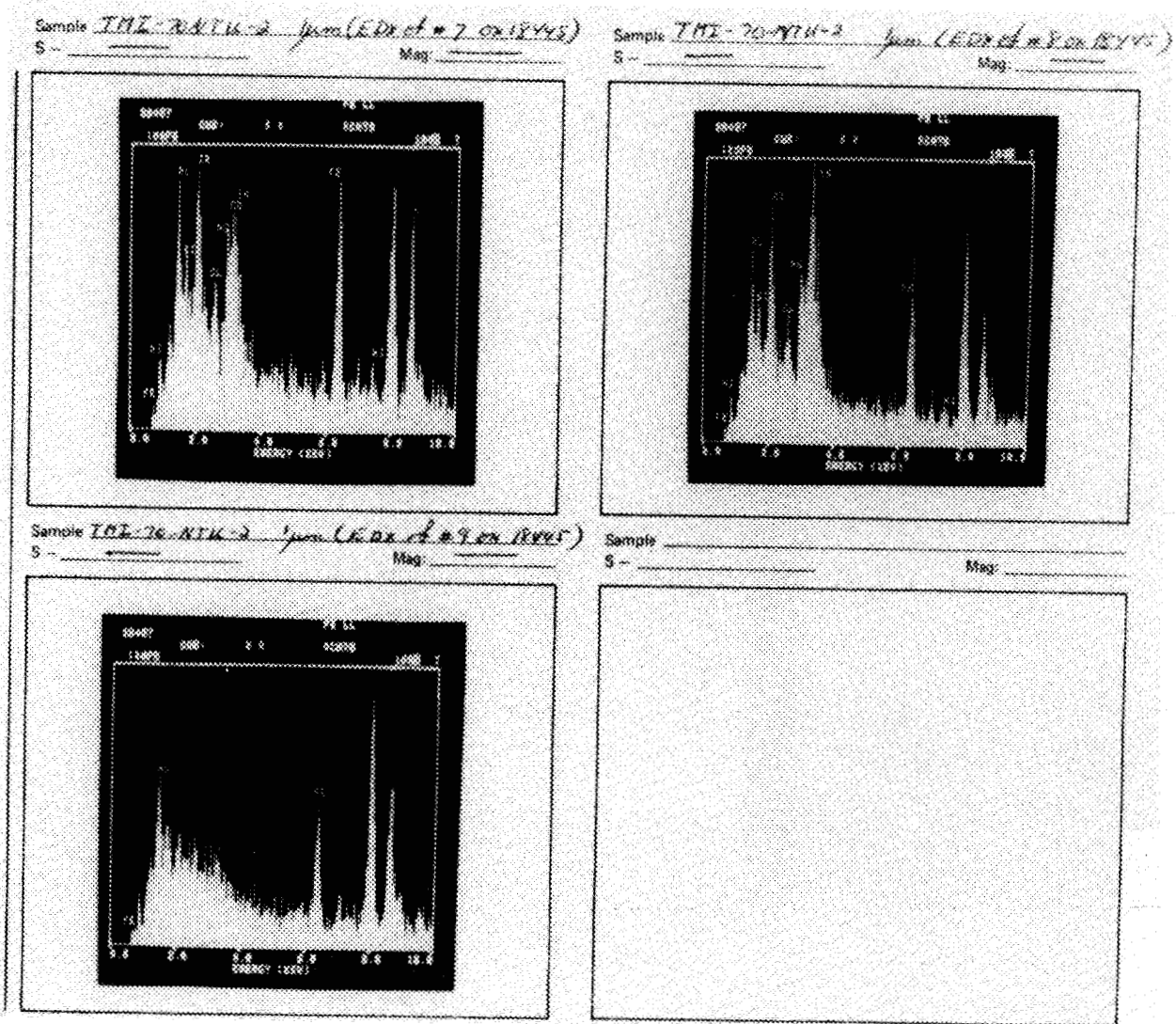


Fig. D.17. Nuclepore filter test 2 with 71-NTU water sample W1, 1-µm filter.

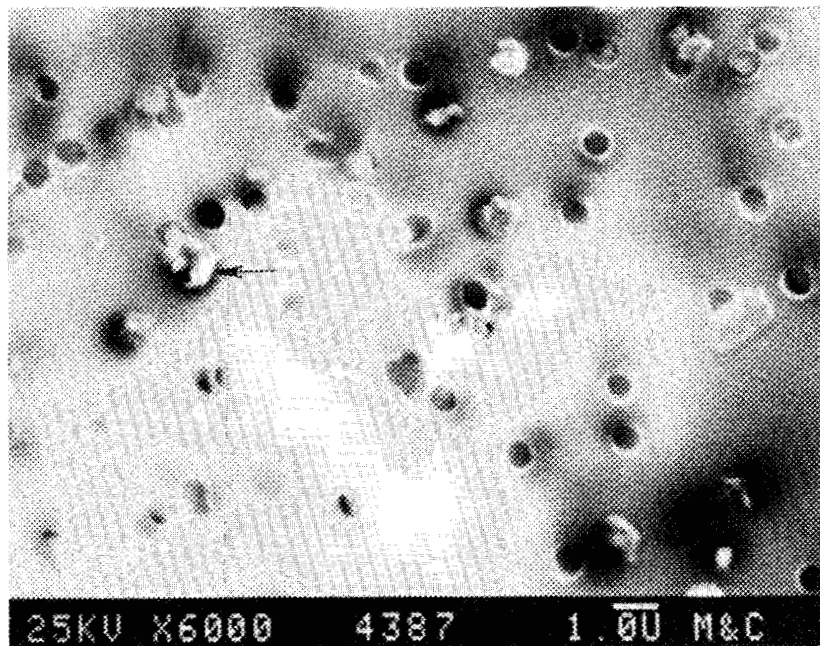


Fig. D.18. Nucleopore filter test 2 with 71-NTU water sample W1, 0.8- μm filter.

ORNL-DWG 87-13755

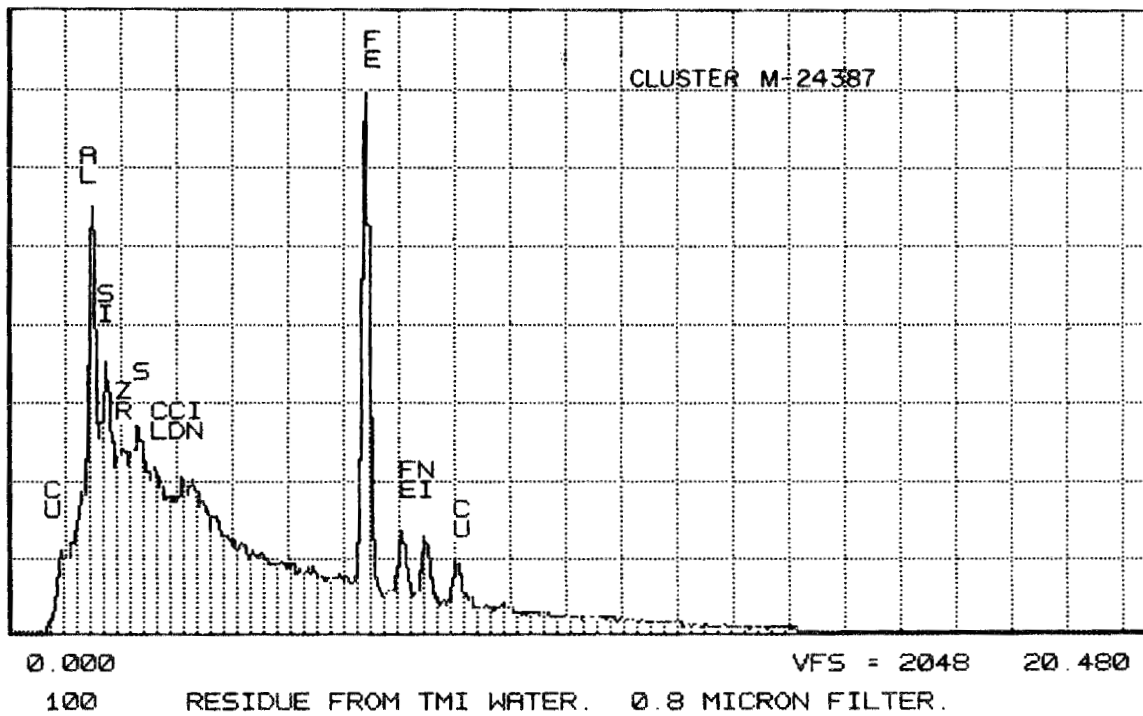


Fig. D.19. EDX of particle cluster, 4387 (see Fig. D.18).

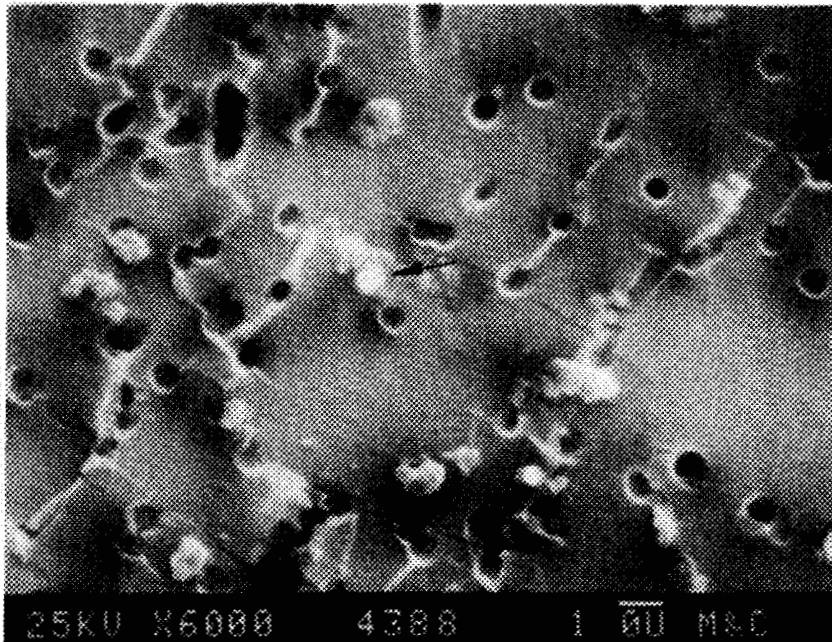


Fig. D.20. Nucleopore filter test 2 with 71-NTU water sample W1, 0.8- μ m filter.

ORNL-DWG 87-13756

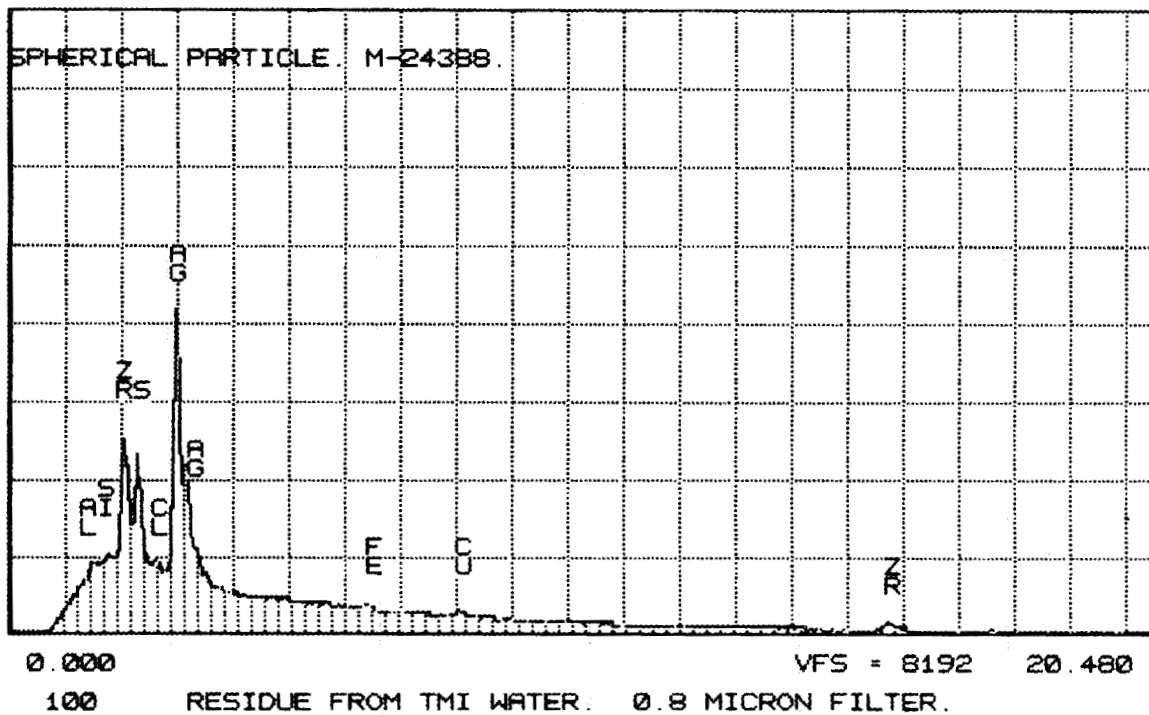


Fig. D.21. EDX of "fish-egg" particle near center, 4388 (see Fig. D.20).

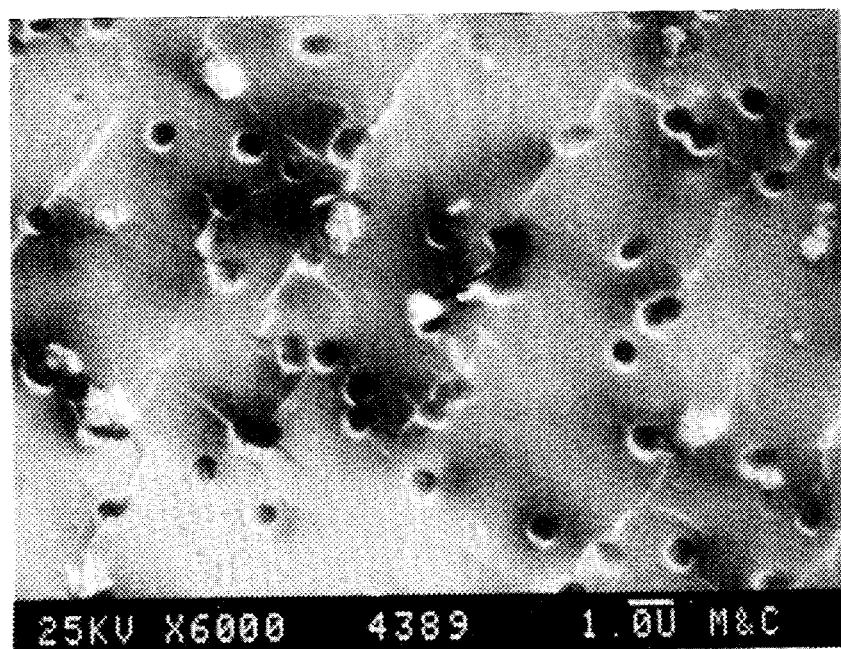


Fig. D.22. Nucleopore filter test 2 with 71-NTU water sample W1, 0.8- μ m filter.

ORNL-DWG 87-13757

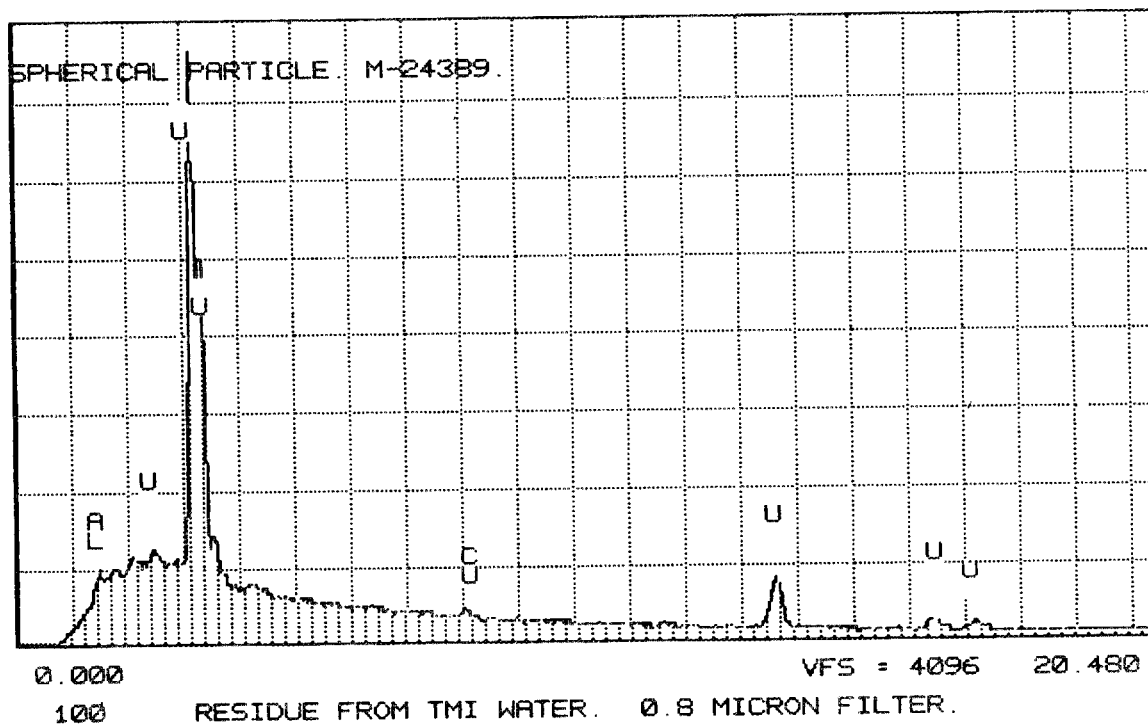


Fig. D.23. EDX of bright particle near center, 4389 (see Fig. D.22).

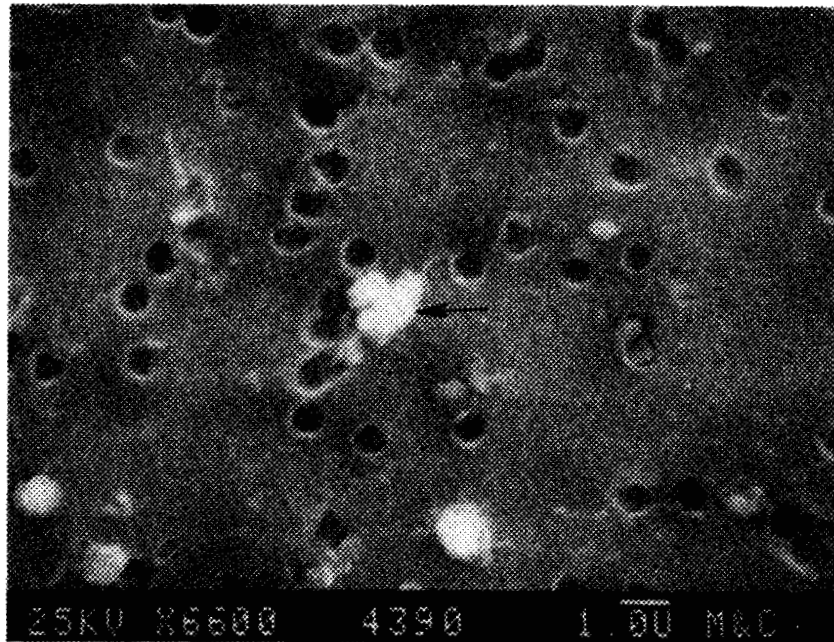


Fig. D.24. Nucleopore filter test 2 with 71-NTU water sample W1, 0.8- μ m filter.

ORNL-DWG 87-13758

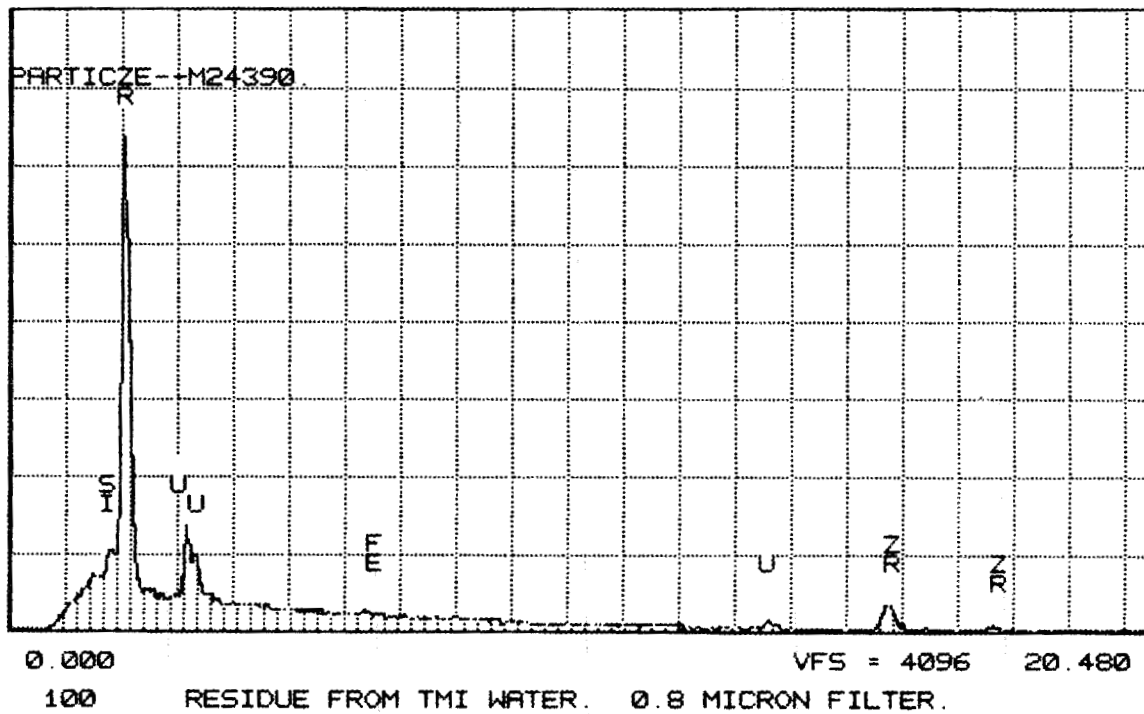


Fig. D.25. EDX of bright cluster near center, 4390 (see Fig. D.24).

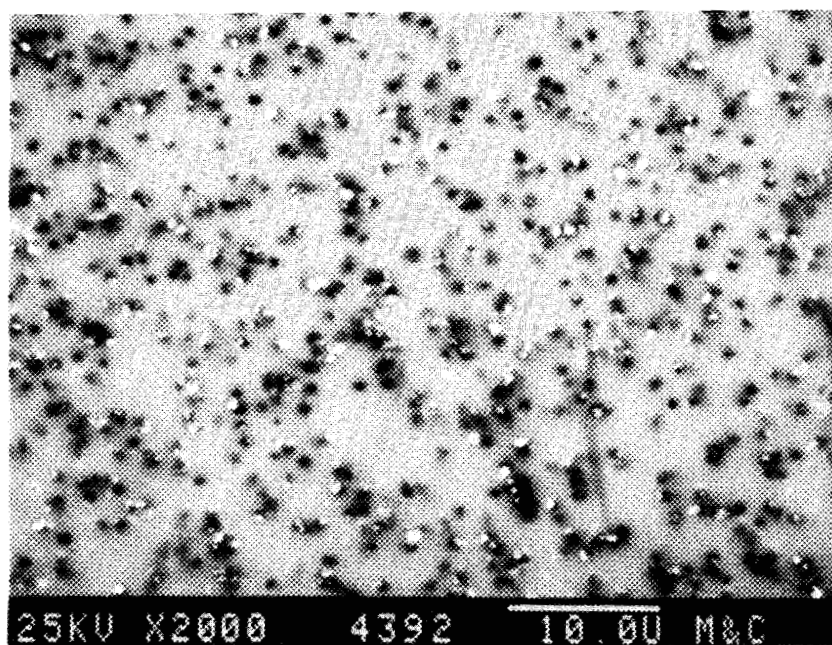


Fig. D.26. Nucleopore filter test 2 with 71-NTU water sample W1, 0.6- μm filter.

ORNL-DWG 87-13759

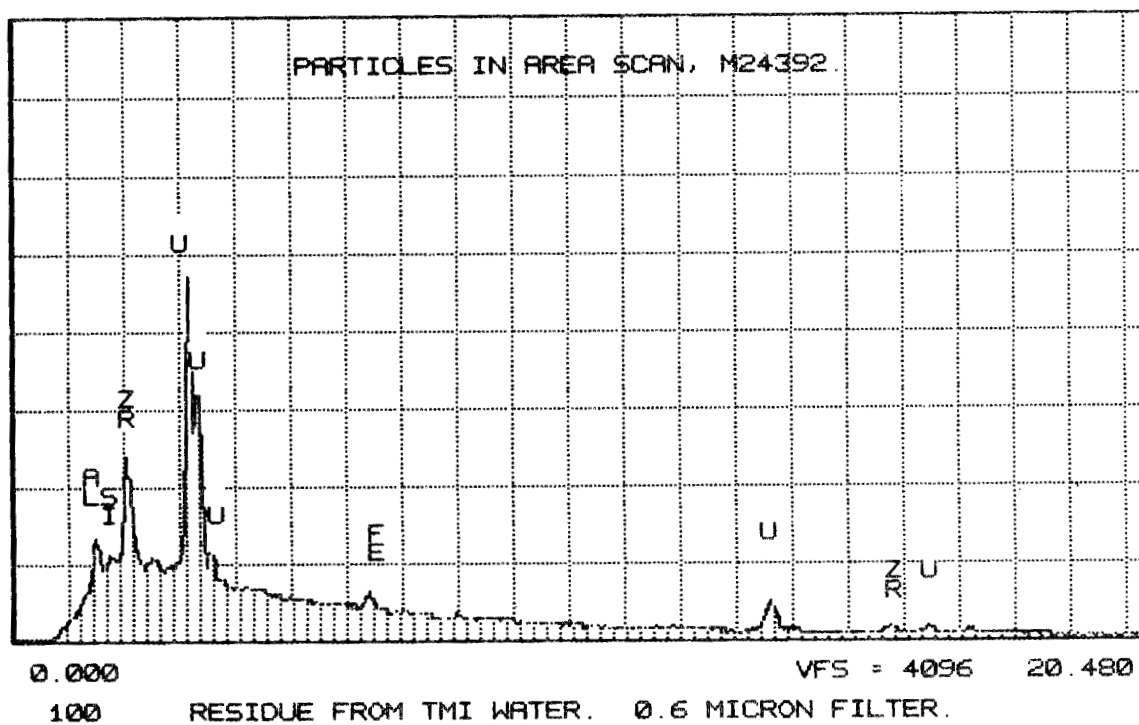


Fig. D.27. EDX of area of 4392 (see Fig. D.26).

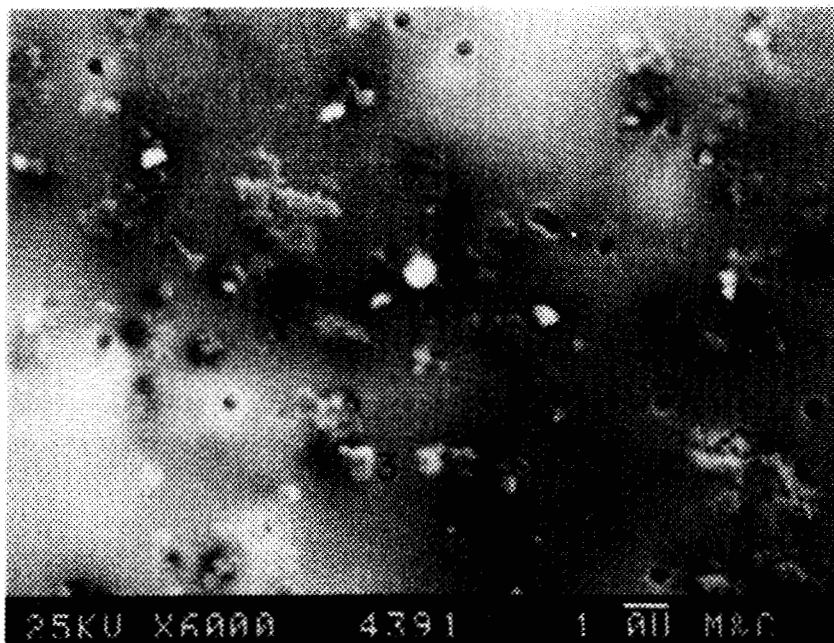


Fig. D.28. Nuclepore filter test 2 with 71-NTU water sample W1, 0.6- μ m filter.

ORNL-DWG 87-13760

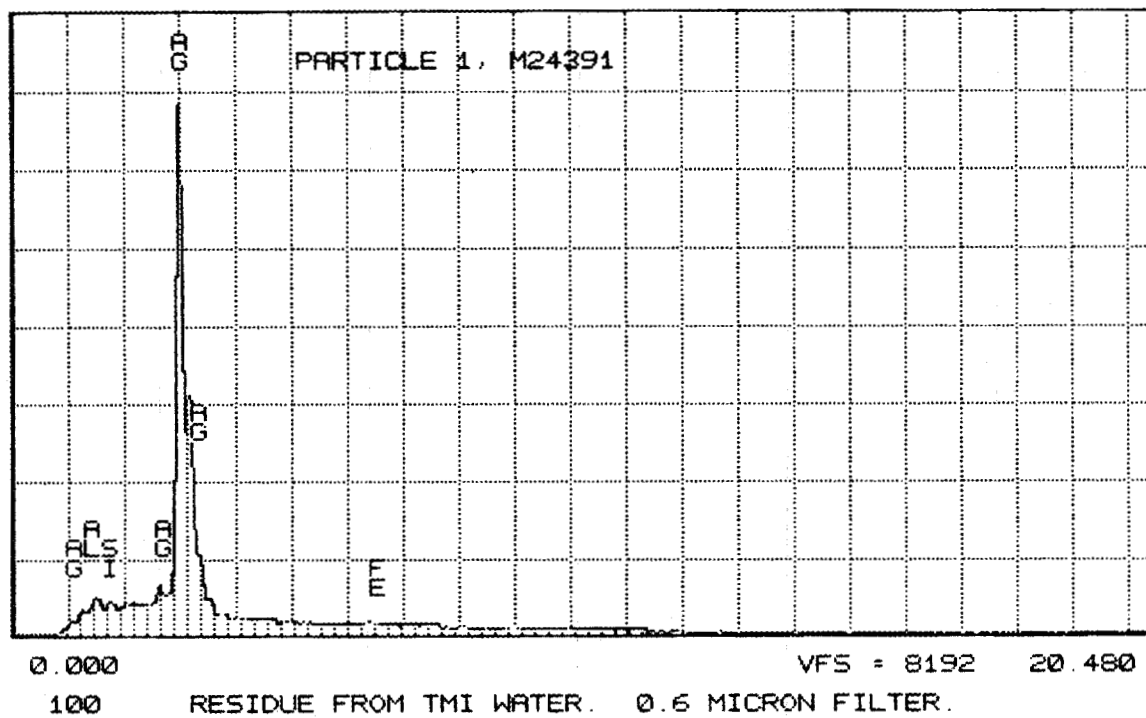


Fig. D.29. EDX of particle No. 1, 4391 (see Fig. D.28).

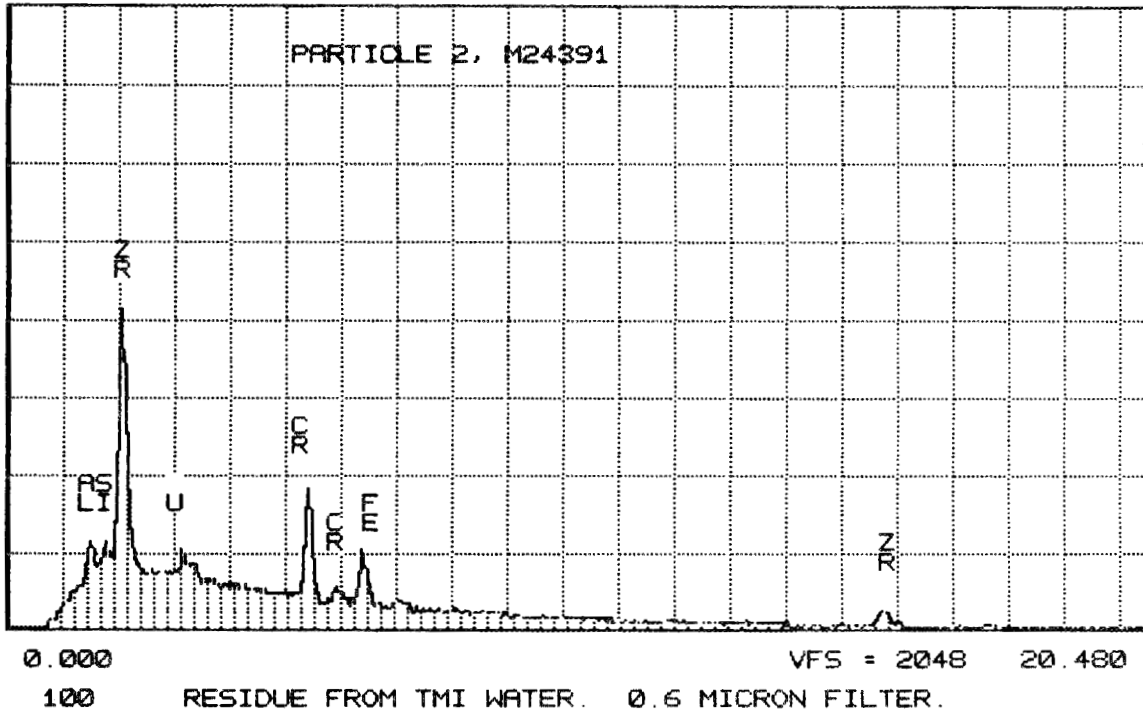


Fig. D.30. EDX of particle No. 2, 4391 (see Fig. D.28).

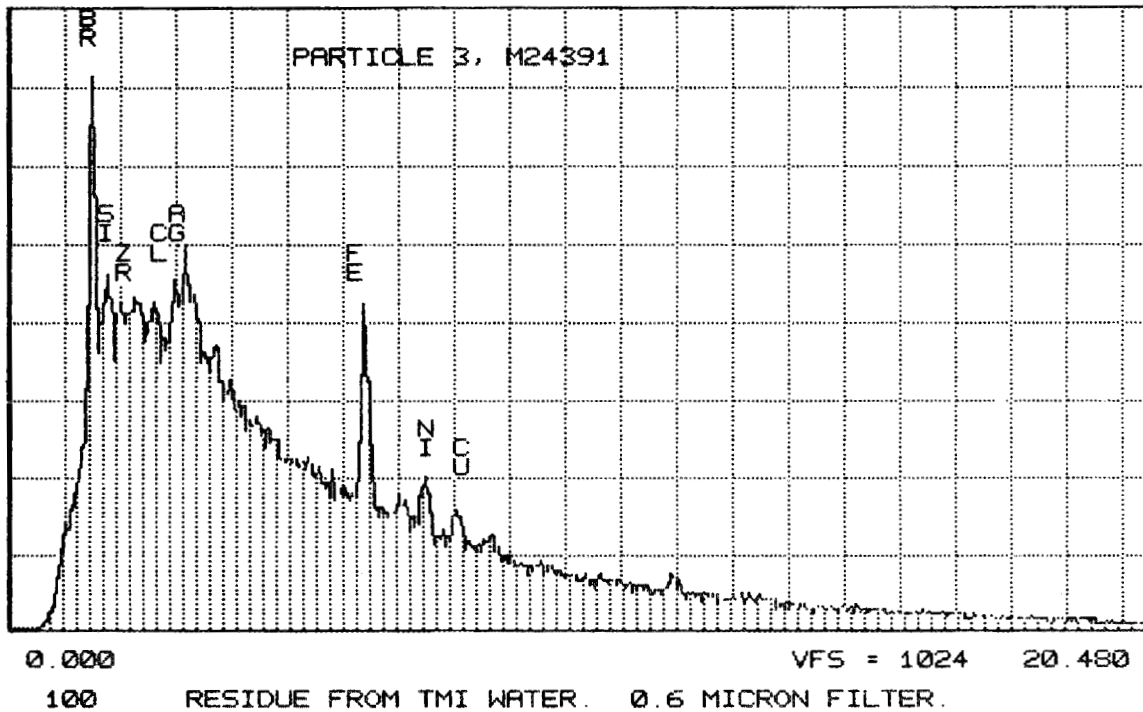


Fig. D.31. EDX of particle No. 3, 4391 (see Fig. D.28).

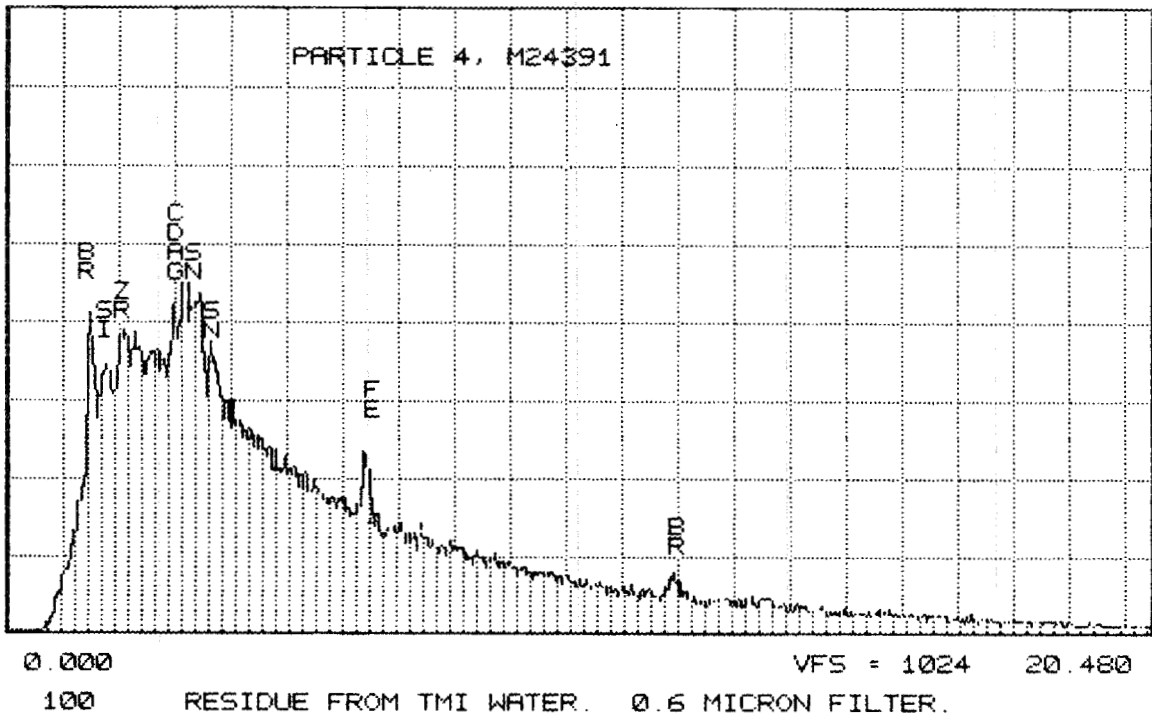


Fig. D.32. EDX of particle No. 4, 4391 (see Fig. D.28).

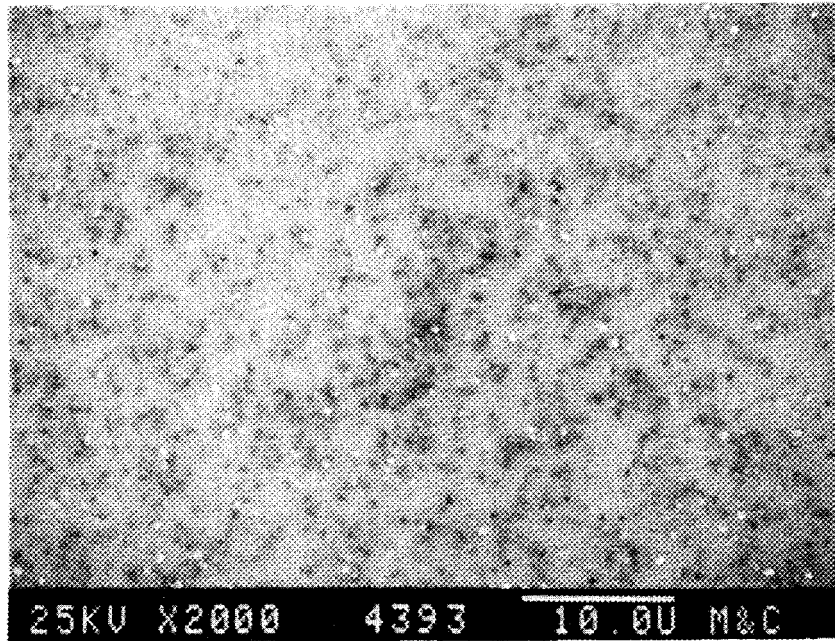


Fig. D.33. Nuclepore filter test 2 with 71-NTU water sample W1, 0.4- μ m filter.

ORNL-DWG 87-13764

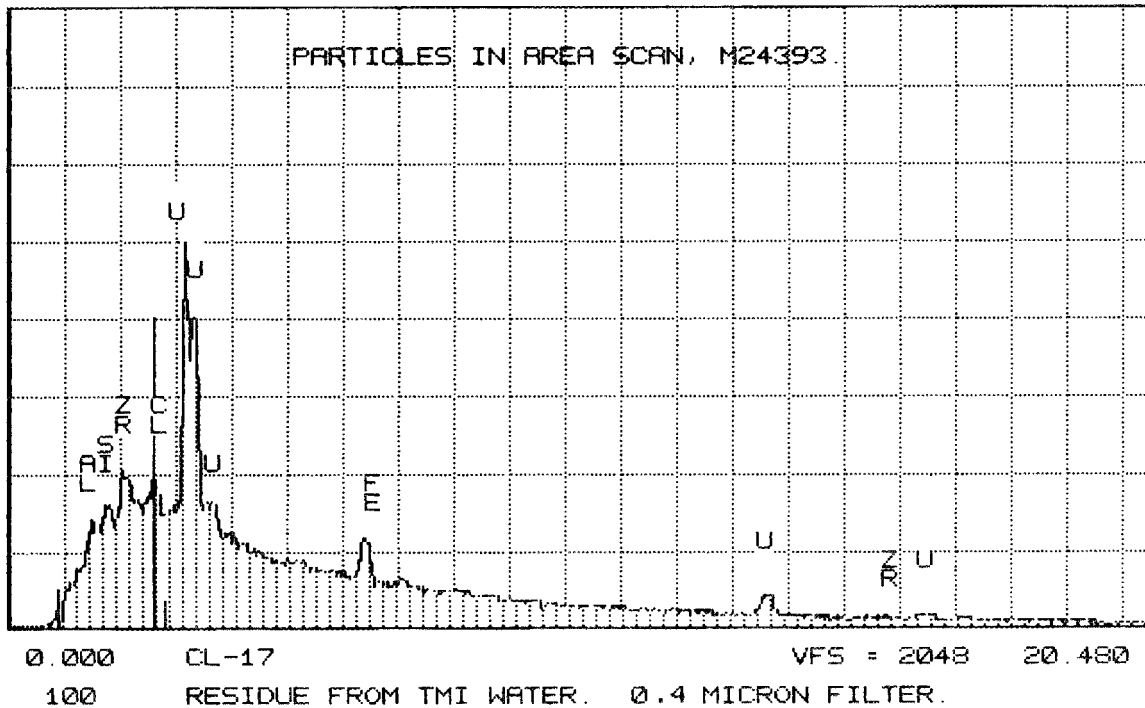


Fig. D.34. EDX of area of 4394 (see Fig. D.33).

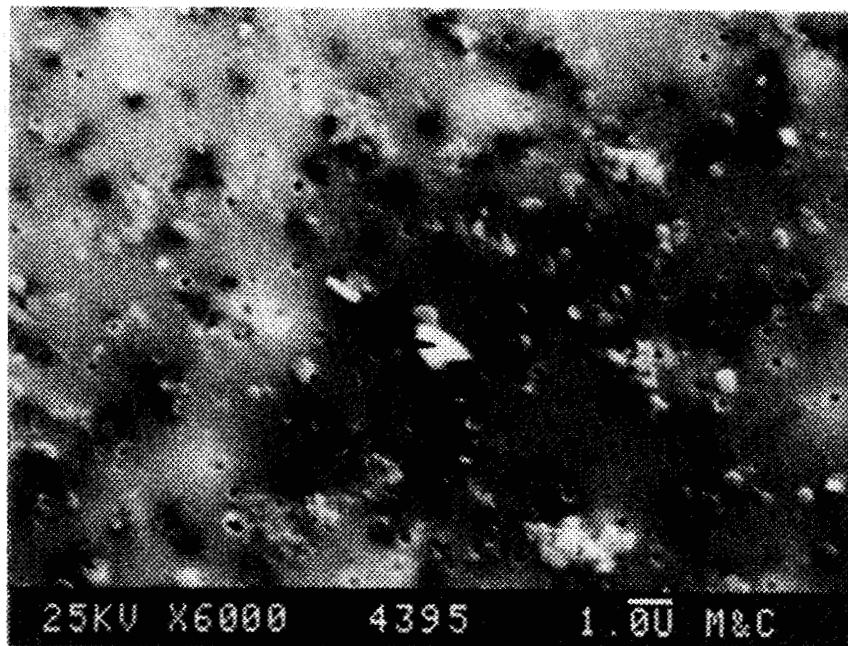


Fig. D.35. Nucleopore filter test 2 with 71-NTU water sample W1, 0.4- μ m filter.

ORNL-DWG 87-13765

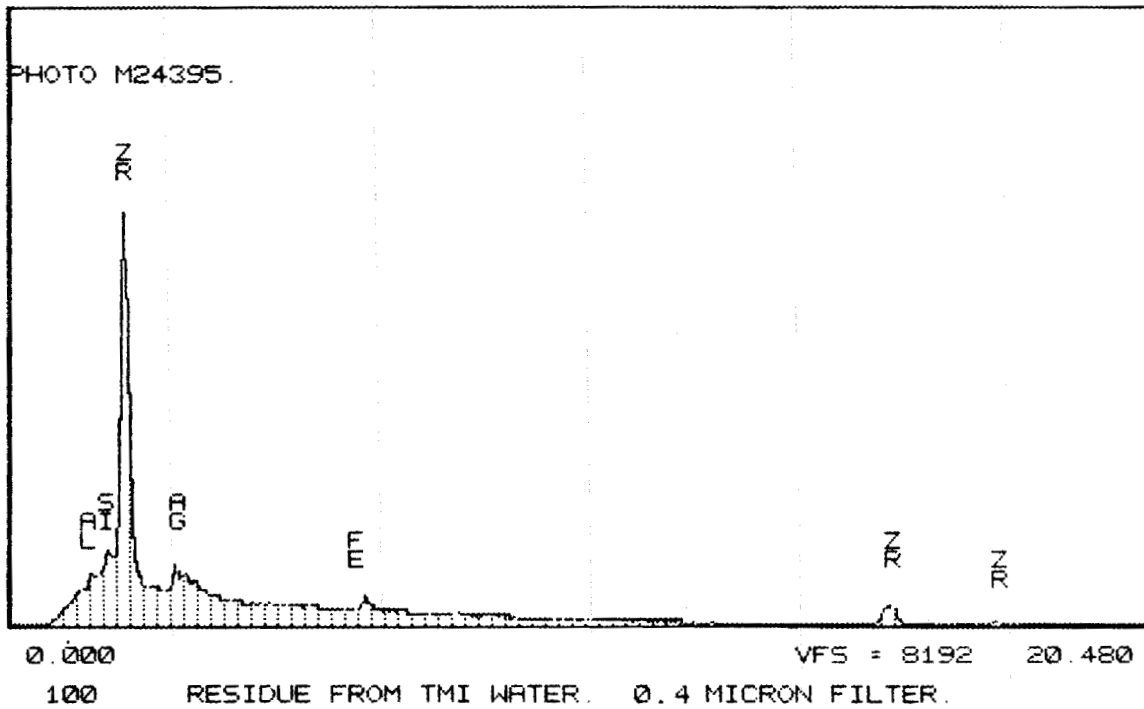


Fig. D.36. EDX of white particle near center, 4395 (see Fig. D.35).

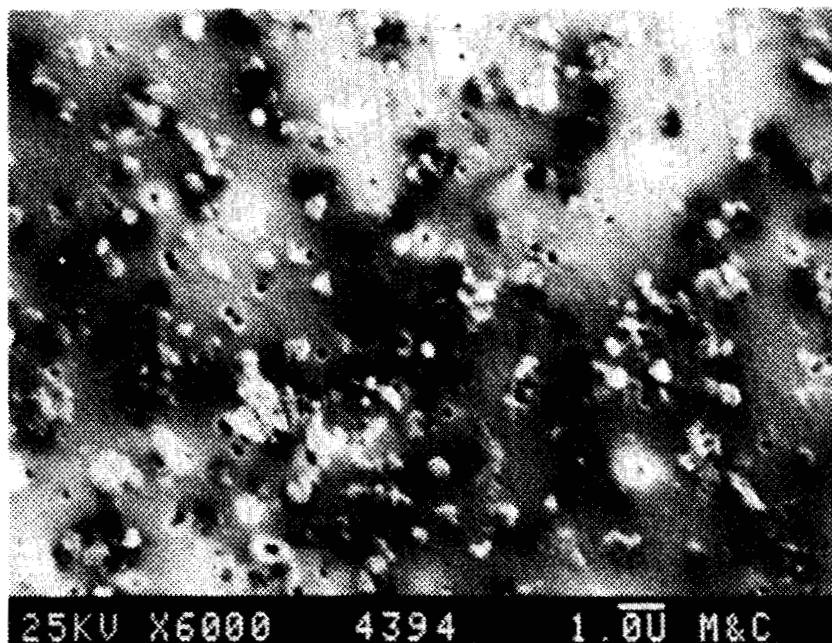


Fig. D.37. Nuclepore filter test 2 with 71-NTU water sample W1, 0.4- μ m filter.

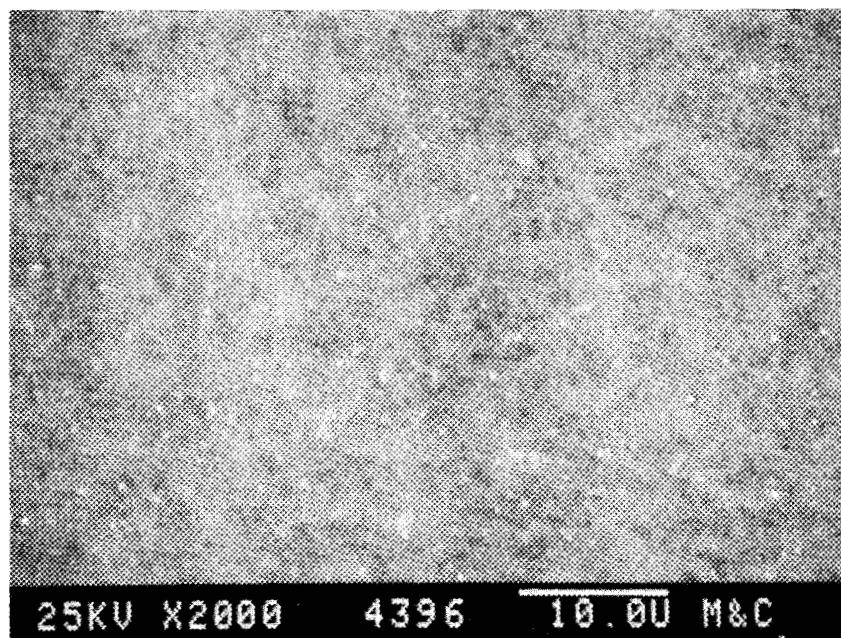


Fig. D.38. Nuclepore filter test 2 with 71-NTU water sample W1, 0.4- μ m filter, BEI.

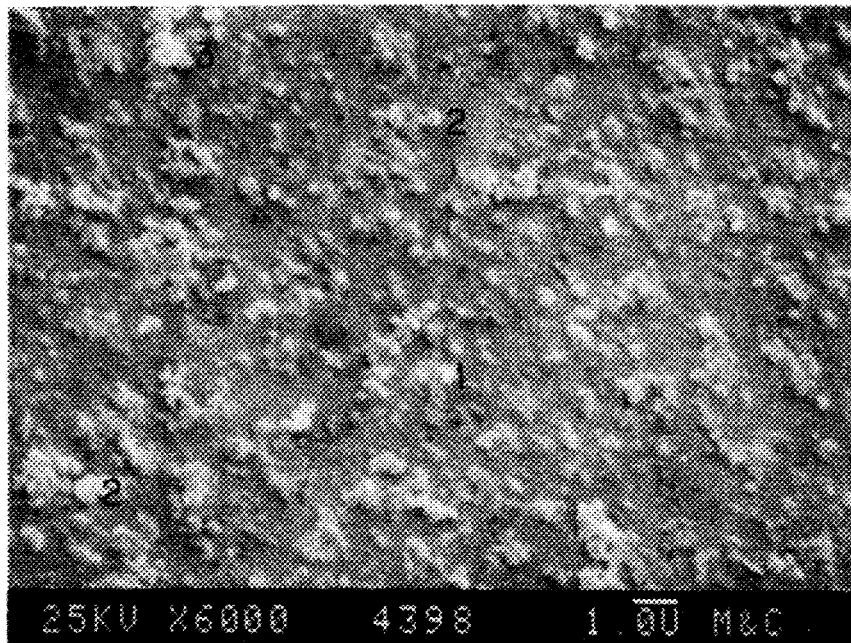


Fig. D.39. Nucleopore filter test 2 with 71-NTU water sample W1, 0.1- μ m filter.

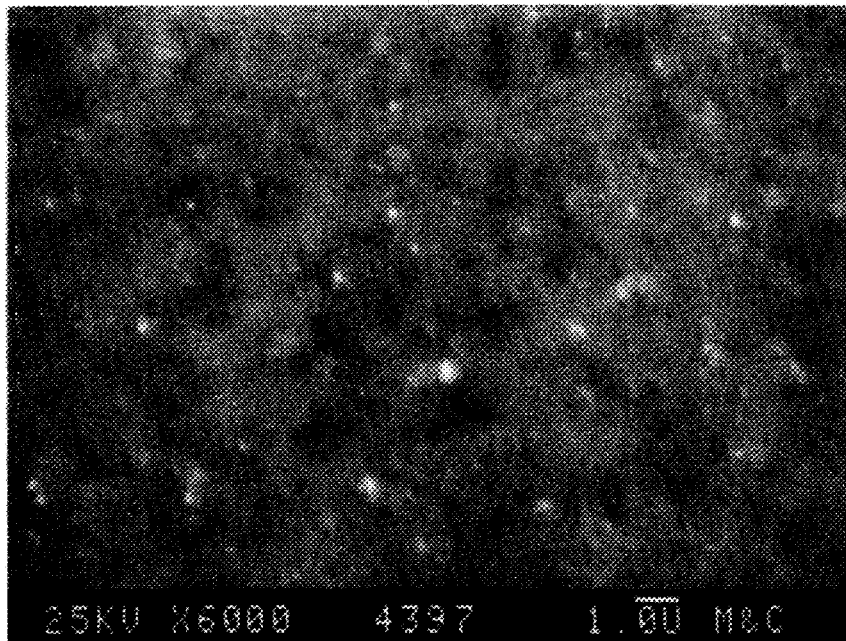


Fig. D.40. Nucleopore filter test 2 with 71-NTU water sample W1, 0.1- μ m filter, BEI.

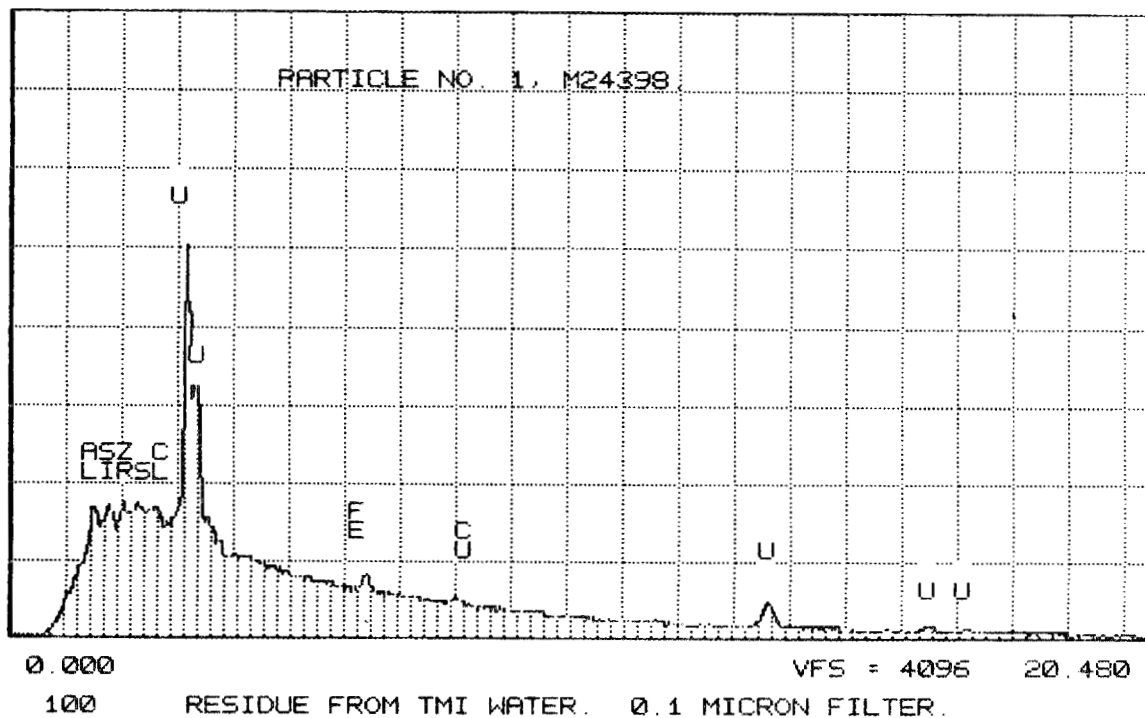


Fig. D.41. EDX of particle No. 1, 4398 (see Fig. D.39).

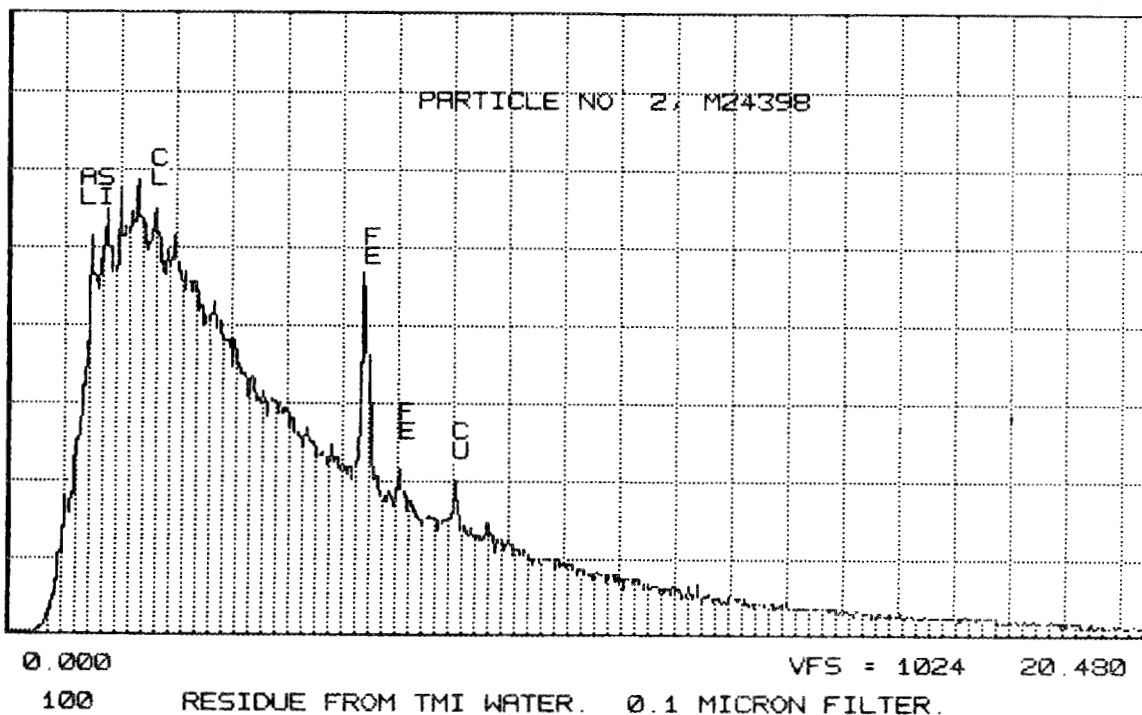


Fig. D.42. EDX of particle No. 2a, 4398 (see Fig. D.39).

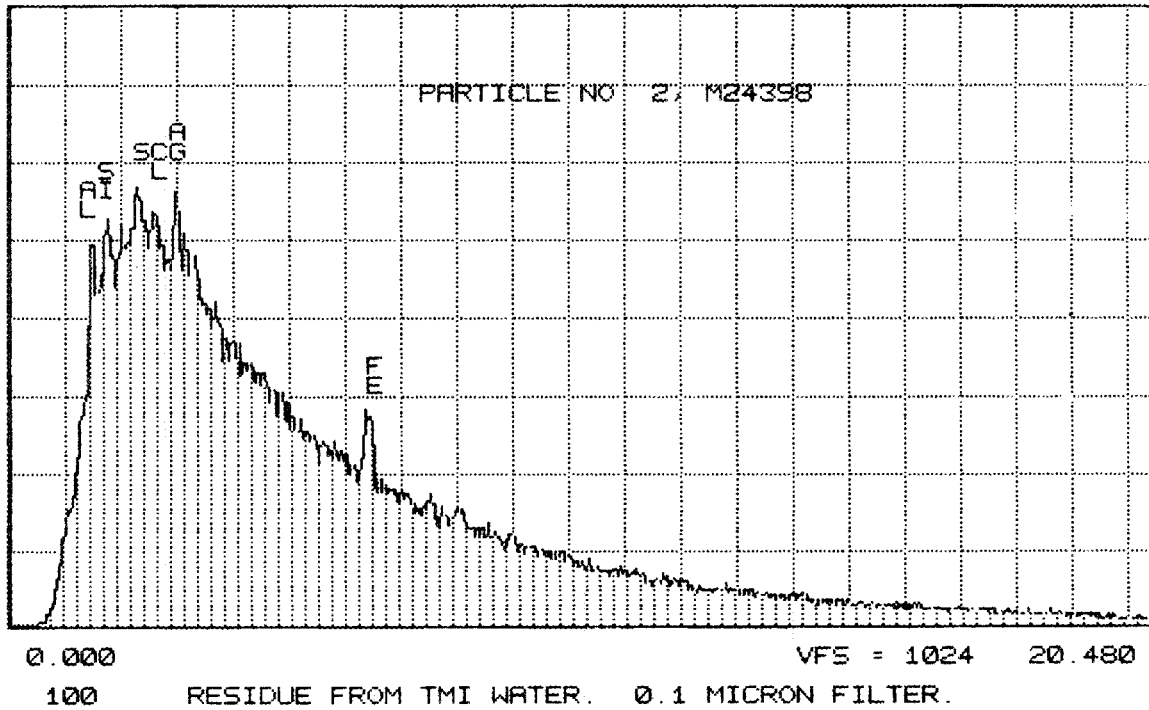


Fig. D.43. EDX of particle No. 2b, 4398 (see Fig. D.39).

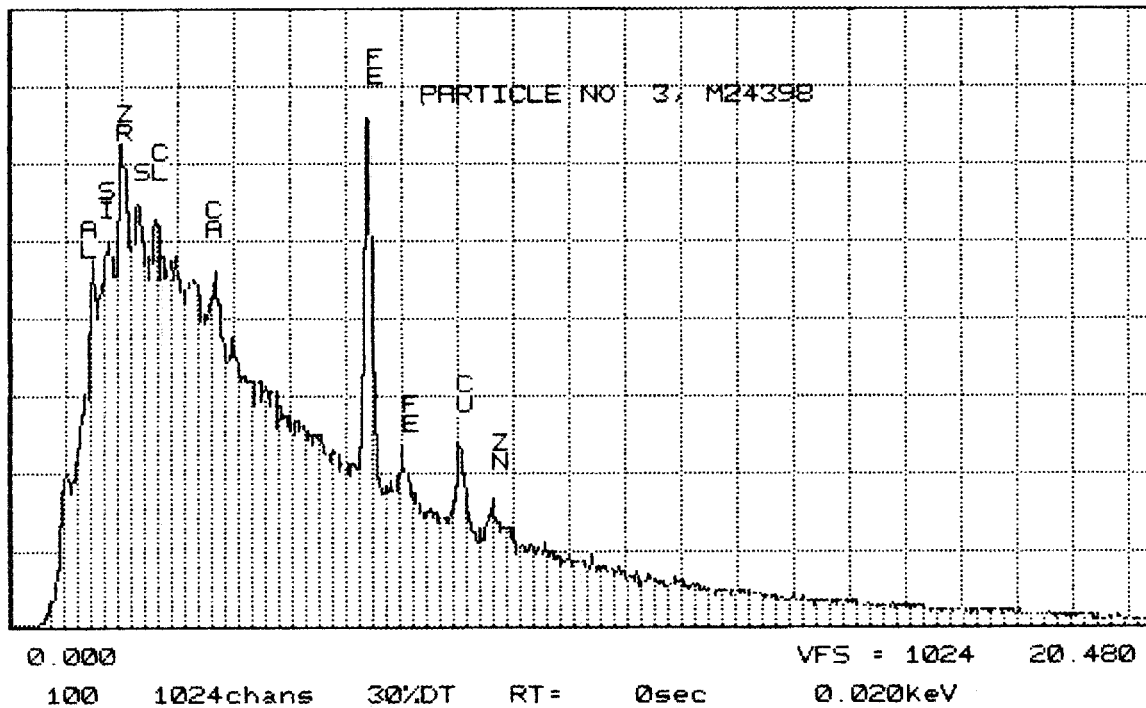


Fig. D.44. EDX of particle No. 3, 4398 (see Fig. D.39).

**Appendix E. PARTICLE CHARACTERIZATION DATA FOR SAMPLE W2
(TURBIDITY = ~25 NTU): FILTRATION TEST 3**

<u>Figure</u>		<u>Page</u>
E.1	Nuclepore filter test 3 with 22-NTU water sample W2, 10- μ m filter	153
E.2	Nuclepore filter test 3 with 22-NTU water sample W2, 10- μ m filter	154
E.3	Nuclepore filter test 3 with 22-NTU water sample W2, 10- μ m filter	155
E.4	Nuclepore filter test 3 with 22-NTU water sample W2, 10- μ m filter	156
E.5	Nuclepore filter test 3 with 22-NTU water sample W2, 10- μ m filter	157
E.6	Nuclepore filter test 3 with 22-NTU water sample W2, 5- μ m filter	158
E.7	Nuclepore filter test 3 with 22-NTU water sample W2, 5- μ m filter	159
E.8	Nuclepore filter test 3 with 22-NTU water sample W2, 5- μ m filter	160
E.9	Nuclepore filter test 3 with 22-NTU water sample W2, 5- μ m filter	161
E.10	Nuclepore filter test 3 with 22-NTU water sample W2, 2- μ m filter	162
E.11	Nuclepore filter test 3 with 22-NTU water sample W2, 2- μ m filter	163
E.12	Nuclepore filter test 3 with 22-NTU water sample W2, 2- μ m filter	164
E.13	Nuclepore filter test 3 with 22-NTU water sample W2, 2- μ m filter	165
E.14	Nuclepore filter test 3 with 22-NTU water sample W2, 1- μ m filter	166
E.15	Nuclepore filter test 3 with 22-NTU water sample W2, 1- μ m filter, BEI	166

<u>Figure</u>		<u>Page</u>
E.16	EDX of particle A, 4399 (see Fig. E.15)	167
E.17	EDX of particle B, 4399 (see Fig. E.15)	167
E.18	EDX of particle C, 4399 (see Fig. E.15)	168
E.19	EDX of particle D, 4399 (see Fig. E.15)	168
E.20	Nuclepore filter test 3 with 22 NTU water sample W2, 1- μ m filter	169
E.21	Nuclepore filter test 3 with 22-NTU water sample W2, 1- μ m filter, BEI	169
E.22	EDX of particle E, 4399 (see Fig. E.15)	170
E.23	EDX of particle F, 4402 (see Fig. E.20)	170
E.24	EDX of particle G, 4399 (see Fig. E.20)	171
E.25	EDX of particle H, 4399 (see Fig. E.20)	171
E.26	Nuclepore filter test 3 with 22-NTU water sample W2, 0.8- μ m filter	172
E.27	Nuclepore filter test 3 with 22-NTU water sample W2, 0.8- μ m filter, BEI	172
E.28	EDX of area of 4411 (see Fig. E.27)	173
E.29	EDX of particle A, 4411 (see Fig. E.27)	173
E.30	EDX of particle B, 4411 (see Fig. E.27)	174
E.31	EDX of particle C, 4411 (see Fig. E.27)	174
E.32	EDX of particle D, 4411 (see Fig. E.27)	175
E.33	EDX of particle E, 4411 (see Fig. E.27)	175
E.34	Nuclepore filter test 3 with 22-NTU water sample W2, 0.8- μ m filter	176
E.35	Nuclepore filter test 3 with 22-NTU water sample W2, 0.8- μ m filter, BEI	176
E.36	EDX of particle F, 4411 (see Fig. E.27)	177
E.37	EDX of particle G, 4413 (see Fig. E.34)	177

<u>Figure</u>		<u>Page</u>
E.38	EDX of particle H, 4413 (see Fig. E.34)	178
E.39	EDX of particle I, 4413 (see Fig. E.34)	178
E.40	Nuclepore filter test 3 with 22-NTU water sample W2, 0.6- μ m filter	179
E.41	Nuclepore filter test 3 with 22-NTU water sample W2, 0.6- μ m filter, BEI	179
E.42	Nuclepore filter test 3 with 22-NTU water sample W2, 0.6- μ m filter	180
E.43	Nuclepore filter test 3 with 22-NTU water sample W2, 0.6- μ m filter, BEI	180
E.44	EDX of area of 4415 (see Fig. E.41)	181
E.45	EDX of particle A, 4418 (see Fig. E.43)	181
E.46	EDX of particle B, 4418 (see Fig. E.43)	182
E.47	EDX of particle C, 4418 (see Fig. E.43)	182
E.48	EDX of particle D, 4418 (see Fig. E.43)	183
E.49	EDX of particle E, 4418 (see Fig. E.43)	183
E.50	EDX of particle F, 4418 (see Fig. E.43)	184
E.51	EDX of particle G, 4418 (see Fig. E.43)	184
E.52	EDX of particle H, 4418 (see Fig. E.43)	185
E.53	EDX of particle I, 4418 (see Fig. E.43)	185
E.54	EDX of particle J, 4418 (see Fig. E.43)	186
E.55	EDX of particle L, 4417 (see Fig. E.42)	186
E.56	EDX of particle M, 4417 (see Fig. E.42)	187
E.57	Nuclepore filter test 3 with 22-NTU water sample W2, 0.4- μ m filter	188
E.58	Nuclepore filter test 3 with 22-NTU water sample W2, 0.4- μ m filter; BEI	188

<u>Figure</u>		<u>Page</u>
E.59	Nuclepore filter test 3 with 22-NTU water sample W2, 0.4- μ m filter	189
E.60	Nuclepore filter test 3 with 22-NTU water sample W2, 0.4- μ m filter; BEI	189
E.61	EDX of area scan of 4587 (see Fig. E.59)	190
E.62	EDX of particle 1, 4587 (see Fig. E.59)	190
E.63	EDX of particle 2, 4587 (see Fig. E.59)	191
E.64	EDX of particle 3, 4587 (see Fig. E.59)	191
E.65	EDX of particle 4, 4587 (see Fig. E.59)	192
E.66	EDX of particle 5, 4587 (see Fig. E.59)	192
E.67	EDX of particle 6, 4587 (see Fig. E.59)	193
E.68	EDX of particle 7, 4587 (see Fig. E.59)	193
E.69	EDX of particle 8, 4587 (see Fig. E.59)	194
E.70	EDX of particle 9, 4587 (see Fig. E.59)	194
E.71	EDX of particle 10, 4587 (see Fig. E.59)	195
E.72	Nuclepore filter test 3 with 22-NTU water sample W2, 0.1- μ m filter	196
E.73	Nuclepore filter test 3 with 22-NTU water sample W2, 0.1- μ m filter; BEI	196
E.74	EDX of area of 4591 (see Fig. E.72)	197
E.75	EDX of particle 1, 4591 (see Fig. E.72)	197
E.76	EDX of particle 2, 4591 (see Fig. E.72)	198
E.77	EDX of particle 3, 4591 (see Fig. E.72)	198
E.78	20,000X enlargement of particle 3, 4591 (see Fig. E.72)	199
E.79	EDX of particle 4, 4591 (see Fig. E.72)	199
E.80	EDX of particle 5, 4591 (see Fig. E.72)	200

<u>Figure</u>		<u>Page</u>
E.81	EDX of particle 6, 4591 (see Fig. E.72)	200
E.82	EDX of particle 7, 4591 (see Fig. E.72)	201
E.83	EDX of particle 8, 4591 (see Fig. E.72)	201
E.84	EDX of particle 9, 4591 (see Fig. E.72)	202

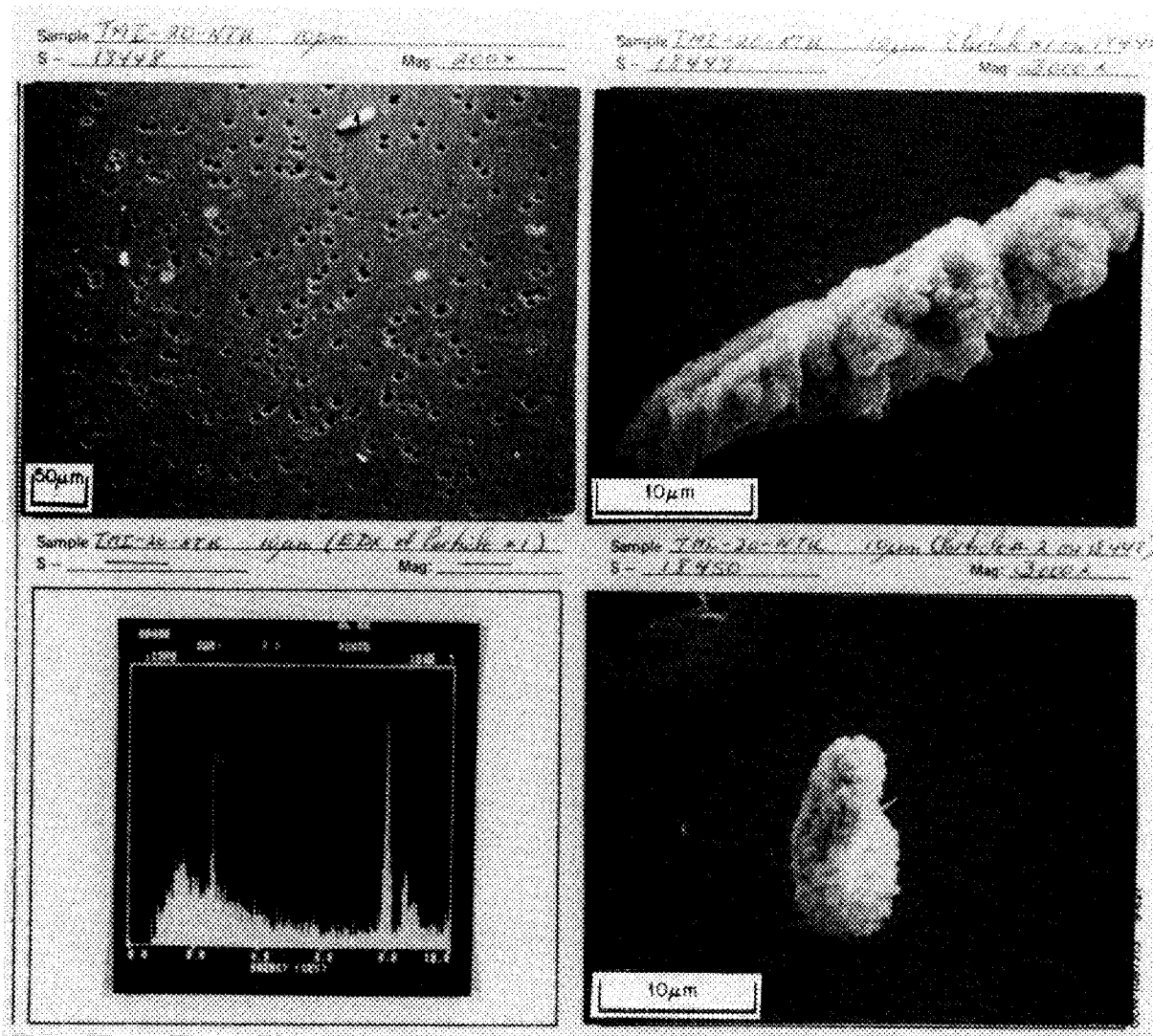


Fig. E.1. Nuclepore filter test 3 with 22-NTU water sample W2, 10-µm filter.

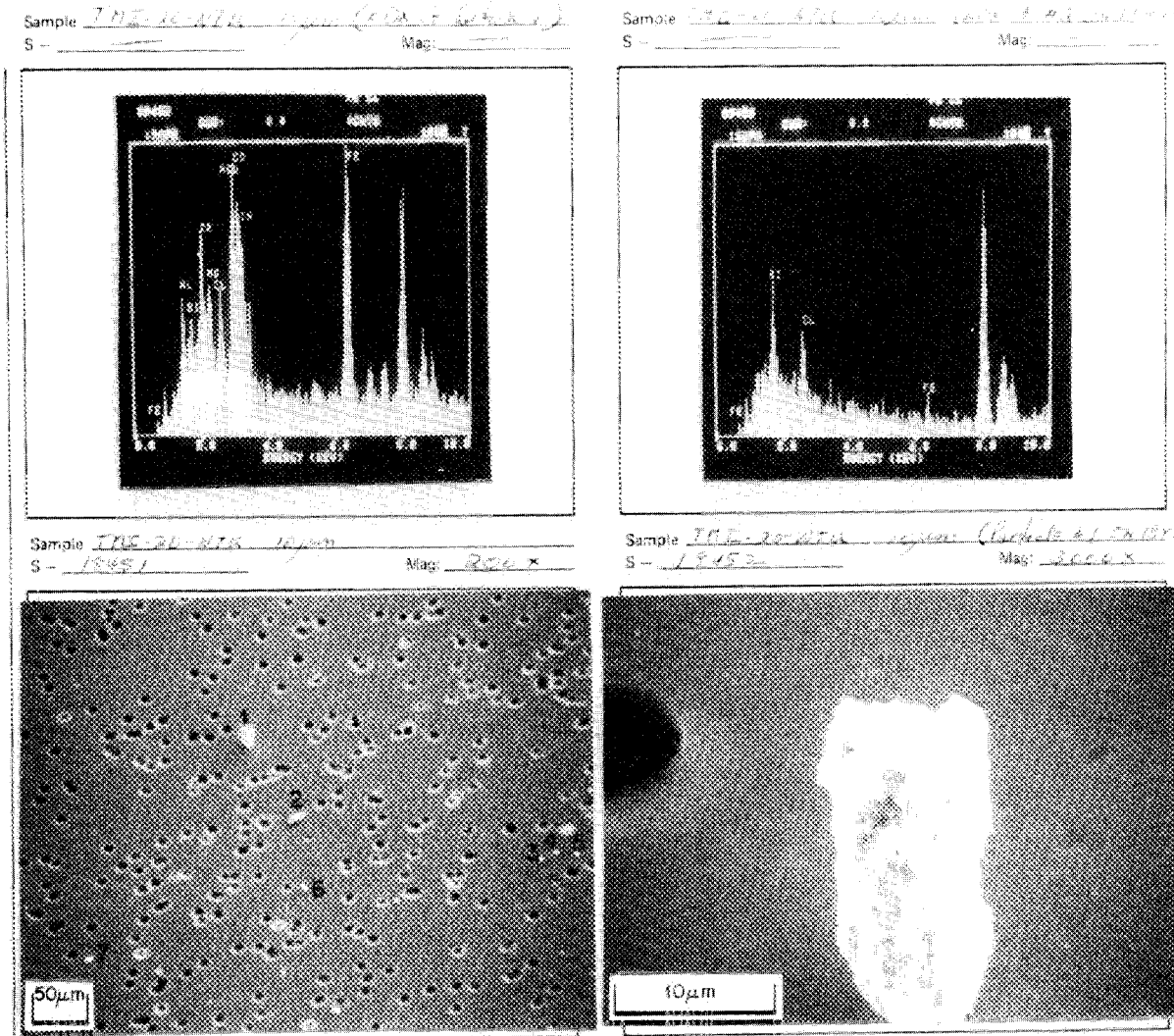


Fig. E.2. Nucleopore filter test 3 with 22-NTU water sample W2, 10- μ m filter.

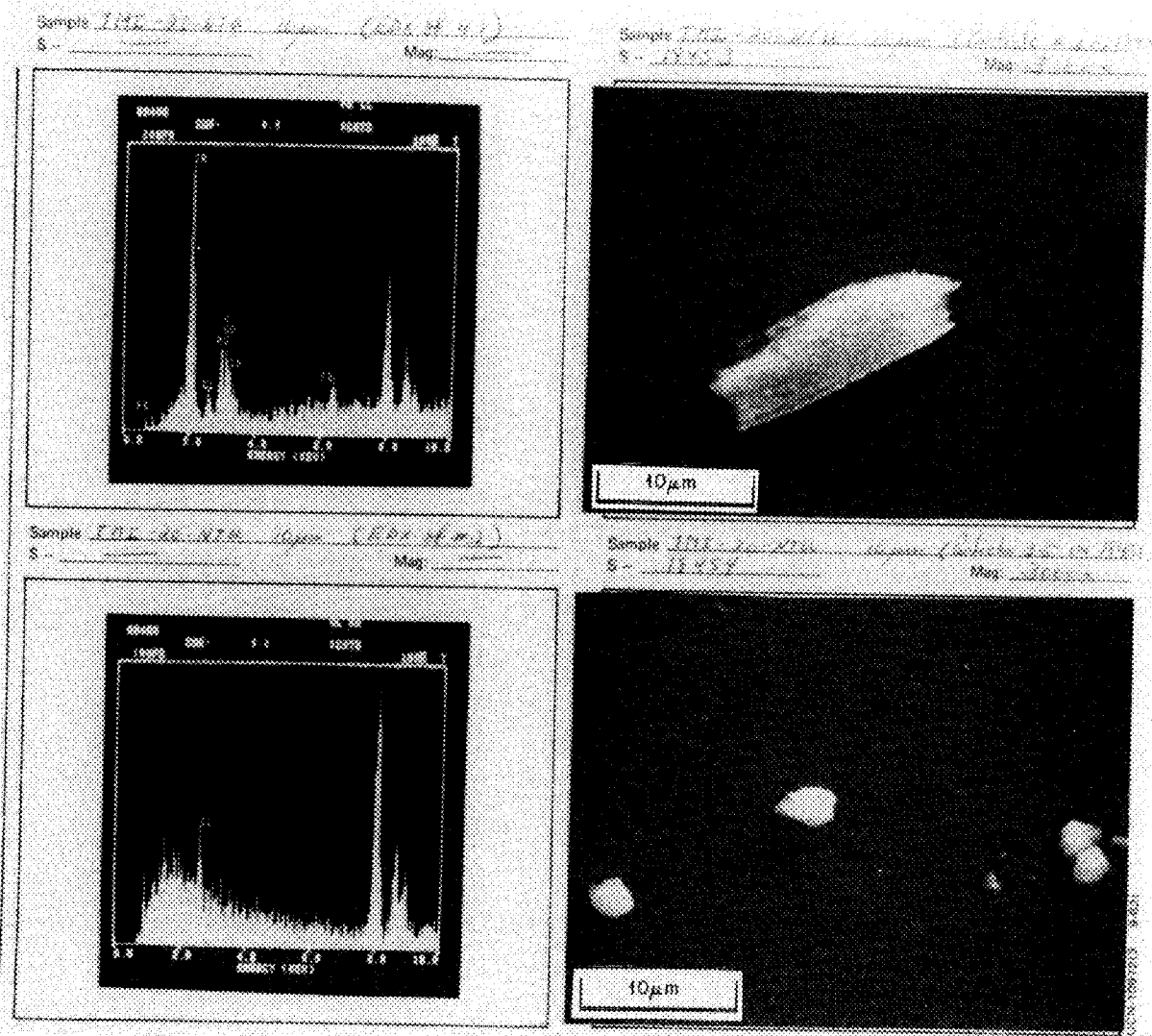
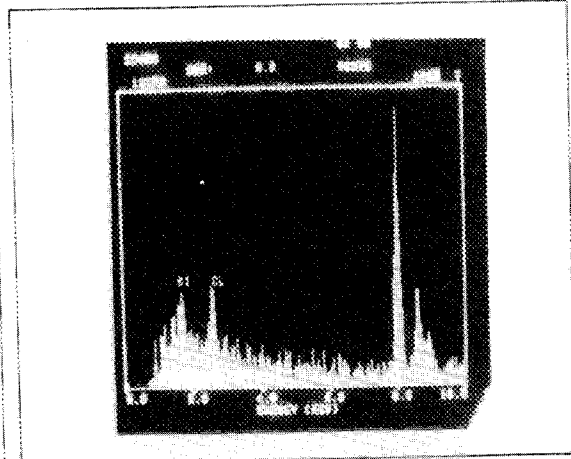
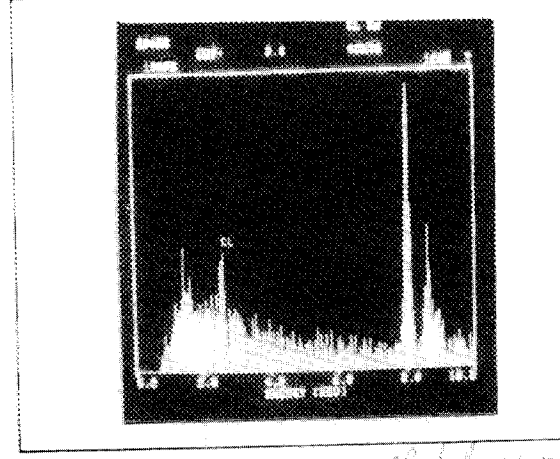


Fig. E.3. Nucleopore filter test 3 with 22-NTU water sample W2, 10-µm filter.

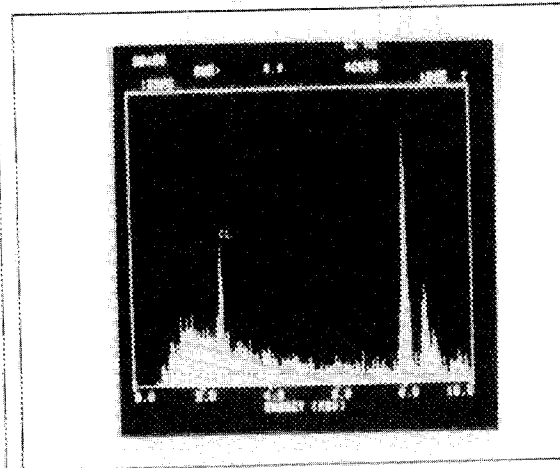
Sample JISE-20-NTU 10µm (Batch #1)
S - _____ Mag: _____



Sample JISE-20-NTU 10µm (Batch #2)
S - _____ Mag: _____



Sample JISE-20-NTU 10µm (Batch #5)
S - _____ Mag: _____



Sample JISE-20-NTU 10µm (Batch #1 on 10µm)
S - 1E435 Mag: 3000x



Fig. E.4. Nuclepore filter test 3 with 22-NTU water sample W2, 10-µm filter.

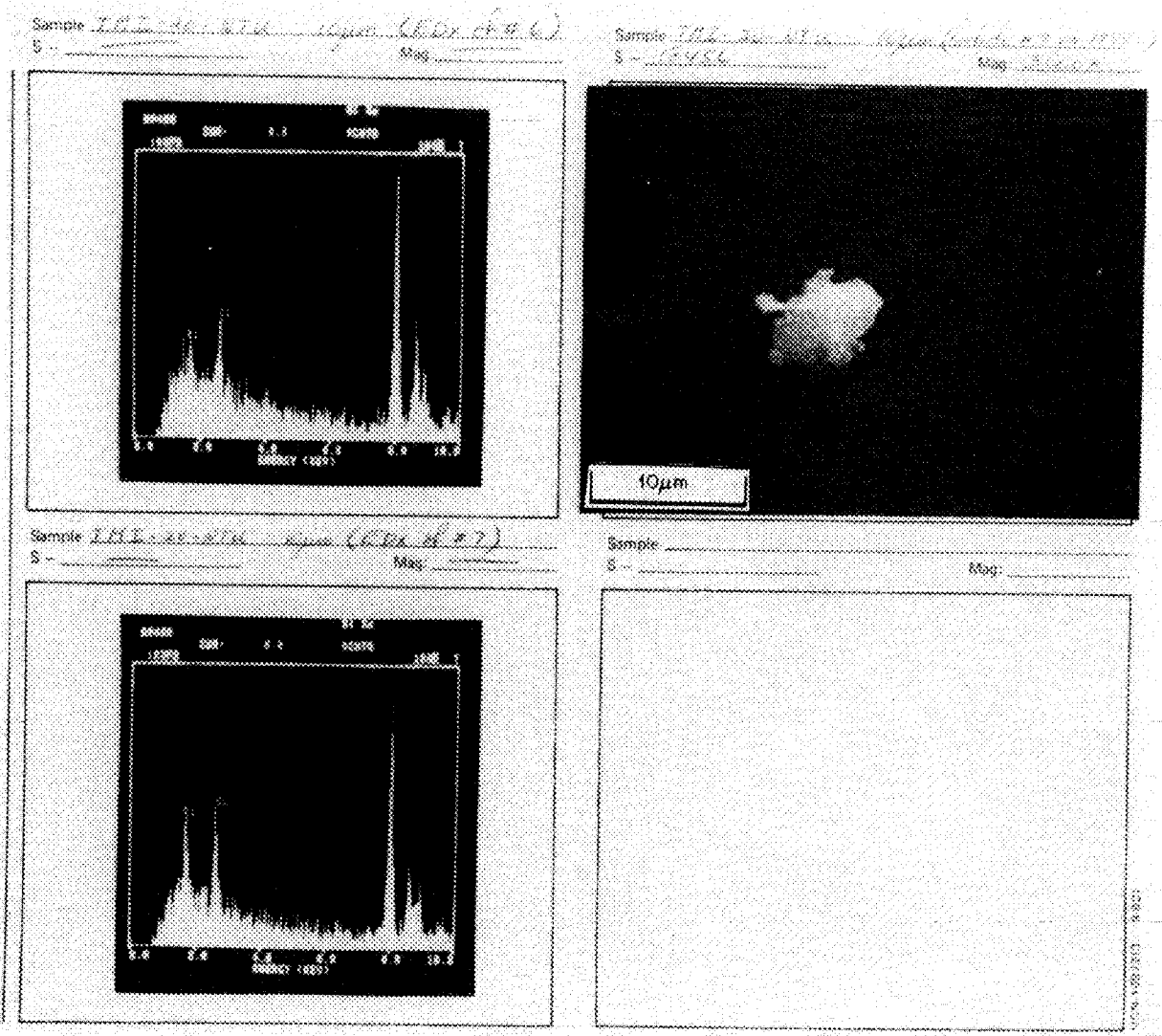


Fig. E.5. Nuclepore filter test 3 with 22-NTU water sample W2, 10-µm filter.

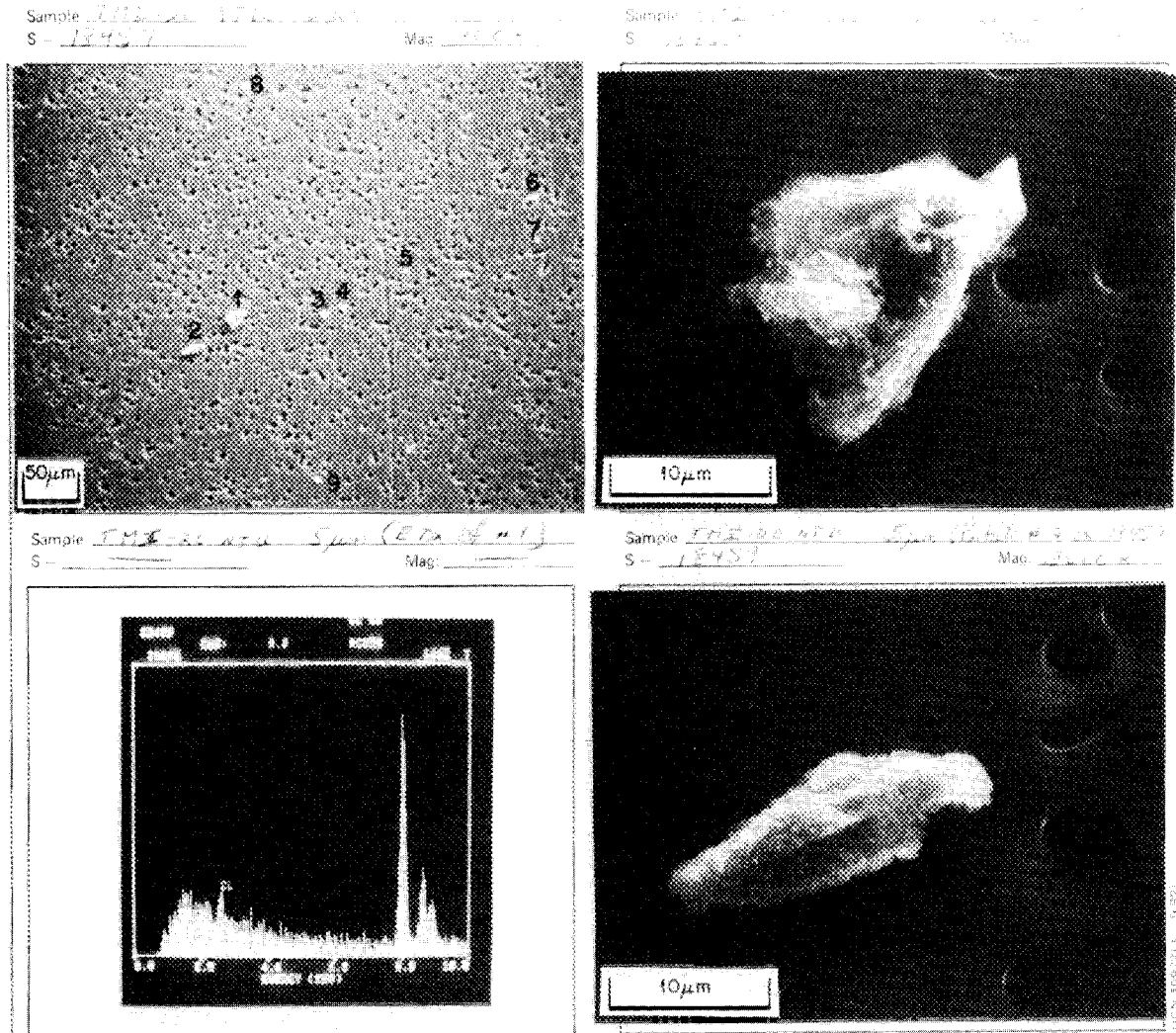


Fig. E.6. Nuclepore filter test 3 with 22-NTU water sample W2, 5-µm filter.

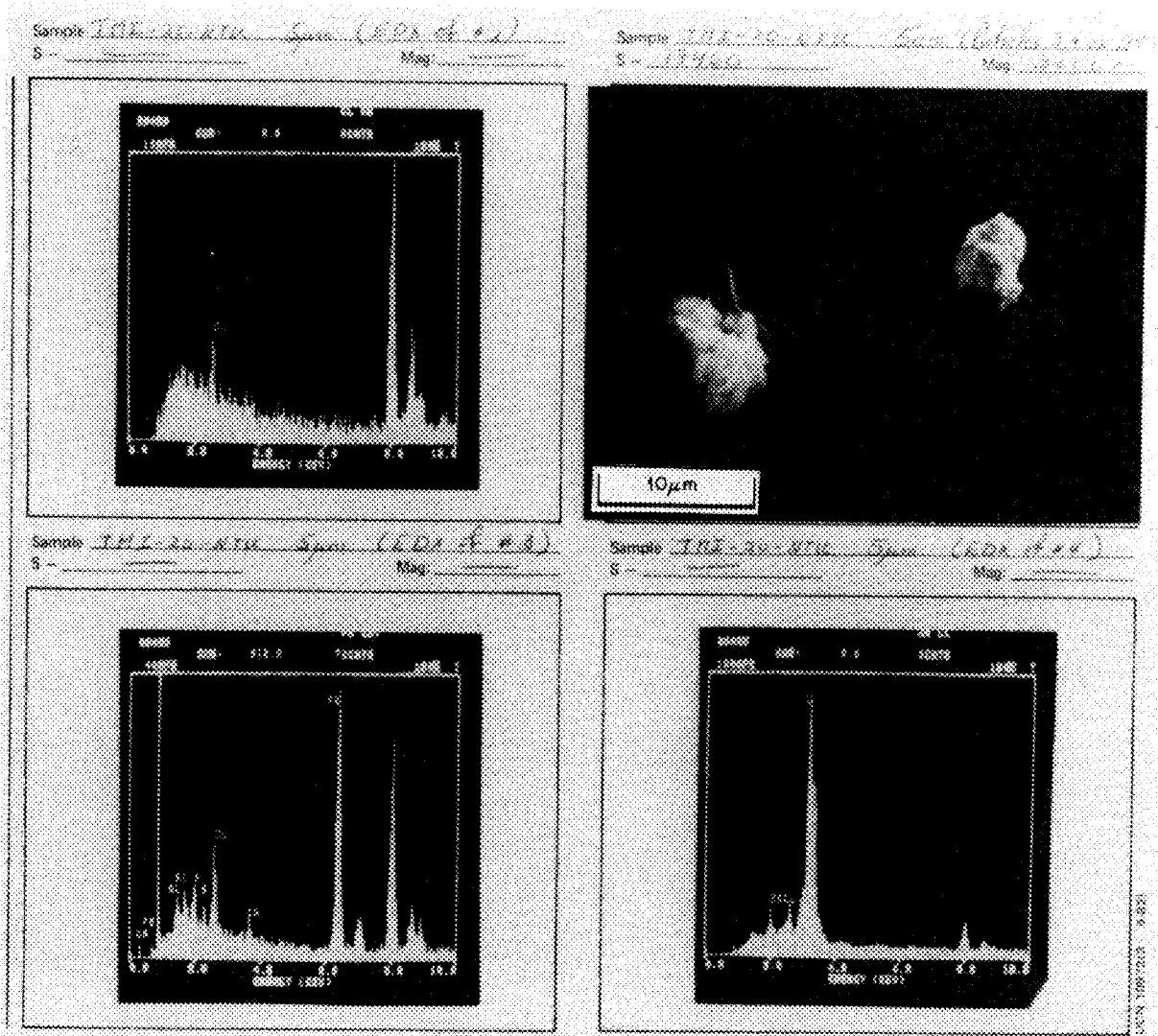
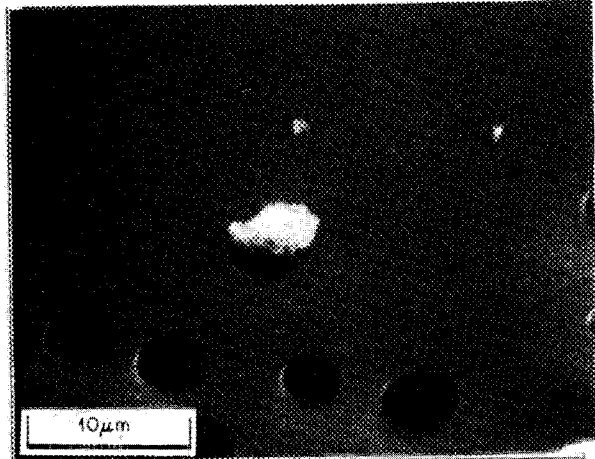
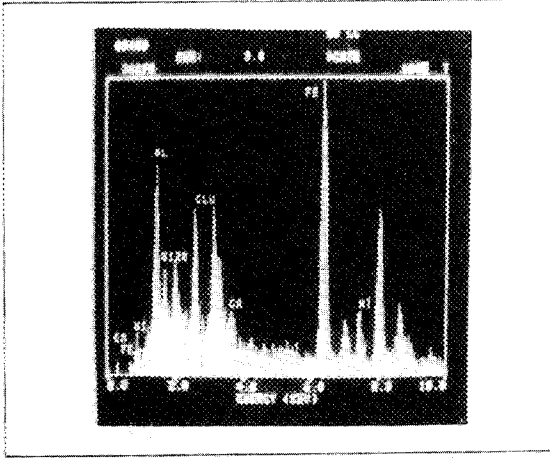


Fig. E.7. Nucleopore filter test 3 with 22-NTU water sample W2, 5-µm filter.

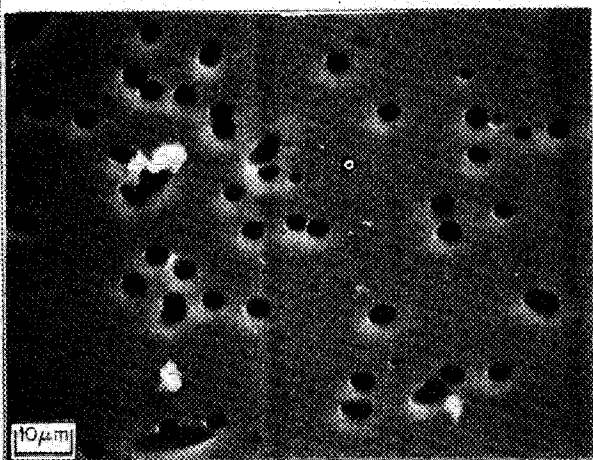
Sample TMT-20-ATM 5µm (C.H. Hsu-195)
 S - 18461 Mag: 2000X



Sample TMT-20-ATM 5µm (C.H. Hsu-195)
 S - 18461 Mag: 2000X



Sample TMT-20-ATM 5µm (C.H. Hsu-195)
 S - 18462 Mag: 1000X



Sample TMT-20-ATM 5µm (C.H. Hsu-195)
 S - 18462 Mag: 1000X

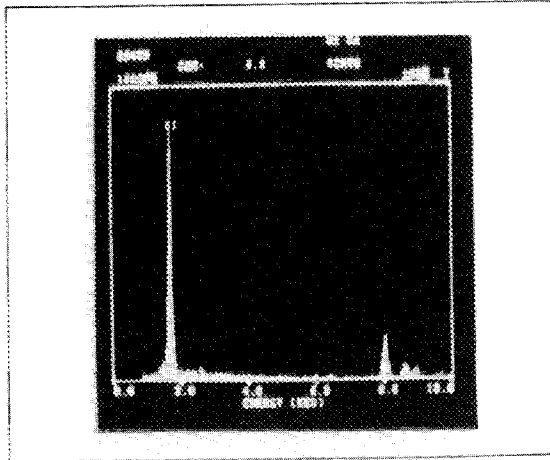


Fig. E.8. Nucleopore filter test 3 with 22-NTU water sample W2, 5-µm filter.

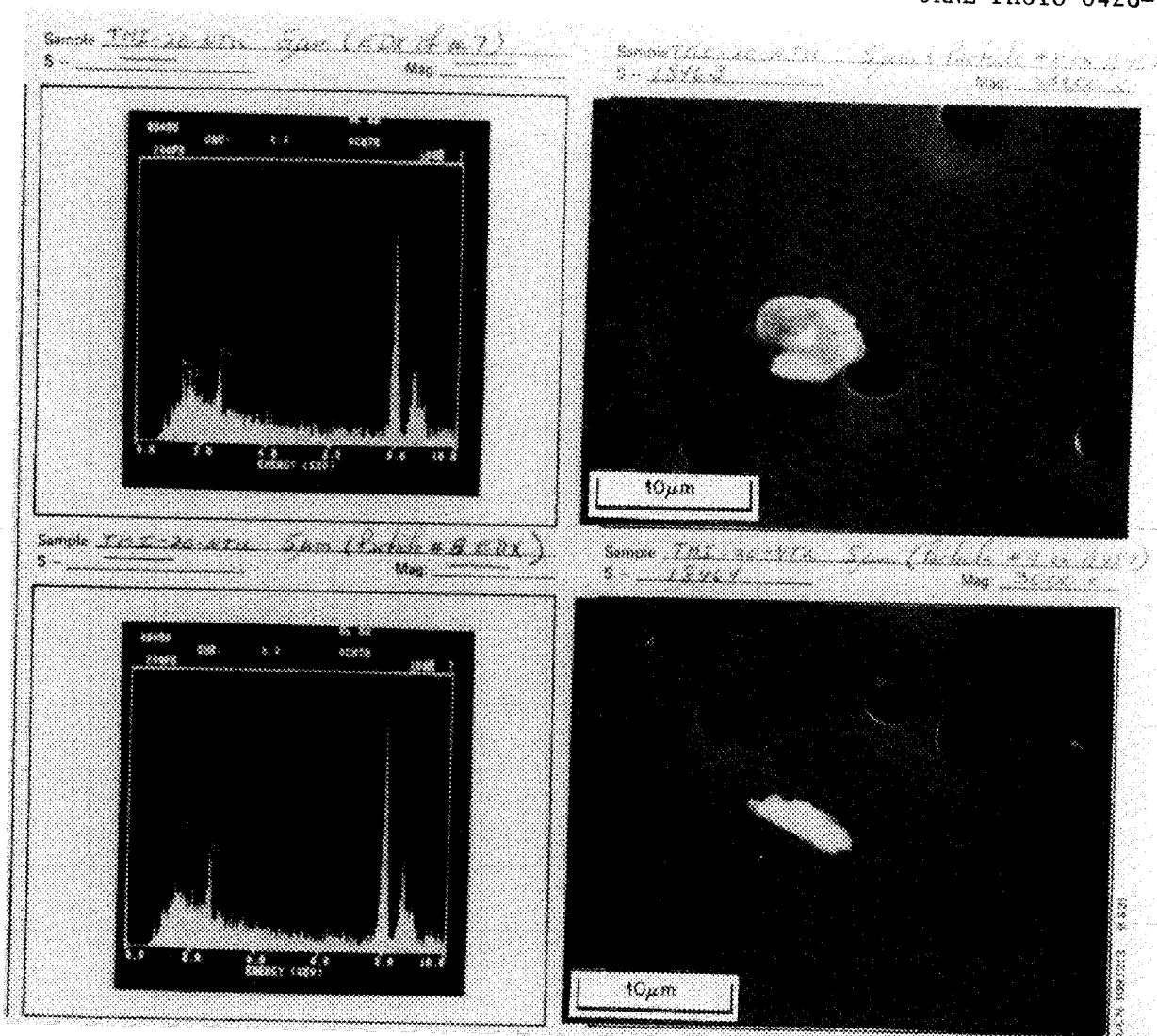
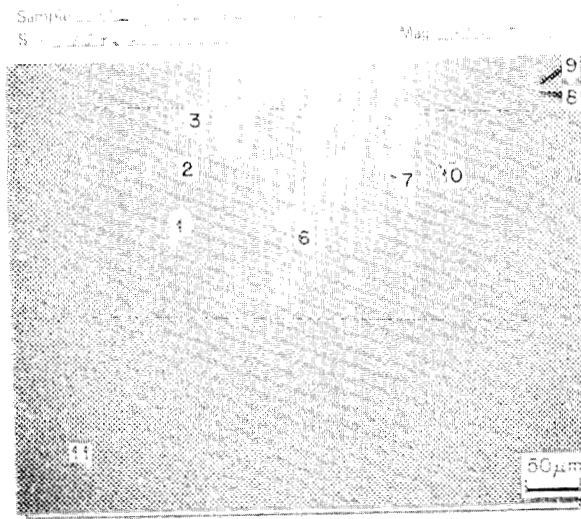
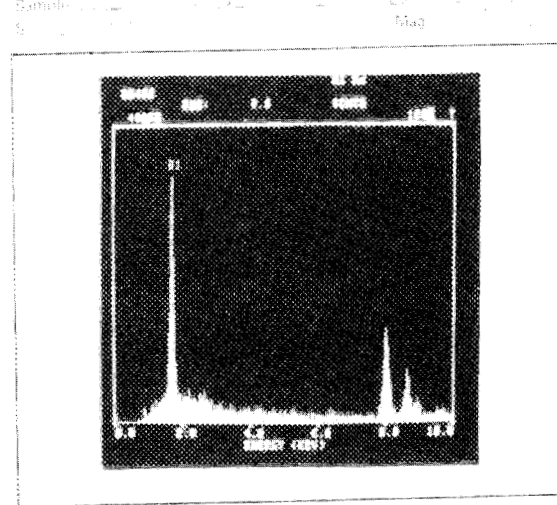


Fig. E.9. Nucleopore filter test 3 with 22-NTU water sample W2, 5-µm filter.



Sample 22-NTU W2 Mag 1000x
 S 22-NTU W2



Sample 22-NTU W2 Mag 1000x
 S 22-NTU W2

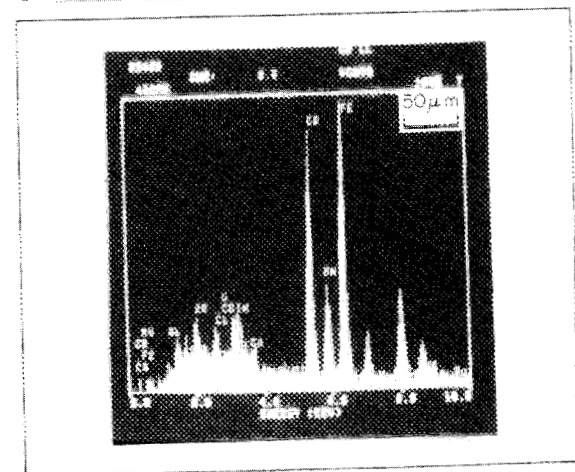
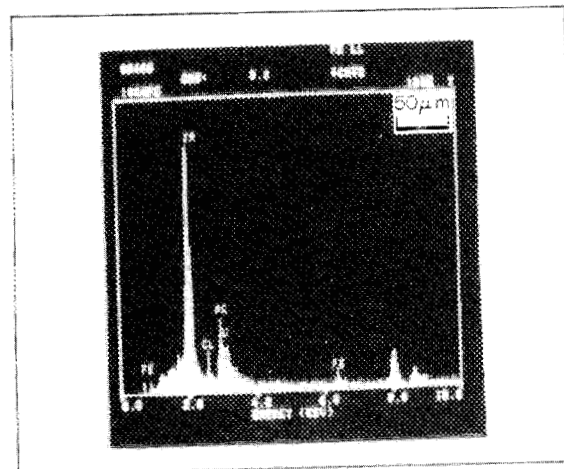


Fig. E.10. Nuclepore filter test 3 with 22-NTU water sample W2, 2-µm filter.

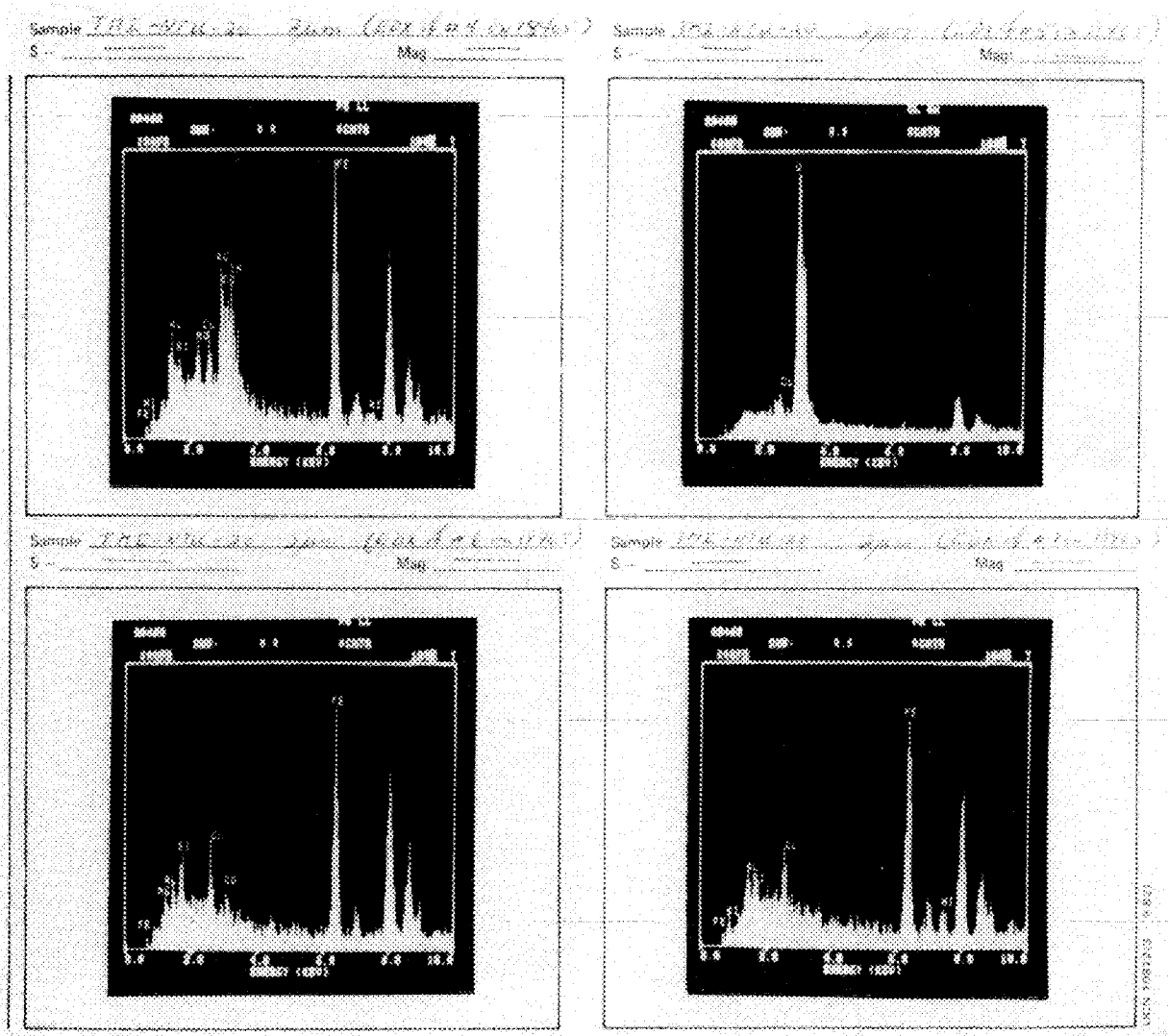
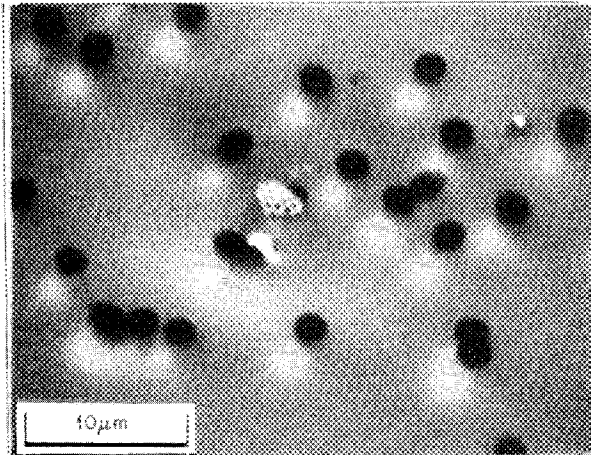
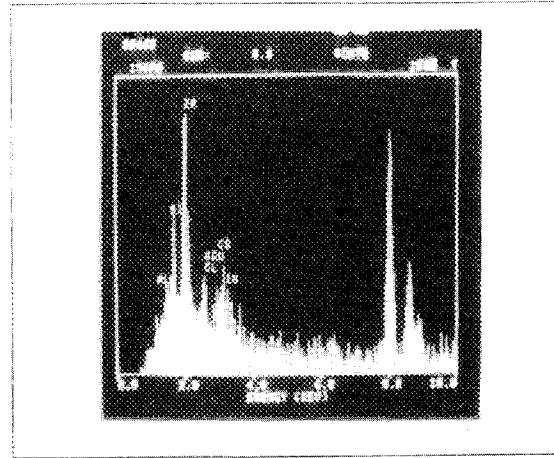


Fig. E.11. Nuclepore filter test 3 with 22-NTU water sample W2, 2- μ m filter.

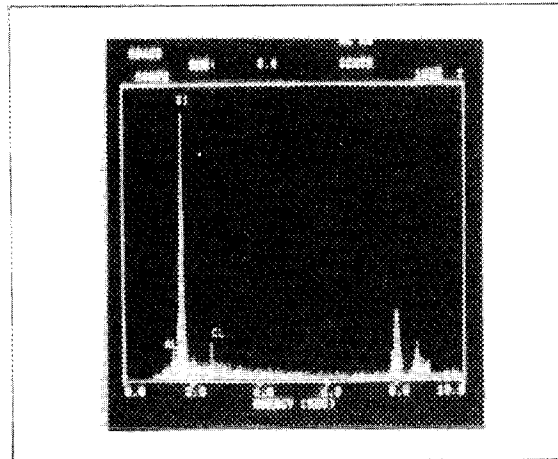
Sample 17A-31400-3um (EDI 4/9)
S- 1796 Mag: 100x



Sample 17A-31400-3um (EDI 4/9)
S- 1797 Mag: 100x



Sample 17A-31400-3um (EDI 4/9)
S- 1798 Mag: 100x



Sample 17A-31400-3um (EDI 4/9)
S- 1799 Mag: 100x

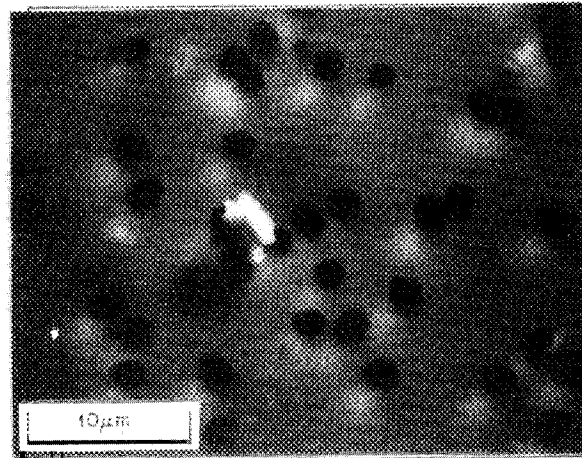
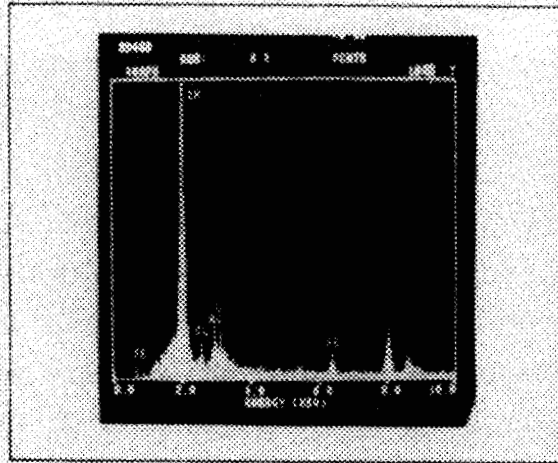


Fig. E.12. Nucleopore filter test 3 with 22-NTU water sample W2, 2- μ m filter.

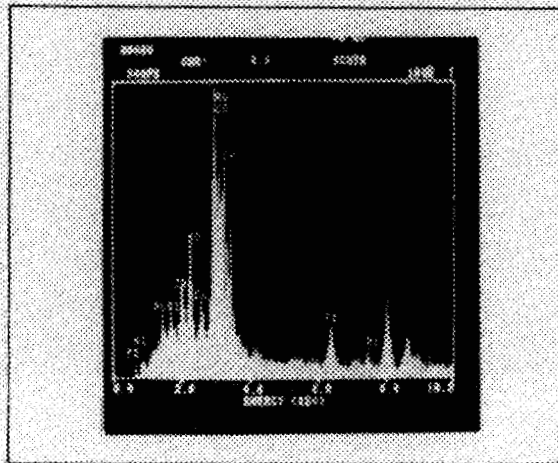
Sample T.M. 2-17-76 2µm (E. W. A. W.)
S _____ Mag _____



Sample T.M. 2-17-76 2µm (E. W. A. W.)
S 18763 Mag 2000x



Sample T.M. 2-17-76 2µm (E. W. A. W.)
S _____ Mag _____



Sample _____
S _____ Mag _____

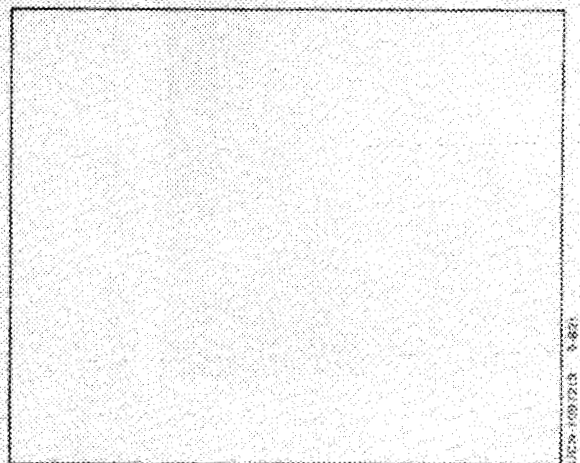


Fig. E.13. Nuclepore filter test 3 with ZZ-NUU water sample W2, 2-µm filter.

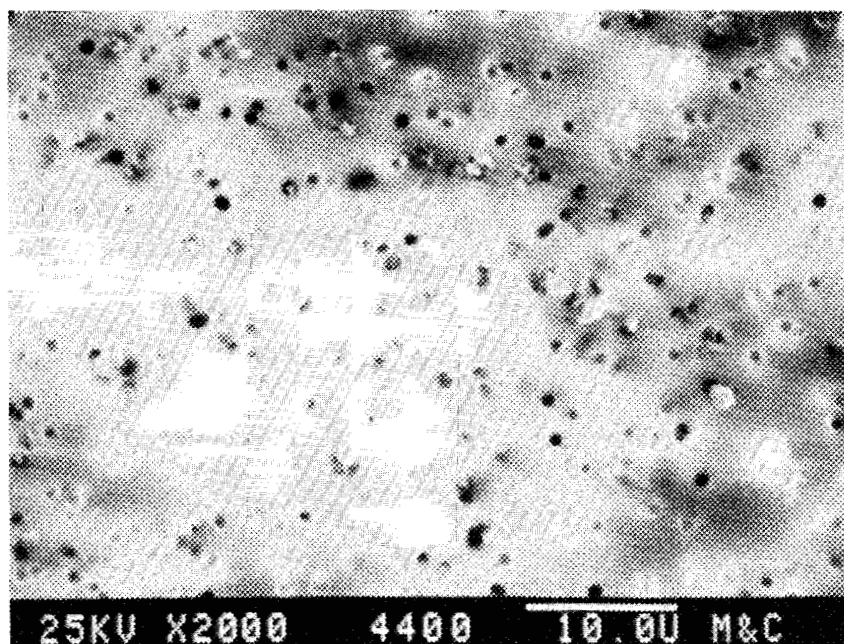


Fig. E.14. Nucleopore filter test 3 with 22-NTU water sample W2, 1- μ m filter.

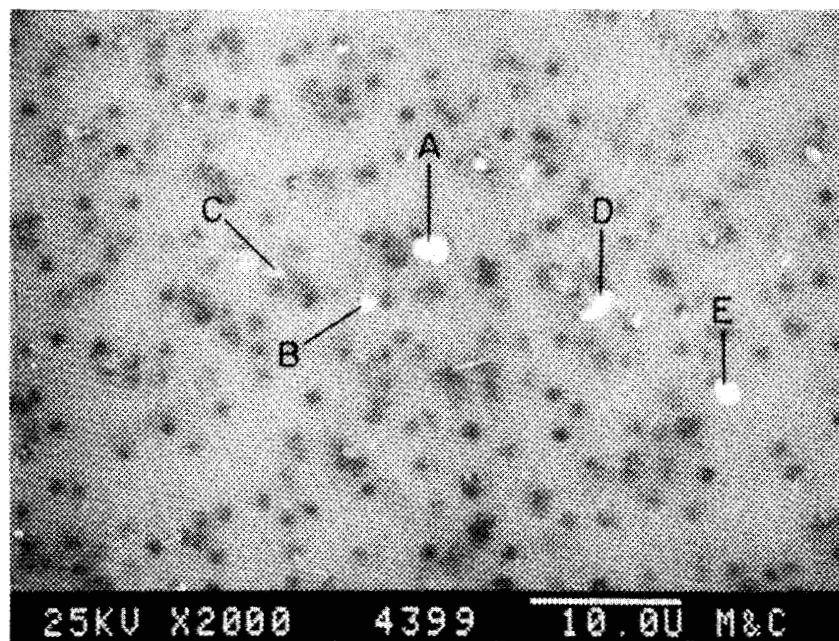


Fig. E.15. Nucleopore filter test 3 with 22-NTU water sample W2, 1- μ m filter, BEI.

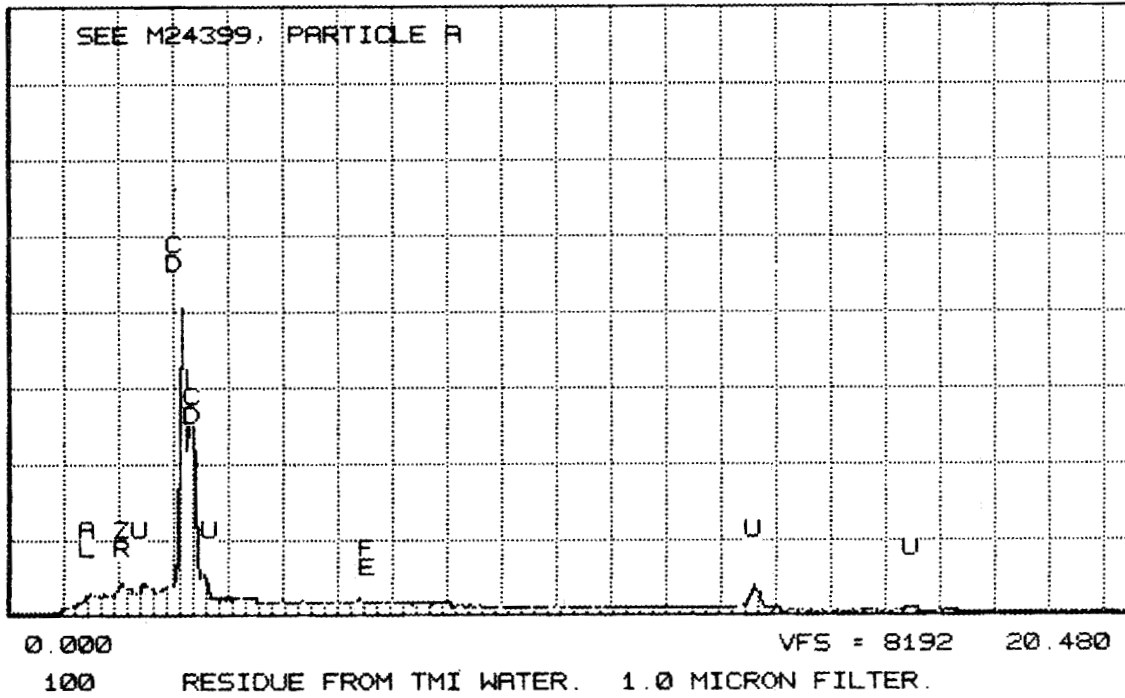


Fig. E.16. EDX of particle A, 4399 (see Fig. E.15).

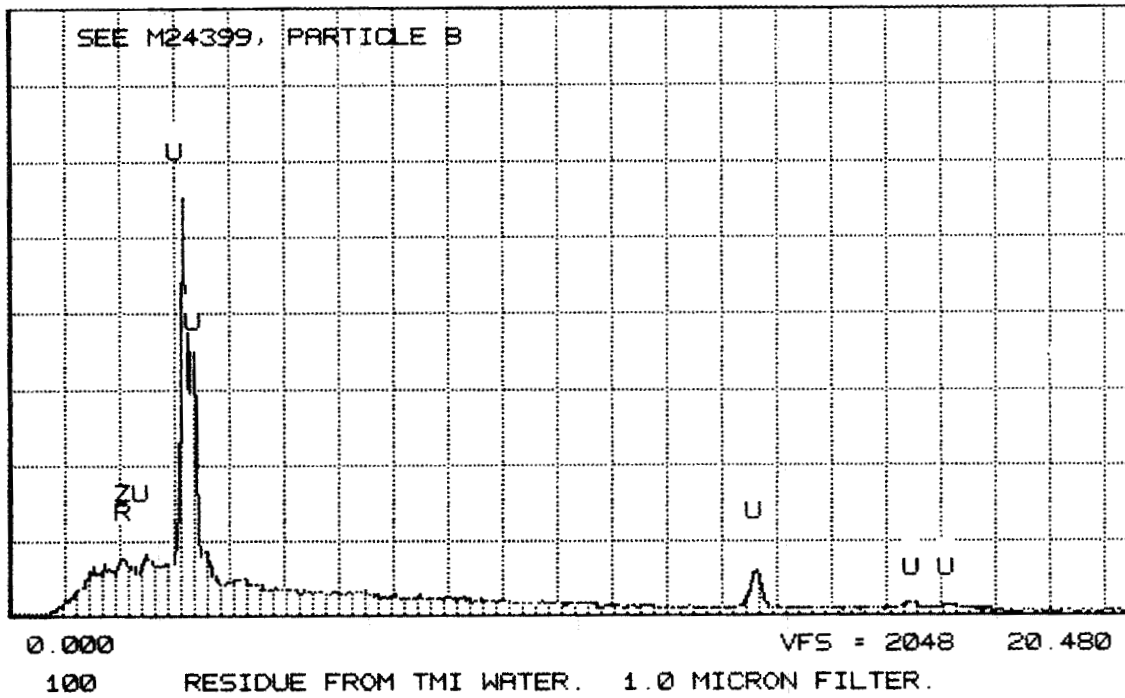


Fig. E.17. EDX of particle B, 4399 (see Fig. E.15).

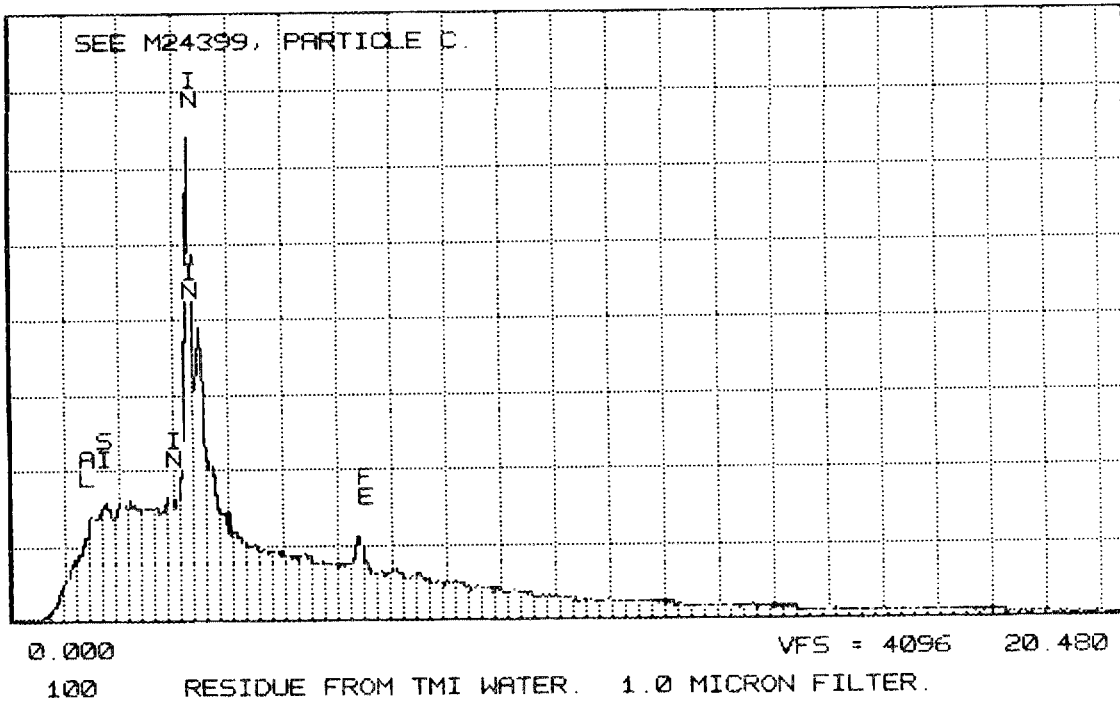


Fig. E.18. EDX of particle C, 4399 (see Fig. E.15).

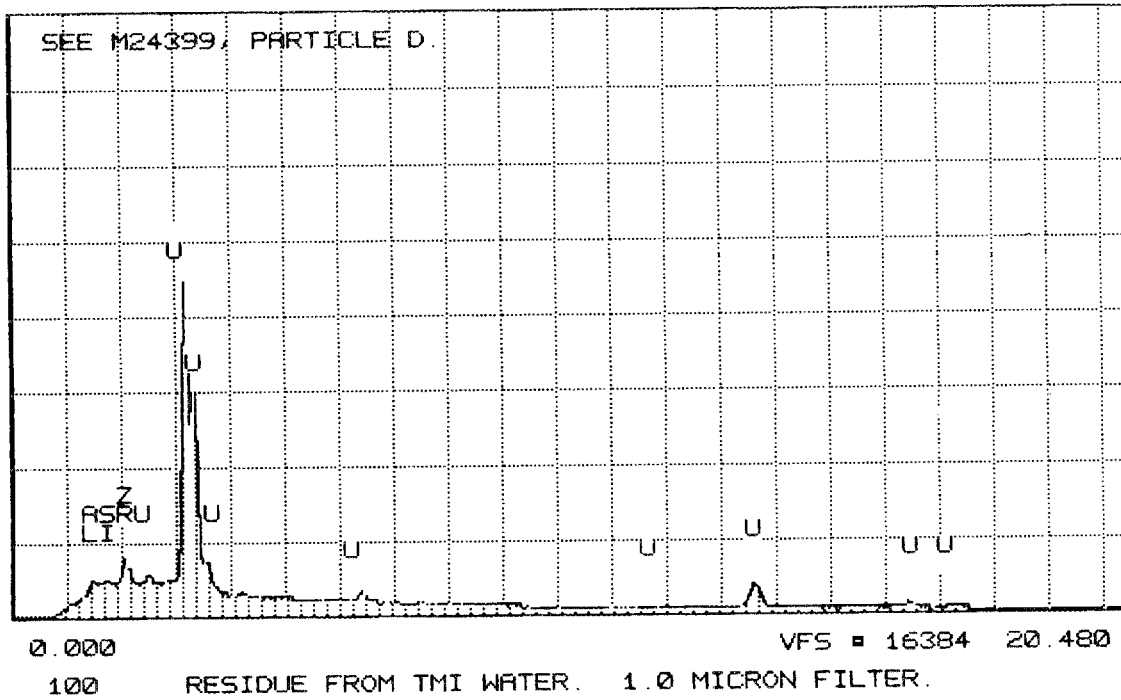


Fig. E.19. EDX of particle D, 4399 (see Fig. E.15).

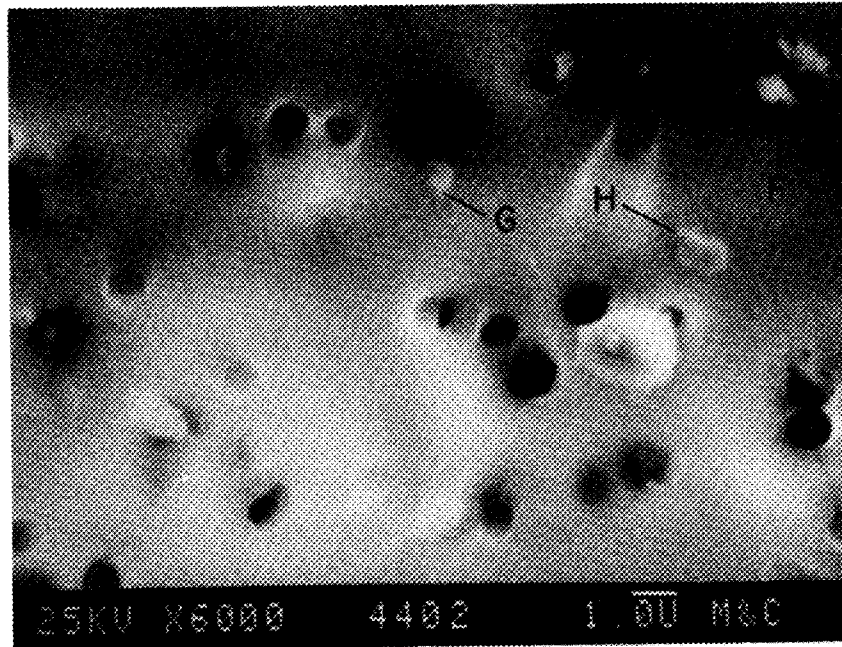


Fig. E.20. Nuclepore filter test 3 with 22-NTU water sample W2, 1- μ m filter.

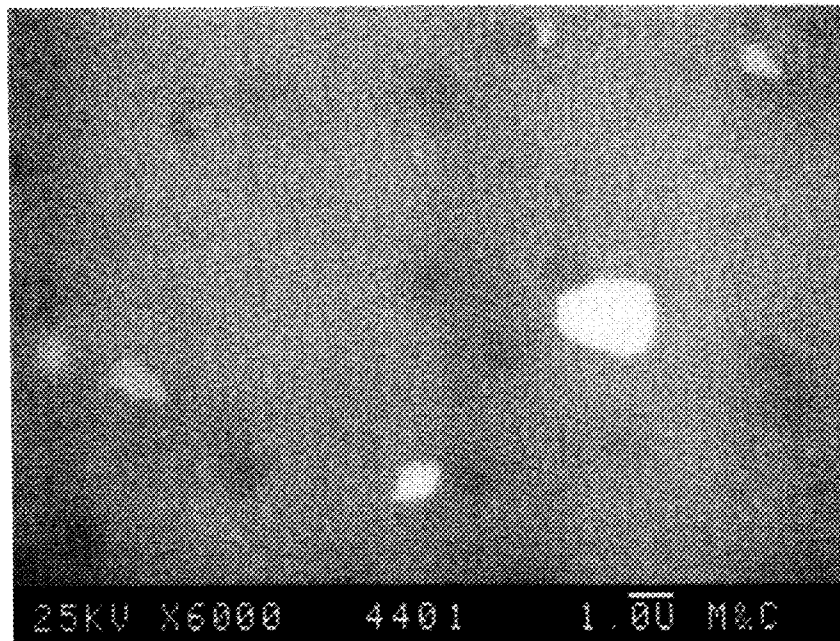


Fig. E.21. Nuclepore filter test 3 with 22-NTU water sample W2, 1- μ m filter, BEI.

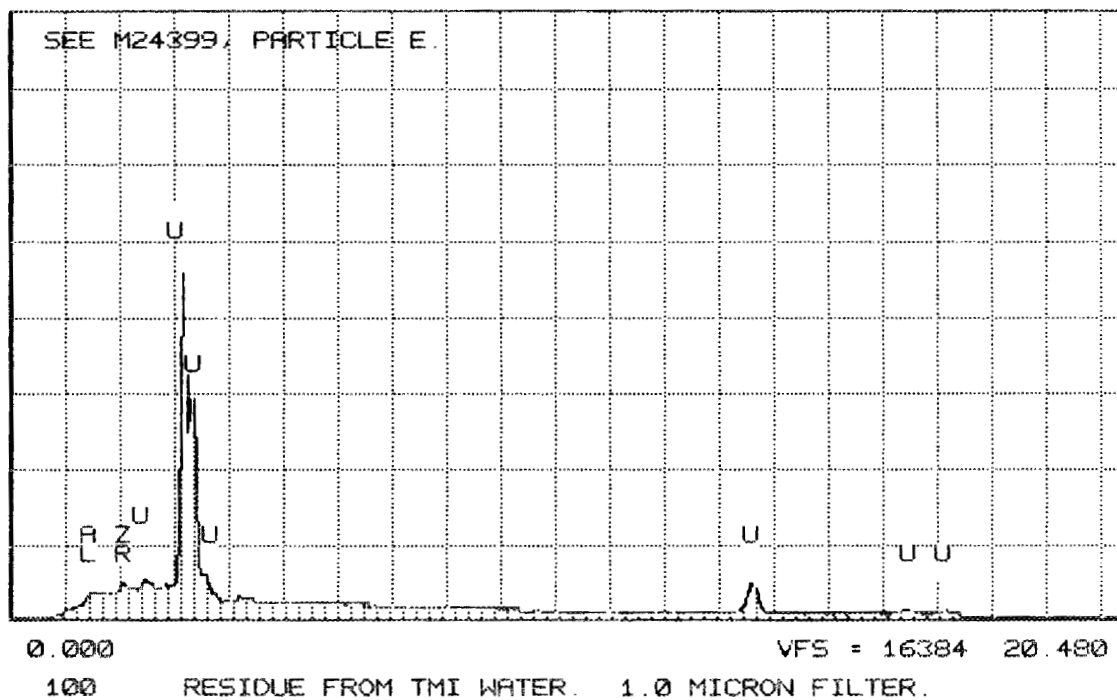


Fig. E.22. EDX of particle E, 4399 (see Fig. E.15).

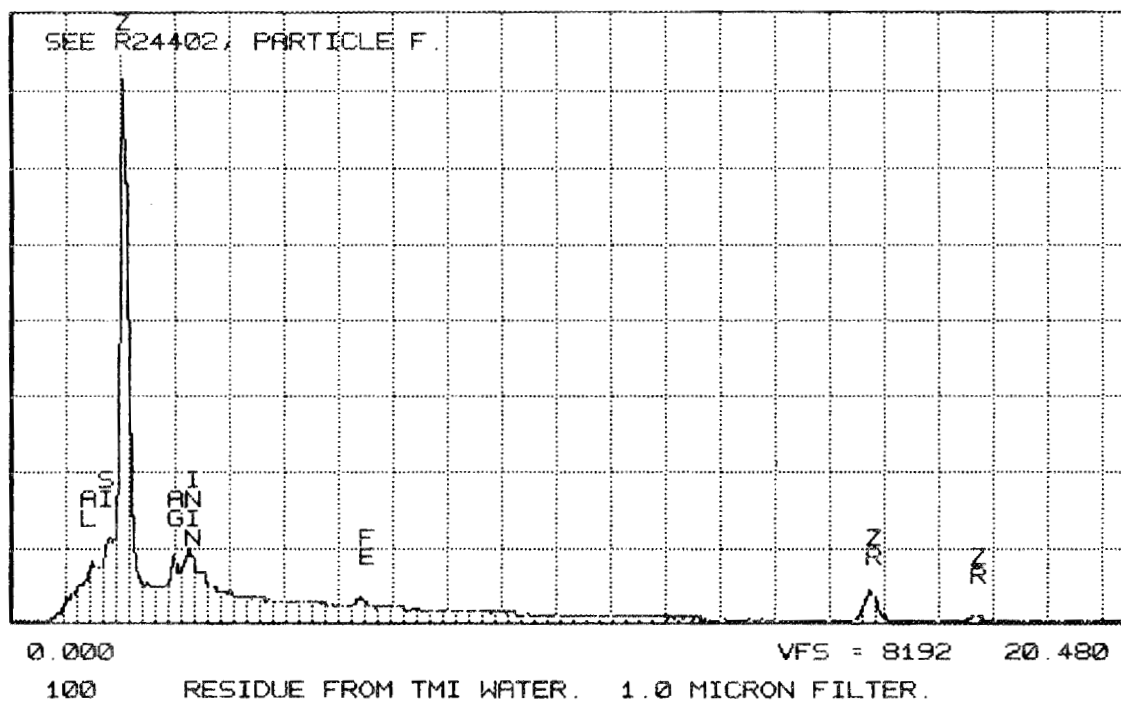


Fig. E.23. EDX of particle F, 4402 (see Fig. E.20).

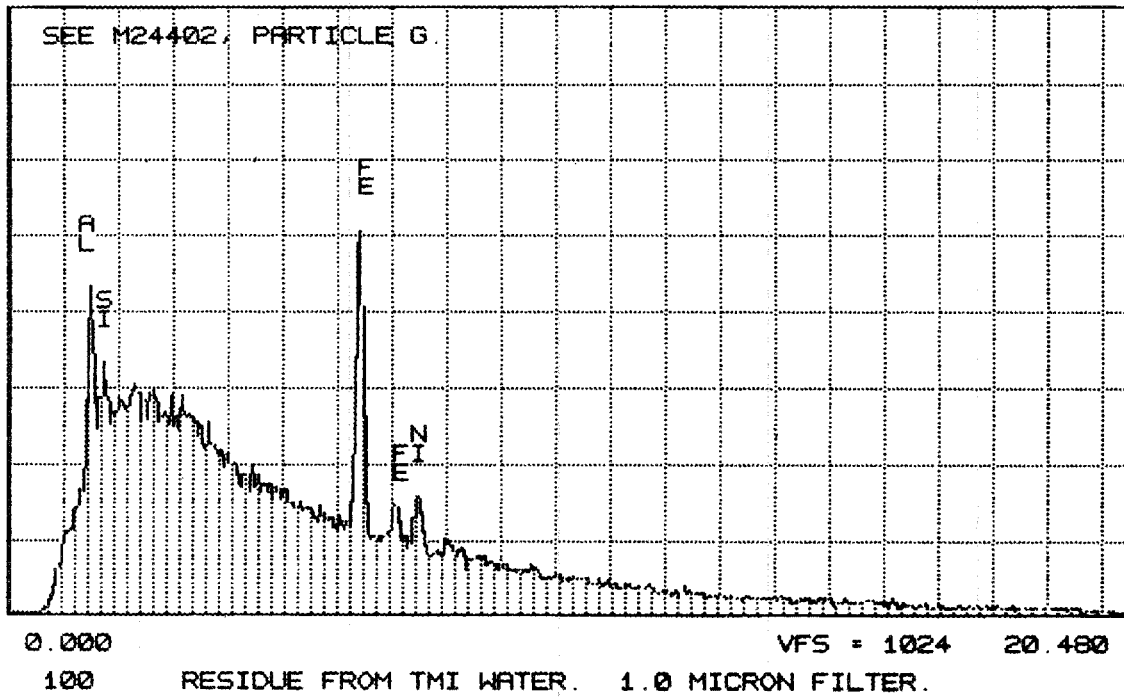


Fig. E.24. EDX of particle G, 4399 (see Fig. E.20).

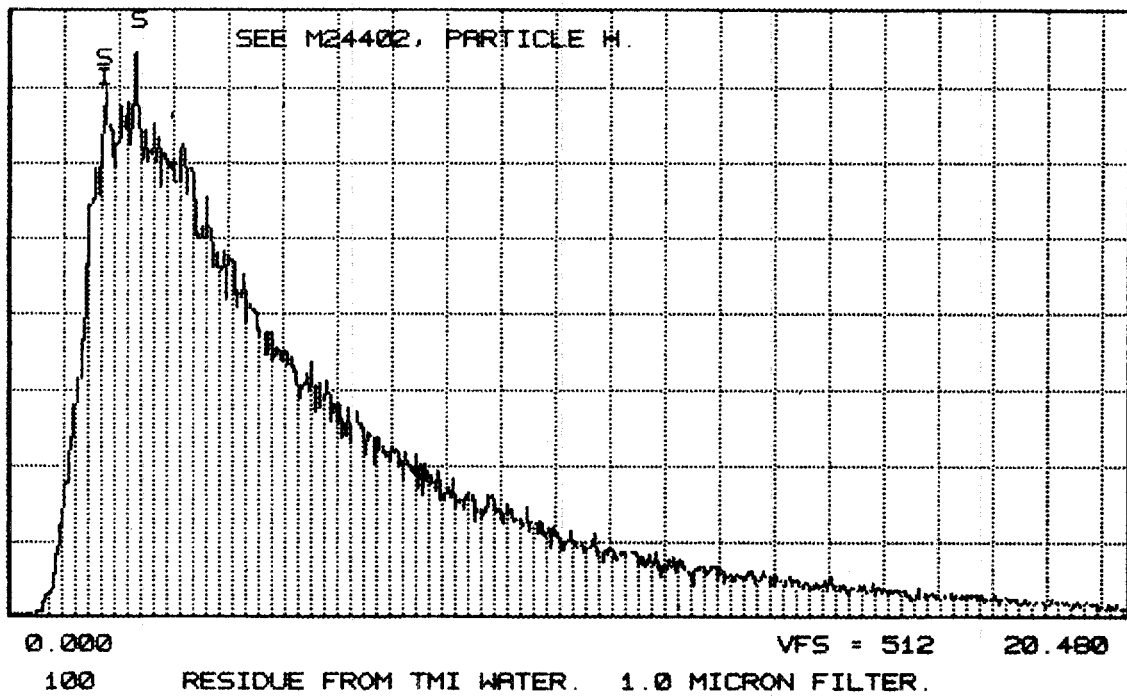


Fig. E.25. EDX of particle H, 4399 (see Fig. E.20).

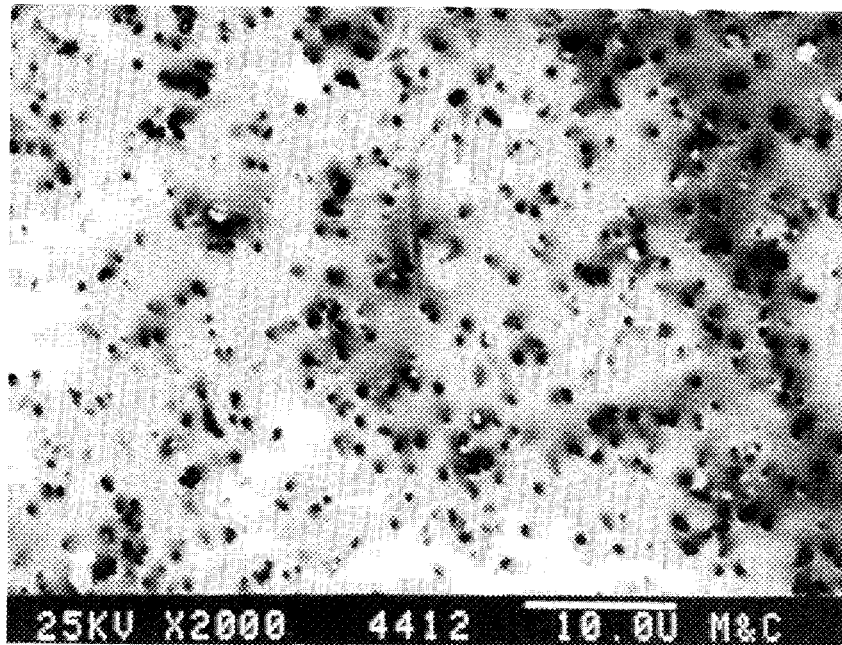


Fig. E.26. Nuclepore filter test 3 with 22-NTU water sample W2, 0.8- μm filter.

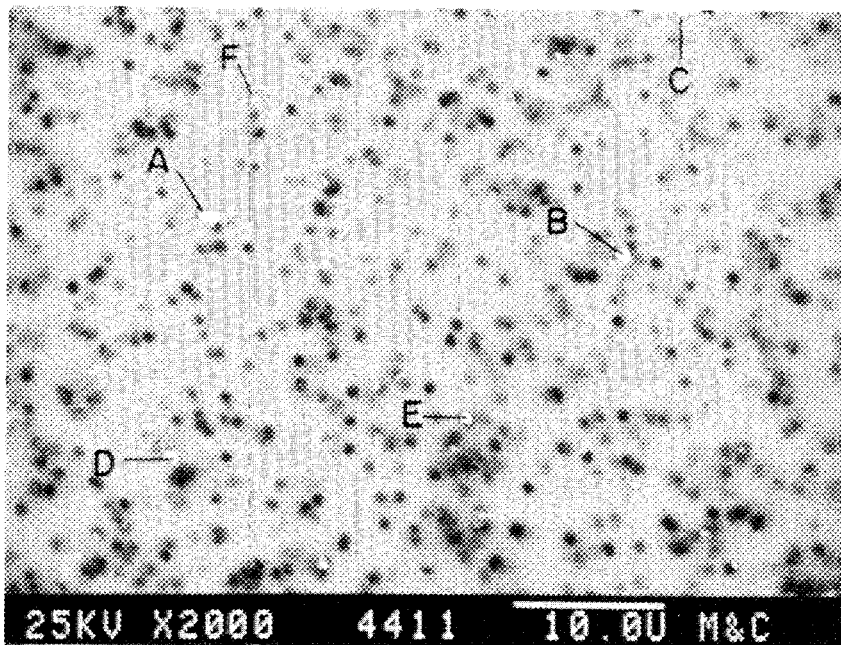


Fig. E.27. Nuclepore filter test 3 with 22-NTU water sample W2, 0.8- μm filter, BEI.

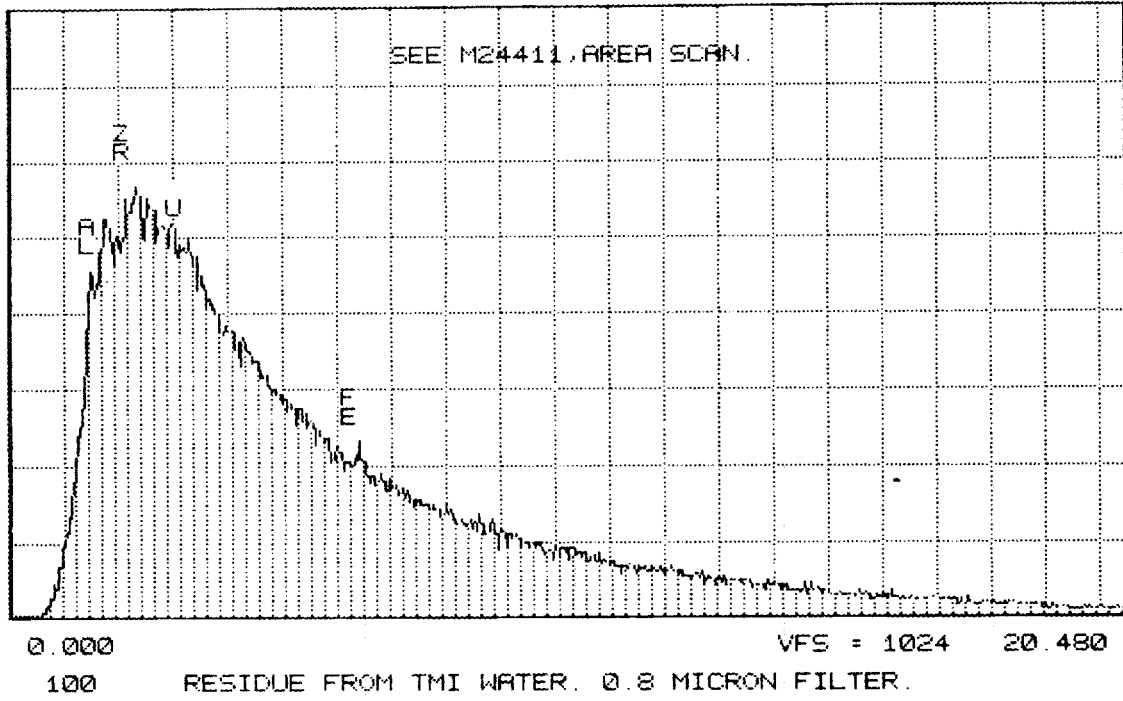


Fig. E.28. EDX of area of 4411 (see Fig. E.27).

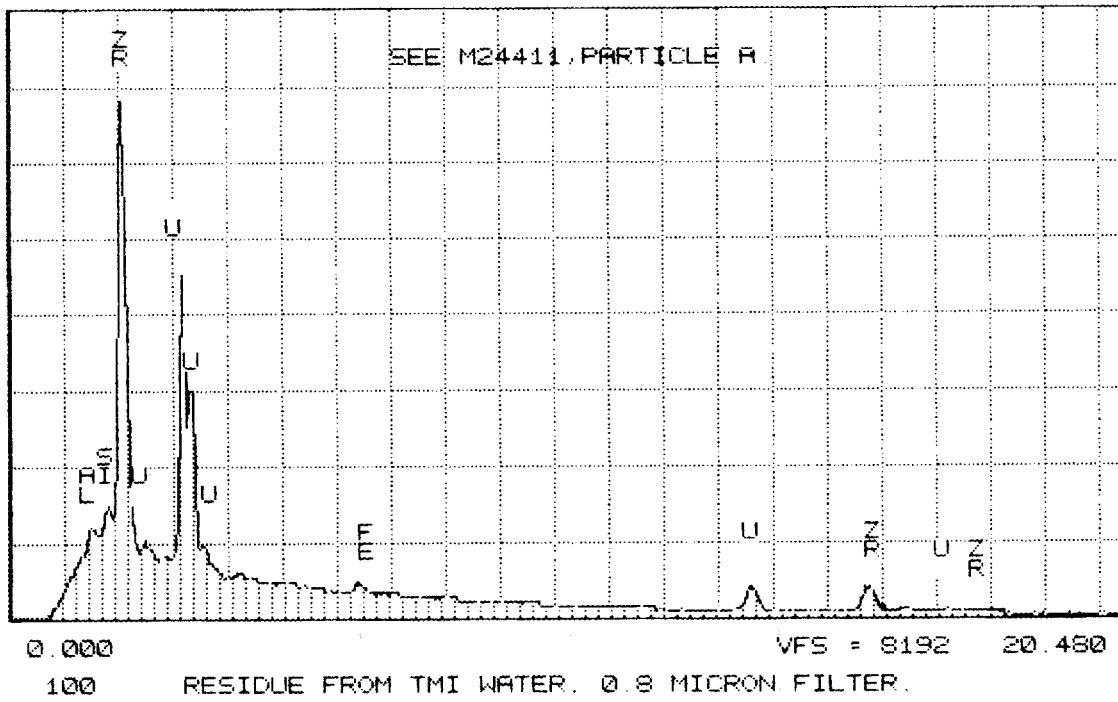


Fig. E.29. EDX of particle A, 4411 (see Fig. E.27).

ORNL-DWG 87-14051

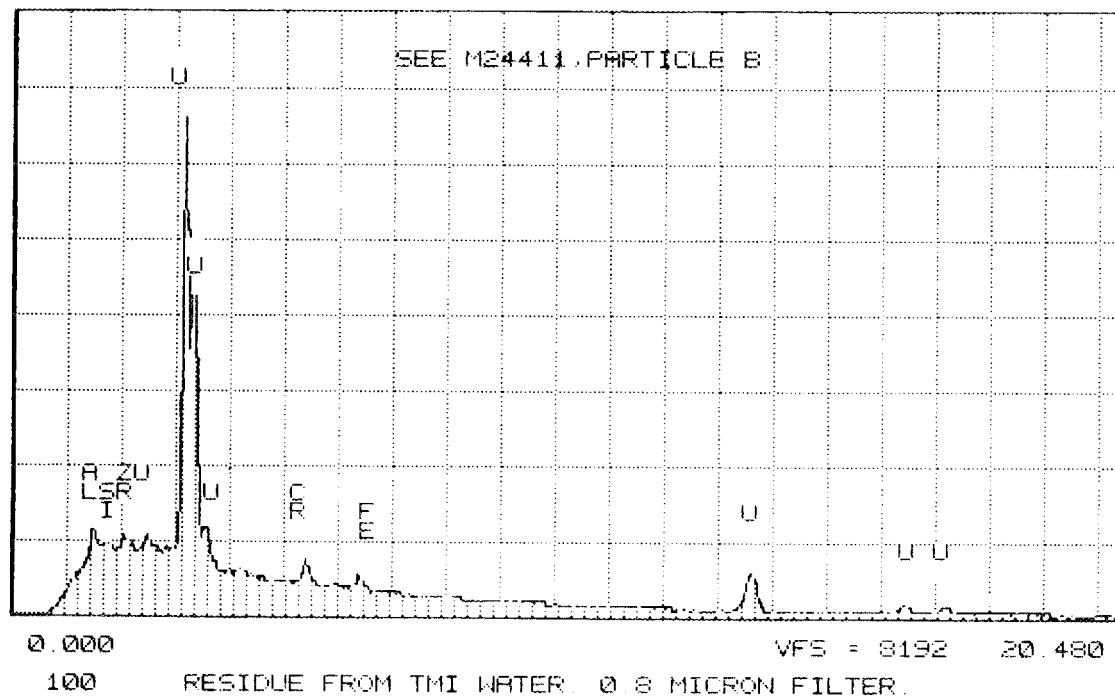


Fig. E.30. EDX of particle B, 4411 (see Fig. E.27).

ORNL-DWG 87-14052

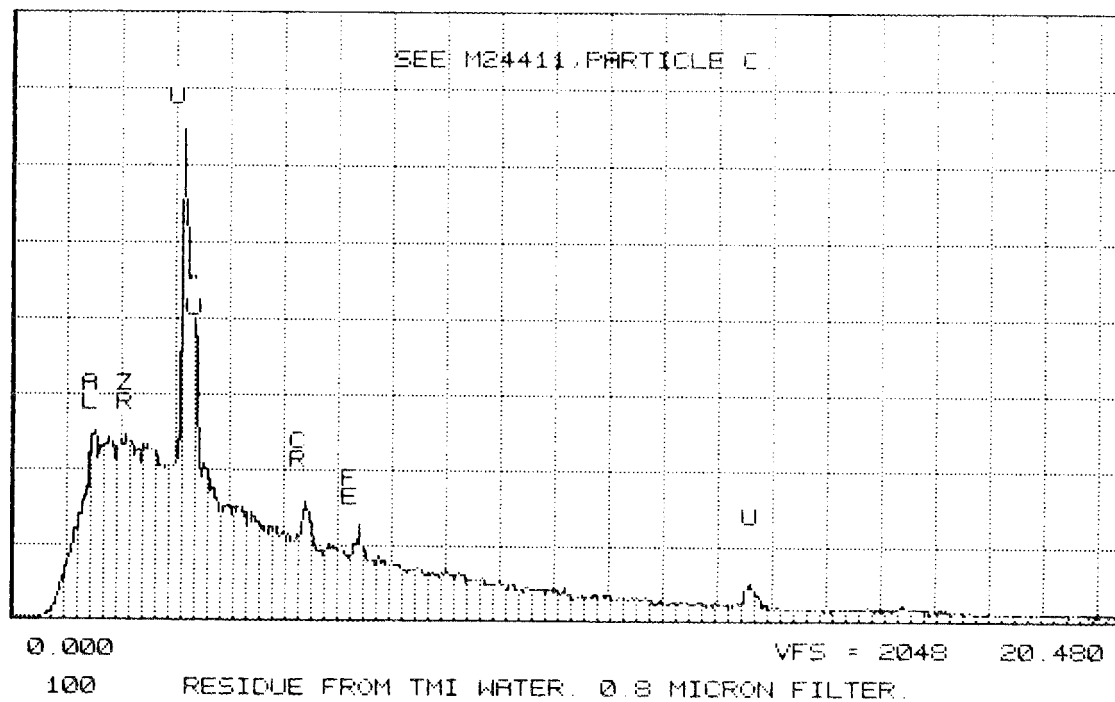


Fig. E.31. EDX of particle C, 4411 (see Fig. E.27).

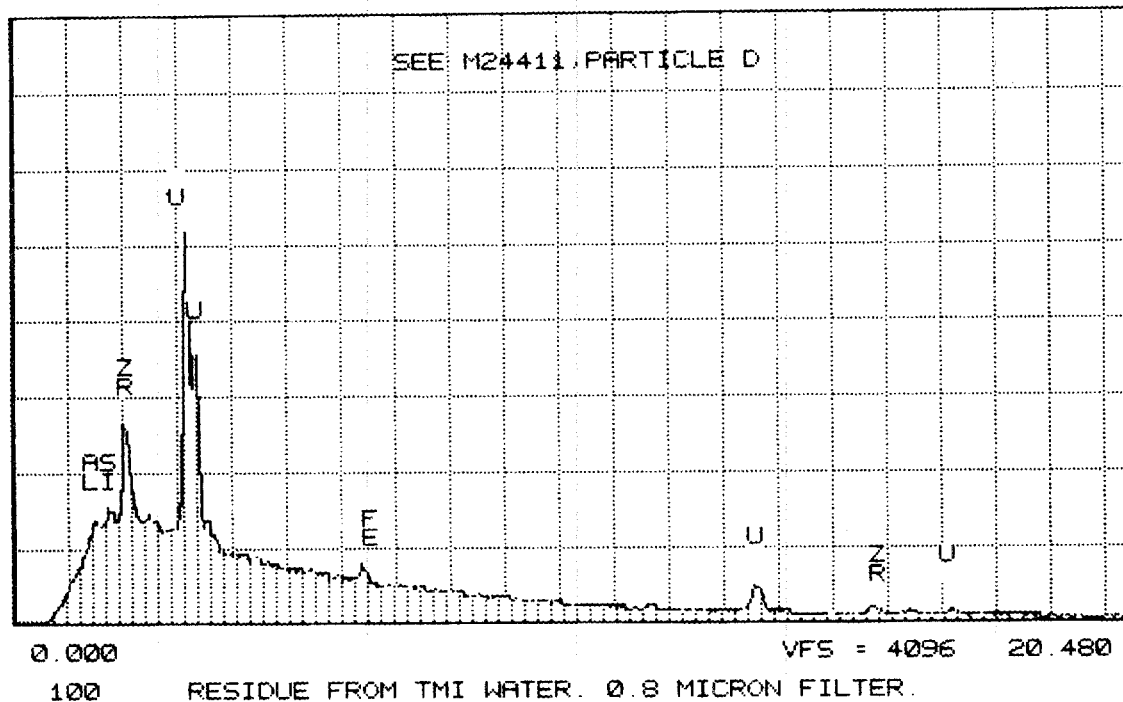


Fig. E.32. EDX of particle D, 4411 (see Fig. E.27).

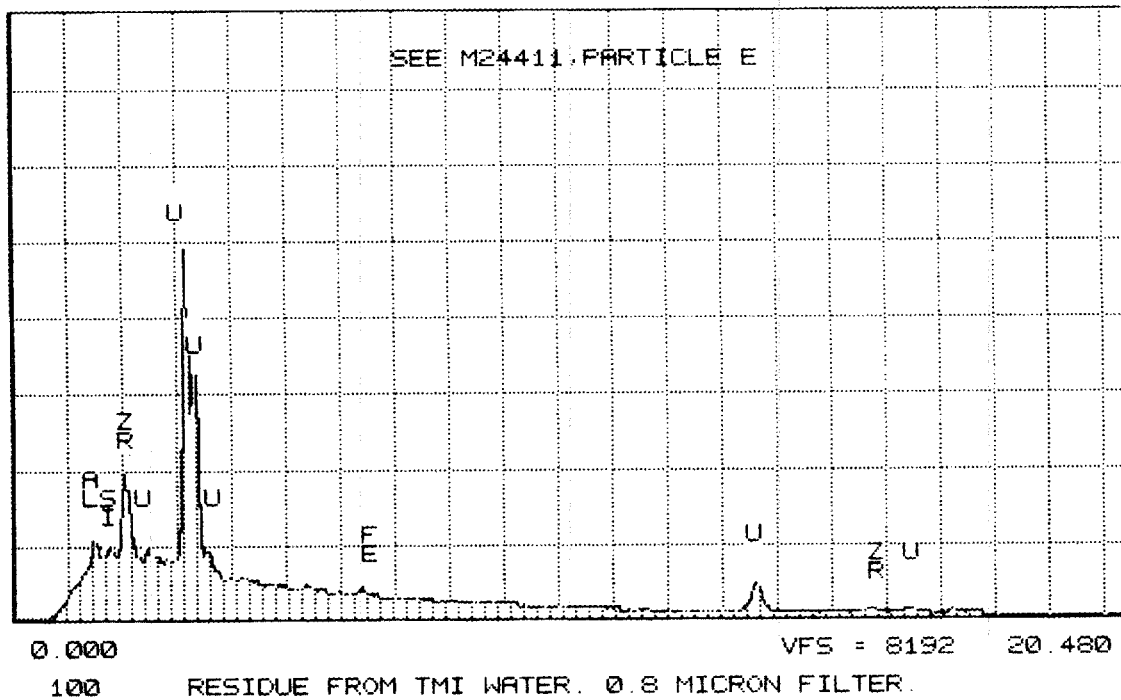


Fig. E.33. EDX of particle E, 4411 (see Fig. E.27).

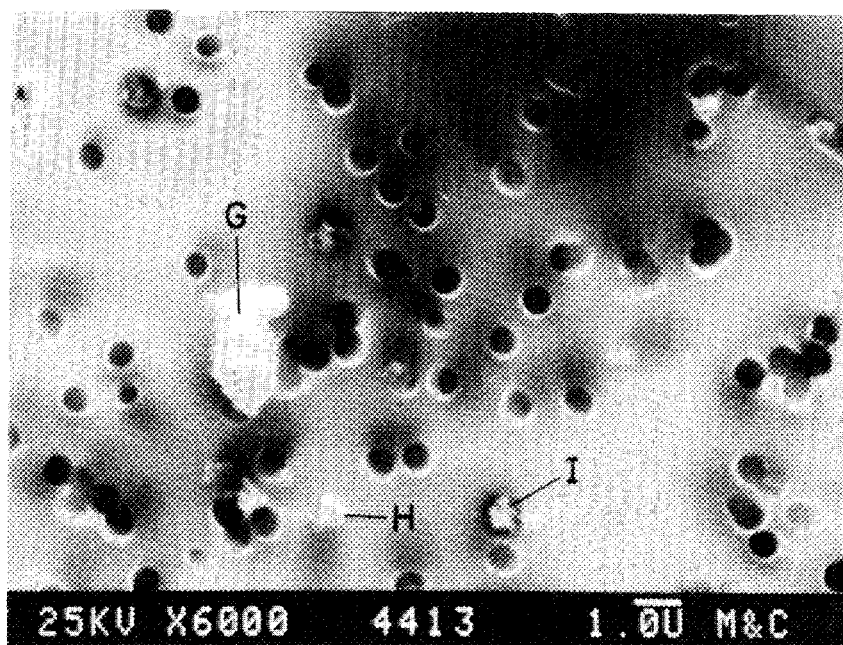


Fig. E.34. Nuclepore filter test 3 with 22-NTU water sample W2, 0.8- μm filter.

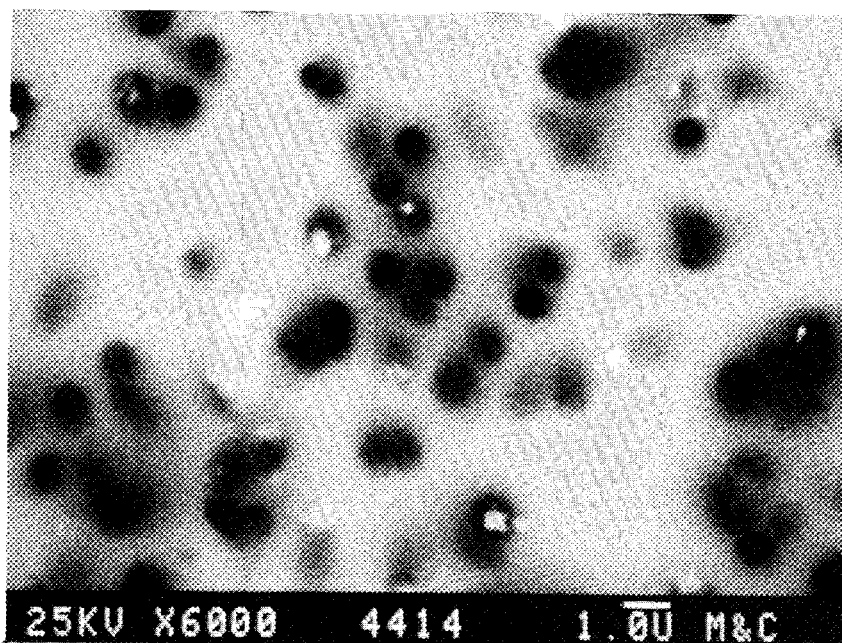


Fig. E.35. Nuclepore filter test 3 with 22-NTU water sample W2, 0.8- μm filter, BEI.

ORNL-DWG 87-14055

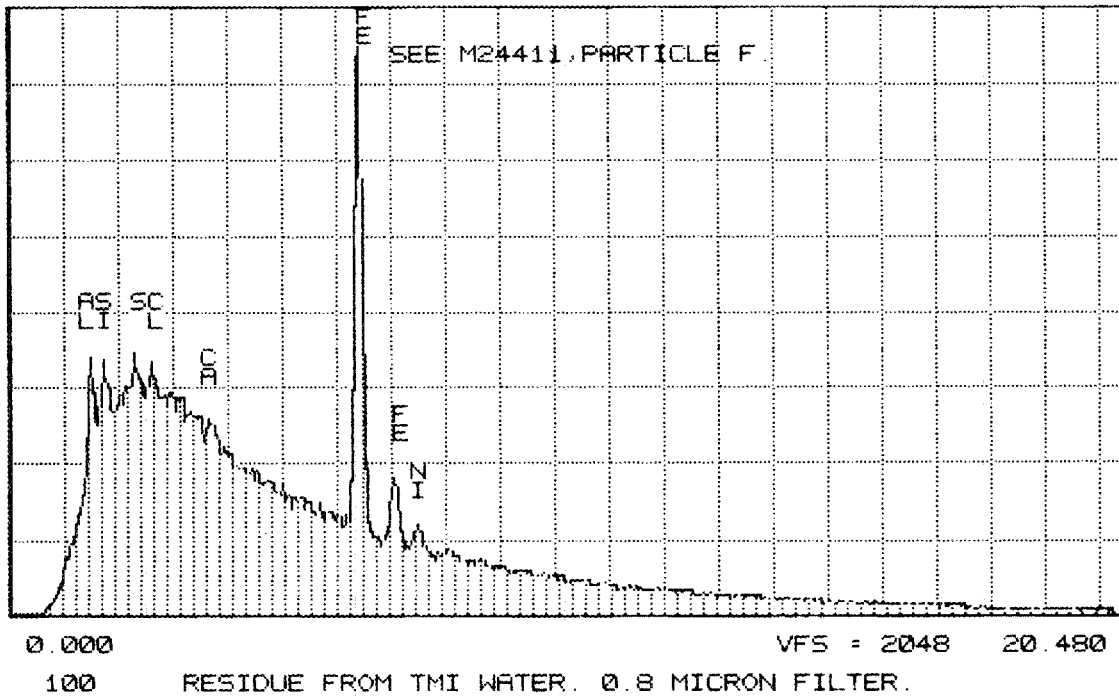


Fig. E.36. EDX of particle F, 4411 (see Fig. E.27).

ORNL-DWG 87-14056

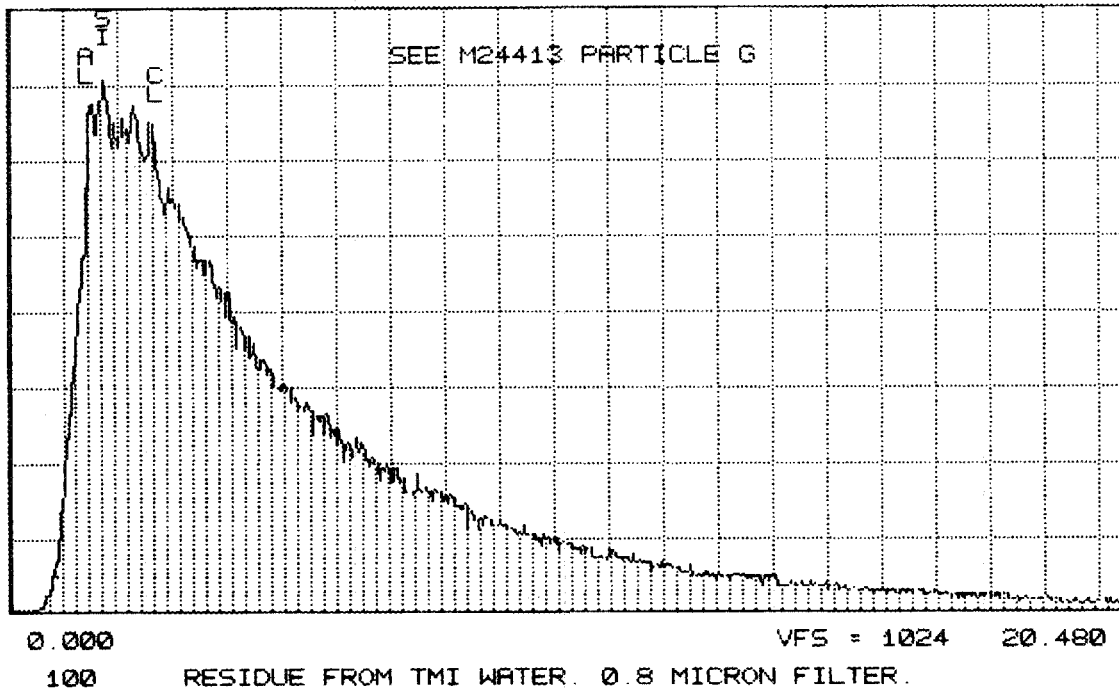


Fig. E.37. EDX of particle G, 4413 (see Fig. E.34).

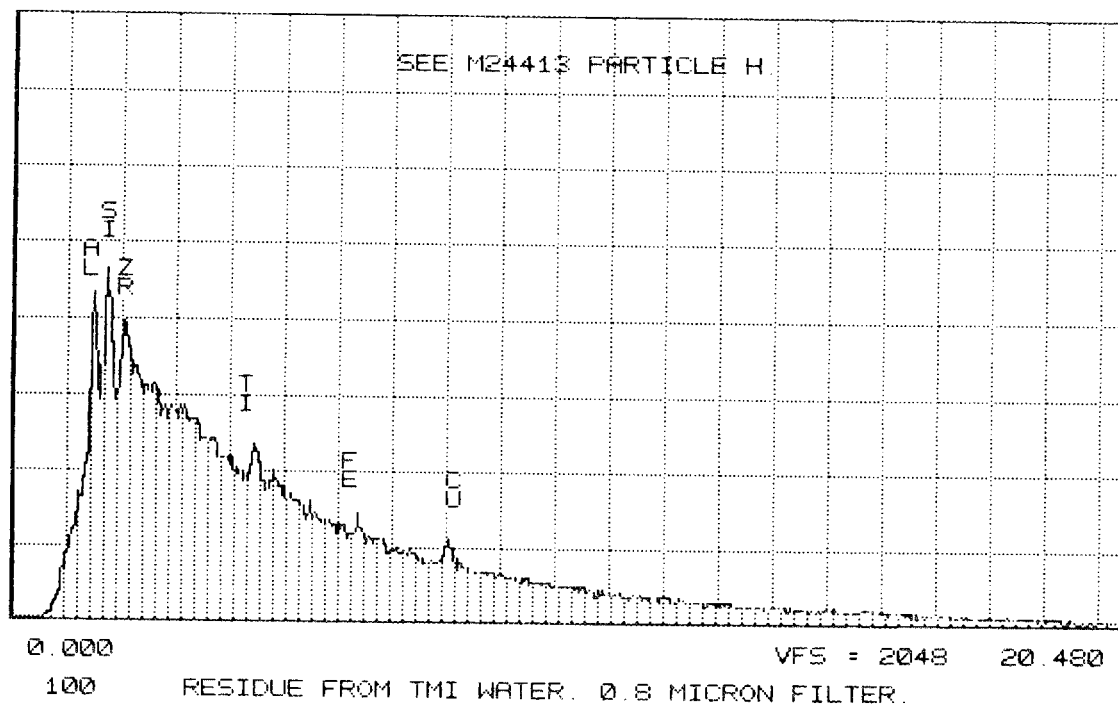


Fig. E.38. EDX of particle H, 4413 (see Fig. E.34).

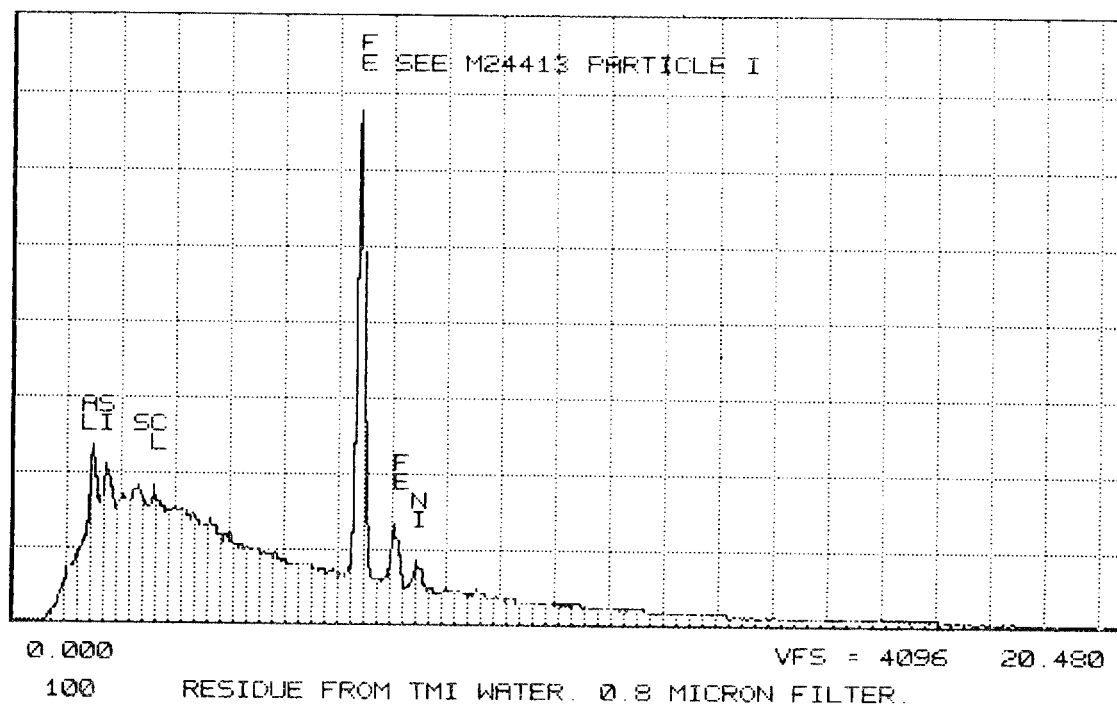


Fig. E.39. EDX of particle I, 4413 (see Fig. E.34).

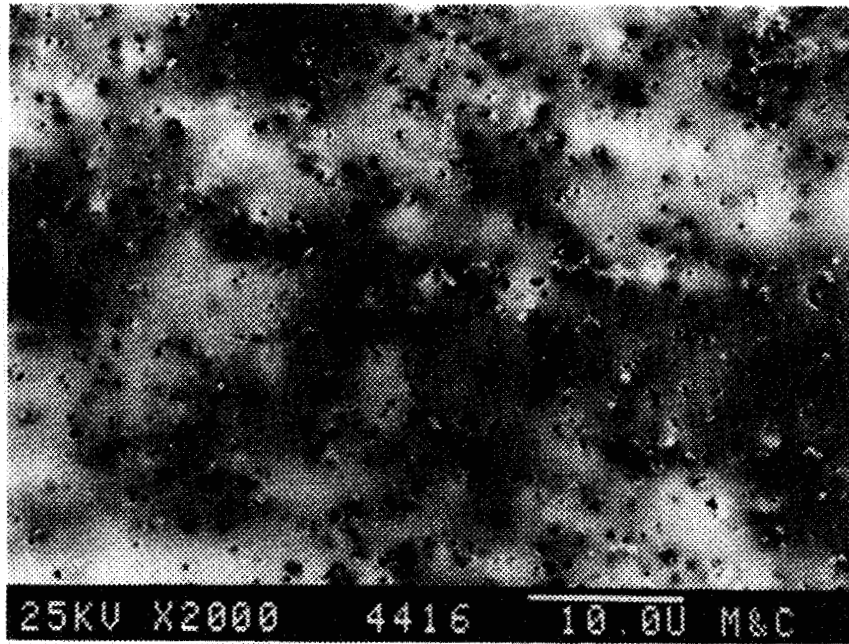


Fig. E.40. Nuclepore filter test 3 with 22-NTU water sample W2, 0.6- μ m filter.

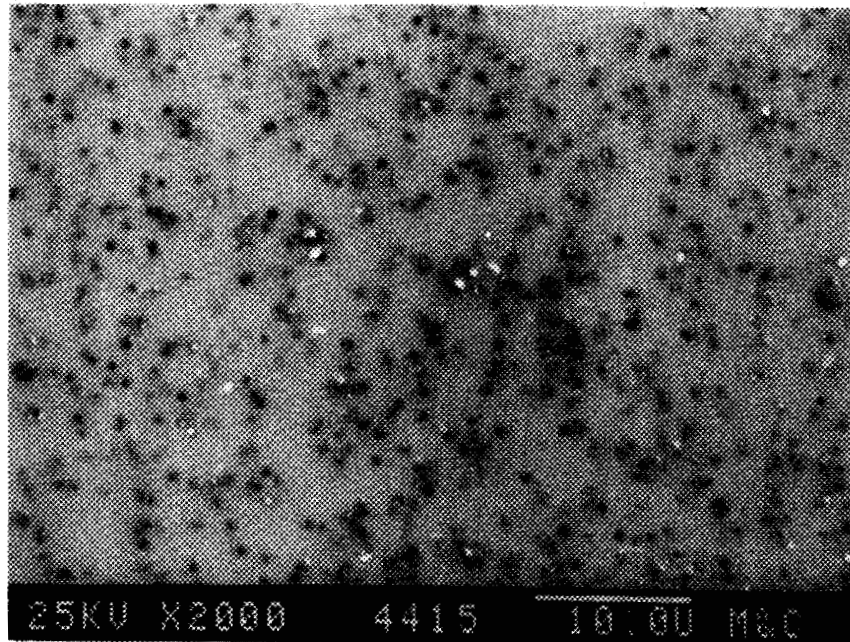


Fig. E.41. Nuclepore filter test 3 with 22-NTU water sample W2, 0.6- μ m filter, BEI.

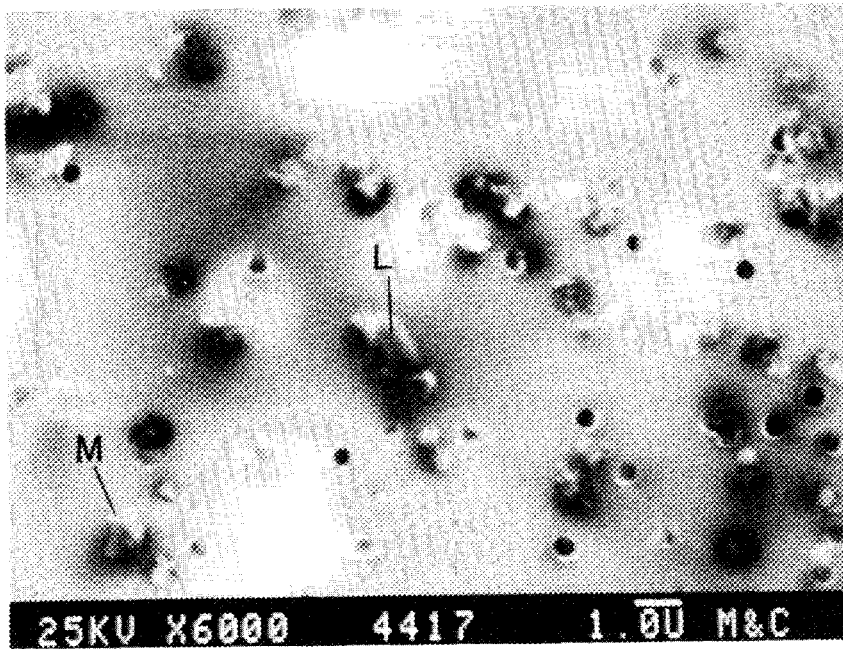


Fig. E.42. Nuclepore filter test 3 with 22-NTU water sample W2, 0.6- μ m filter.

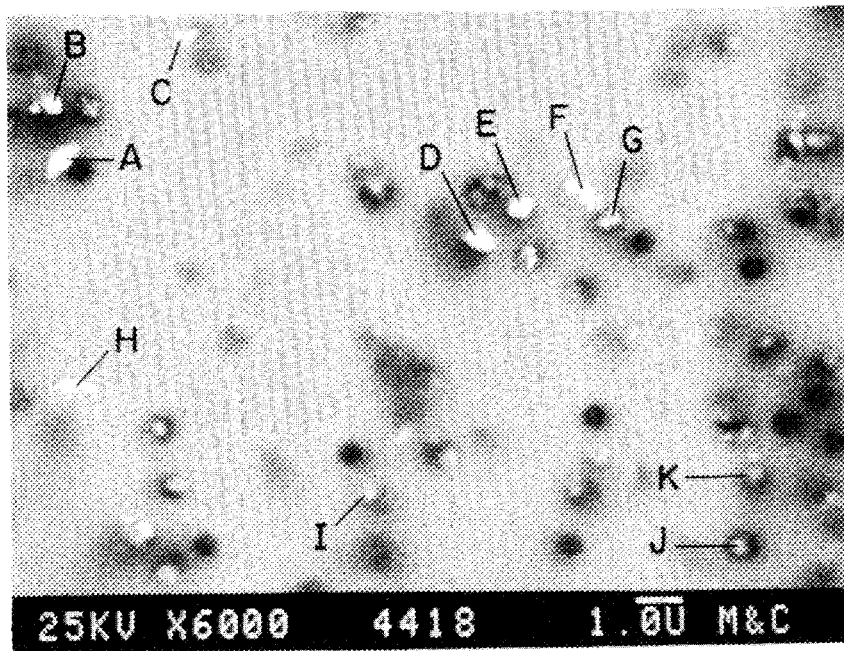


Fig. E.43. Nuclepore filter test 3 with 22-NTU water sample W2, 0.6- μ m filter, BEI.

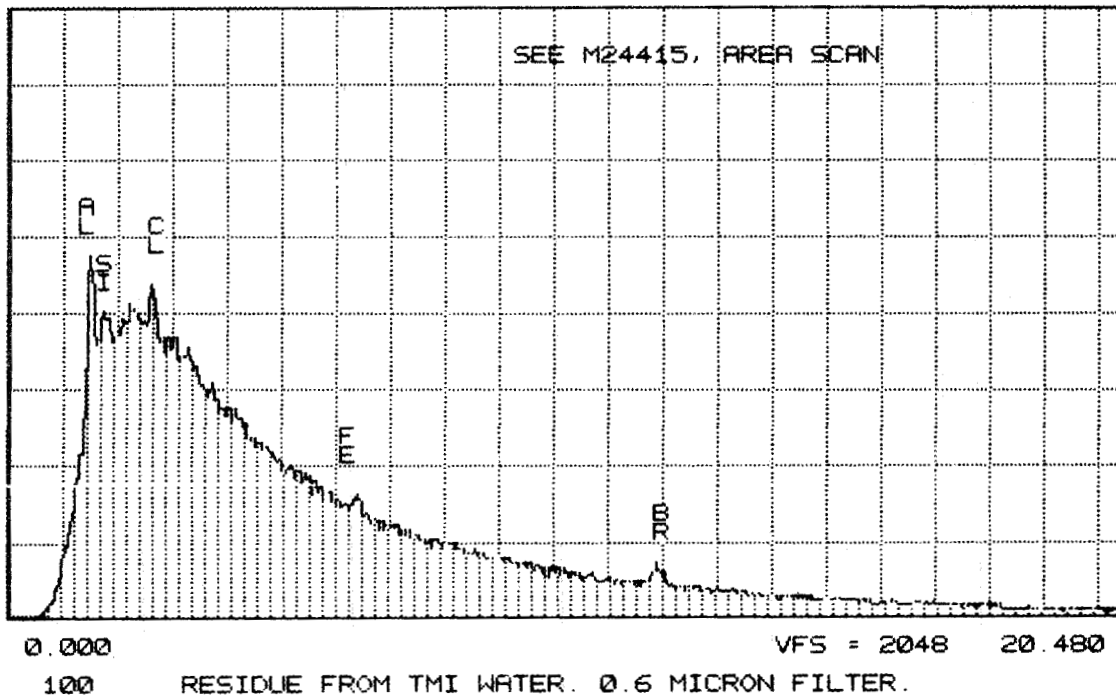


Fig. E.44. EDX of area of 4415 (see Fig. E.41).

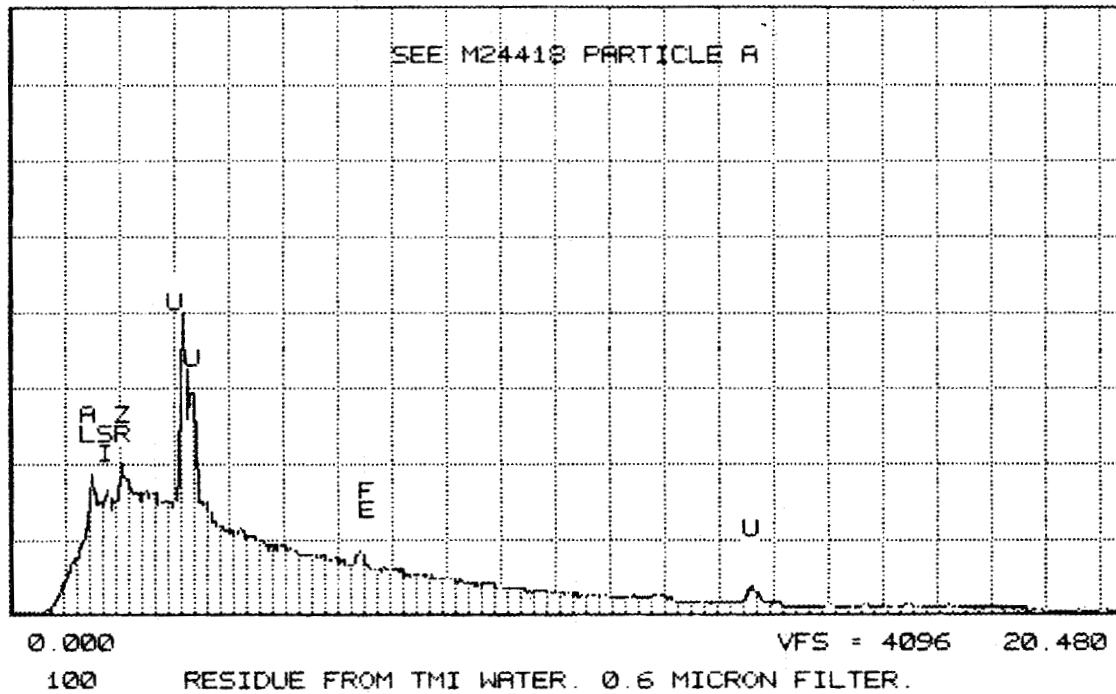


Fig. E.45. EDX of particle A, 4418 (see Fig. E.43).

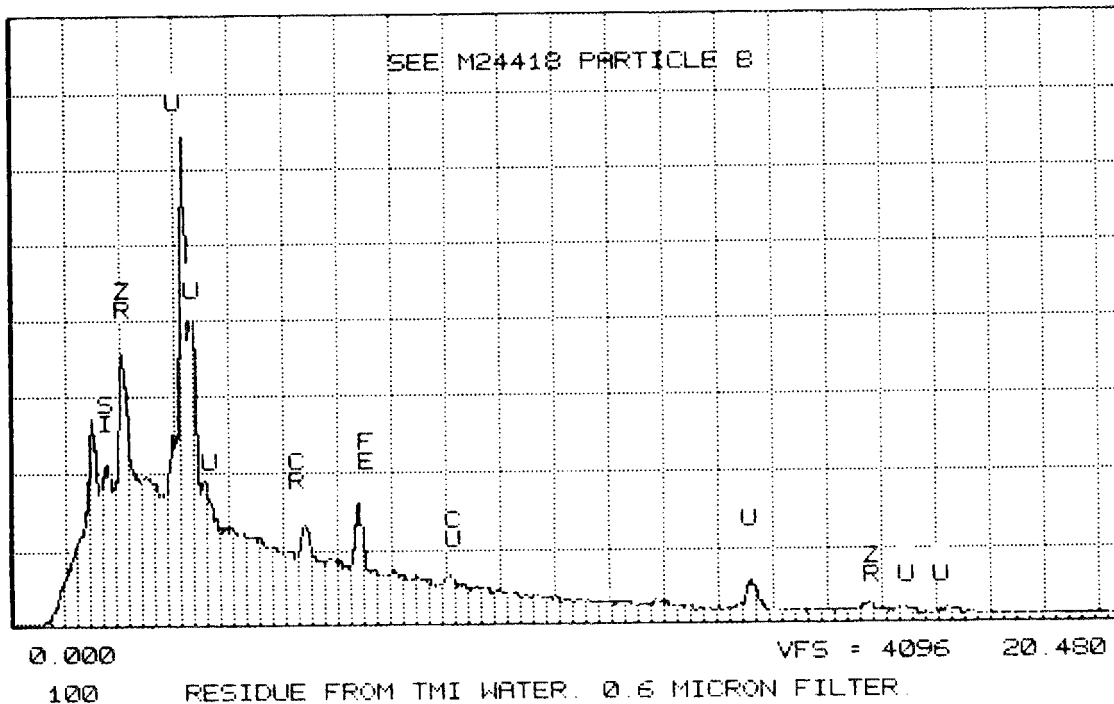


Fig. E.46. EDX of particle B, 4418 (see Fig. E.43).

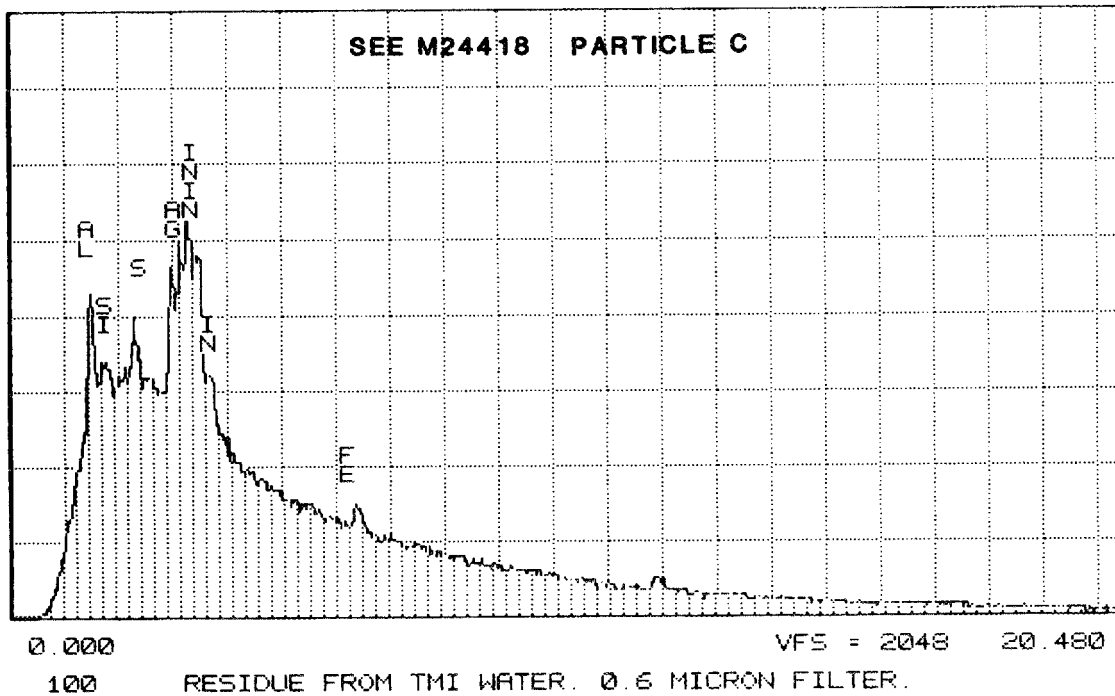


Fig. E.47. EDX of particle C, 4418 (see Fig. E.43).

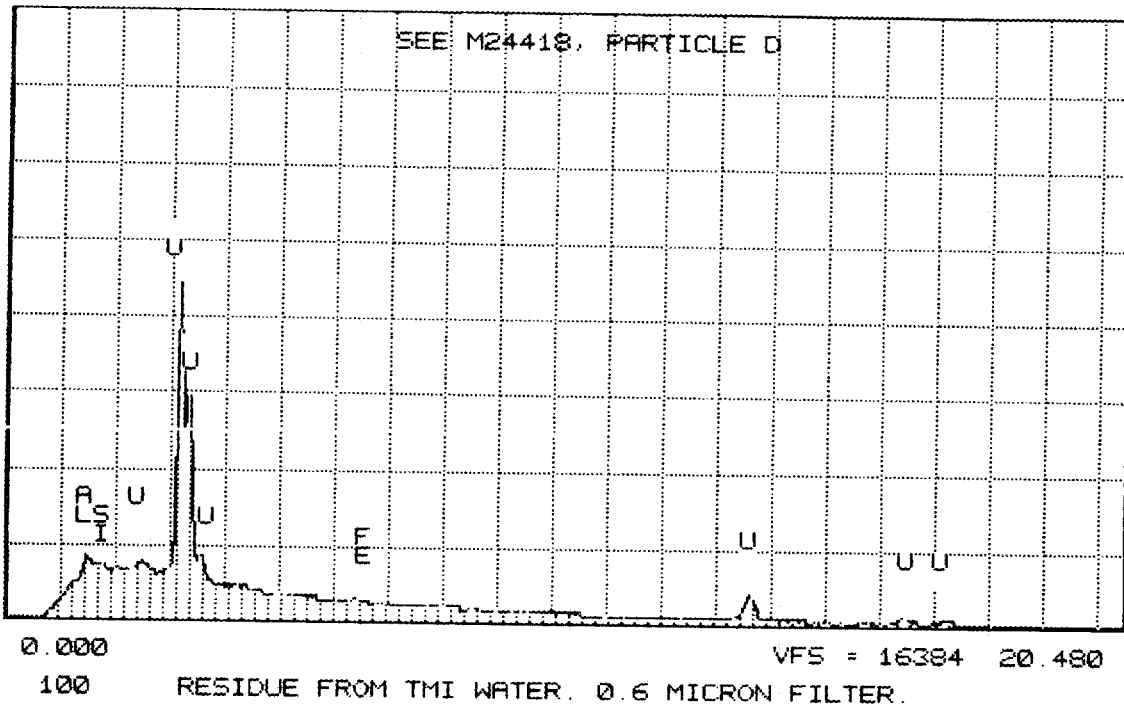


Fig. E.48. EDX of particle D, 4418 (see Fig. E.43).

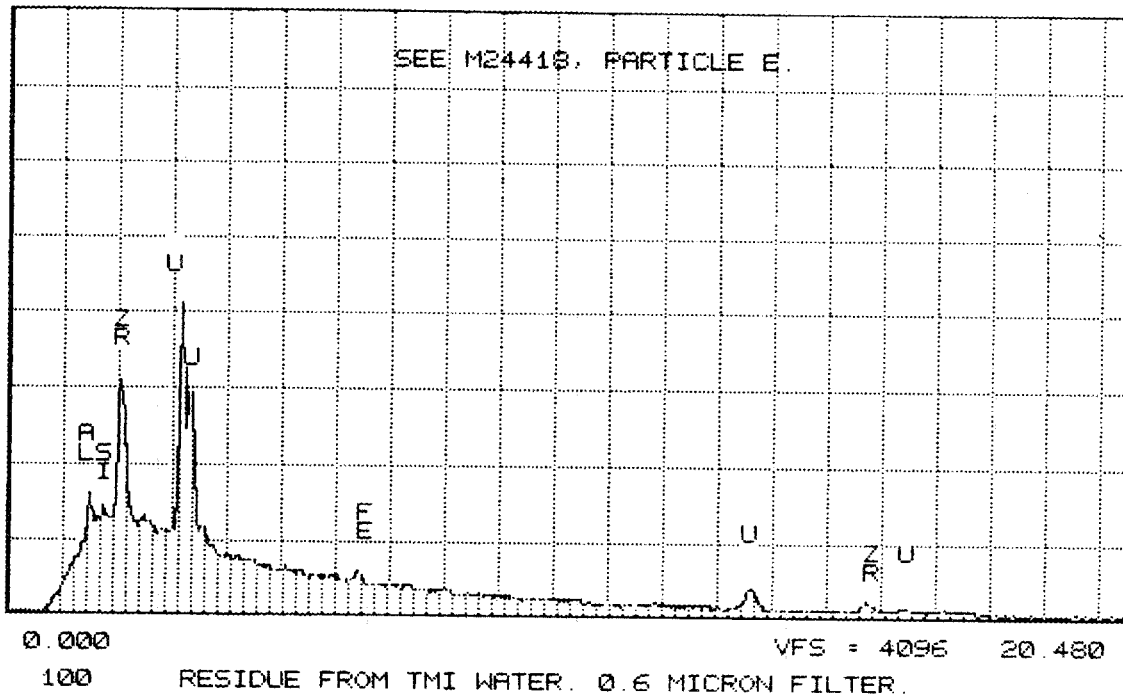


Fig. E.49. EDX of particle E, 4418 (see Fig. E.43).

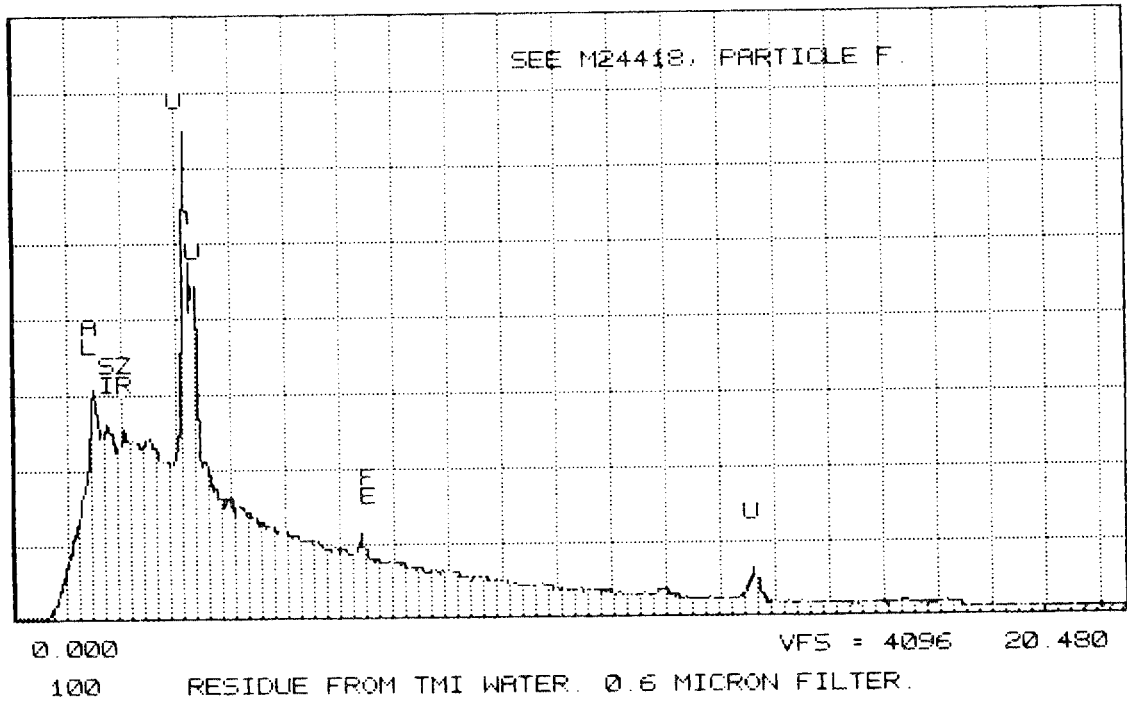


Fig. E.50. EDX of particle F, 4418 (see Fig. E.43).

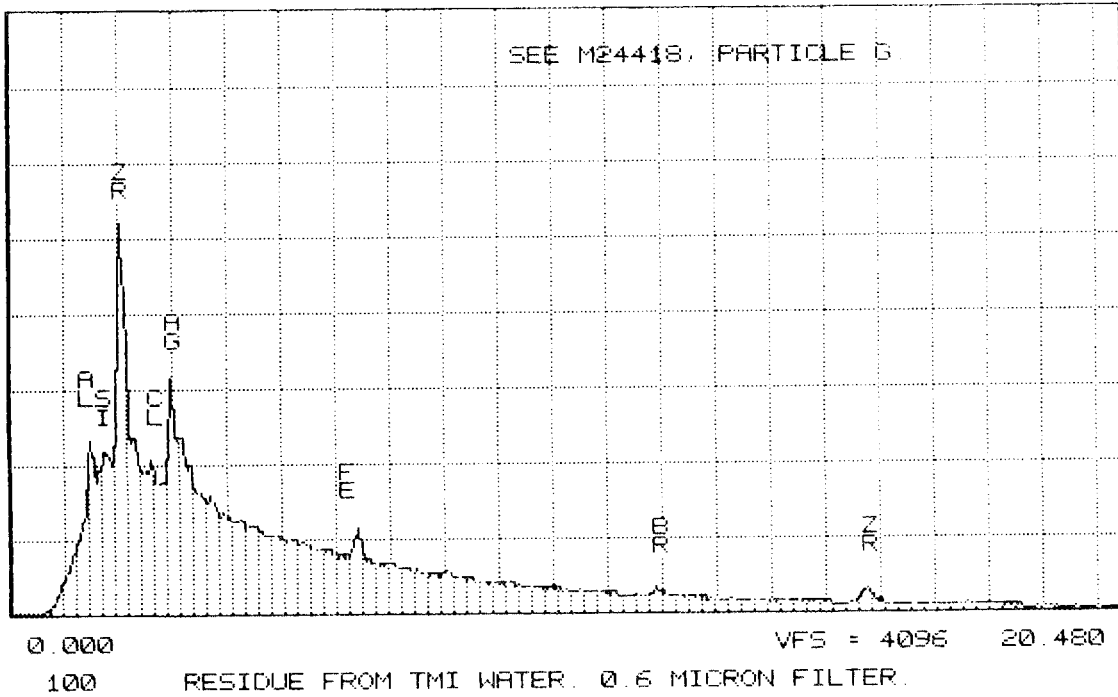


Fig. E.51. EDX of particle G, 4418 (see Fig. E.43).

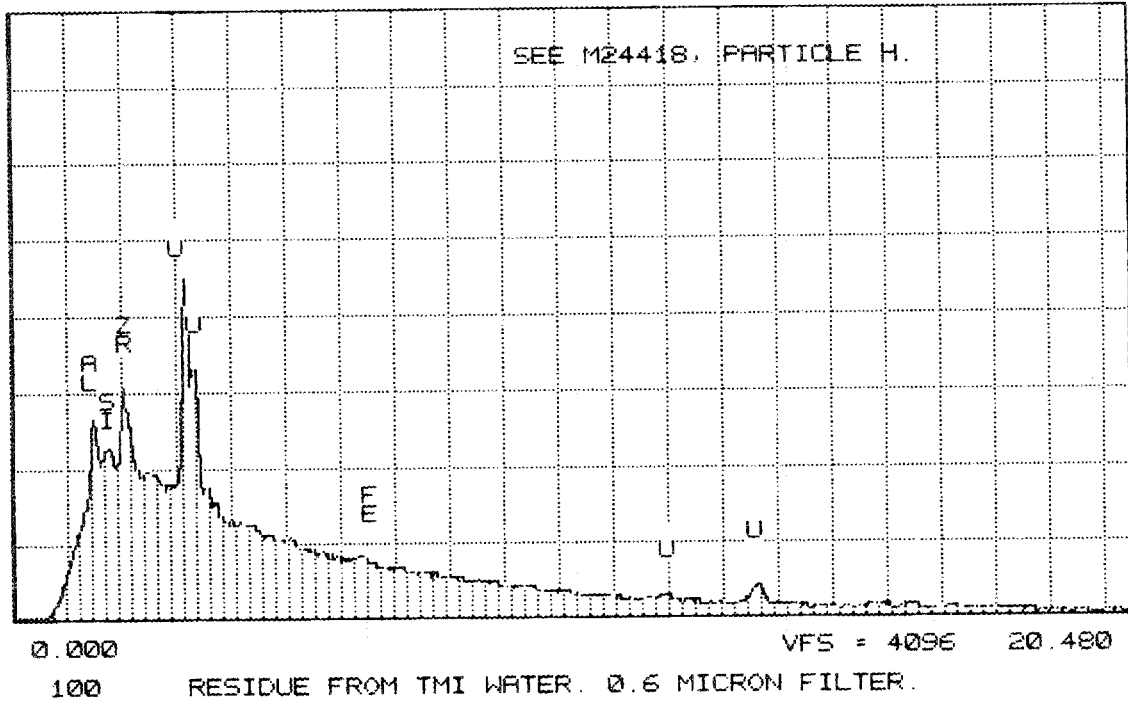


Fig. E.52. EDX of particle H, 4418 (see Fig. E.43).

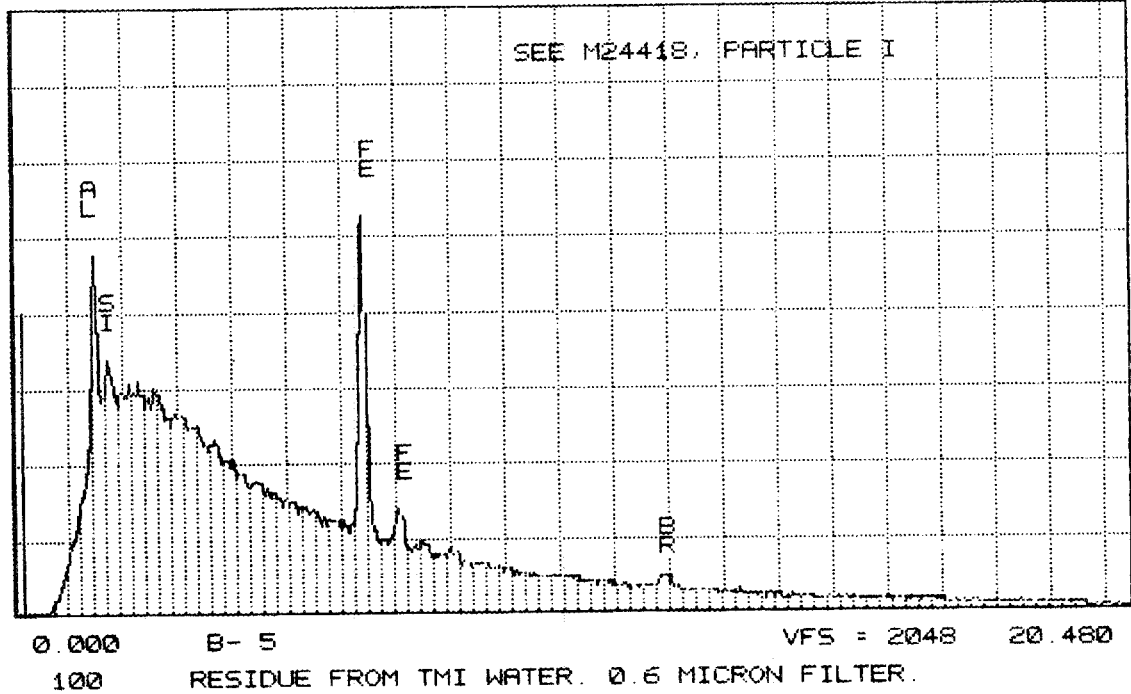


Fig. E.53. EDX of particle I, 4418 (see Fig. E.43).

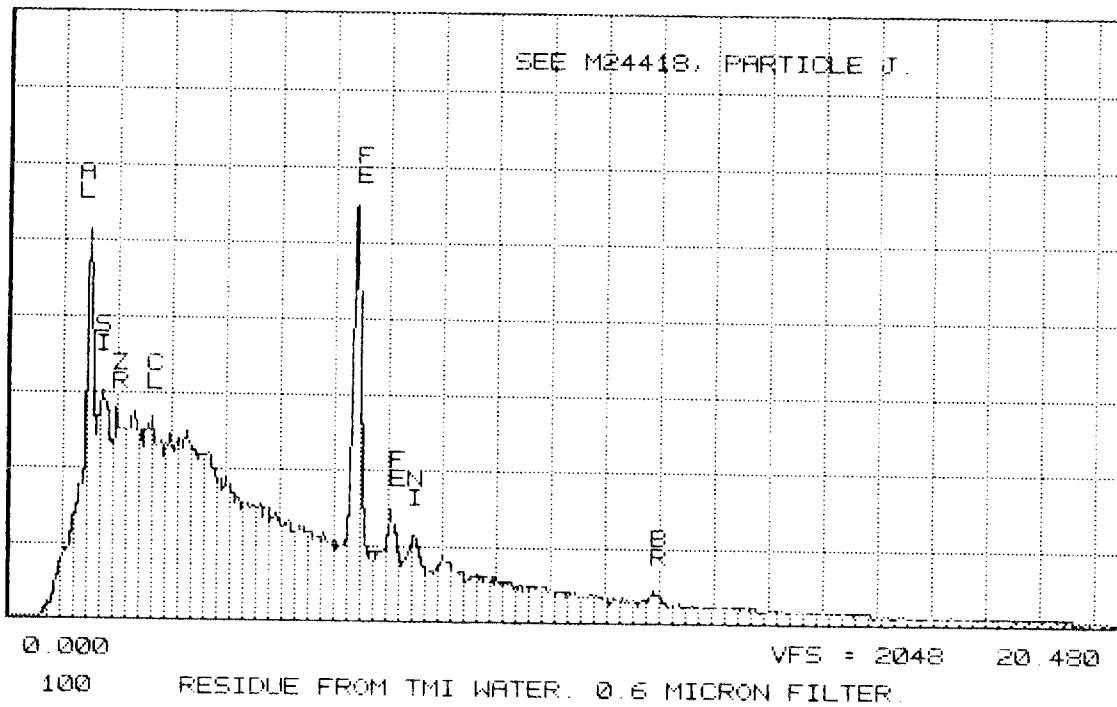


Fig. E.54. EDX of particle J, 4418 (see Fig. E.43).

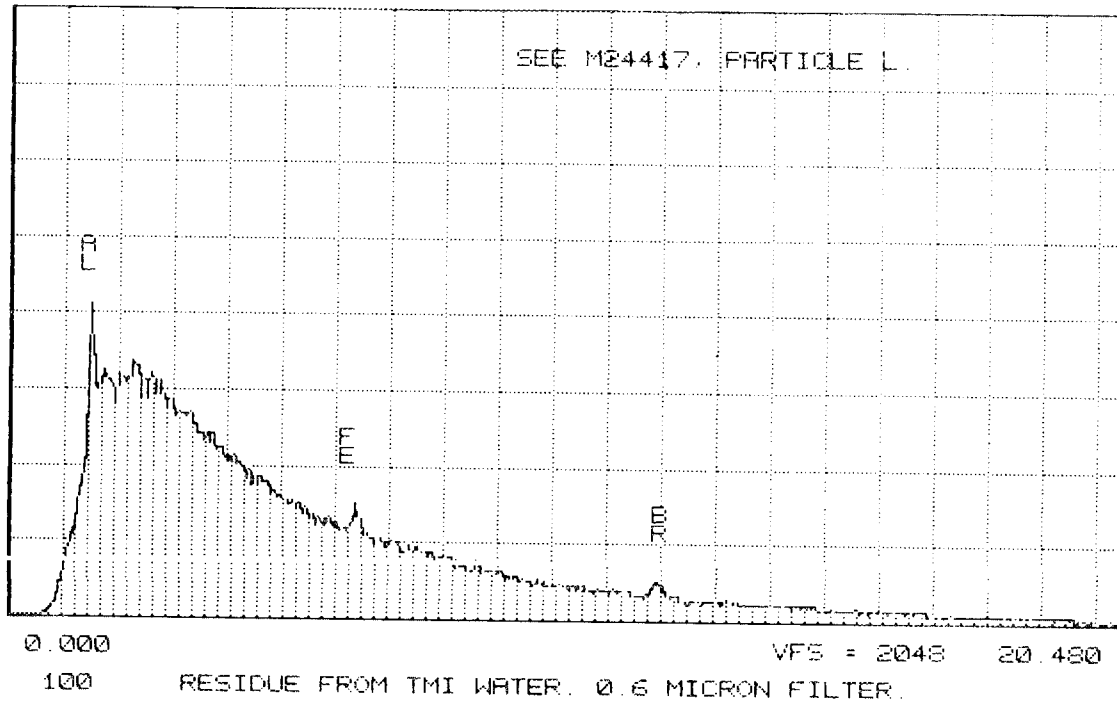


Fig. E.55. EDX of particle L, 4417 (see Fig. E.42).

ORNL-DWG 87-14071

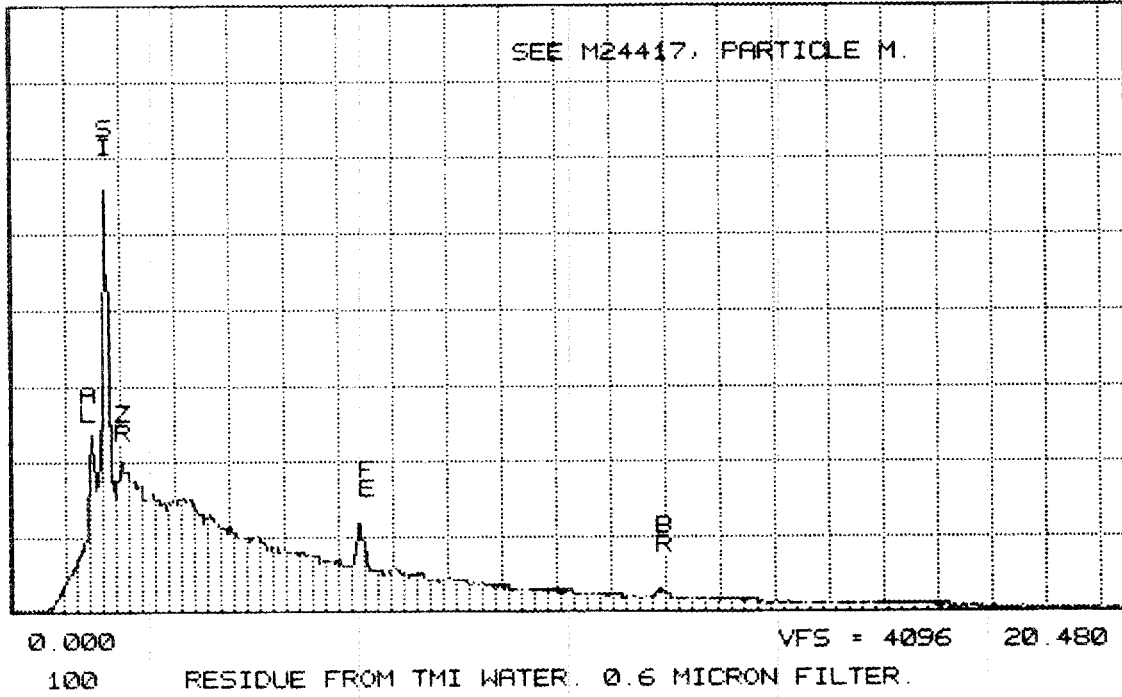


Fig. E.56. EDX of particle M, 4417 (see Fig. E.42).

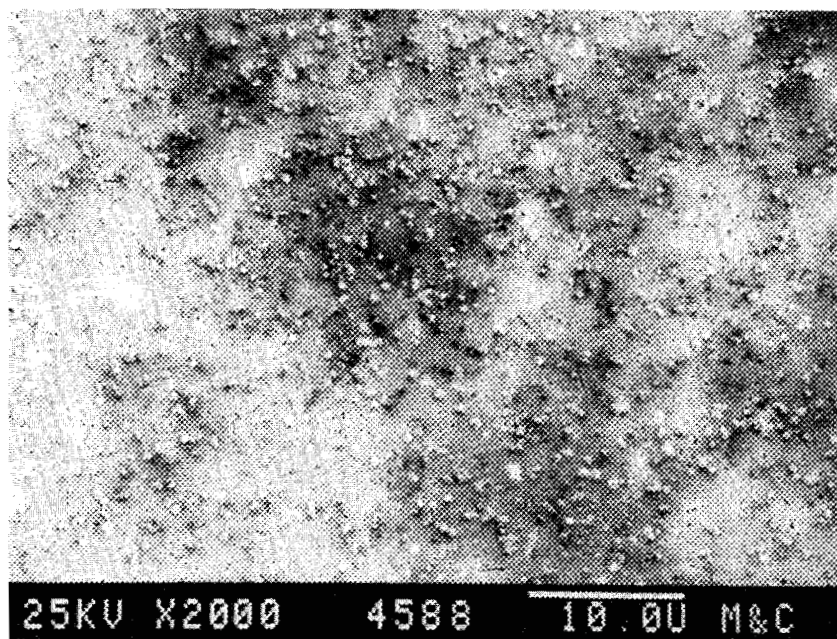


Fig. E.57. Nuclepore filter test 3 with 22-NTU water sample W2, 0.4- μm filter.

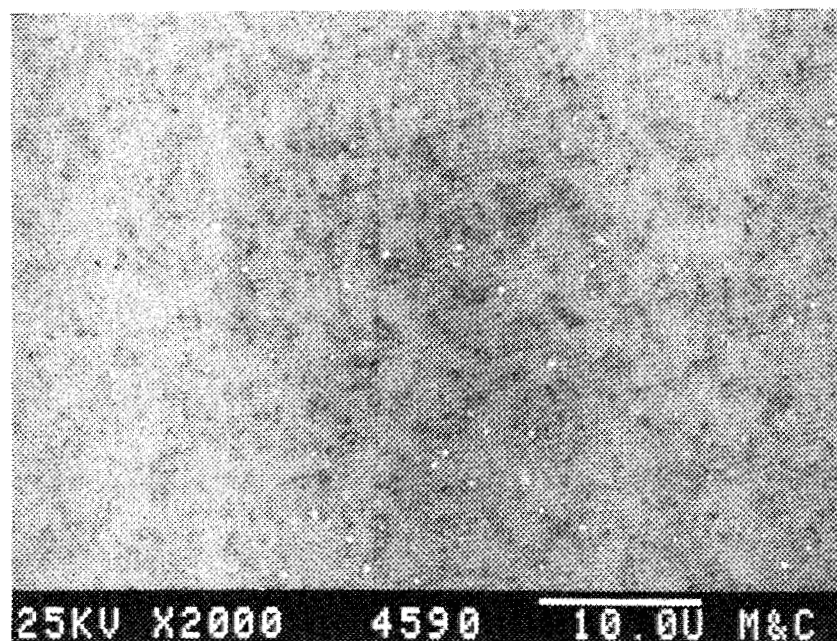


Fig. E.58. Nuclepore filter test 3 with 22-NTU water sample W2, 0.4- μm filter, BEI.

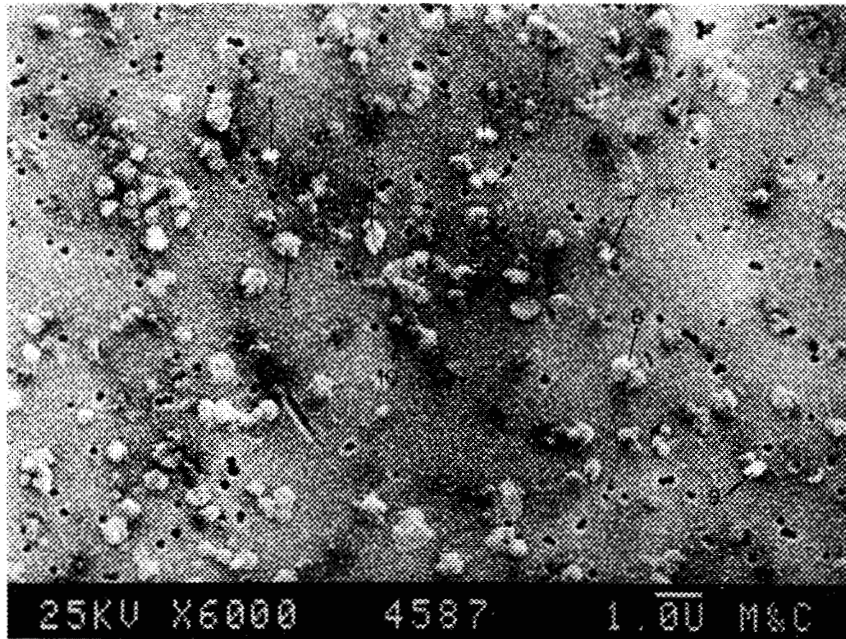


Fig. E.59. Nuclepore filter test 3 with 22-NTU water sample W2, 0.4- μm filter.

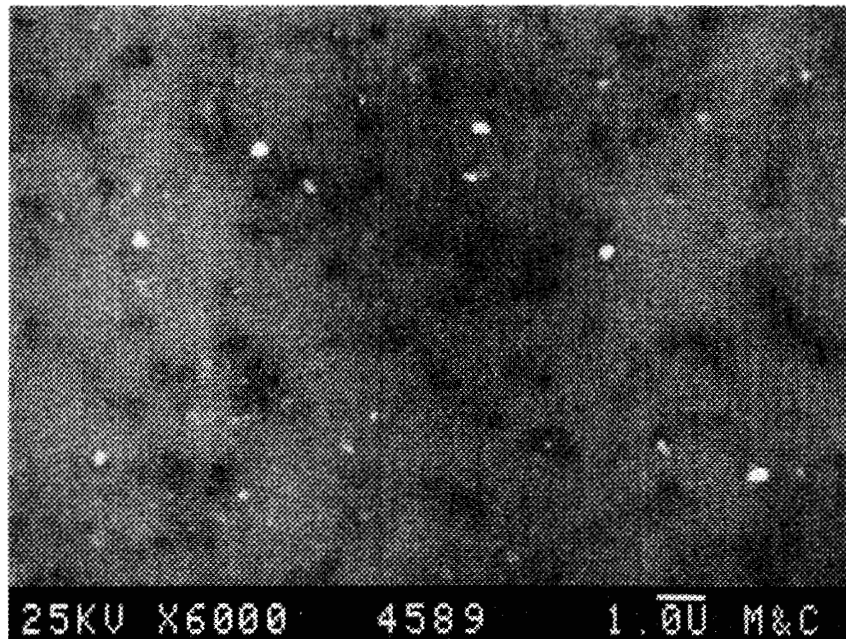


Fig. E.60. Nuclepore filter test 3 with 22-NTU water sample W2, 0.4- μm filter, BEI.

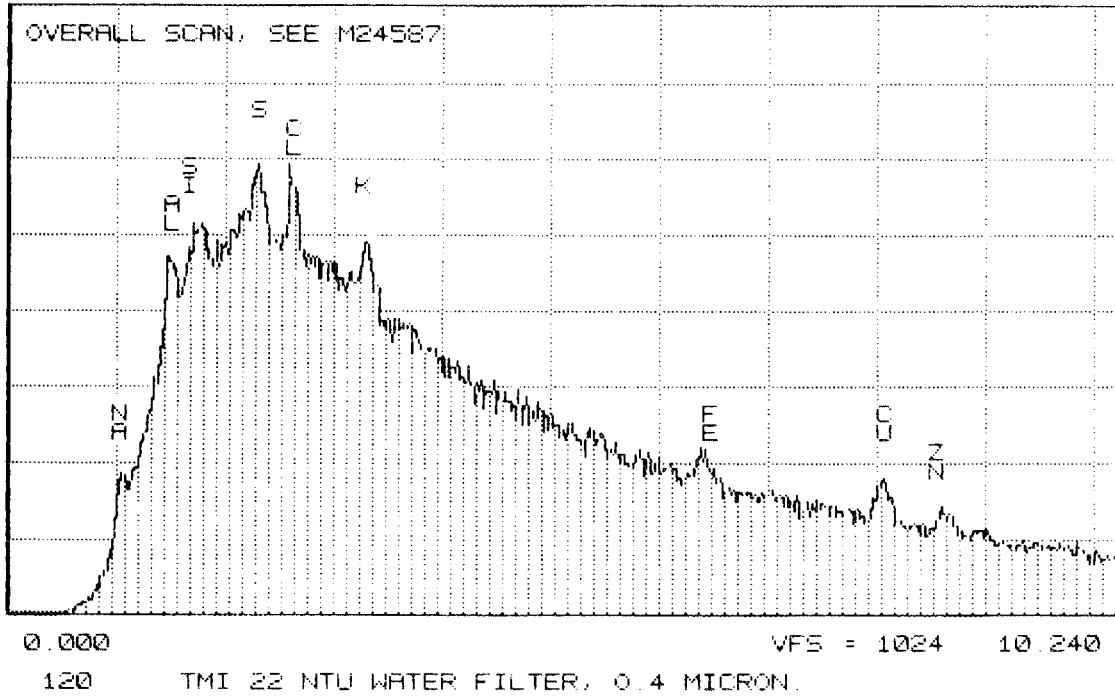


Fig. E.61. EDX of area scan of 4587 (see Fig. E.59).

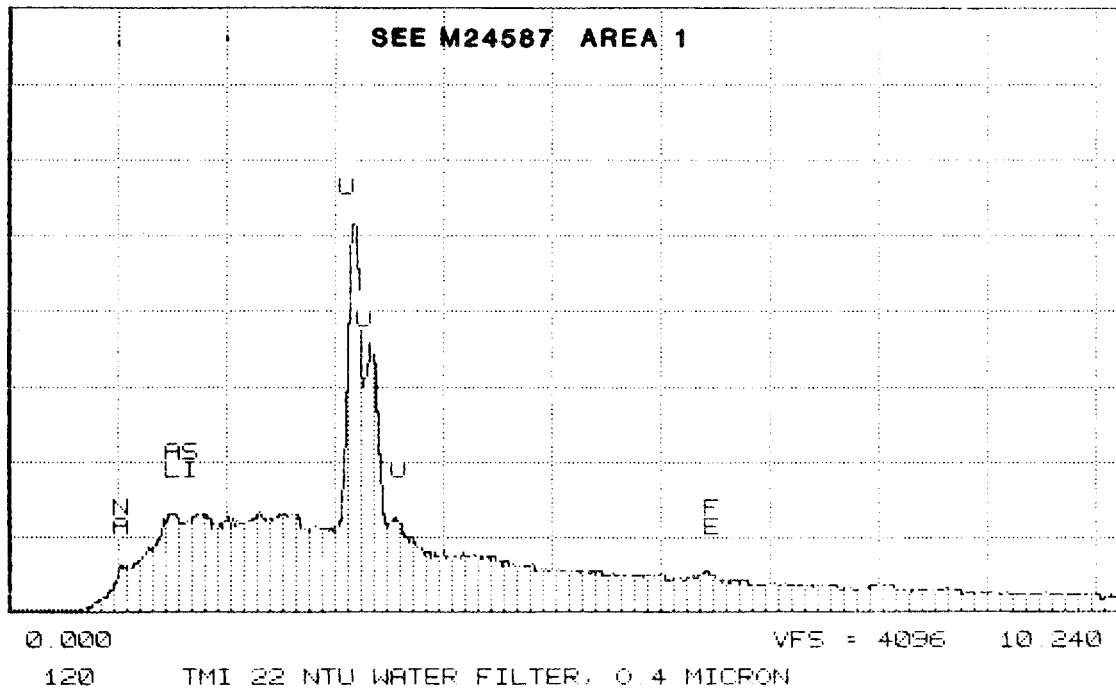


Fig. E.62. EDX of particle 1, 4587 (see Fig. E.59).

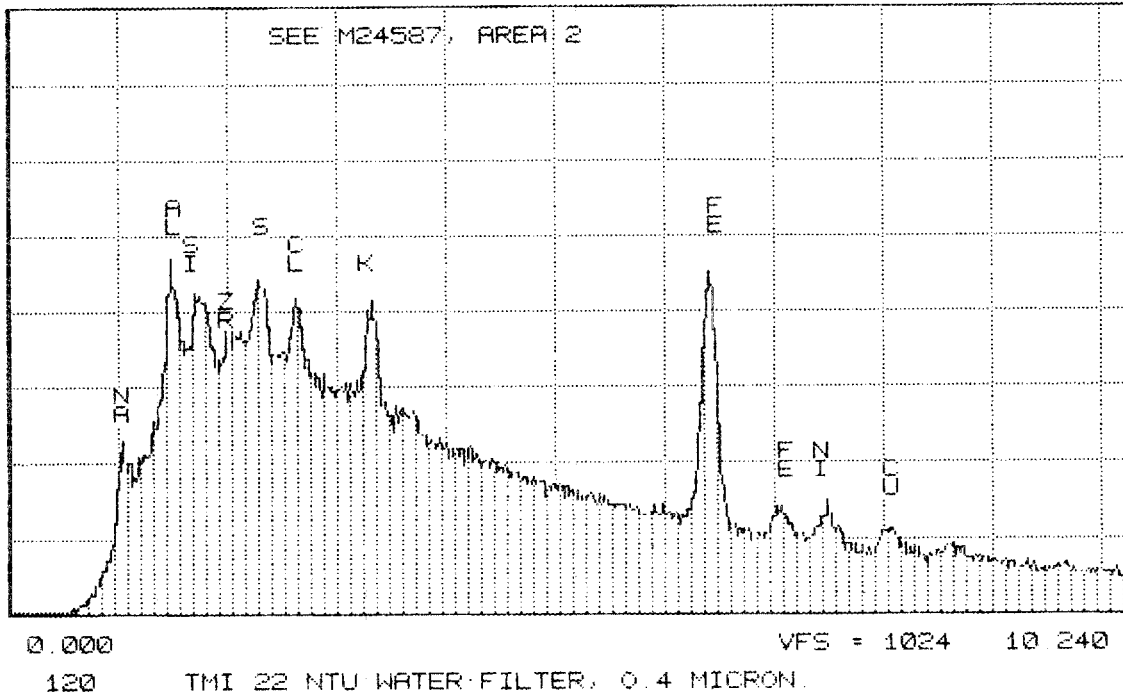


Fig. E.63. EDX of particle 2, 4587 (see Fig. E.59).

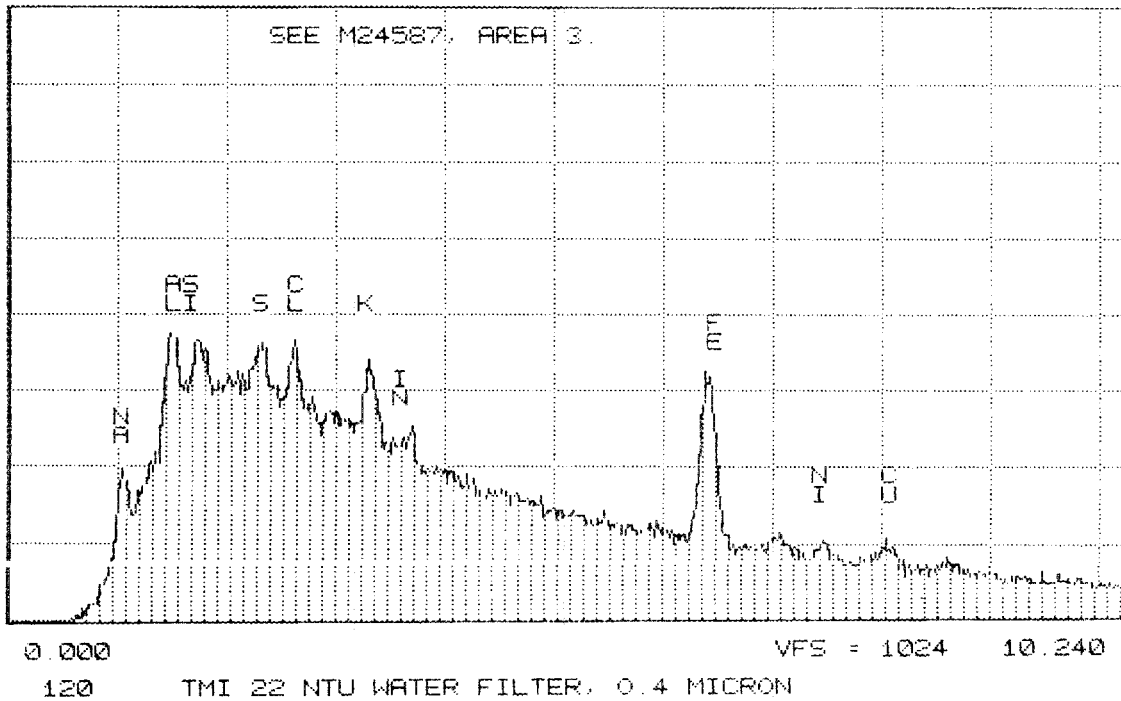


Fig. E.64. EDX of particle 3, 4587 (see Fig. E.59).

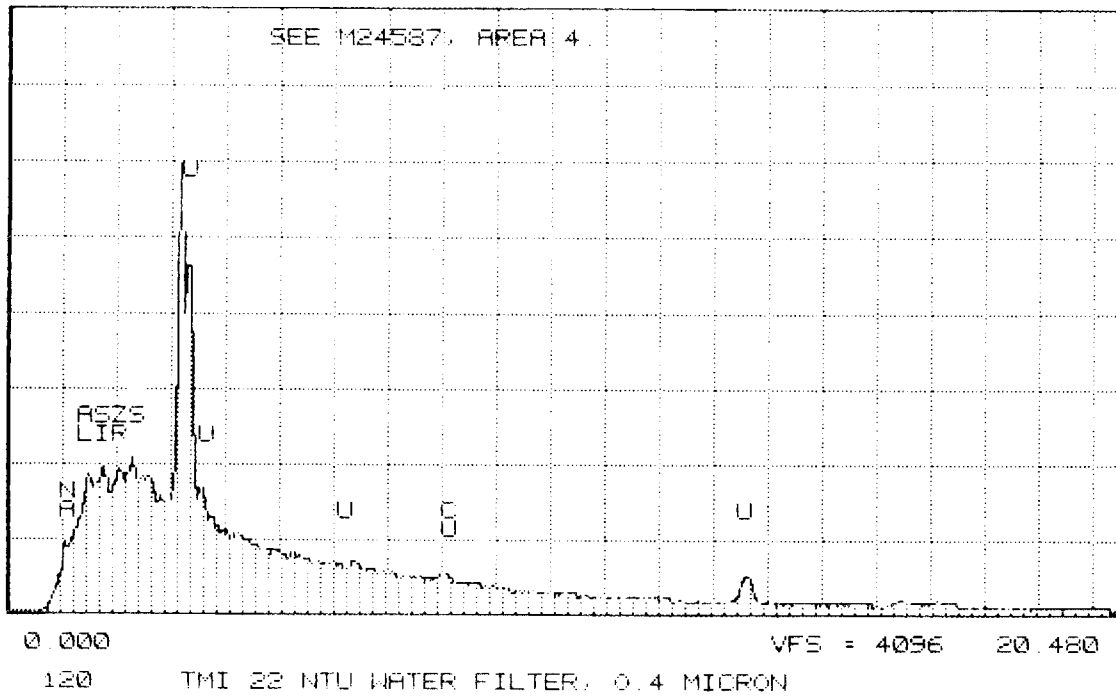


Fig. E.65. EDX of particle 4, 4587 (see Fig. E.59).

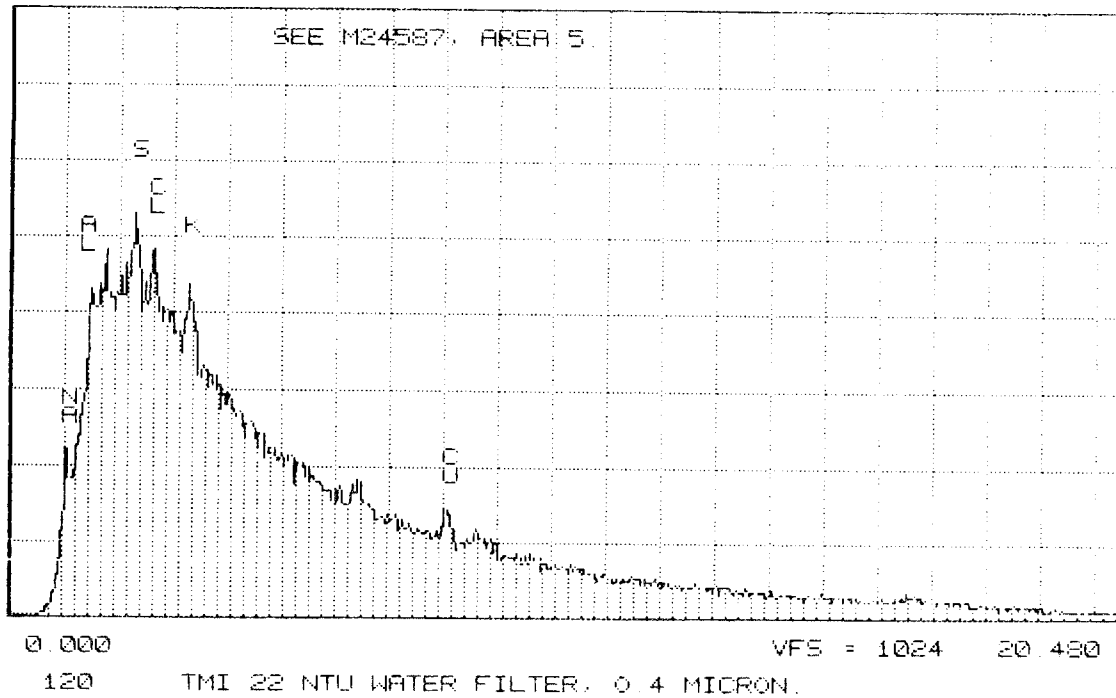


Fig. E.66. EDX of particle 5, 4587 (see Fig. E.59).

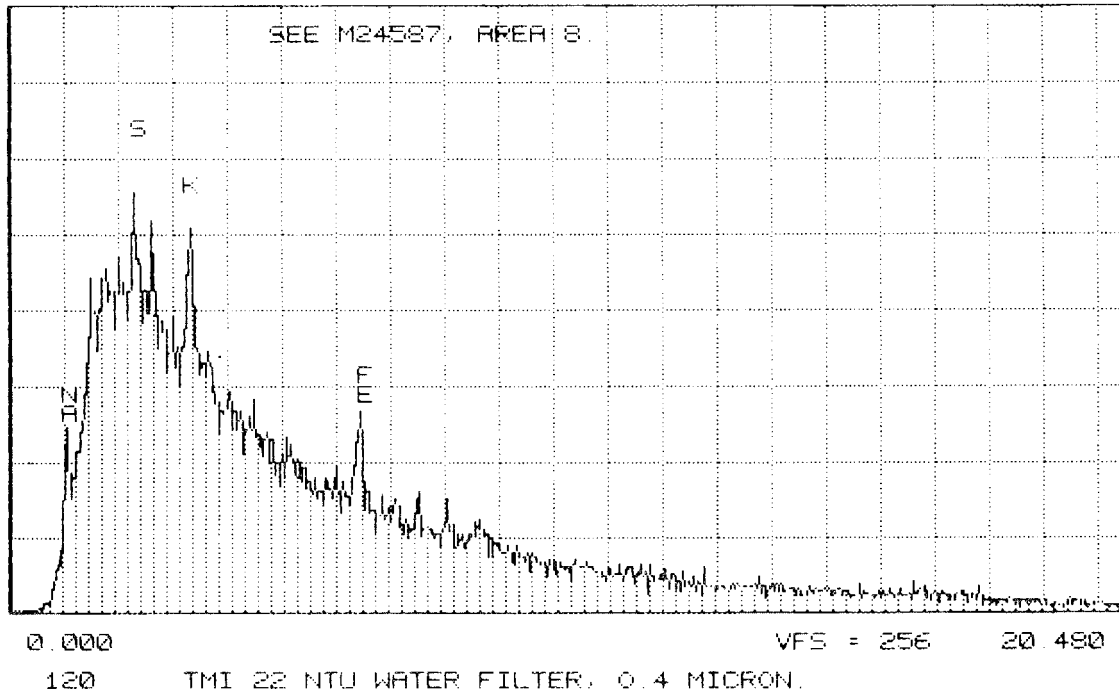


Fig. E.69. EDX of particle 8, 4587 (see Fig. E.59).

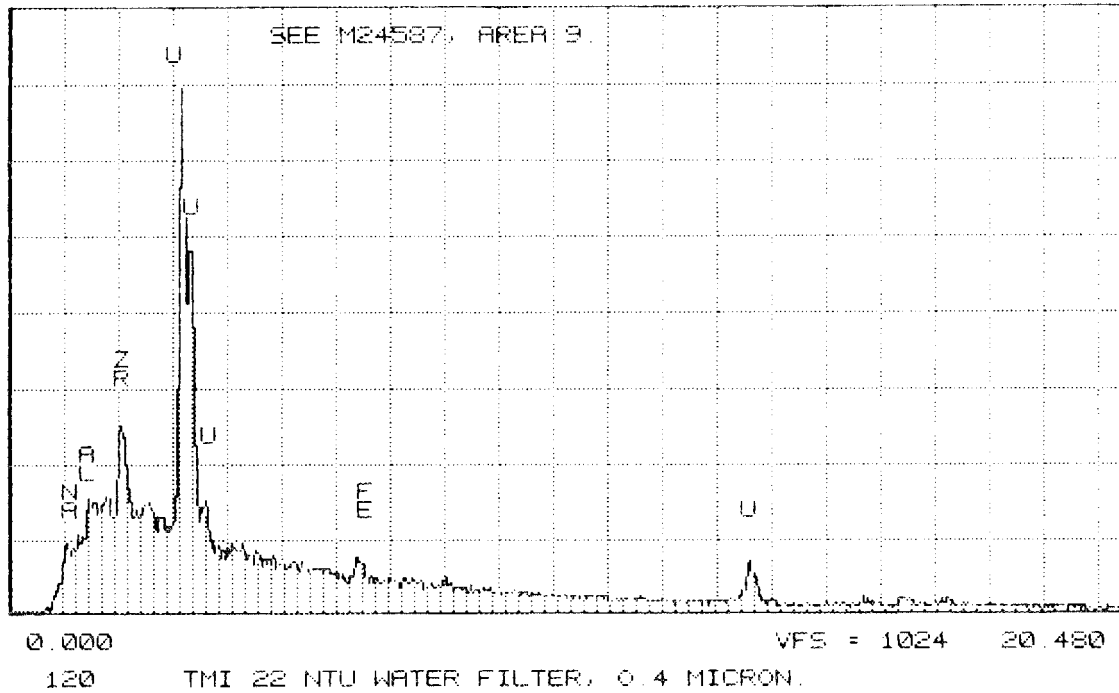


Fig. E.70. EDX of particle 9, 4587 (see Fig. E.59).

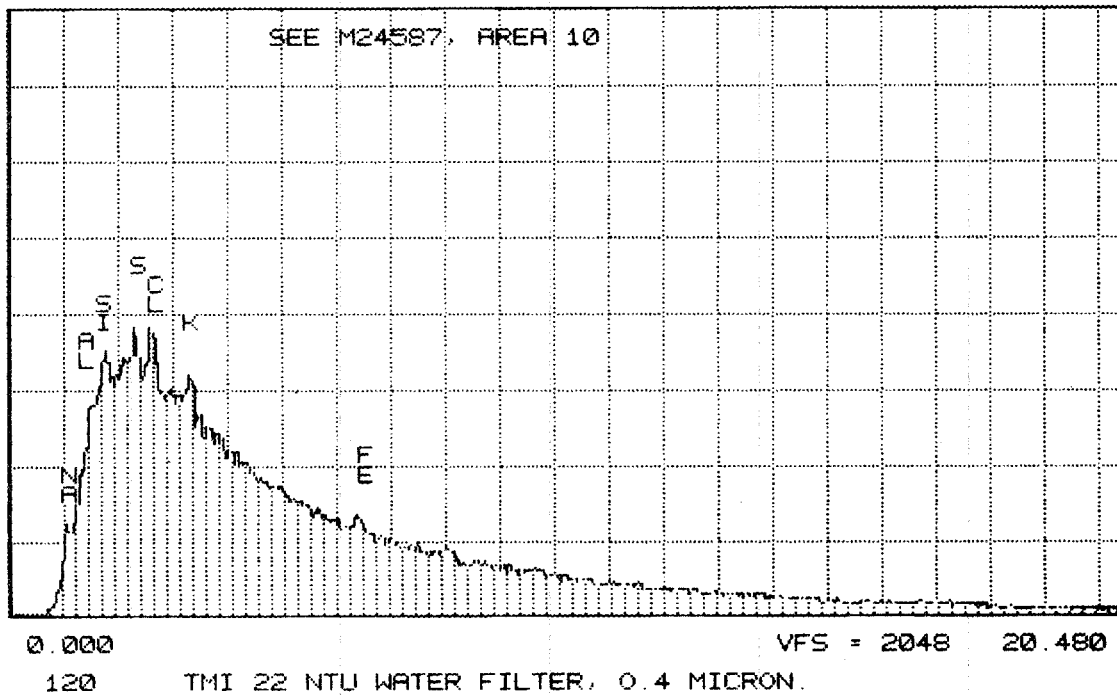


Fig. E.71. EDX of particle 10, 4587 (see Fig. E.59).

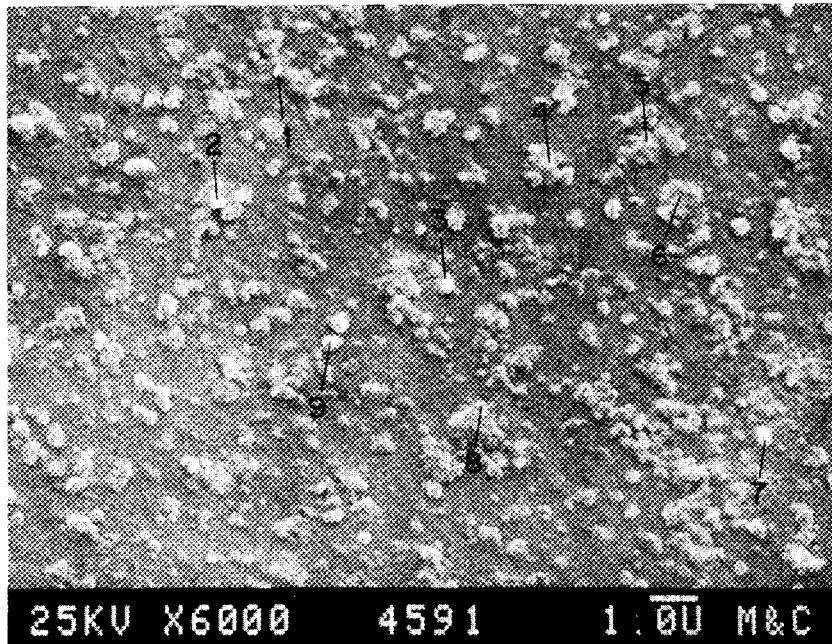


Fig. E.72. Nuclepore filter test 3 with 22-NTU water sample W2, 0.1- μ m filter.

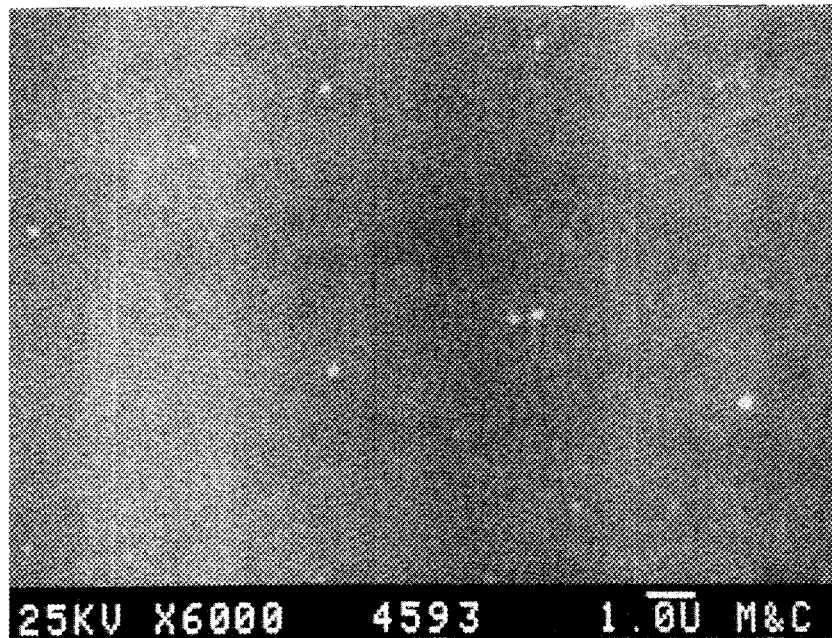


Fig. E.73. Nuclepore filter test 3 with 22-NTU water sample W2, 0.1- μ m filter, BEI.

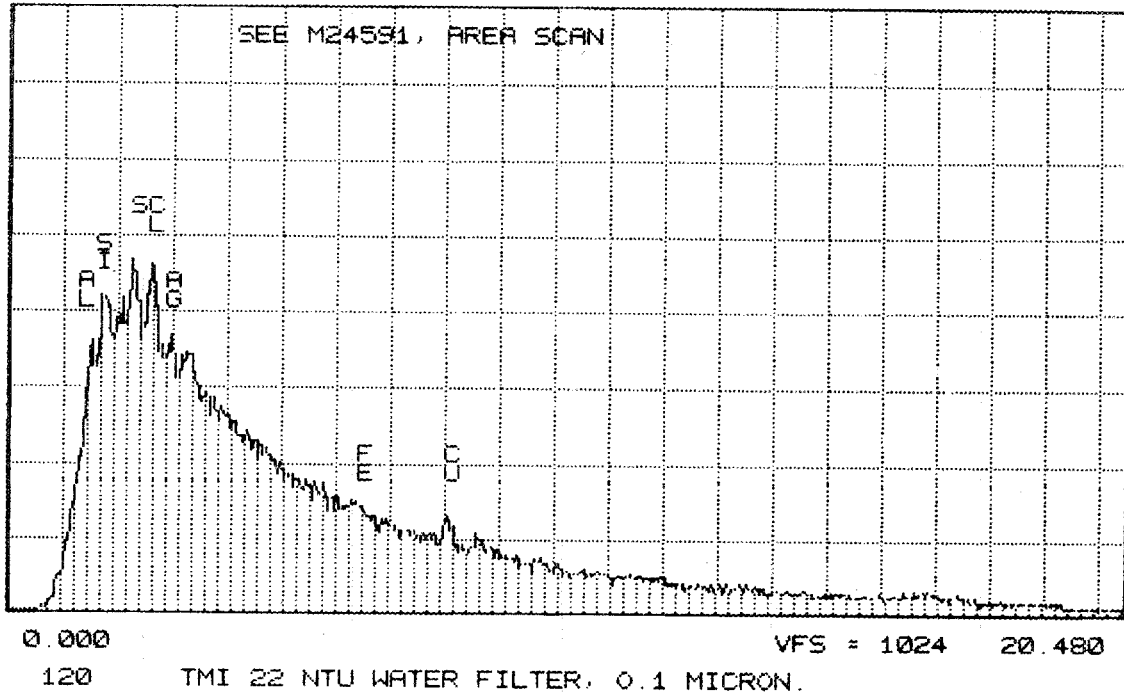


Fig. E.74. EDX of area of 4591 (see Fig. E.72).

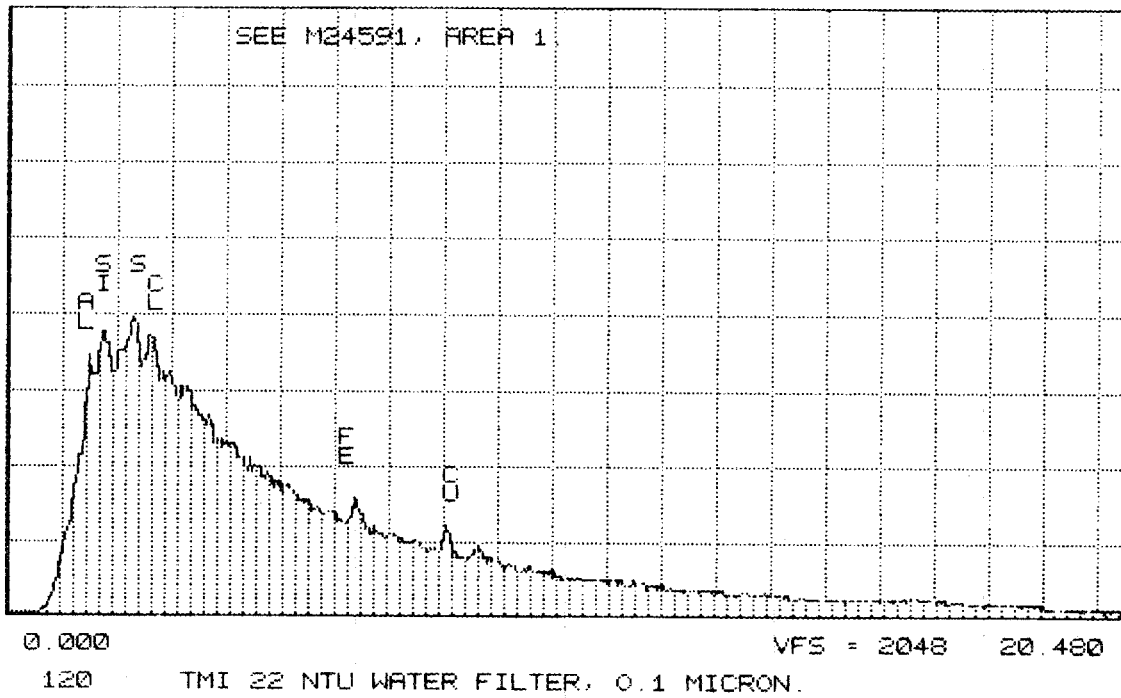


Fig. E.75. EDX of particle 1, 4591 (see Fig. E.72).

ORNL-DWG 87-14085

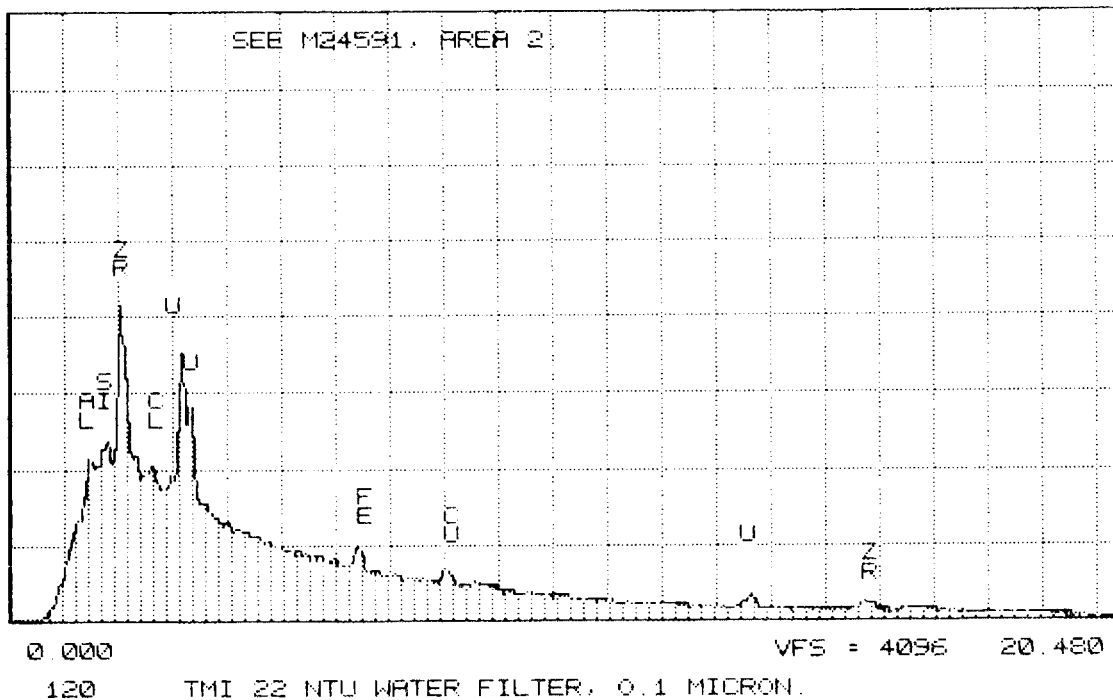


Fig. E.76. EDX of particle 2, 4591 (see Fig. E.72).

ORNL-DWG 87-14086

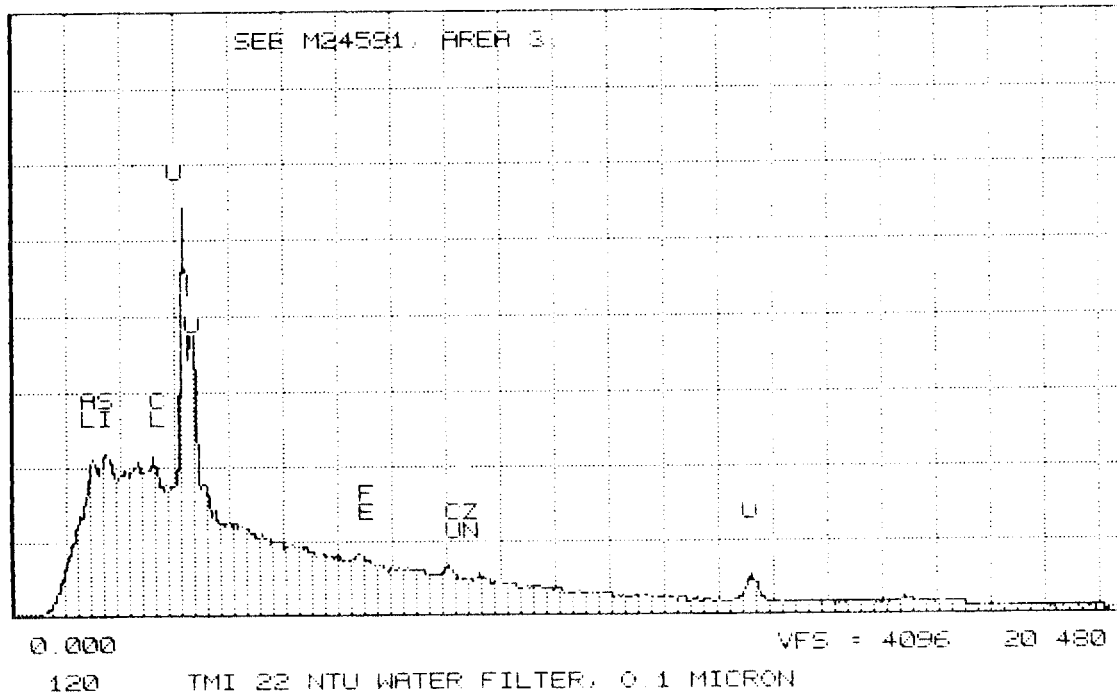


Fig. E.77. EDX of particle 3, 4591 (see Fig. E.72).

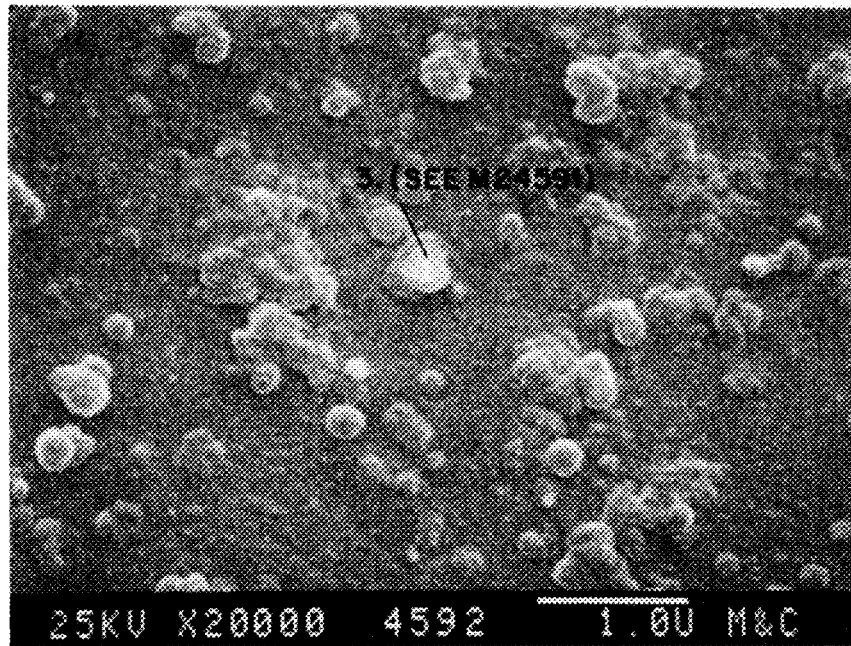


Fig. E.78. 20,000X enlargement of particle 3, 4591 (see Fig. E.72).

ORNL-DWG 87-14087

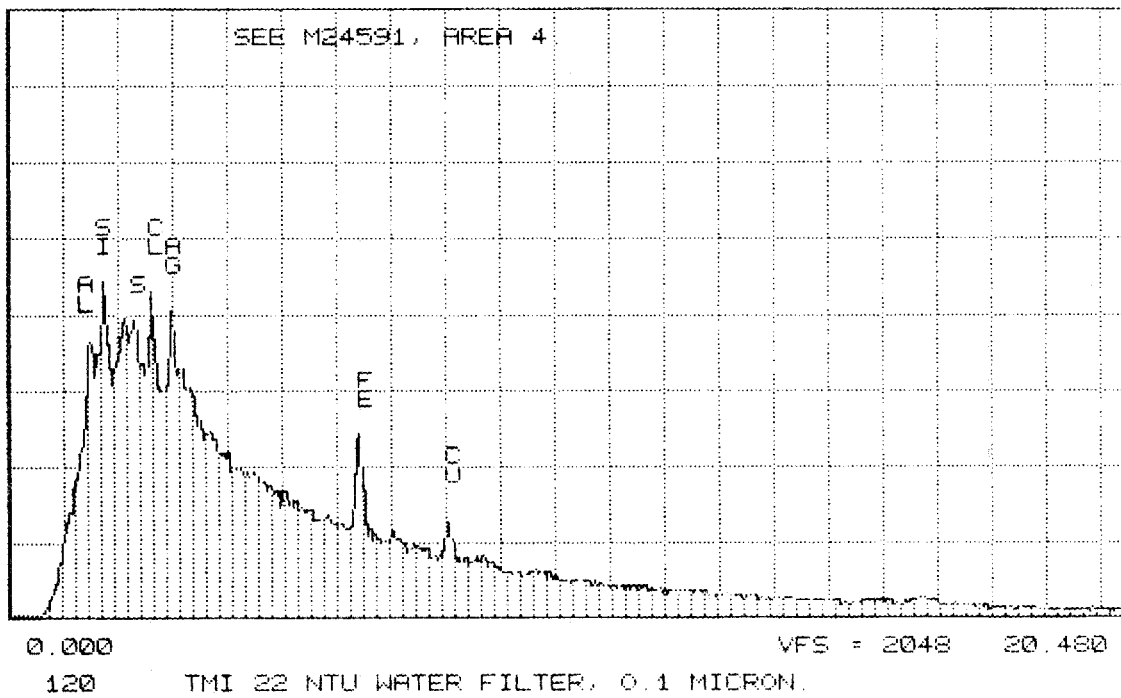


Fig. E.79. EDX of particle 4, 4591 (see Fig. E.72).

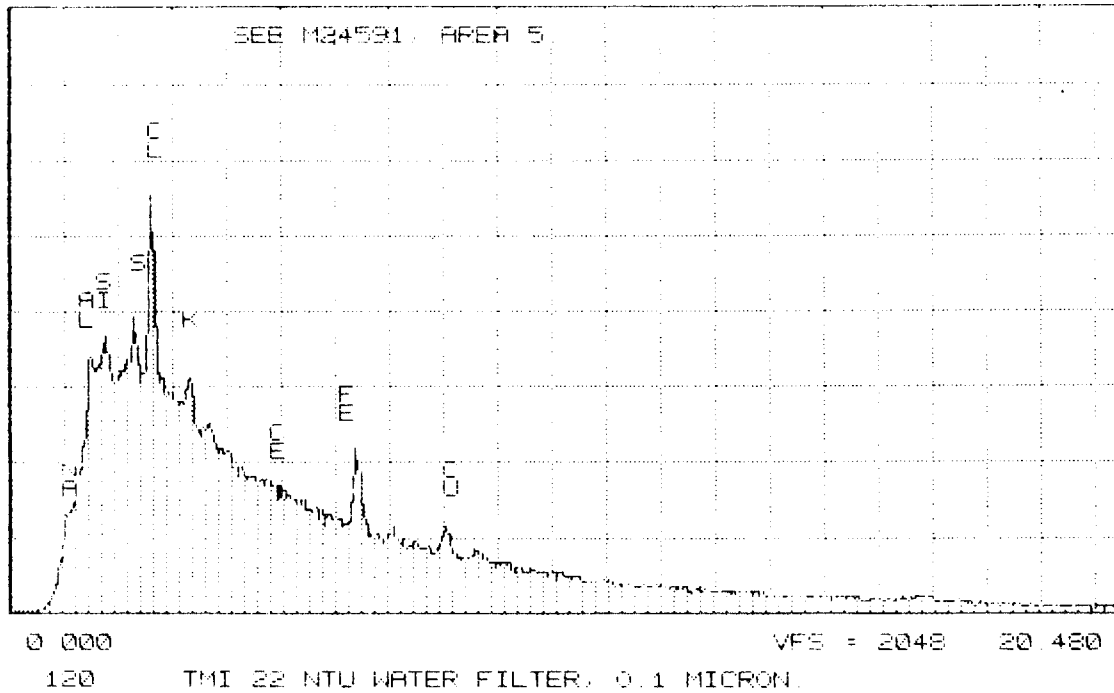


Fig. E.80. EDX of particle 5, 4591 (see Fig. E.72).

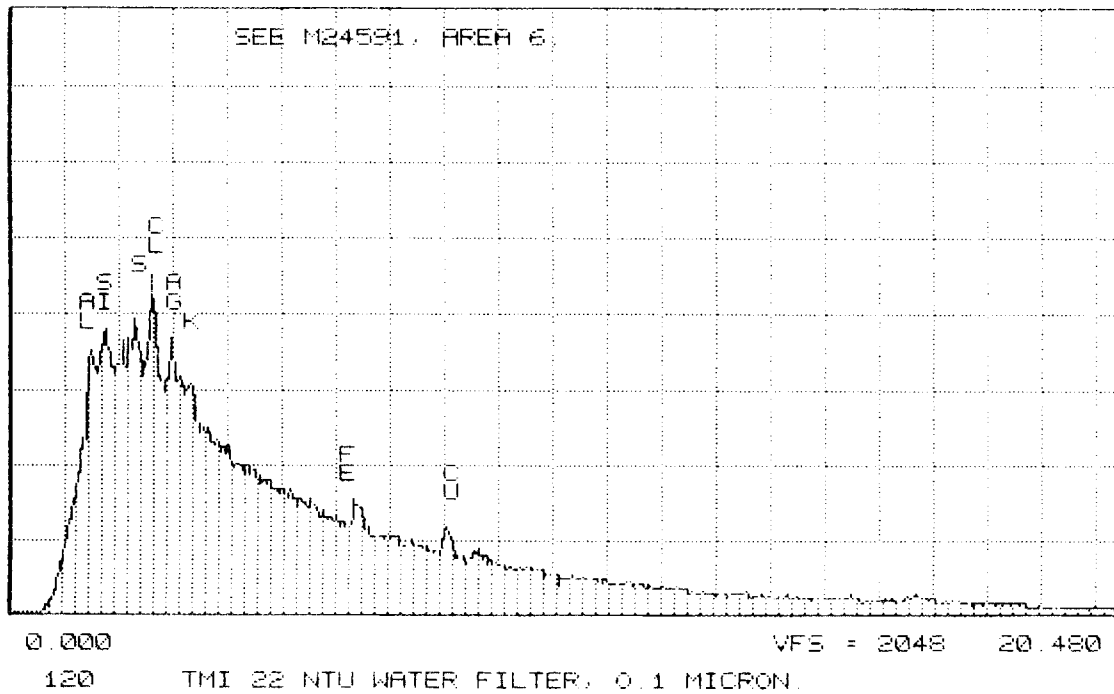


Fig. E.81. EDX of particle 6, 4591 (see Fig. E.72).

ORNL-DWG 87-14646

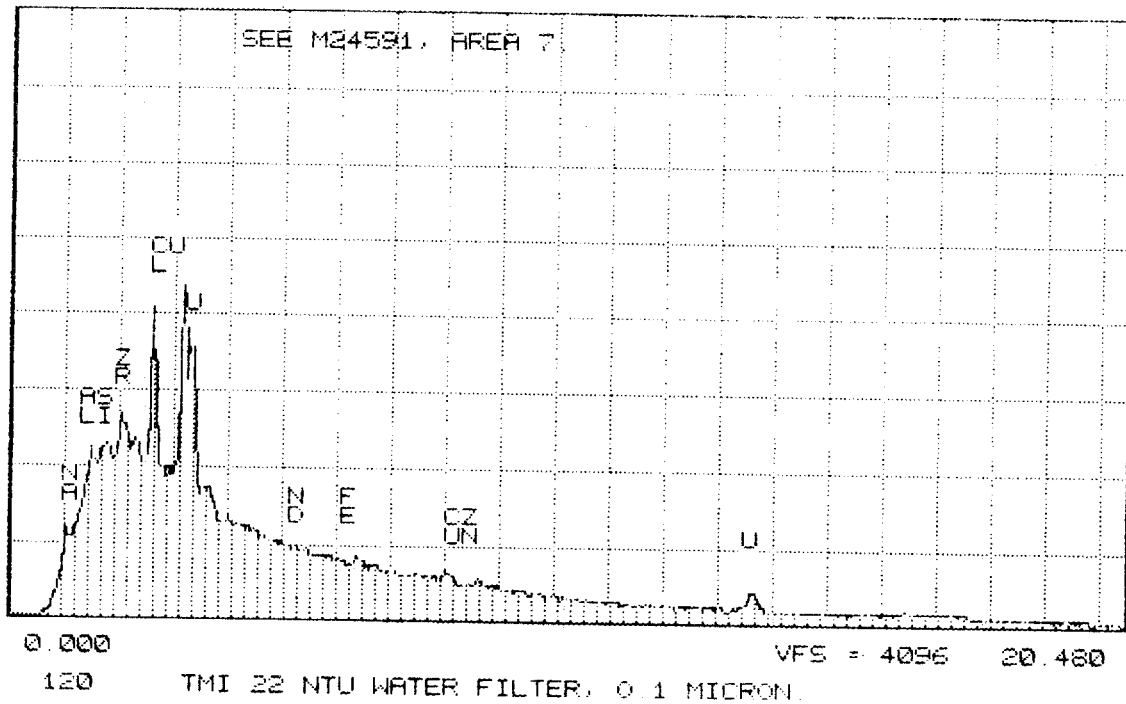


Fig. E.82. EDX of particle 7, 4591 (see Fig. E.72).

ORNL-DWG 87-14647

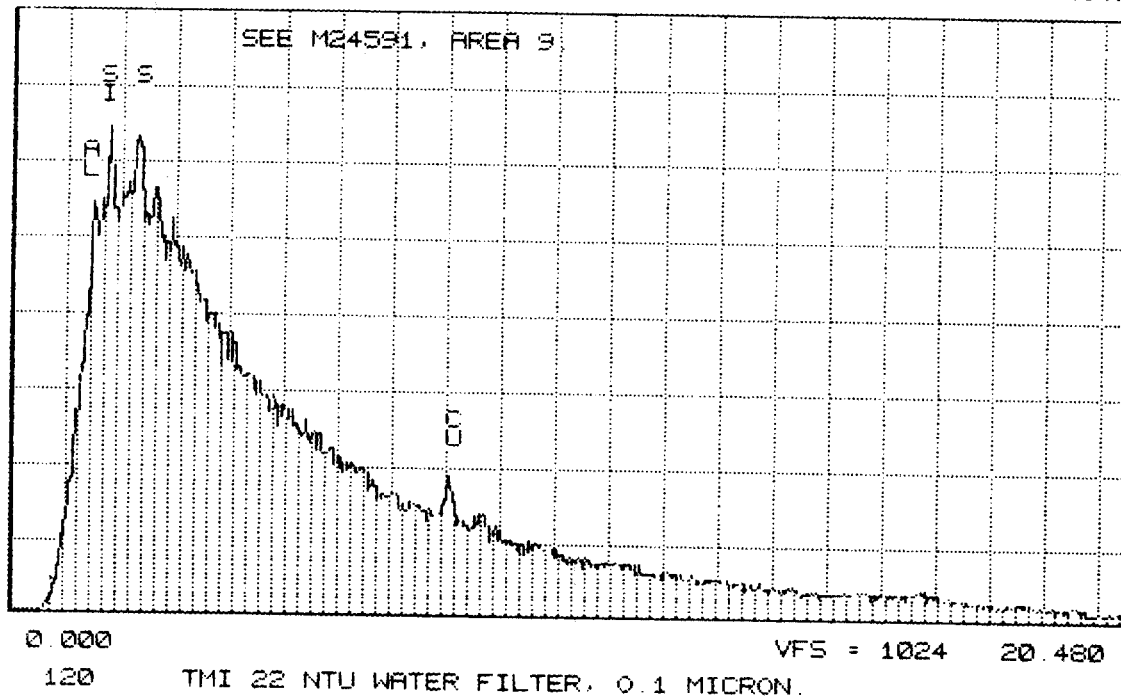


Fig. E.83. EDX of particle 8, 4591 (see Fig. E.72).

ORNL-DWG 87-14648

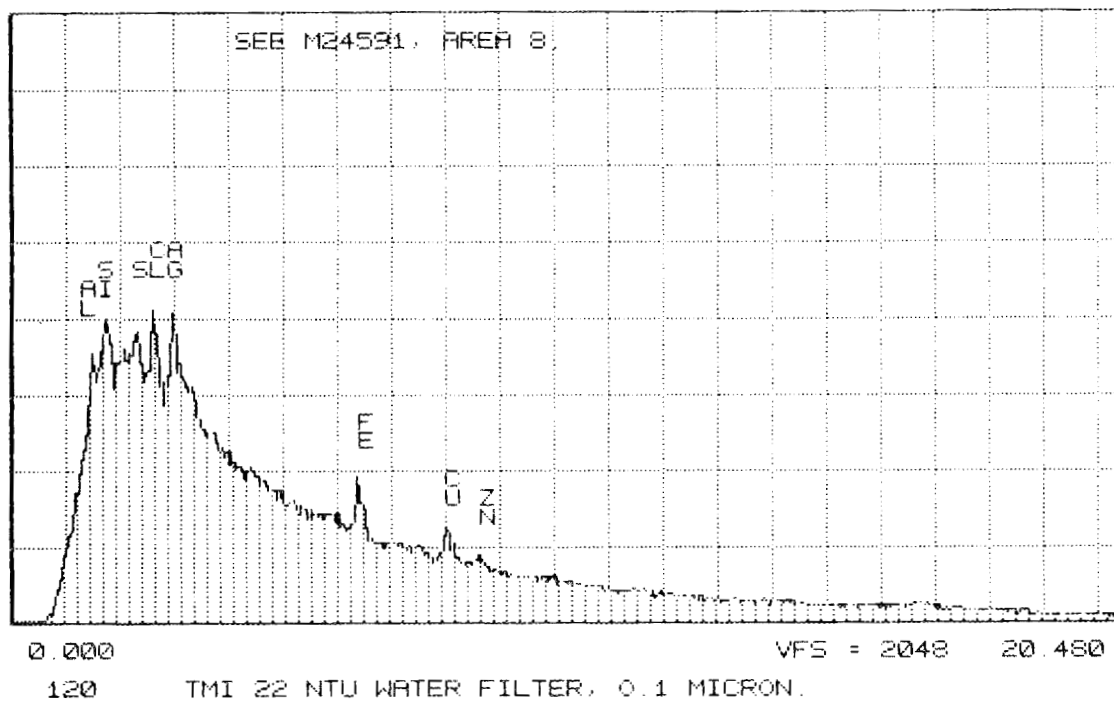


Fig. E.84. EDX of particle 9, 4591 (see Fig. E.72).

**Appendix F. PARTICLE CHARACTERIZATION DATA FOR SAMPLE W3
(TURBIDITY = ~4 NTU): FILTRATION TEST 4**

<u>Figure</u>		<u>Page</u>
F.1	Nuclepore filter test 4, 4-NTU water, 10- μ m filter	205
F.2	Nuclepore filter test 4, 4-NTU water, 10- μ m filter	206
F.3	Nuclepore filter test 4, 4-NTU water, 10- μ m filter	207
F.4	Nuclepore filter test 4, 4-NTU water, 10- μ m filter	208
F.5	Nuclepore filter test 4, 4-NTU water, 5- μ m filter	209
F.6	Nuclepore filter test 4, 4-NTU water, 5- μ m filter	210
F.7	Nuclepore filter test 4, 4-NTU water, 5- μ m filter	211
F.8	Nuclepore filter test 4, 4-NTU water, 5- μ m filter	212
F.9	Nuclepore filter test 4, 4-NTU water, 2- μ m filter	213
F.10	Nuclepore filter test 4, 4-NTU water, 2- μ m filter	214
F.11	Nuclepore filter test 4, 4-NTU water, 2- μ m filter	215
F.12	Nuclepore filter test 4, 4-NTU water, 2- μ m filter	216
F.13	Nuclepore filter test 4, 4-NTU water, 1- μ m filter	217
F.14	Nuclepore filter test 4, 4-NTU water, 1- μ m filter	218
F.15	Nuclepore filter test 4, 4-NTU water, 1- μ m filter	219
F.16	Nuclepore filter test 4, 4-NTU water, 1- μ m filter	220

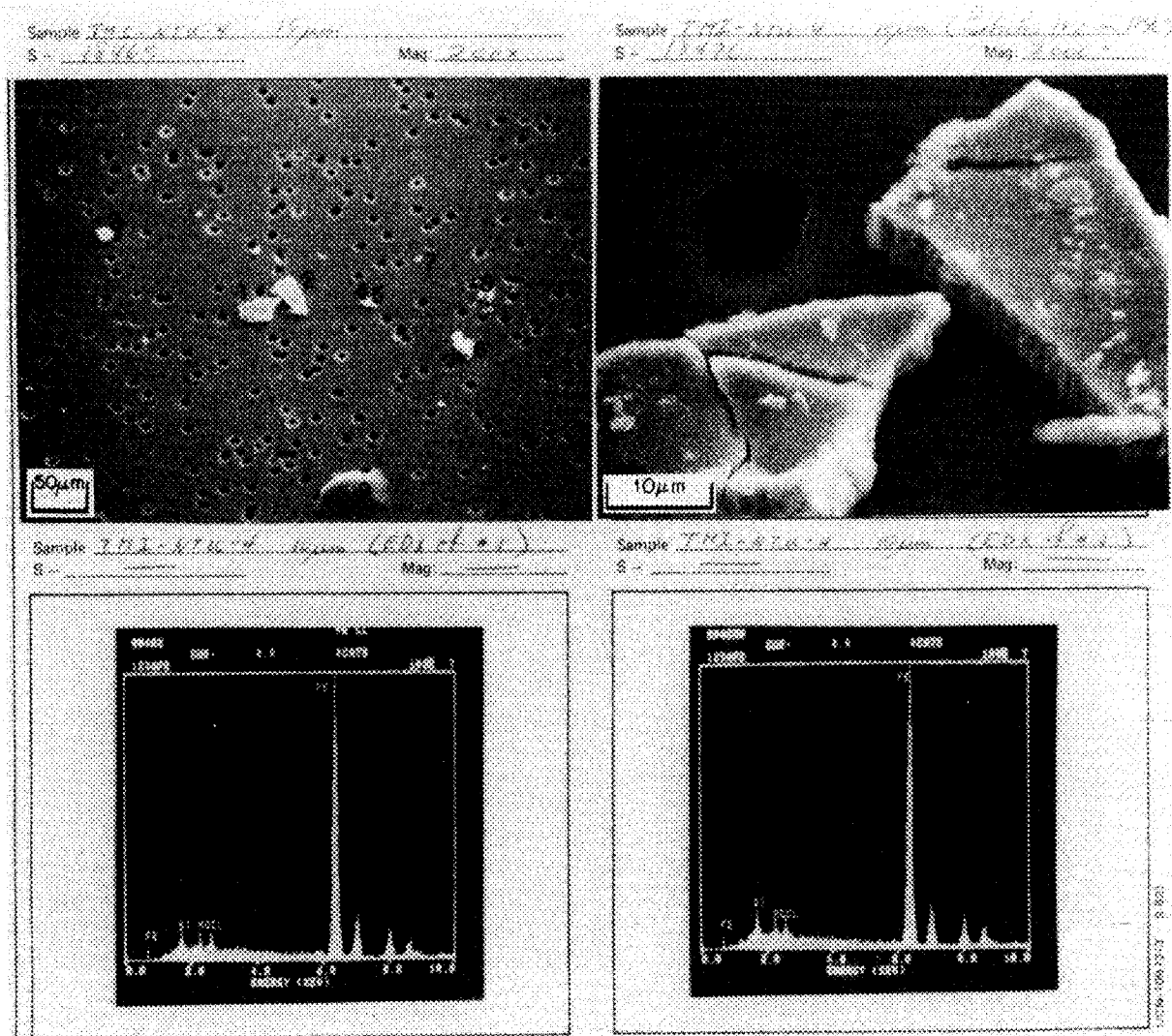
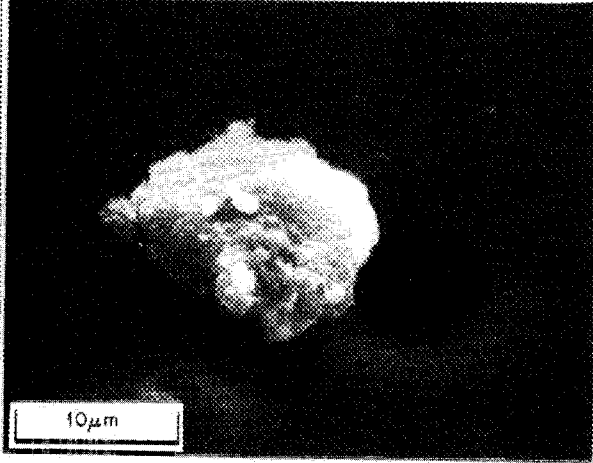
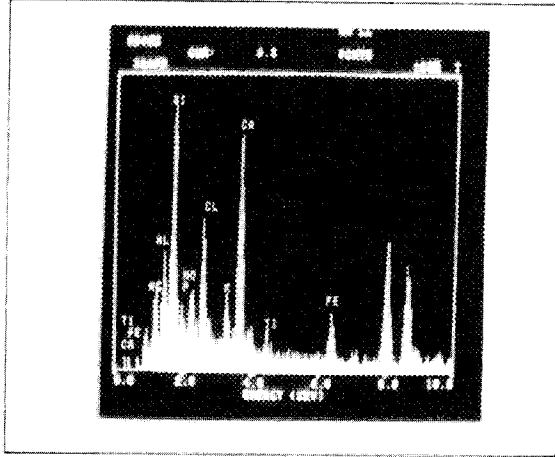


Fig. F.1. Nucleopore filter test 4, 4-NTU water, 10-µm filter.

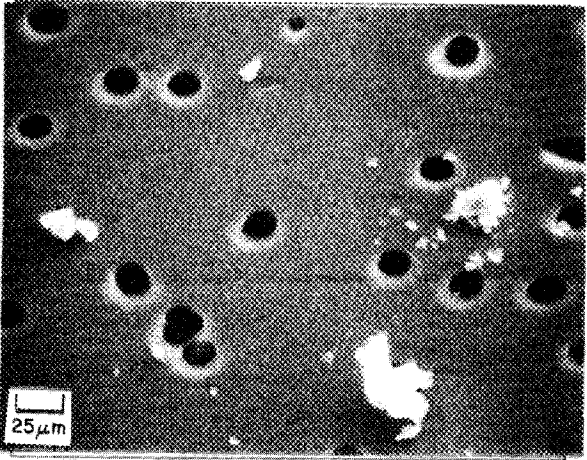
Sample 292-NTU-4 4µm (Nuclepore Filter)
S - 1247 Mag: 2000x



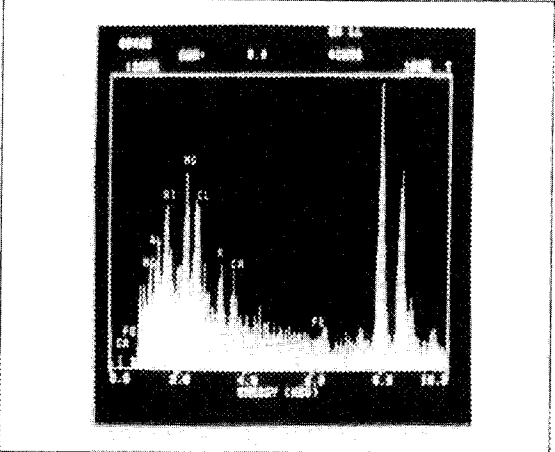
Sample 1M2-NTU-4 4µm (Nuclepore Filter)
S - _____ Mag: _____



Sample 292-NTU-4 4µm (Nuclepore Filter)
S - 1247 Mag: 7000x



Sample 1M2-NTU-4 4µm (Nuclepore Filter)
S - _____ Mag: _____



129 6 E12E01 N03

Fig. F.2. Nuclepore filter test 4, 4-NTU water, 10-µm filter.

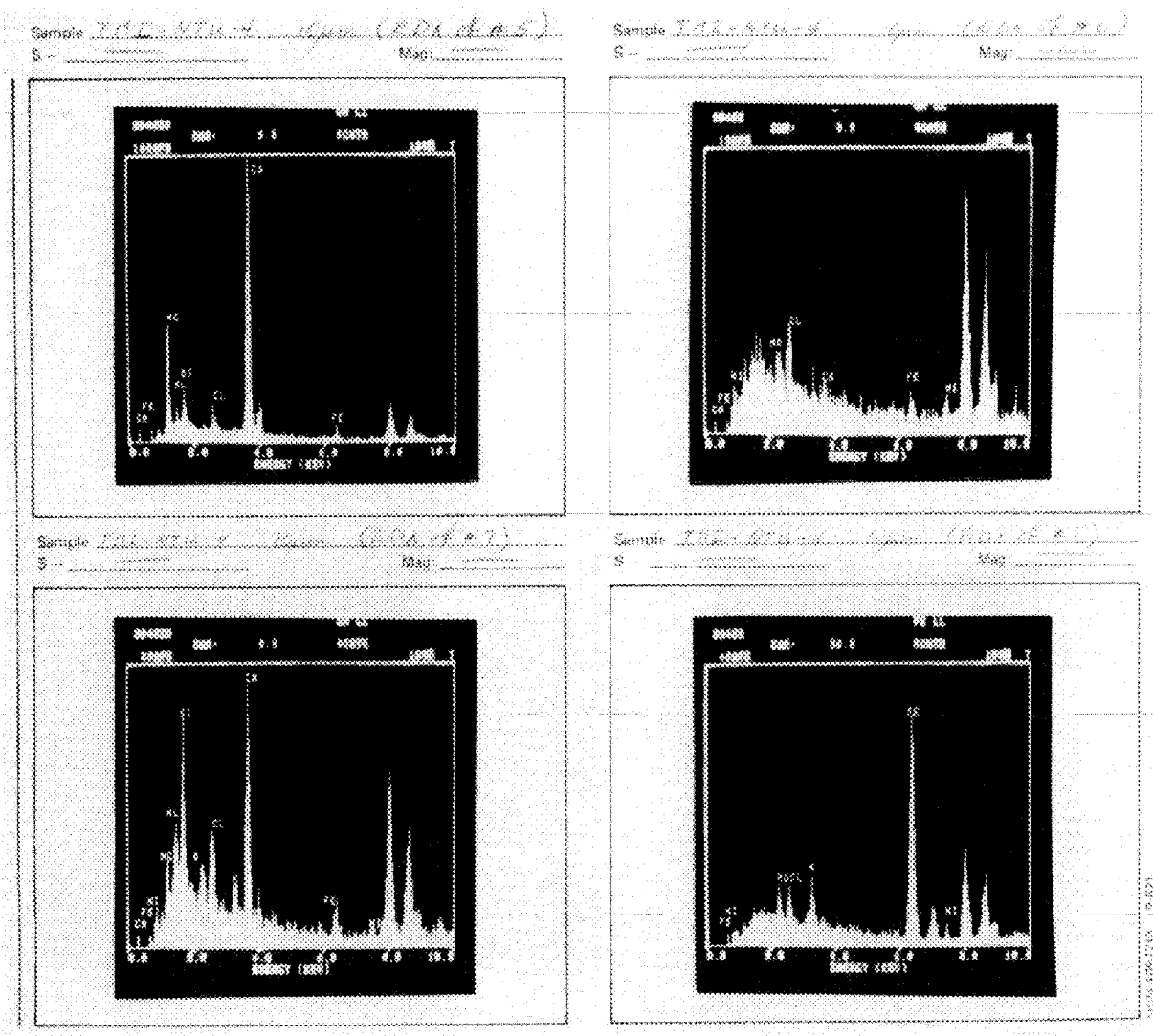
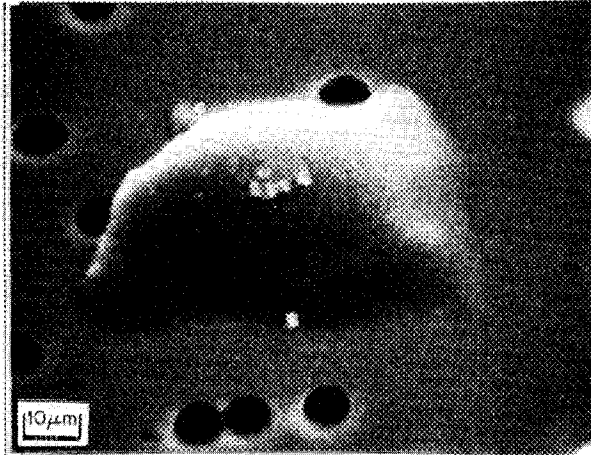
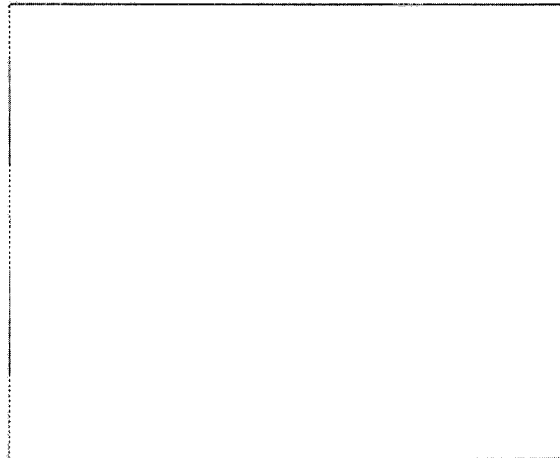


Fig. F.3. Nuclepore filter test 4, 4-NTU water, 10-µm filter.

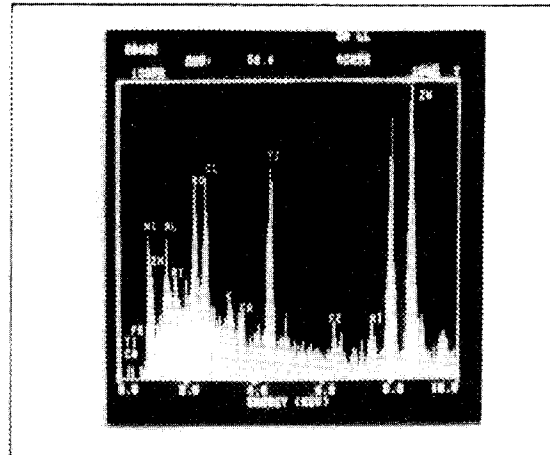
Sample TMI-NTU-4 10µm Sintered #42 (1987)
S - 18473 Mag: 1000x



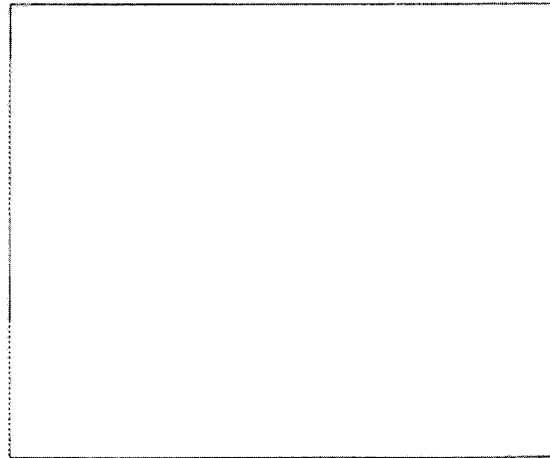
Sample _____
S - _____ Mag: _____



Sample TMI-NTU-4 10µm (EPA #42)
S - _____ Mag: _____



Sample _____
S - _____ Mag: _____



128-6 01/1/01 N3M

Fig. F.4. Nucleopore filter test 4, 4-NTU water, 10-µm filter.

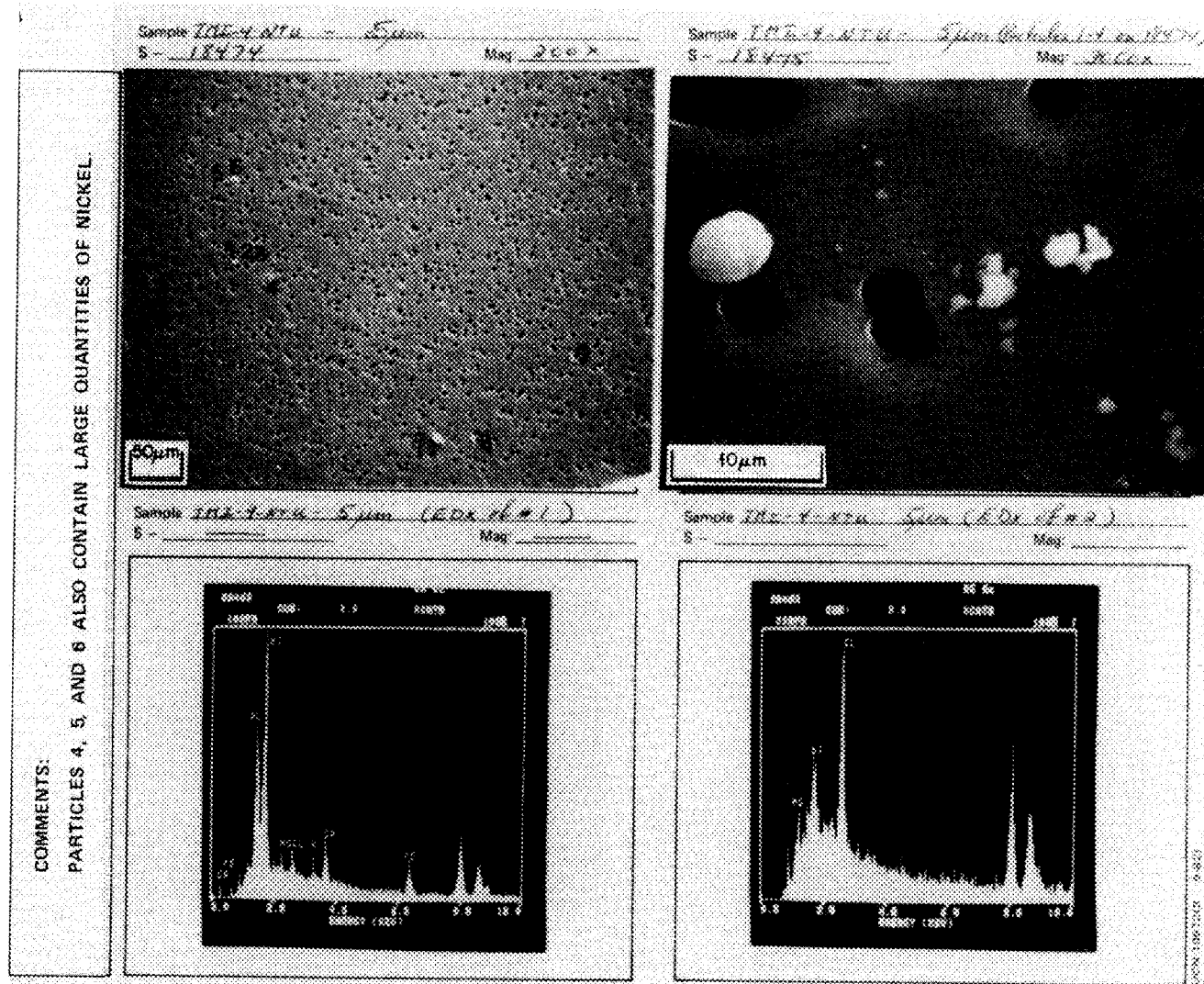


Fig. F.5. Nucleopore filter test 4, 4-NTU water, 5-µm filter.

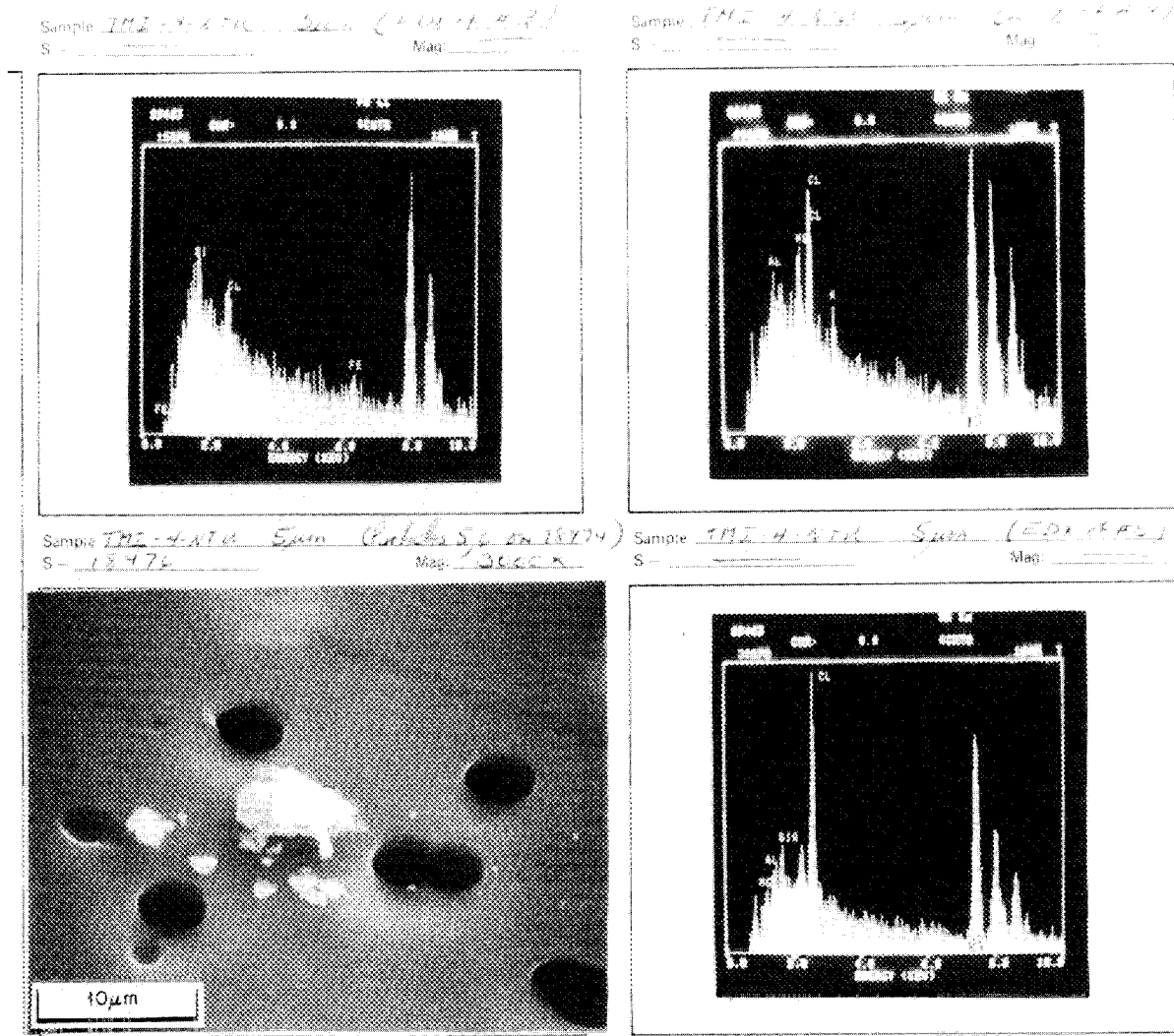


Fig. F.6. Nucleopore filter test 4, 4-NTU water, 5-µm filter.

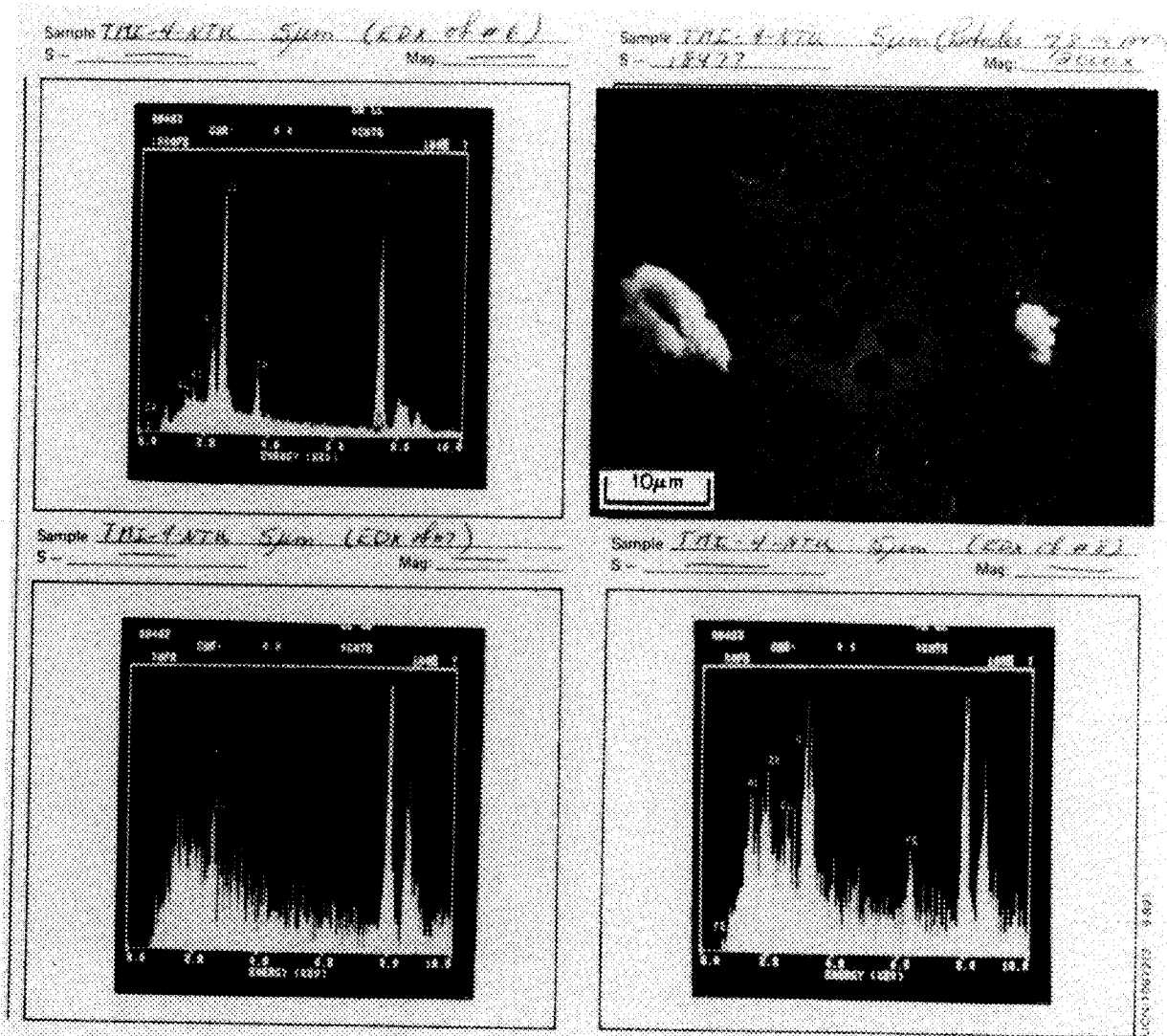


Fig. F.7. Nucleopore filter test 4, 4-NTU water, 5-µm filter.

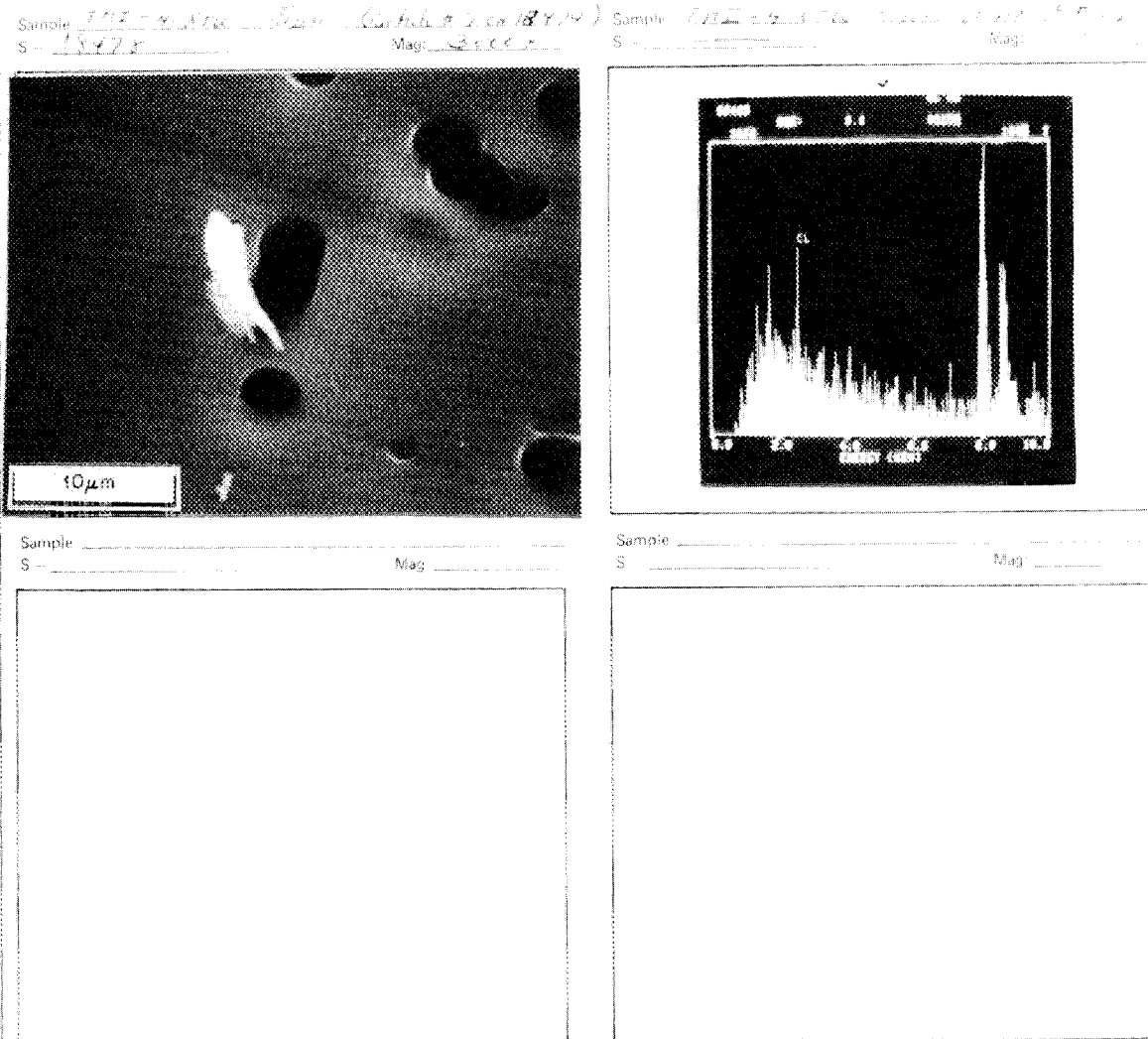


Fig. F.8. Nucleopore filter test 4, 4-NTU water, 5-µm filter.

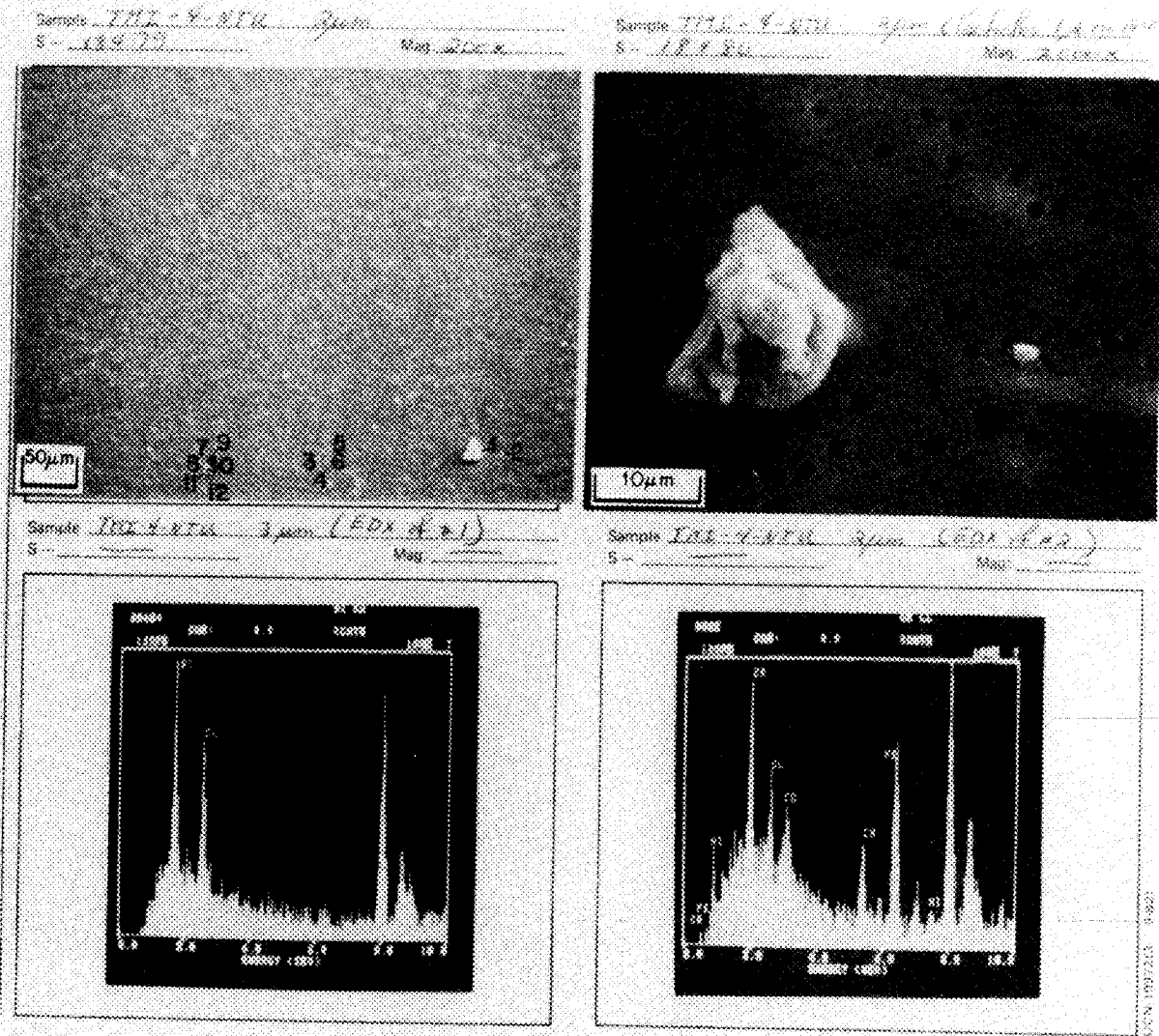


Fig. F.9. Nucleopore filter test 4, 4-NTU water, 2-µm filter.

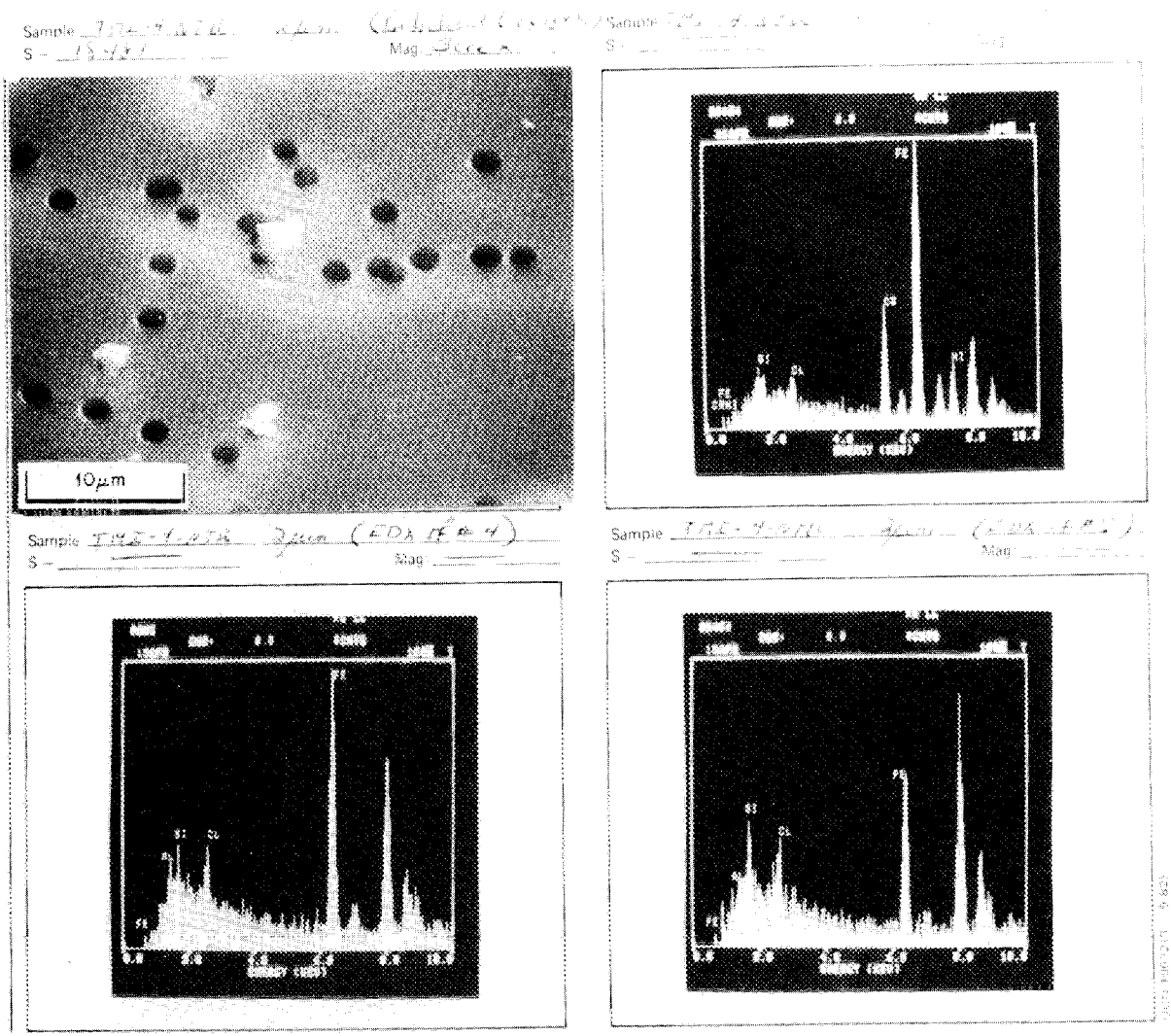


Fig. F.10. Nucleopore filter test 4, 4-NTU water, 2-µm filter.

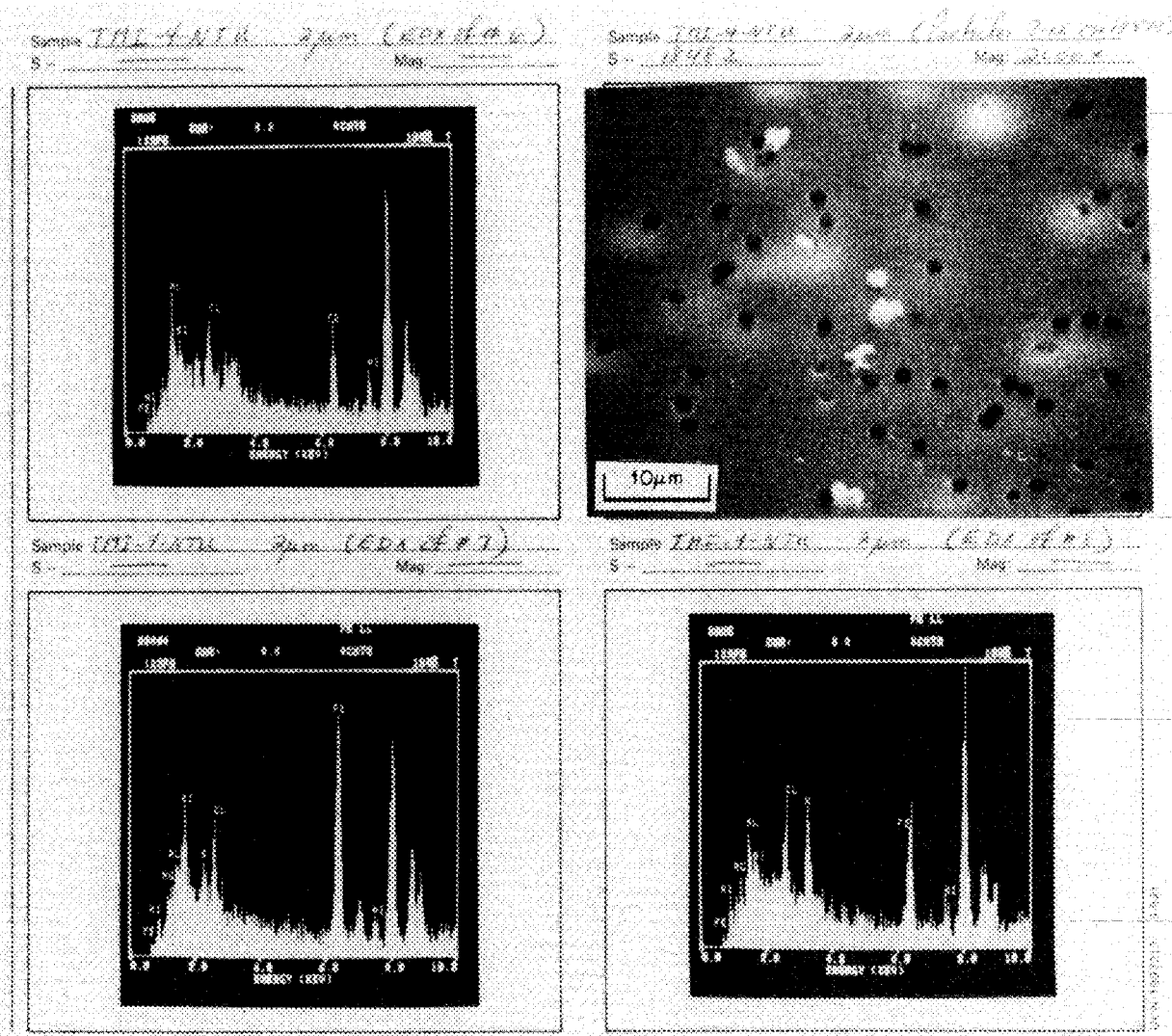
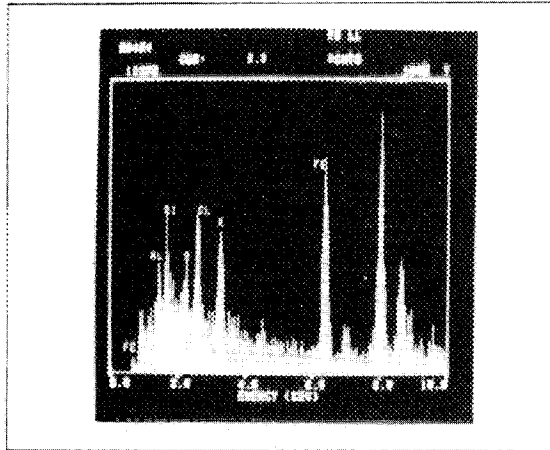
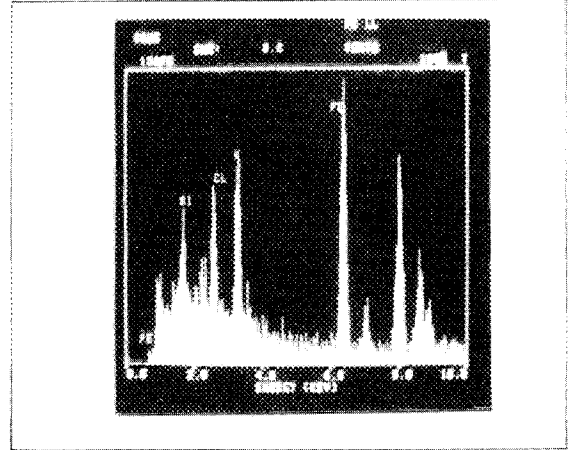


Fig. F.11. Nucleopore filter test 4, 4-NTU water, 2-µm filter.

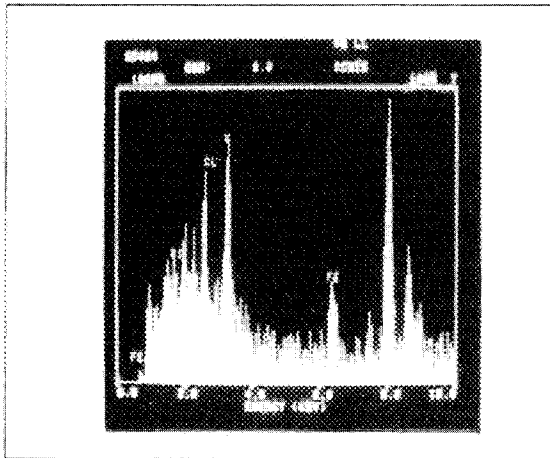
Sample IDE-4-NTU 2um (EDX # 10)
S _____ Mag _____



Sample IDE-4-NTU 2um (EDX # 11)
S _____ Mag _____



Sample IDE-4-NTU 2um (EDX # 12)
S _____ Mag _____



Sample IDE-4-NTU 2um (EDX # 13)
S _____ Mag _____

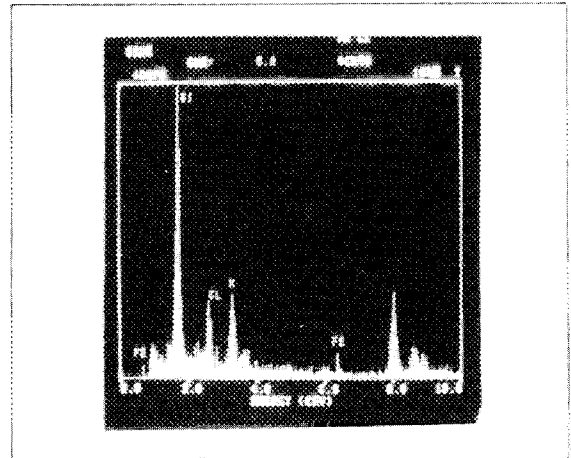


Fig. F.12. Nuclepore filter test 4, 4-NTU water, 2- μ m filter.

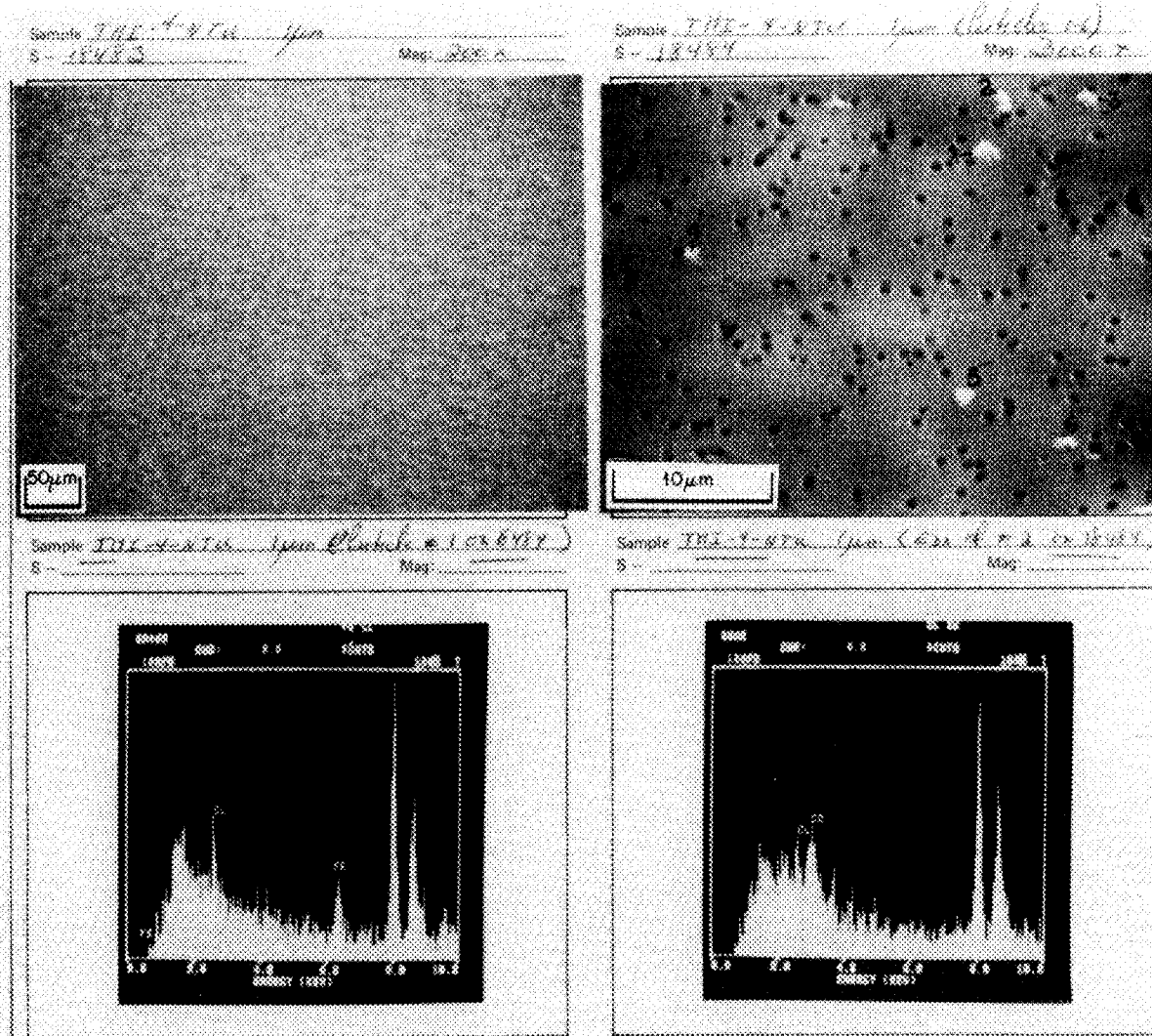
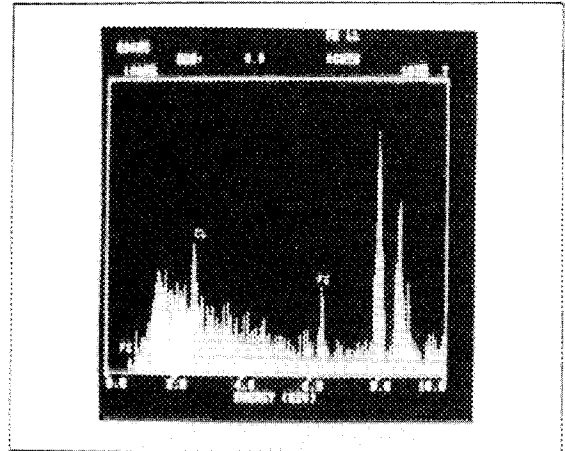
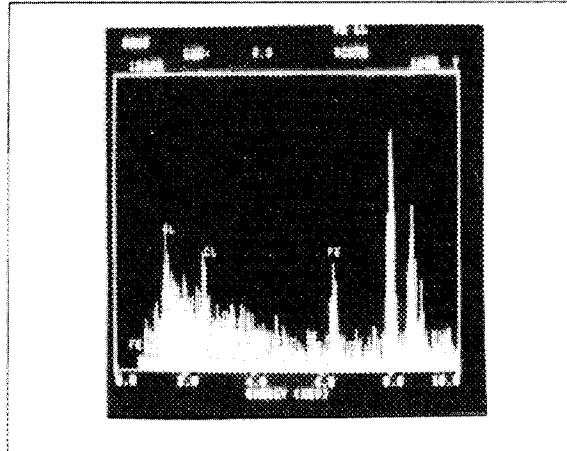


Fig. F.13. Nucleopore filter test 4, 4-NTU water, 1-µm filter.

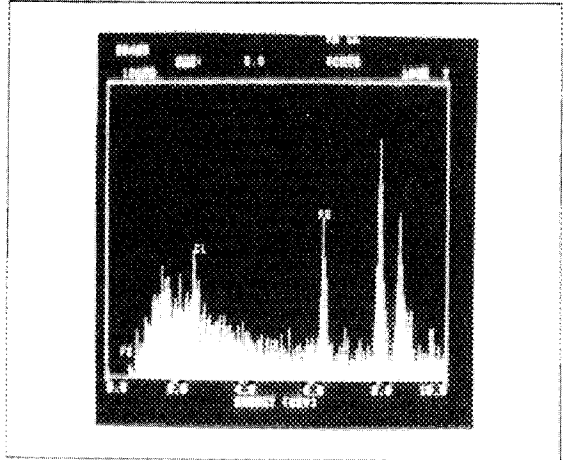
Sample IDE-4-NTH 1µm (EDA # 2-1884)
S _____ Mag: _____



Sample IDE-4-NTH 1µm (EDA # 4-1884)
S _____ Mag: _____



Sample IDE-4-NTH 1µm (EDA # 5-1884)
S _____ Mag: _____



Sample IDE-4-NTH 1µm (EDA # 6-1884)
S _____ Mag: _____

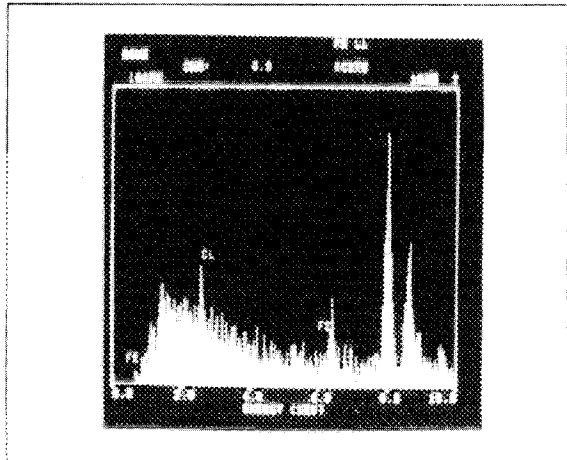


Fig. F.14. Nuclepore filter test 4, 4-NTU water, 1-µm filter.

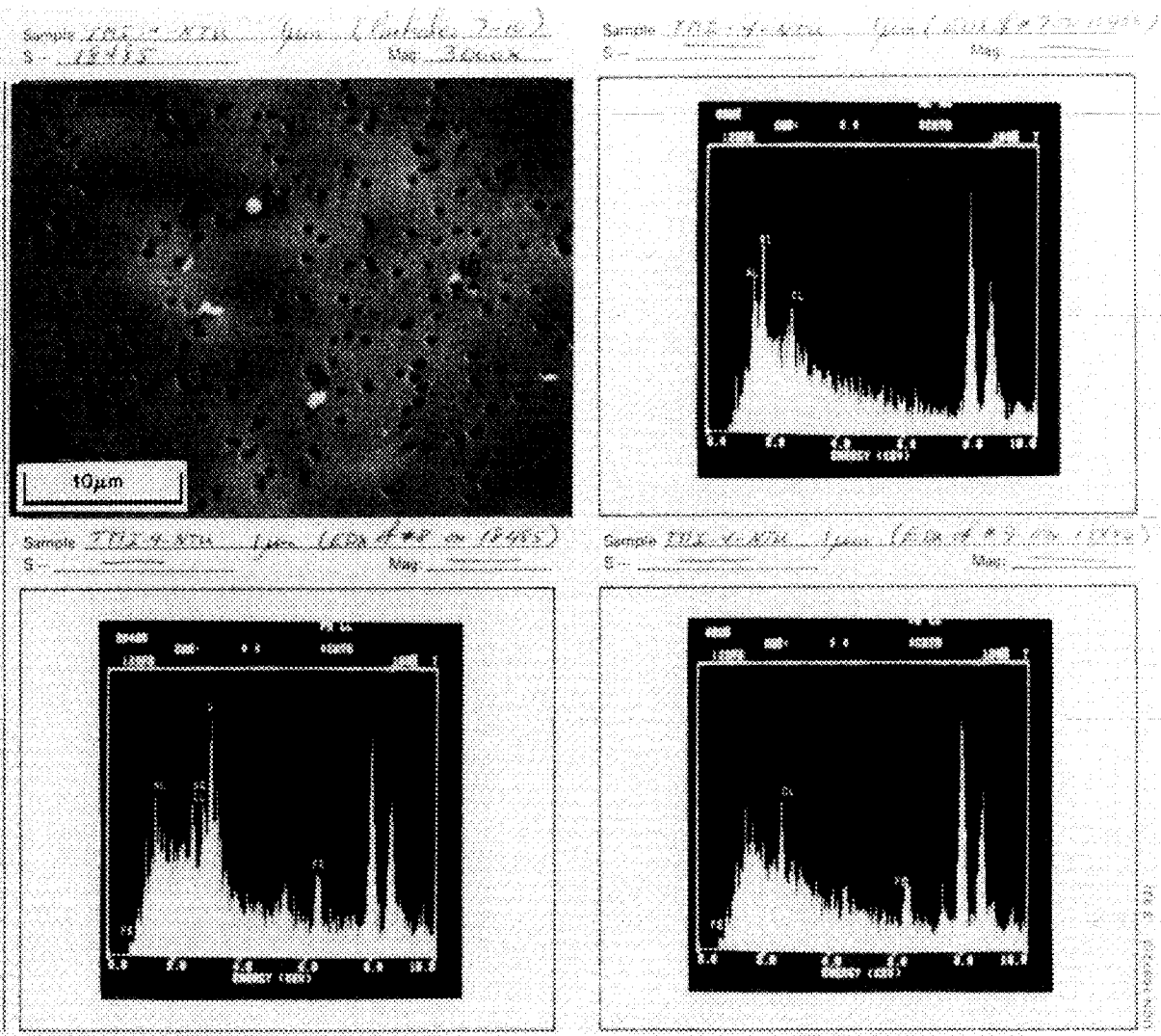


Fig. F.15. Nucleopore filter test 4, 4-NTU water, 1-µm filter.

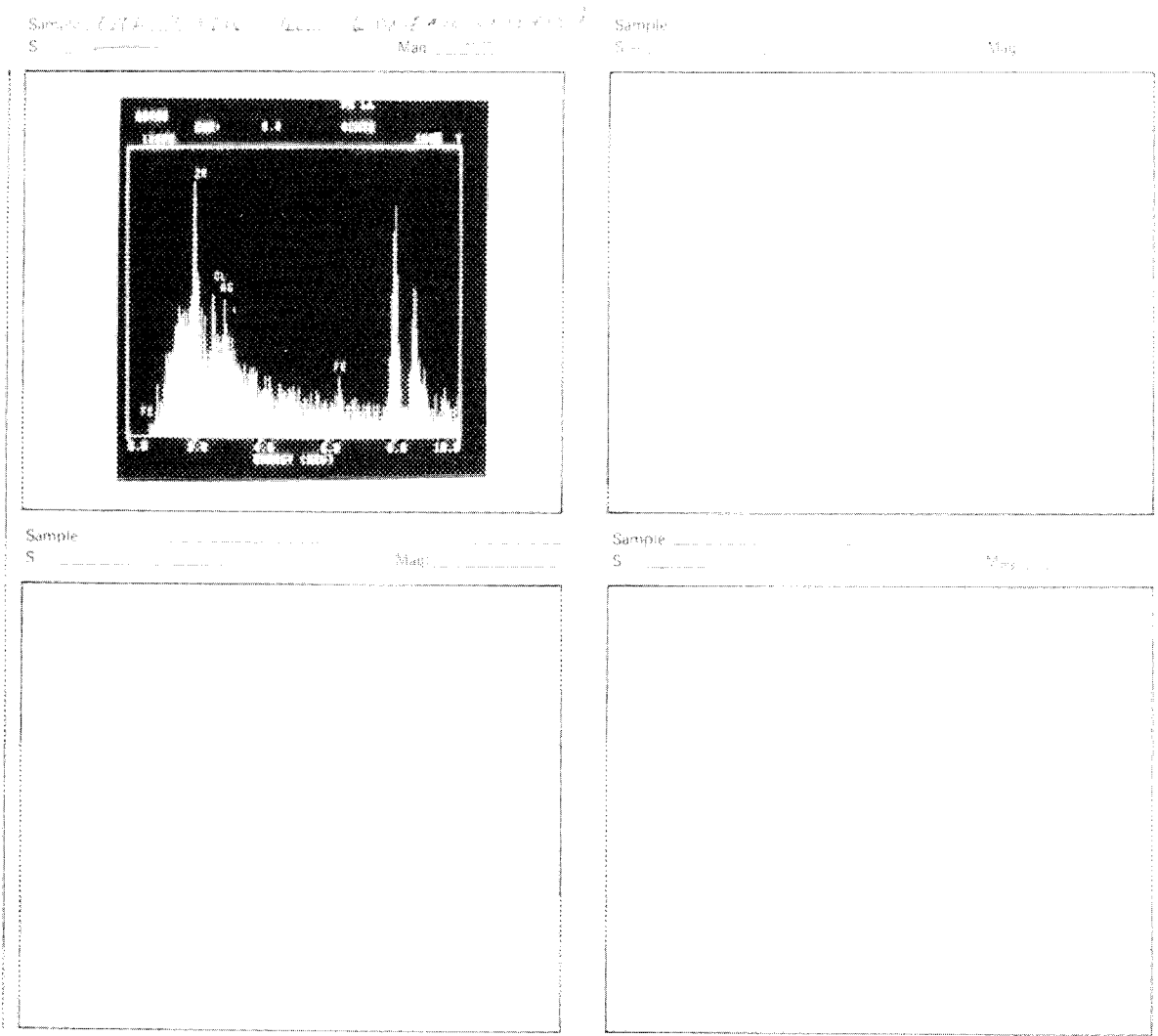


Fig. F.16. Nucleopore filter test 4, 4-NTU water, 1- μ m filter.

INTERNAL DISTRIBUTION

- 1-3. J. T. Bell
- 4-8. D. O. Campbell
- 9-11. E. D. Collins
- 12. D. A. Costanzo
- 13. R. S. Crouse
- 14. R. W. Glass
- 15-16. J. R. Hightower
- 17. E. K. Johnson
- 18. J. C. Mailen
- 19. A. P. Malinauskas
- 20. J. R. Merriman
- 21-22. J. H. Stewart, Jr.
- 23-24. M. G. Stewart
- 25. R. G. Wymer
- 26-27. Central Research Library
- 28. ORNL-Y-12 Technical Library Document Reference Section
- 29-30. Laboratory Records
- 31. Laboratory Records — ORNL R.C.
- 32. ORNL Patent Section

EXTERNAL DISTRIBUTION

- 33. Office of Assistant Manager, Energy Research and Development, DOE/ORO
- 34. N. M. Cole, NPR Associates, 1050 Connecticut Ave., Washington, DC 20036
- 35. R. S. Daniels, GPU Nuclear Corporation, P.O. Box 480, Middletown, PA 17057
- 36. T. F. Demitt, GPU Nuclear Corporation, P.O. Box 480, Middletown, PA 17057
- 37. G. R. Eidam, Manager, Data Management and Analysis, GPU Nuclear Corporation, P.O. Box 480, Middletown, PA 17057
- 38. W. H. Hamilton, 410 East Church Street, P.O. Box 613, Ligonier, PA 15658
- 39. K. J. Hofstetter, GPU Nuclear Corporation, P.O. Box 480, Middletown, PA 17057
- 40. E. E. Kintner, Executive Vice-President, GPU Nuclear Corporation, 100 Interpace Parkway, Parsippany, NJ 07054
- 41. C. B. Leek, EG&G Idaho, TMI Site Office, P.O. Box 88, Middletown, PA 17057
- 42. W. E. Potts, GPU Nuclear Corporation, P.O. Box 480, Middletown, PA 17057
- 43. F. R. Standerfer, Director, TMI-2, GPU Nuclear Corporation, P.O. Box 480, Route 441 South, Middletown, PA 17057
- 44. W. R. Young, DOE/TMI Site Office, P.O. Box 88, Middletown, PA 17057
- 45-46. Technical Information Center, Oak Ridge, TN 37831